_____

Timo Huttula (Ed.)

FLOW, THERMAL REGIME AND SEDIMENT TRANSPORT STUDIES IN LAKE TANGANYIKA

Timo Huttula (Ed.)

FLOW, THERMAL REGIME AND SEDIMENT TRANSPORT STUDIES IN LAKE TANGANYIKA

ABSTRACT

A report on hydrodynamical results of Lake Tanganyika Research within the Interagency
Agreement between FAO and UNOPS for the years 1996 and 1997.

Life out there

Lake clear and deep,
- moving waters and us.
Mountains so steep,
- bringing wind and gust.
They sail and fish
- in night and thunder.
You have it fresh
- we strange with wonder

TH/98

CONTENTS

1. Introduction

1.1. The project aims and its organisation

To complement the special studies in the UNOPS Project, "Pollution Control and Other Measures to Protect Biodiversity of Lake Tanganyika" (RAF/92/G32), Lake Tanganyika Biodiversity (LTBP), a set of hydrodynamic Circulation and Sediment Transport Models for Lake Tanganyika were developed and validated. The implementation of the work was carried out through **an Inter-Agency agreement (IAA)** between the UNOPS and FAO (explanations of acronyms in Appendix 1). FAO has been executing a regional project, "Research for the Management of the Fisheries on Lake Tanganyika", Lake Tanganyika Research (LTR) since 1992. This particular project is mainly funded by the Finnish International Development Agency (FINNIDA) and it comprises a number of research and development elements that share common interests with LTBP. This is the case particularly in the assessment of the environmental state and natural resources in the lake.

The plan for the joint activities in hydrodynamics was prepared on July 3, 1995 by the University of Kuopio. The agreement between UNOPS and FAO was signed in January 1996. The **overall objectives** of the hydrodynamic work were:

1. to study the wind driven water circulation
2. to study the major upwelling phenomena in the southern lake basin and their role in vertical transport of hypolimnetic waters
3. to study the secondary upwellings and spreading of these waters along eastern and western shore of the lake
4. to study the periodic oscillations in the lake
5. to study the horizontal dispersion and transport of suspended matter in the lake, especially near the main river inlets

Activities in the hydrodynamic program within IAA were undertaken in 1996 and 1997 (Table 1.1./1). The study was conducted by using the LTR hydrodynamic measurement network which already existed around and on the lake. The data collection was based on several meteorological stations, which were set up in 1993 and 1994 (Huttula et al. 1993, Kotilainen et al. 1994), and on weekly measurements conducted in the vicinity of the three main field stations. The lake wide expeditions played an important role in the data collection.

Table 1.1./1. Measurement activities sharing within LTBP and LTR during the years 1996 - 1997. MET = meteorological stations, CUR = water current measurements, CTD = conductivity-temperature-depth profiler with oxygen sensor, SED = sediment and sedimentation measurements

	LTR	LTBP
Fixed stations		
MET on the shore	+	
MET and temperature profiles	+	
on the buoys		
Expeditions		
CUR		+
CTD profiles		+
SED		+
MET on the ship		+

During the years 1996 - 97 three hydrodynamic **expeditions** were conducted in addition to a few testing surveys. The agreement made it possible to collect data all around the lake using the ship meteorological station and to measure water currents with three Acoustic Doppler Current Profilers (ADCP).

The **characteristics of LTR and LTBP models** are described in Table 1.1./2. The further development of the circulation model was a logical extension for the earlier modelling work done in LTR. This circulation model was developed for pelagic areas, although near shore currents were also described. It was designed to simulate wind driven circulation and upwelling phenomena in Lake Tanganyika.

Table 1.1./2. Main characteristics of numerical models applied to the Lake Tanganyika during the years 1996 - 97.

	LTR model	LTBP models
Main emphasis	Wind-driven circulation Upwelling	Wind-driven circulation Sediment transport
Spatial resolution	3 - 5 km	1 - 2 km
Wind forcing	quasi 3D wind model	3D mesoscale meteorological model
Visualisations	simple	IDL graphics

In the modelling work within the present study **two regional sediment transport models** were introduced. This together with field observations made it possible to study the dynamics of suspended matter transportation from the River Malagarasi and rivers in the south end of the lake. The vertical transport of hypolimnetic waters was studied mainly from field observations. The chart in Fig. 1.1./1 visualises the work phases and the links between the field work and modelling.
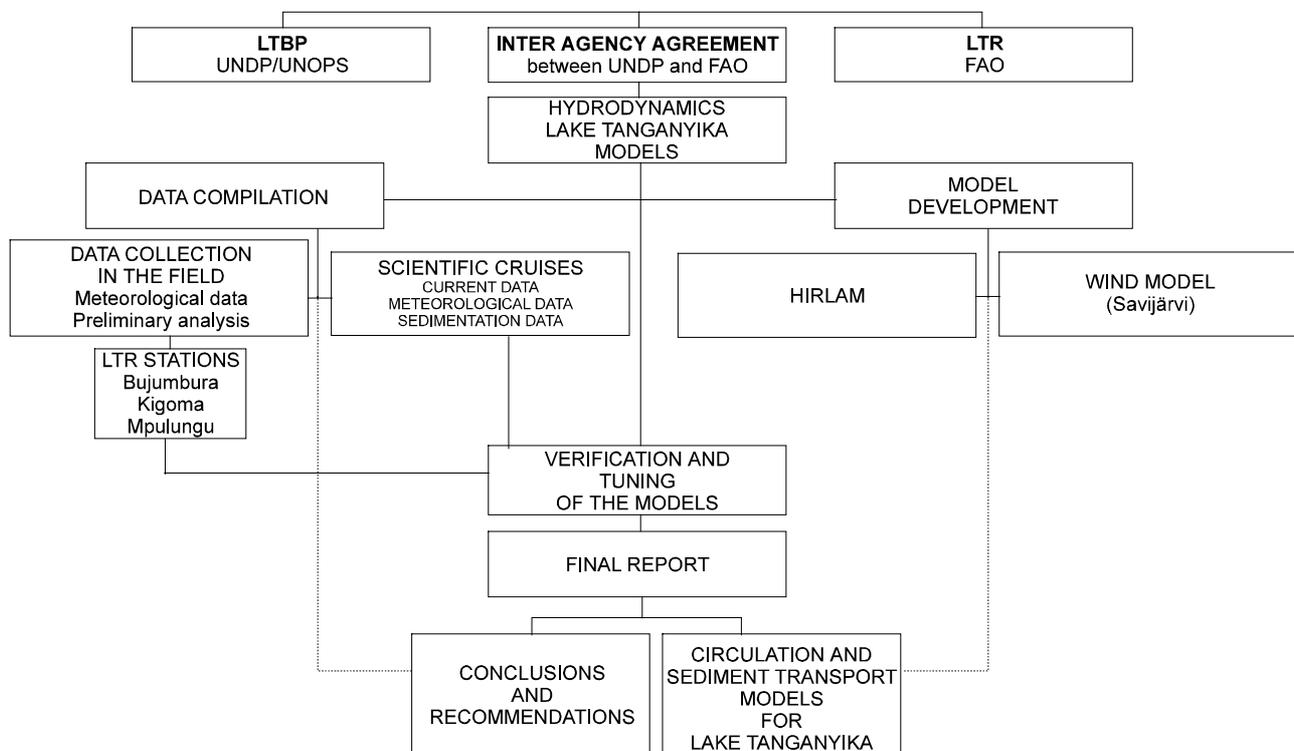

Figure 1.1./1 Organizational chart of LTR/LTBP circulation and sediment transport model development work.

LTR Technical Documents (TD's) by Huttula & Podsetchine (1994) and Podsetchine & Huttula (1995 and 1996) describe the model development work done within LTR before the LTBP activities started.

The IAA was designed to meet the specific requirements of LTBP. **The integration of different research sub-programs of the LTBP project and LTR team working under the IAA** took place during the visits of the model developer (Dr. Victor Podsetchine) to Natural Research Institute (NRI), UK in May 1996 and the sediment transport sub-program leader, Dr. G. Patterson, to Finland in September 1996. In parallel with the three major expeditions several meetings with Dr. Menz (the co-ordinator of LTBP) have also been held in the LTBP field office in Dar-Es-Salaam. During these visits the work plans of the model development were updated. The outline of this report was sent for an approval to the LTBP project and sub-program leaders in June 1997. As a result, the LTBP models having higher spatial resolution near the main river mouths were developed. This made it possible to predict the transport and dispersion of the river waters and suspended particulate matter (SPM).

Soon after the development of the LTR model had started, the need for **a separate model to describe the meteorological regime** over the lake region became evident. Analysis of collected meteorological data showed high spatial and temporal variability of the wind fields due to the mountain terrain and the very narrow and elongated shape of the lake. Intensive solar radiation and cooling during the nights also contribute as thermal winds to the general wind pattern over the lake. Numerical lake circulation models are very sensitive to the wind forcing. The meteorological modelling has been conducted in a separate research project funded by the Academy of Finland. Two different models have been applied, a quasi 3D meteorological model (Savijärvi 1995 and 1997) and later on a 3D mesoscale meteorological model (High Resolution Limited Area Model - HIRLAM).

The data collection of the development work for LTBP circulation model was conducted by **LTR staff**. A hydrodynamic specialist (Pekka Kotilainen) worked in Bujumbura during the period of 12.5.1996 - 19.5.1997 and continued the data analysis (ADCP, CTD and ship meteostation with GIS) after his return to Finland. This arrangement was necessary for complementing the highly demanding data processing and in the absence of suitable national personnel. The national scientists participating in the basic LTR data collection and analysis were: Messrs. Jean-Marie Tumba and Eduard Nikomeze from Burundi, Aderico Kihakwi and Mathias Kissaka from Tanzania, Bombi Kakogozo from Zaire and Lawrence Makasa from Zambia. Mr. Piet Verburg in LTR Kigoma was responsible for maintaining LTR data collection and analysis. The University of Kuopio (Prof. Hannu Mölsä) was responsible for the overall administration of the work. The hydrodynamic team lead by Dr. Timo Huttula at the Regional Environmental Agency of Häme (REAH), Tampere conducted the ADCP data processing and the hydrodynamic modelling. Lic. Phil. Anu Peltonen was responsible for the whole data processing and archiving. Messrs. Markku Lakkisto and Mika Salomäki assisted in the ADCP data analysis at REAH. Dr. Victor Podsetchine was responsible for the model development and application. Mr. Matti Savinainen, an electrical engineer, from the University of Joensuu was responsible for installation and maintenance of automatic instruments on board of *R/V TANGANYIKA EXPLORER*.

In Appendix 2 the used resources are tabulated as man months during the years according to the funding source.

In this report the collected meteorological and hydrodynamic data of the period of 1.1.1996 to 10.9.1997 and the obtained results are discussed. They are compared to the previous results within

LTR. The 3D circulation and regional sediment transport models are also described. The models have been used to calculate the transport of river waters and suspended matter carried by them during two main seasons. Non-steady wind fields produced by the HIRLAM-model for dry and wet seasons were used as an input to lake circulation and transport models. The report also includes an order form for a simple version of the model with detailed user instructions. In this way the modelling results will be available for anybody interested in the subject.

1.2. Lake Tanganyika and earlier studies

Lake Tanganyika (Fig. 1.2./1) is the second in size of the African Great Lakes. It is situated in the Western Rift Valley of Central Africa at an altitude of 773 m above mean sea level. Elongated along the N - S axis, the lake is approximately 630 km long and 50 km wide in average. It is the second largest freshwater lake in the world (Hutchinson 1957). The lake has three main basins. In the north, the Kigoma basin extends to the depth of 1310 m. The middle basin is separated from the Kigoma basin by a broad sill with a depth of 655 m. In the south, the middle basin is separated from the Kipili basin by another sill with a depth of 700 m. The basin near Kipili is the deepest of the three basins, its maximum depth being 1472 m. The lake is meromictic with stable hypolimnetic waters, and the salt content is low for this type of lake (Degens et al. 1971).

The **abiotic deep waters** of Lake Tanganyika have been studied since the beginning of this century. Cunnington (1920) measured the surface temperatures in 1904 - 05, and almost 10 years later Stappers and Jakobs carried out a bathymetric survey to find the deepest parts of the lake (Stappers 1914). In 1938, Beauchamp (1939) conducted a survey on the temperature and oxygen stratification and major nutrients off Kigoma and also to the south of Kigoma in the southern part of the lake. He recorded the vertical stratification during the rainy season and noticed that upwelling of hypolimnetic waters took place during the dry season in the south. Furthermore, he noticed that the water in the deeper layers was deoxygenated. The Belgian 'Exploration Hydrobiologique' in 1946 - 47 proved the existence of internal waves in the thermocline (Servais 1957) and also measured the lake water temperature more accurately than ever before (Capart 1952). Another result of the same expedition was the first bathymetric chart of the lake by Capart (1949). In the late 1950s, Dubois made the first depth-time-series of temperature and oxygen data. In the early 1960s, Coulter (1963, 1968) continued the studies in the south and later on, in 1973 - 75, in the northern part of the lake.

Upwelling in Lake Tanganyika has been observed at the very southern end of the lake during the dry season in May - August. The relation between the upwelling and biological production has been studied in Lake Tanganyika by Coulter and Spiegel (1991) and Hecky and Bugenyi (1991).

There are **two main seasons** with different weather conditions within the yearly cycle in the Lake Tanganyika region (Capart 1952). The **wet season** from September to May is characterised by weak winds over the lake, high humidity, considerable precipitation and frequent thunderstorms.

The **dry season** from May until the end of August is characterised by moderate precipitation and strong, regular southerly winds. The seasonal changes of weather and winds result from large-scale atmospheric processes. During the dry season, a global wind convergence zone (Inter Tropical Convergence Zone, ITCZ) is reaching to lake region. In January, in the middle of wet season, it is situated on the northern side of the equator.

Surface area   32.900 km^2
Depth max.   1435 m; 700 m (mean)
Volume   18.940 km^3
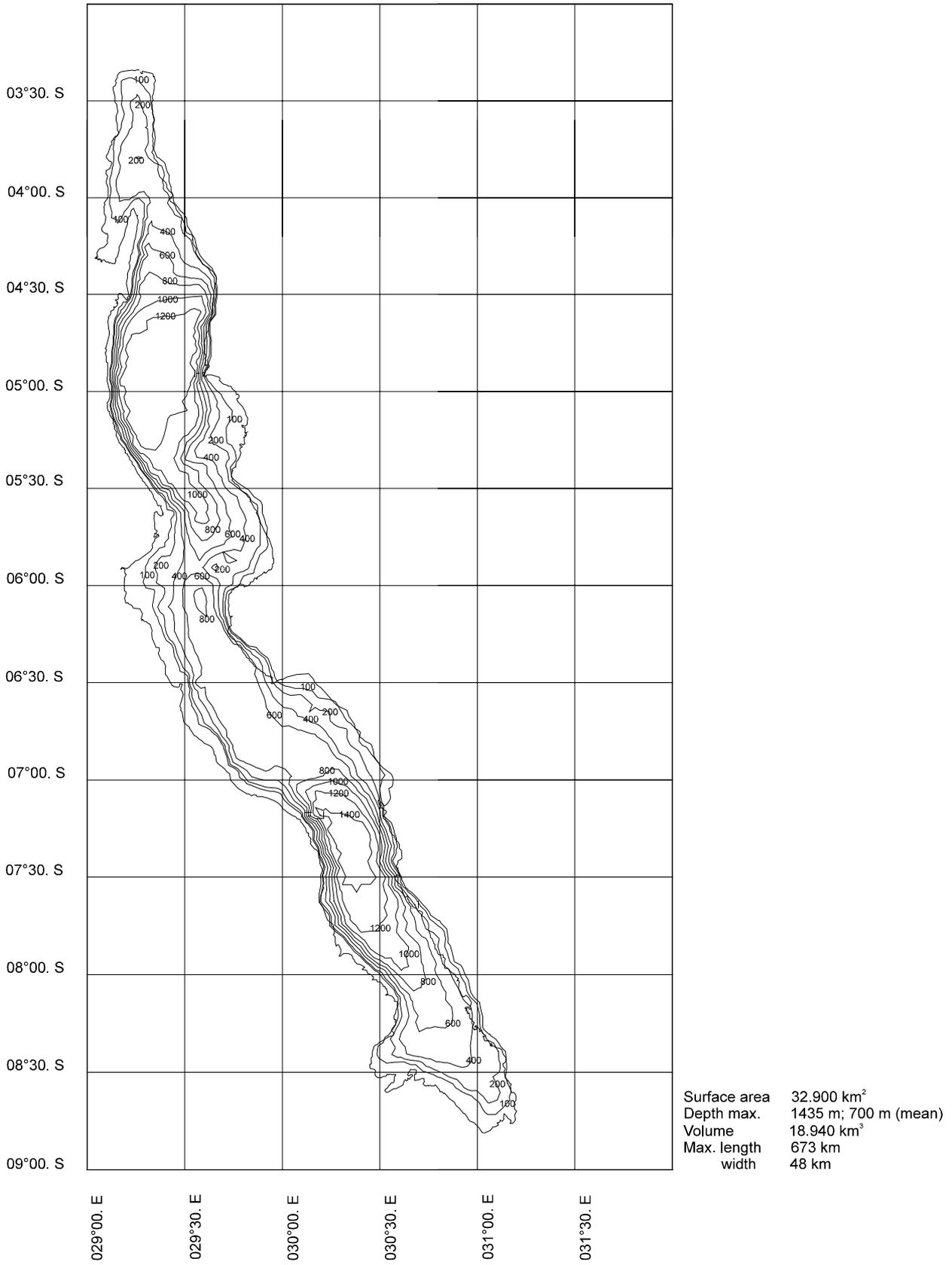Max. length   673 km
     width   48 km

Figure 1.2./1 Lake Tanganyika and its characteristics.

The **seasonal thermal regime** of the lake has been discussed by Capart (1952), Coulter (1963, 1968) and Coulter and Spiegel (1991). Heating of the lake takes place mainly in the beginning of the wet season in September - November (Coulter and Spiegel 1991). As a result, thermal stratification is established all over the lake, with the temperature difference of 4 °C between the surface water and bottom layers. The lake loses heat through evaporation caused by strong winds during the dry season (Coulter and Spiegel 1991). This cooling is strongest in the southern basin. In the epilimnion, the temperature varies between 25 °C in August to 27 °C in April. Within the thermocline, the temperature drops down to 25 °C. In the hypolimnion, the temperature varies only between 23.43 and 23.48 °C. The thermocline is situated at the depth of 40 - 60 m.

Until the FAO/FINNIDA Lake Tanganyika Research, the only known **water flow measurements** conducted earlier in the lake were by van Well and Chapman (1976) as quoted by Vandelannote et al. (1997). Van Well and Chapman reported a mean southward currents of 11 cms^{-1} at a depth of 5 m off coast near Kigoma. During the dry season, the current speed was lower.

Many studies deal indirectly with the **mixing and the substance transport in Lake Tanganyika**. The stability of 70 % of the lake volume and the great age of the lake should lead to a high depth gradient of salts. However, the measurements by Degens et al. (1973) show that no such a gradient exists in the lake's deep waters. This indicates some kind of deep water circulation. The vertical mixing has been discussed also by Tietze (1982) in connection with his study on the methane content of Lake Tanganyika waters. He estimated that the decrease in density due to temperature changes within the metalimnion was about 1 kgm^{-3}. He also conducted laboratory studies on density variations in the lake due to dissolved substances. The results indicated that these density variations were 5 % of those due to temperature variations. Capart (1949) reported that the water coming from the Rusizi River flows at the depth of 53 m due to its density. He also chemically traced runoff waters at the depth of 400 m. Coulter (1968) suggested that the dense water penetration occurs every night everywhere along the lake margins. On the basis of temperature observations and theoretical analysis, he also came to the conclusion that a clockwise general circulation prevails in the lake and that strong coastal jets exist, especially near the eastern shore.

2. Data collection and analysis

2.1 Equipment

Basic **hydrodynamic instruments and data recorders** have been used within LTR since 1993, before the IAA. Within IAA it was possible to expand this network and instrumentation. As this report is based on the data that have been collected with all these instruments and used for hydrodynamic studies and for model verification, all hydrodynamic instruments are described in the next chapter.

Since March 1993, LTR has equipped three stations around the lake and two other offshore buoy stations with automatic meteorological and hydrodynamical data recording instruments (Fig. 2.1/1.). A weather station and a water level recorder were located at Bujumbura, Burundi. At Kigoma, Tanzania, a wind station (Appendix 3, Fig. A) and a water level recorder were installed and also at Mpulungu, Zambia. Later on, the Mpulungu wind station was extended, it served as a meteorological station as four new sensors were installed. Two LTR meteorological offshore stations were installed, one outside Kigoma, in the northern main basin, and the another one 40 km to the north of Mpulungu in the southern main basin. The installed recorders collected data continuously all around the lake and ensured satisfactory coverage of the lake, more complete than previous studies. The installations started in March 1993 and the last recorder was set up in August 1994. The extension of Mpulungu wind station took place in May 1995.

Some of the instruments have collected data for more than four years, excluding breaks in recording due to instrument failure or maintenance. The lake meteorological station outside Kigoma was lost at the end of November 1996 and the one outside Mpulungu in January 1997. A list of collected data up to the end of May 1997 is presented in Appendix 4.

In addition to the equipment listed above, a Conductivity-Temperature-Dissolved oxygen profiler (CTD), a ship based Acoustic Doppler Current Profiler (ADCP), two buoy based Workhorse Sentinel ADCP's (Appendix 3, Fig. D) and a meteorological station on board *R/V TANGANYIKA EXPLORER* have been used for extensive data recordings on the lake (Appendix 3, Fig. C).

The Bujumbura weather station was installed in the Bujumbura port, on a pier, in March 1993. The station has a recording unit and 9 sensors at two different heights, 4 and 13 m above the lake surface. A total of 11 parameters is recorded at an interval of 10 min. The sensors at 4 m are for wind speed, air temperature and relative humidity, and at 13 m for wind speed and wind gust, wind direction, air temperature, relative humidity, air pressure, solar radiation and rainfall. The parameters are mainly recorded as momentary values or as total sums within an interval. The structure of the weather station and technical specifications have been described in detail by Huttula, Peltonen and Nieminen (1993).

At Mpulungu a weather station with three sensors was installed in April 1994 on a hill above a water tower 40 m above the lake surface and 300 m away from the lake. In May 1995 it was extended to 7 sensors. The sensors are for wind speed, wind gust, wind direction, air temperature, air pressure, relative humidity and solar radiation. The parameters are recorded similarly to the Bujumbura weather station.
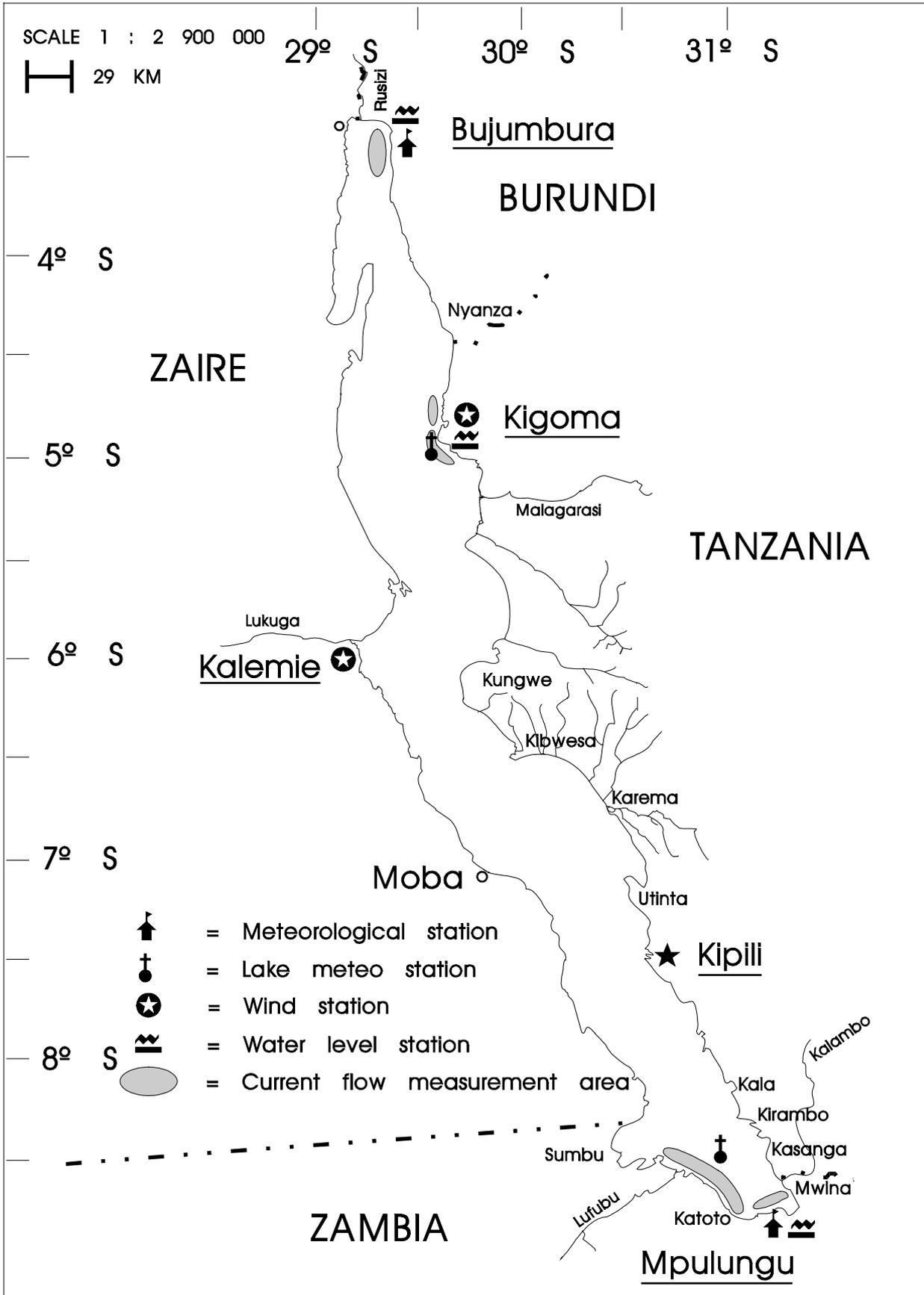
Figure 2.1./1 Data collection network of LTR.

The Kigoma wind station was installed on a cliff south of Kigoma port in July 1993 (see Appendix 3, Fig. A). It has a scanning unit and two sensors 50 m above the lake surface and less than 50 m away from the lake shore. The measured parameters are wind speed, wind gust and wind direction. The recording interval has been set to 10 min.

The lake buoy station off Mpulungu was installed during the first hydrodynamic expedition in March 1993. It consists of a data recording unit, wind speed, wind direction and air temperature sensors and a sub surface temperature sensor chain with eleven temperature sensors. The accuracy of used sensor is 0.1 ^{o}C. The data recording interval has been set to 60 min and observations are stored in the memory unit as momentary values from each depth. The depths are 1, 5, 30, 50, 70, 90, 110, 150, 200, 250 and 300 m. The structure of the station has been described in detail by Huttula, Peltonen and Nieminen (1993). From May 1995 a new chain was installed with an extra sensor at 15 m depth and no sensor at 250 m depth.

A similar type of **lake buoy station** as off Mpulungu is located **outside Kigoma**. It was installed in March 1994. The depths of the sensors are the same as in the second Mpulungu chain (see above). The sensors above the surface are similar to the ones outside Mpulungu. The recording interval of the lake meteo station off Kigoma has been set to 30 min. The water depth at the Kigoma and Mpulungu buoys was c. 400 m and 350 m respectively.

Each **water level recorder** located at Bujumbura, Kigoma and Mpulungu, three in total, has a data recording unit and a pressure sensor. The sensor was placed inside a tube to avoid wave effects. The tube was fixed to a jetty. Each installation was done similarly. Instrument record momentary values of water pressure i. e. the depth of the sensor every 2 s. This means that the observations are not fixed to any absolute value and only the periodicity and the amplitude of oscillation can be obtained. Hourly means of water level were recorded within the depth range of 0 cm to 70 cm. The water pressure recorders were all installed in March 1993. Further information concerning the structure and operation of the water level recorder is provided by Huttula *et al*. (1993) and Kotilainen *et al.* (1995a). The seasonal variation of water level was sometimes higher than the measuring range of the sensors and their depth in the protection tube had to be adjusted accordingly.

In 1993 a **CTD-profiler, model STD-12 Plus,** was purchased for the LTR project. It is a self-contained, intelligent instrument, which is designed for precision measurements in fresh and saline water. The measured parameters are conductivity, temperature, pressure and dissolved oxygen. Deployment range is 0 - 2000 meters. The accuracy of the temperature sensor is 0.01 ^{o}C and for the depth 0.01 % in the range of 0 - 200 bar. It has a solid state memory and can be set up to record in certain time or depth intervals. The programming is executed with a PC software, AML. The instrument can be used for several successive measurements without re-programming. The size of the CTD memory is 640 Kb. The instrument has been used during scientific expeditions and circulated between the LTR stations for regional measurements. More information about the structure and functioning of the STD-12 Plus is provided by Huttula, Peltonen and Nieminen (1993).

Based on the IAA, three new hydrodynamic instruments were purchased in order to expand hydrodynamic studies.

The first one, **an Acoustic Doppler Current Profiler (ADCP)** was installed on R/V Tanganyika Explorer in May 1996. It has 4 transducers of 150 kHz transmitting frequency (Fig. 2.1./2a).

Configuration of the transducers is convex and the beam angle is 20°. Apart from the transducers, the ADCP has a temperature, a heading and a pitch and roll sensor. The ADCP is connected via a deck box to a computer. The deck box is also interfaced to a Gyro compass, GY 700, and a GPS (Global Positioning System), Raytheon Raystar 390 (Fig. 2.1./2b). The GY700 gives heading and the GPS position of the vessel while sailing. The ADCP has an in-built system for bottom tracking. The configuration of the ADCP is done on the computer.
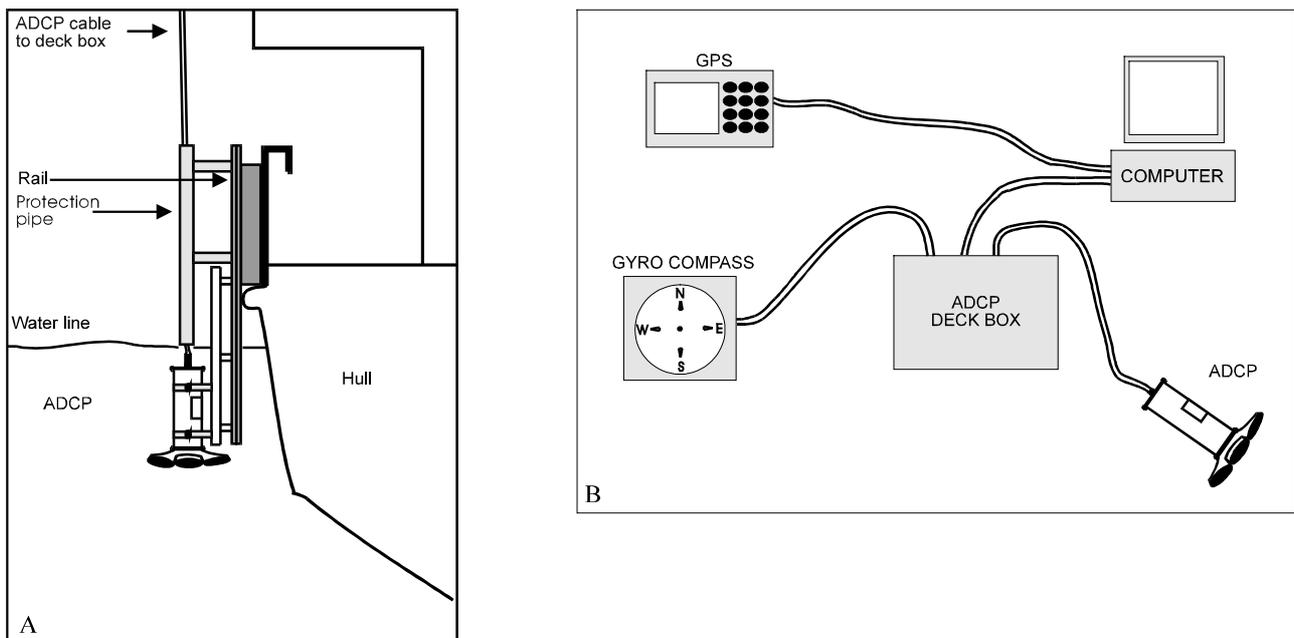
Figure 2.1./2 Acoustic Doppler Current Profiler (ADCP) installation on the side of R/V Tanganyika Explorer (a) and the interfacing of ADCP-Deckbox-Computer-DGPS (b).

The ADCP's function is based on transmitted pulses and received echoes from the moving scattered particles in the water. The assumption is that the scattered particles move at the same average speed as currents, so the measured velocities of these scattered particles correspond with current. The movement of the ship can be traced by different means. The standard method is the bottom tracking. Lake Tanganyika was the deepest fresh water body where this instrument has been used to date. The nominal range for bottom detection was 450 m for this frequency, but due to the low density of the water it was possible to track the bottom even at the depth of 800 m on some occasions. For the deeper areas a use of a DGPS system was planned in order to obtain reference velocity of the ship (Appendix 3, Fig. B). The equipment consisted of DGPS by Trimble and two VHF radios for communication.

More information can be found in the Technical Manual of Acoustic Doppler Current Profiler (Anon. 1995).

Two other moored ADCP's, called **Workhorse Sentinel ADCP'**s were purchased in June 1996 (Fig. 2.1./3). The instrument is designed for self-contained current measurements at depths 0 - 200 m. It consists of a transducer and a three-board system electronics. Frequency and bandwidth of the transducer is 300 kHz. Transducer's configuration is convex with an angle of 20º. Mooring accessories consist of an external battery case and a spherical buoy. This buoy is designed to hold

up the top of a mooring and is made of syntactic foam. The instrument is fit and fixed inside the buoy with mooring frames. A special software assists in testing, deployment planning and preparation, data recovery and data analysis. Data are recorded in a DOS-compatible format.
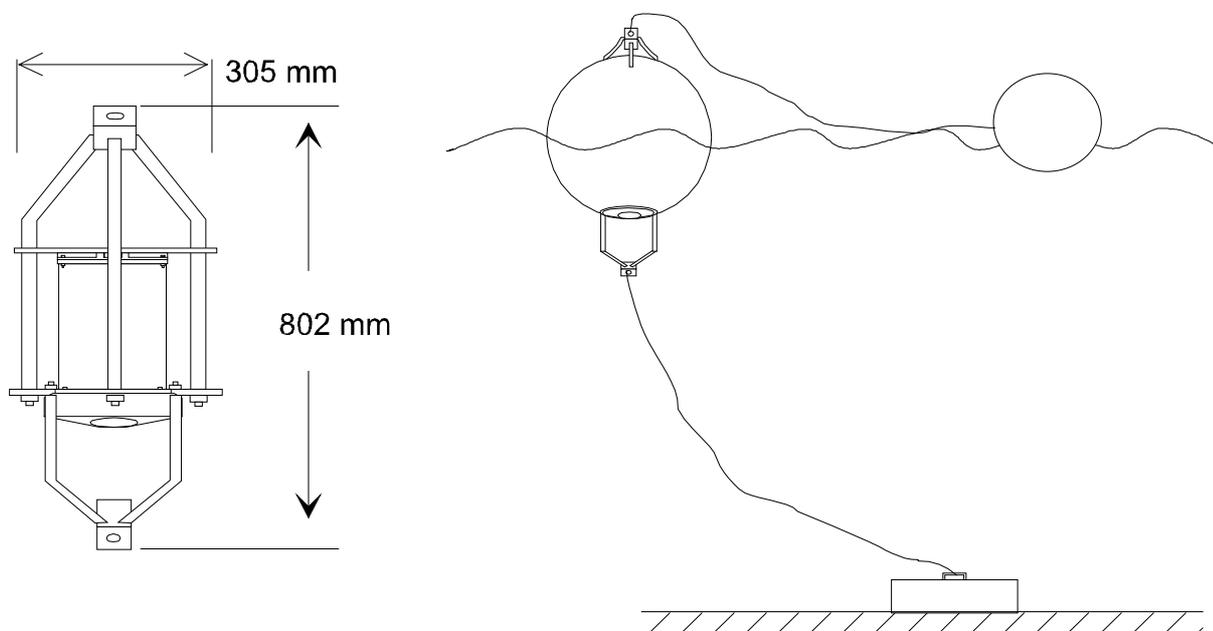
Figure 2.1./3 Buoy based Acoustic Doppler Current Profiler, model "Workhorse" and its installation in the lake.

A **meteorological station** was installed on *R/V TANGANYIKA EXPLORER* in April - May 1995. The station is based on Aanderaa Instruments instrumentation and the data logging software was tailored by Navarc Ltd. The station consists of the following sensors: wind speed, wind direction, air temperature, relative humidity, sun minutes, air pressure, solar radiation and rainfall. They were installed on the roof of the vessel. Wind speed and direction sensors are installed in mast of the vessel's main headlights, and the rest of the sensors on a separate pole of 4.5 meters starboard side on the wheelhouse roof. Both installations have been designed not to be affected by the vessel itself or any equipment on the deck. The height of the sensors off the water surface was 10 meters. Ship speed and direction is determined from GPS of the main deck. The installation is presented in the Fig. 2.1./4.

Flow cylinders were used for measuring current speed and direction. They are of standard size, 60 x 100 cm. During use they are attached with a rope to a buoy. The depth of a measurement is determined with the length of the rope. The usual depths are 2, 5, 10, 20 and 40 m, the most common depth is 2 m. Normally 5 to 6 cylinders were used on one measurement line. When the cylinders are put in the water the position and the time of installation of each cylinder are recorded. The Global Positioning System (GPS) is used for that. One measurement lasts 1 - 2 h. The execution of the measurements is given in more detail by Huttula, Peltonen, Nieminen (1993) and Kotilainen (1993). Current flow measurements were conducted once a week in three areas, off Bujumbura, Kigoma and Mpulungu, each having 4 to 5 measurement lines, but also during hydrodynamics expeditions on *R/V TANGANYIKA EXPLORER*.
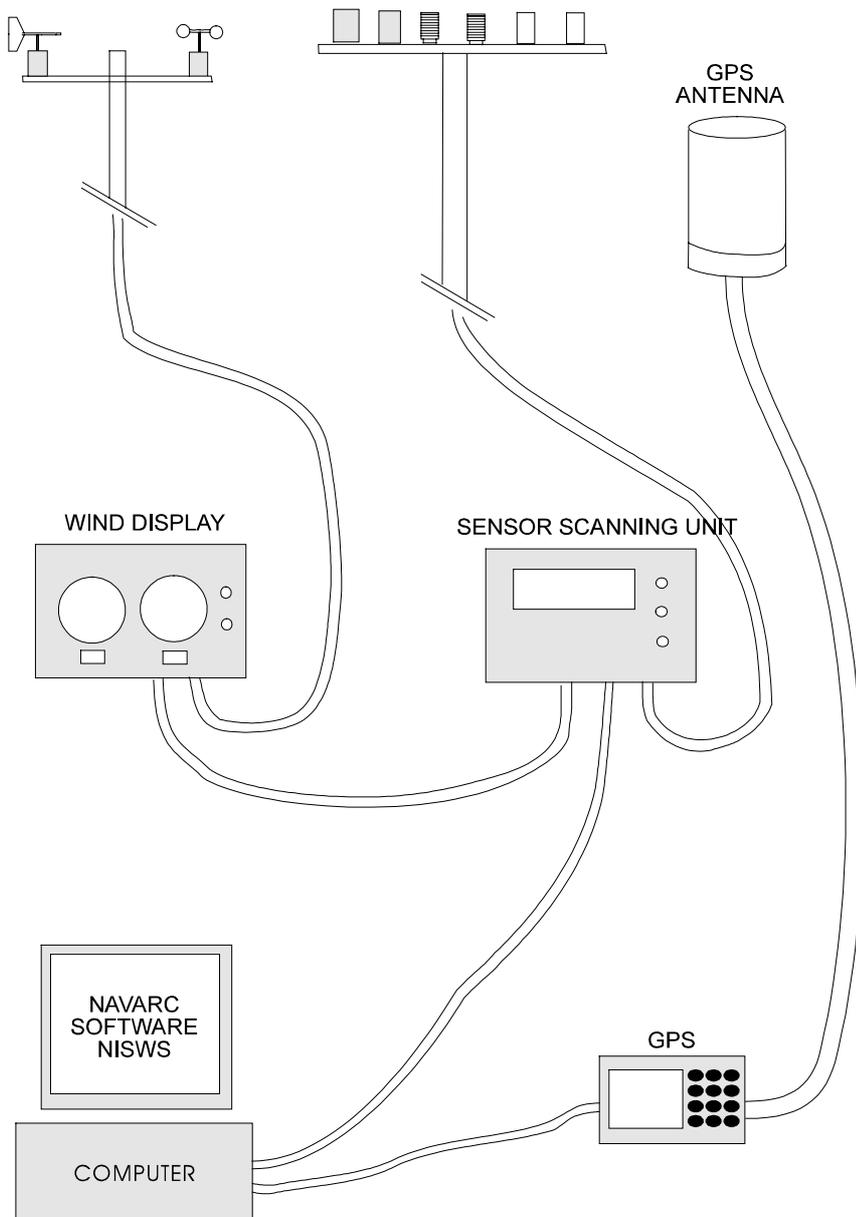
Figure 2.1./4 Installation meteorological station on R/V Tanganyika Explorer.

During expeditions 14 and 16 **sedimentation measurements** were conducted. The sampling was done near the main river mouths. Two different samplers were used: a LIMNOS sediment corer and sedimentation traps.

The surface sediment samples were taken during expedition 14 with LIMNOS sediment corer. A total 8 sediment samples were cored. The sampling sites were in the Malagarasi, Kalambo and Lufubu river mouths. The water depth at the sampling sites varied from 20 to 60 m.

Sedimentation traps were used during expedition 16 for sedimentation flux measurements. The traps were made of plexi glass (Fig. 2.1./5). The diameter of a sampler is 5 cm and the height 50 cm. The

traps were placed 1 m above the bottom. At each site 6 traps were deployed. The traps were collecting material over a period, which varied from 43 to 48 hours. The water from each tube was decanted to half volume, mixed and preserved in one litre bottles. In the laboratory the six samples from each site were put together and total mass analysed. The samples were analysed in the laboratory of Regional Environmental Agency of Häme, Tampere in Finland.
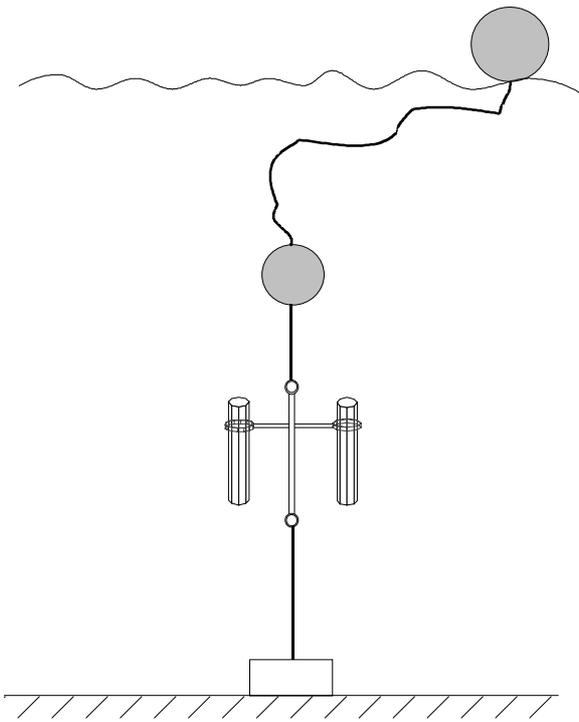
Figure 2.1./5 Sedimentation trap and its installation in the lake.

2.2. Expeditions

Three main **expeditions on *R/V TANGANYIKA EXPLORER*** were conducted during the IAA. They were expeditions number 10, 14 and 16 of the vessel. These numbers have been used to refer to each expedition in the present report. Expedition and sampling characteristics for each expedition are presented in Table 2.2./1

Table 2.2./1 Expedition characteristics: sampling dates, recorded ship ADCP transects, buoy ADCP deployments, number of CTD profiles, usage of ship meteo station and number of sediment samples taken.

EXPEDITION	DATE	DATA COLLECTION/SAMPLING				
		ADCP TRANSECTS (KM)	BUOY ADCP (HRS)	NO. OF CTD PROF.	MET. STATION (HRS)	NO. OF SEDIMENT SAMPLES
10	16 - 27.11.1996	590	59	20	175	-
14	08 - 16.04.1997	650	59	72	124	8
16	24.08 - 04.09.1997	720	115	100	203	6

The **objectives** of the expeditions were to collect data on meteorology, hydrodynamics and sedimentation of the lake during different seasons. The data were used for to improve the knowledge of the lake hydrodynamics and for validation of numerical models i.e. the LTR flow and upwelling model and regional sediment transport models.

There were **severe logistic problems** due to delayed shipments and needed replacements of the instruments. The laborious installation of the ADCP and unstable voltage on board caused additional problems. Furthermore, political unrest in the region hampered the execution of the expeditions. Finally a test expedition of the hull mounted ADCP was conducted in the southern part of the lake in June 1996. This was the first time such an ADCP was deployed in such a deep fresh water body as Lake Tanganyika and in a tropical environment.

The first data collection, **expedition 10**, took place in **November 1996 during the wet season.** The expedition was focused on the southern part of the lake, the important upwelling region, and the main river estuaries to scope **the study to the dispersion of sediment transport of the inflowing rivers**. During the expedition the moored ADCP's were used for the first time to collect data about temporal variation of currents at one place.

The second expedition 14 was conducted **at the end of the wet season in April 1997**. The following **expedition 16** took place **in the late dry season in August - September 1997** and was the widest of all as the northern part of the lake could be covered for the first time. The expedition was the most successful one not only in terms of the amount of collected data but also in terms of quality. A major drawback for the study was that both the lake buoy stations were found lost. The one off Mpulungu was hit by lightning and most probably sunk in early 1997 and the other off Kigoma was stolen or sabotaged. It was discovered to be missing in February 1997 by the LTR/Kigoma personnel. Both stations, off Kigoma and Mpulungu were operational 3 and 4 years, respectively and their loss left a huge gap for data collection and lake monitoring in the future.

Expedition 10 started in Kigoma 16.11.1996. All three ADCP's were tested in the Kibwesa area, south of Kungwe mountains for 3 hours (Fig 2.2./1.). Both buoy ADCP's were placed in deep

waters, 112 and 128 m. Water currents were recorded on five transects, water temperature and conductivity at two CTD stations. Additional measurements were conducted in the Utinta area. Intensive current measurements were conducted in the southern part of the lake with the ship ADCP and CTD as well as with the buoy ADCP's. Outside the main river outlets, namely the Lufubu and Malagarasi rivers, the buoy ADCP's were also deployed (Appendix 5). In the Lufubu area buoy ADCP's were set up for 11 hours at 50 and 177 m depths on 18 - 19.11.1996. Simultaneously with the buoy ADCP measurements, eight ADCP transects were covered to measure currents. Four CTD measurements were also conducted. In the Malagarasi delta buoy ADCP's were deployed between 25. - 27.11.1996 for 40 hours at 47 and 125 m deep sites. Simultaneously with the buoy ADCP measurements 47 ADCP transects of water currents and 6 CTD profiles were measured. The vessel returned to Kigoma 27.11.1996 wherein the expedition ended. A total of 108 transects of water currents and 20 CTD profiles of water temperature, conductivity were measured during the expedition (Appendix 6 and 7). The vessel's meteorological station recorded information about meteorological parameters such as wind speed and direction, air temperature, relative humidity, solar radiation and rainfall, although some minor gaps could not be avoided.

Winds around the lake at the stations during the November expedition varied between the regions (Fig 2.2./2). A 24-hour wind pattern was clear in Bujumbura. Average wind speed was slow during the night and in the morning. Prevailing direction was NE. Around noon average wind speed increased and shifted to blow S - SE. The strong S - SE winds lasted a few hours. At the time winds were strongest in the afternoon as highest hourly means were 10 - 12 ms^{-1}. This pattern indicates that winds in Bujumbura, in the northern part of the lake, were thermal in origin. The daily wind pattern off Kigoma and Mpulungu was not as clear as at the land stations, although average wind speed varied from less than 1 ms^{-1} to 10 ms^{-1}. Off Kigoma the highest averages were 8 ms^{-1} during the expedition. At Mpulungu a similar 24-hour periodicity in wind speed and direction as in Bujumbura was observed. Average speed was less than in Bujumbura and the highest speeds of a day were recorded around noon or early afternoon. This is typical for thermal winds in the area. Prevailing wind direction gave evidence for thermality as well.

Expedition 14 was conducted 8. - 16.4.1997. Only the Tanzanian, Zambian and Zairian waters south of Kigoma to Mpulungu could be covered as the political unrest continued in the northern part of the lake. A total of 72 CTD profiles were taken and 70 transects were sailed to measure the currents (Fig. 2.2./3 and Appendix 8 and 9).

This expedition started with intensive measurements outside the Malagarasi River estuary 08 - 10.04.1997. Buoy ADCP's were deployed at two stations at 38 and 127 m deep sites (Appendix 5). Simultaneously 10 CTD profiles were taken and 26 ADCP transects to measure currents were covered. The expedition continued in the Kungwe region to estimate the water exchange in the main strait of the lake. In the Moba region 9 transects of water currents were measured and a total of 10 CTD profiles of water temperature and conductivity were taken. In the southern part of the lake intensive recordings outside the Lufubu and Kalambo River outlets were undertaken with all three ADCP's to measure water currents and CTD to gather information about vertical stratification of water. In general, the southern part of the lake was the area of intensive measurements. A total of 22 CTDs profiles were collected and 210 km of ADCP transects were sailed in the area. Vessel's meteorological station collected information for circa 40 hours.

Figure 2.2/1 Schematic map of the transects and CTD profiles measured during the expedition 10
(15. - 27.11.96) on R/V TANGANYIKA EXPLORER. Data from the areas surrounded with boxes are
discussed in results.

24

Figure 2.2./2 Hourly means of wind speed and wind components at the LTR stations during expedition 10.

Figure 2.2./3 Schematic map of the transects and CTD profiles measured during the expedition 14 (8. - 16.4.97) on R/V TANGANYIKA EXPLORER. Data from the areas surrounded with boxes are discussed in results.

Sediment samples were cored in the Kalambo, Malagarasi and Lufubu River estuaries. A LIMNOS corer was used for sampling. The cores were sliced into 1 cm slices. Samples were stored and taken to Finland for grain size analysis. These analysis were done with a SediGraph analyser at the Finnish Environment Institute's laboratory in Helsinki.

During the April expedition the same daily wind pattern was recorded in the north as in November (Fig. 2.2./4). The highest average wind speed during the expedition in Bujumbura was > 12ms^{-1}. Similar to November wind shifted from the N - NE to the S - SE around noon. At Kigoma wind station, on shore, a clear 24-hour pattern could be seen. Highest speeds were recorded around early or late afternoon. Wind shifted simultaneously from land to lake wind i.e. from the E to the W - SW. A strong lake wind at Kigoma in the afternoon is very typical for the region. At Mpulungu average wind speed was slow. Highest averages were only 6 ms^{-1} and a diurnal pattern as in the north and at Kigoma could not been defined.

ADCP transects and CTD measurements during **expedition 16** can be seen in Figure 2.2./5. The expedition started from Kigoma on 21.8. The northern part of the lake was covered in 21.8. - 23.8 and the southern part 24.8. - 4.9.97. During the expedition 117 transects (720 km) and 100 CTD profiles were collected (Appendix 10 and 11).

Moored ADCP's were deployed outside three main inflowing rivers, Rusizi, Malagarasi and Lufubu (Appendix 5). In the Rusizi delta moored ADCP's were placed at sites 46 and 108 m deep on 21.8. and they recorded continuously for 22 hours. Nine ADCP transects and nine CTD profiles were measured in the same area 21.8. Outside the Malagarasi River, buoy ADCP measurements were conducted 25.8. - 27.8. (43 hours) at 35 and 124 m deep sites simultaneously with 23 transect lines and 26 CTD measurements. Buoy ADCP's measured currents continuously 48 hours outside Lufubu in 30.8. - 1.9., but no intensive ADCP or CTD measurements were done in that area.

Sedimentation traps were deployed near Malagarasi and Lufubu rivers to collect sedimenting material at the depths of 16 to 23 and 20 to 22 meters. The time of deployment in the Malagarasi was 43 and in the Lufubu estuary 48 hours. Samples were stored and taken to Finland for analysis.

During the last expedition in August - September 1997 wind data from two recorders were available (Fig. 2.2./6). Winds at Bujumbura seemed to follow the same 24-hour pattern; strong average winds 8 ms^{-1} blew in the afternoon S - SE and ceased for the night till noon. At Mpulungu stronger average winds than during the previous expeditions were observed. A clear daily pattern could be observed as well. This indicated the start of the dry season, but also gave more clear evidence for thermal winds in the region. The prevailing direction was during the night S - SE and during the day N - NW, just the opposite compared to the Bujumbura area.
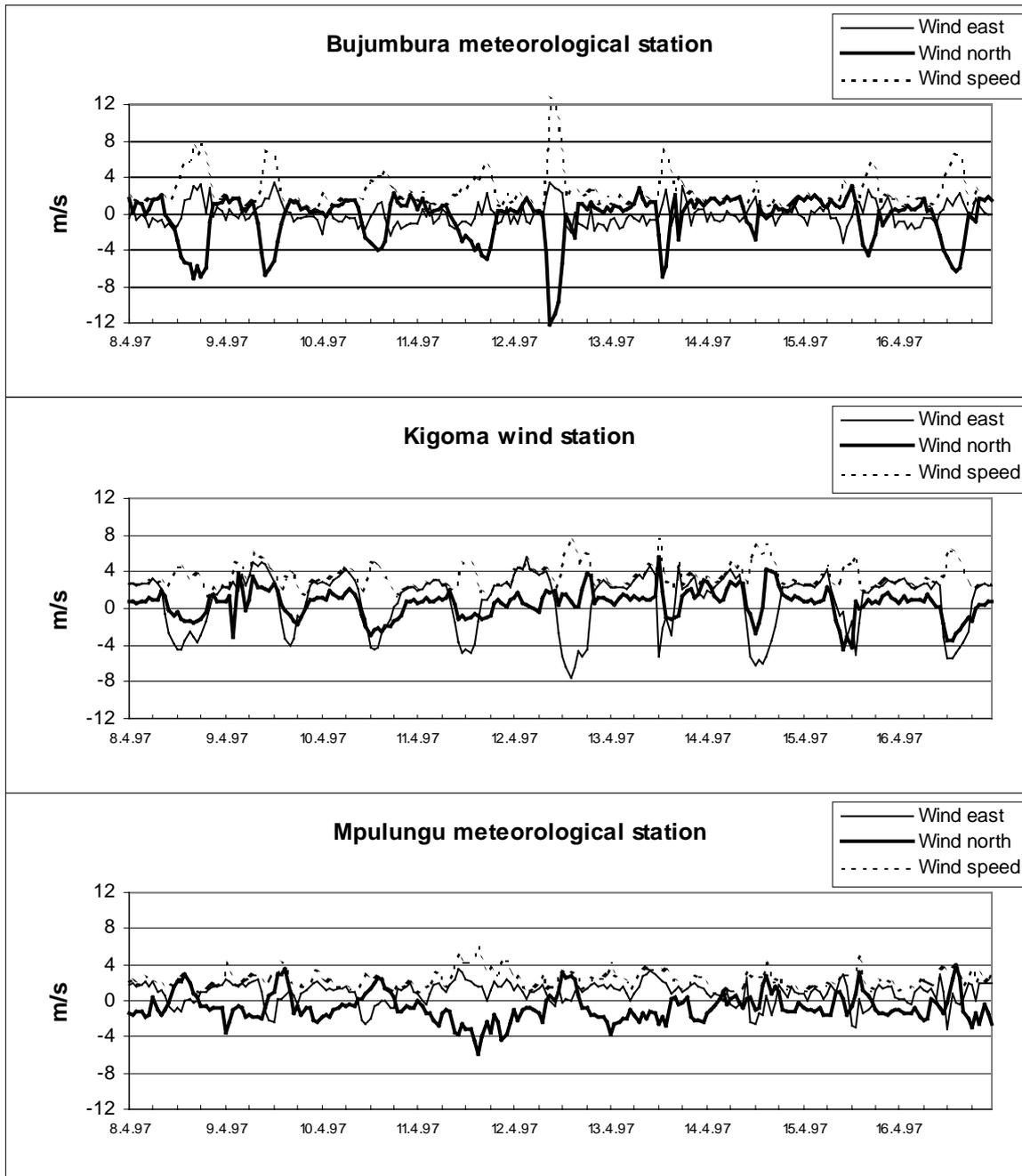
Figure 2.2./4 Hourly means of wind speed and wind components at LTR stations during expedition 14.
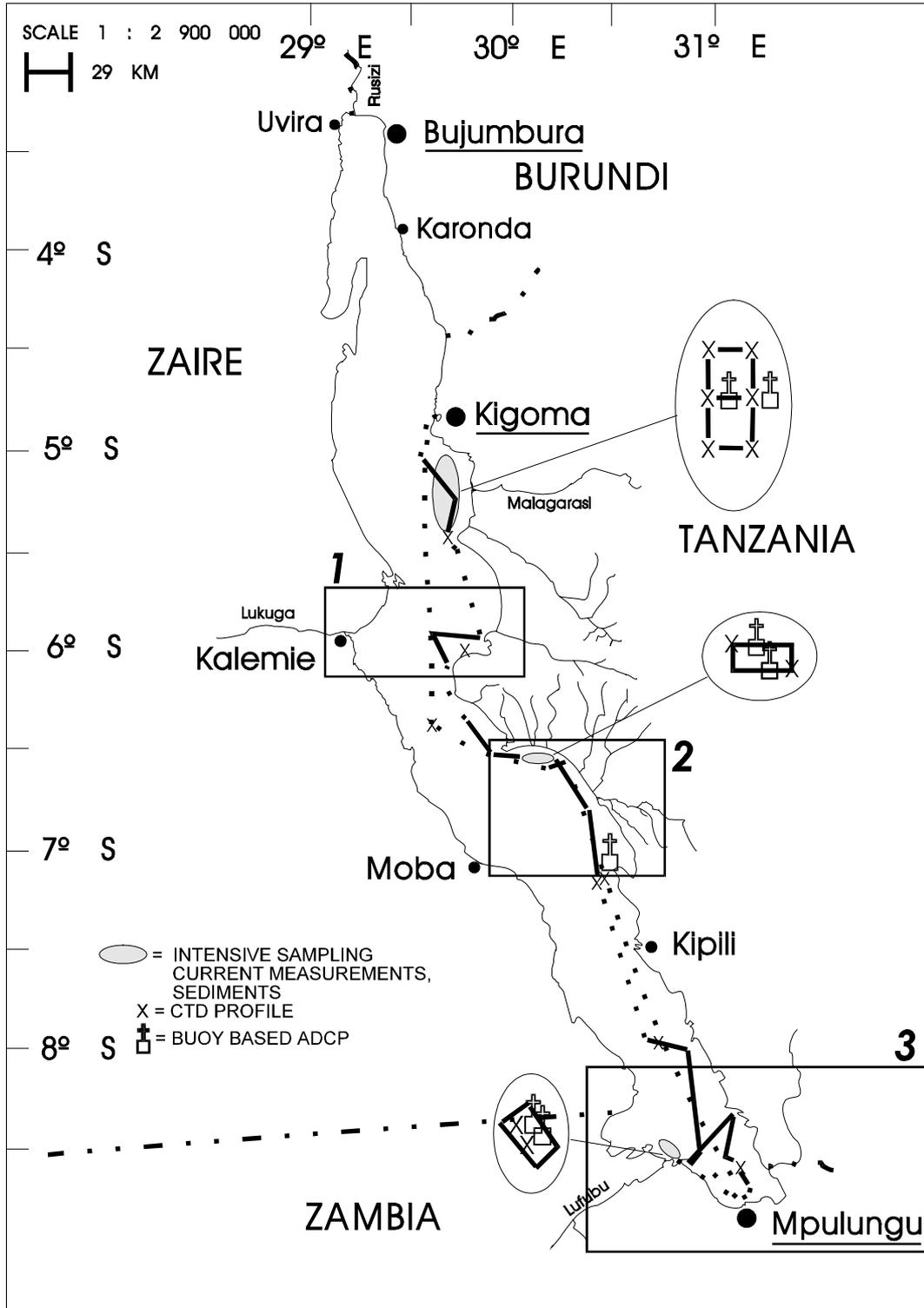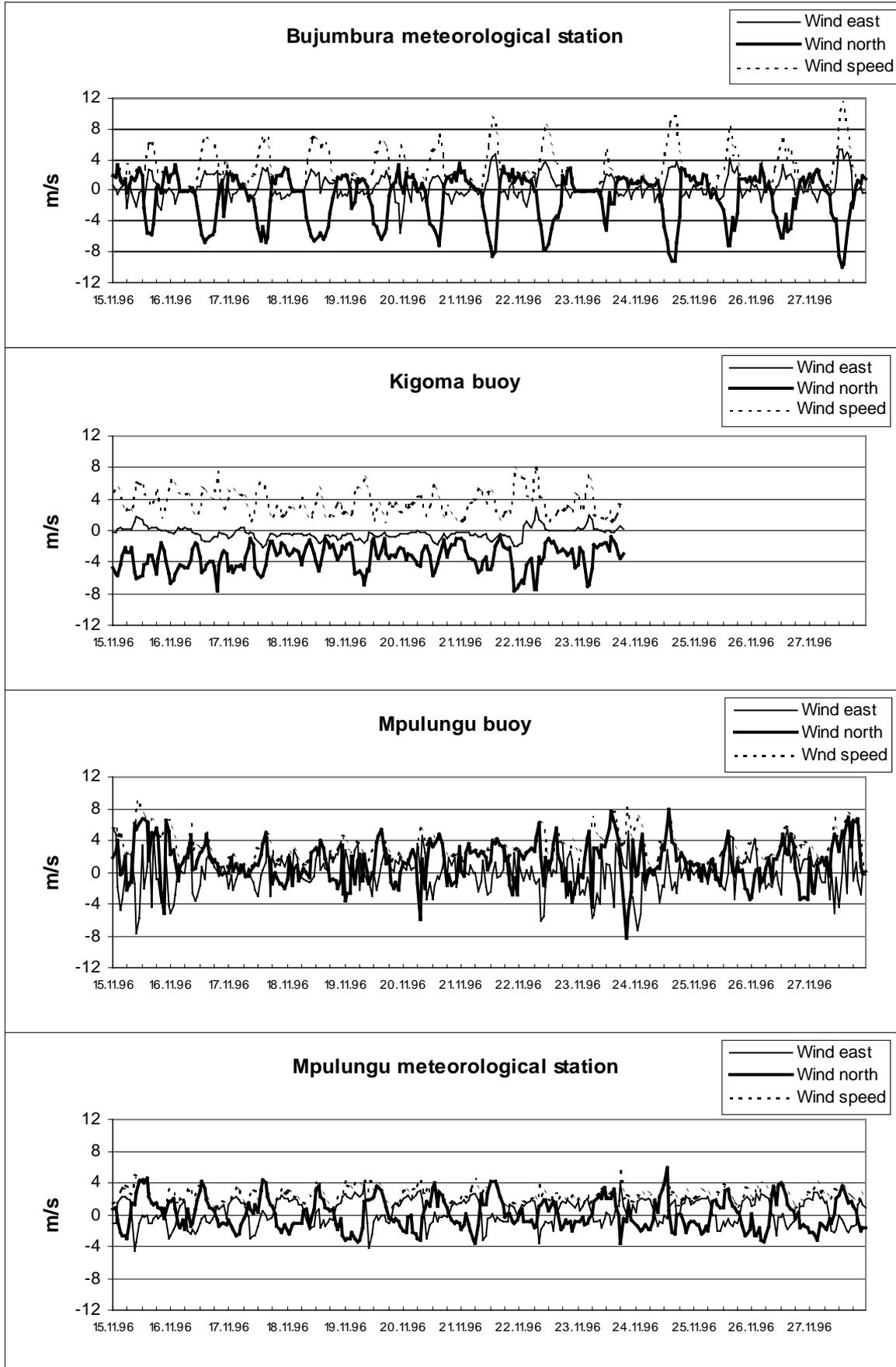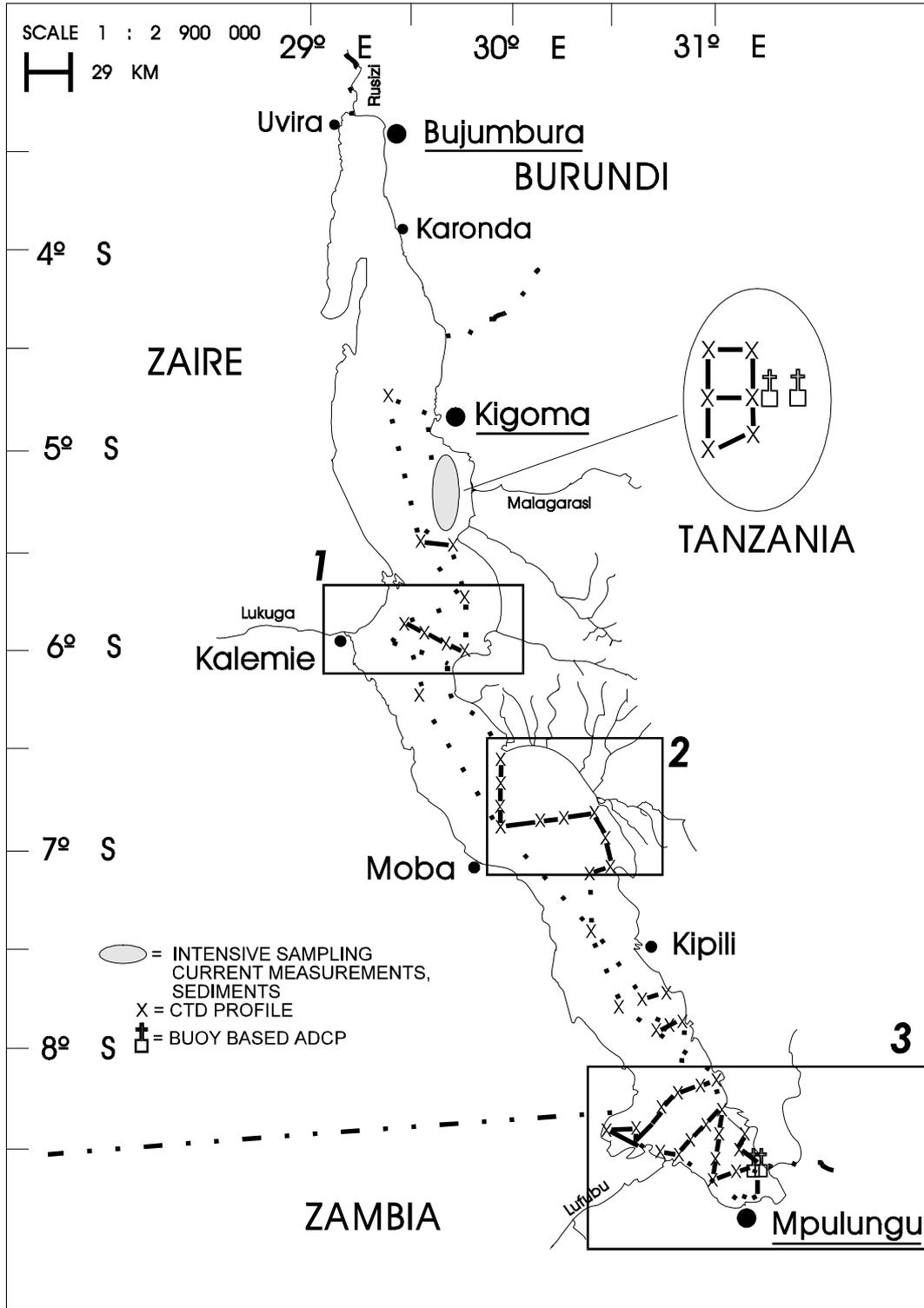
28
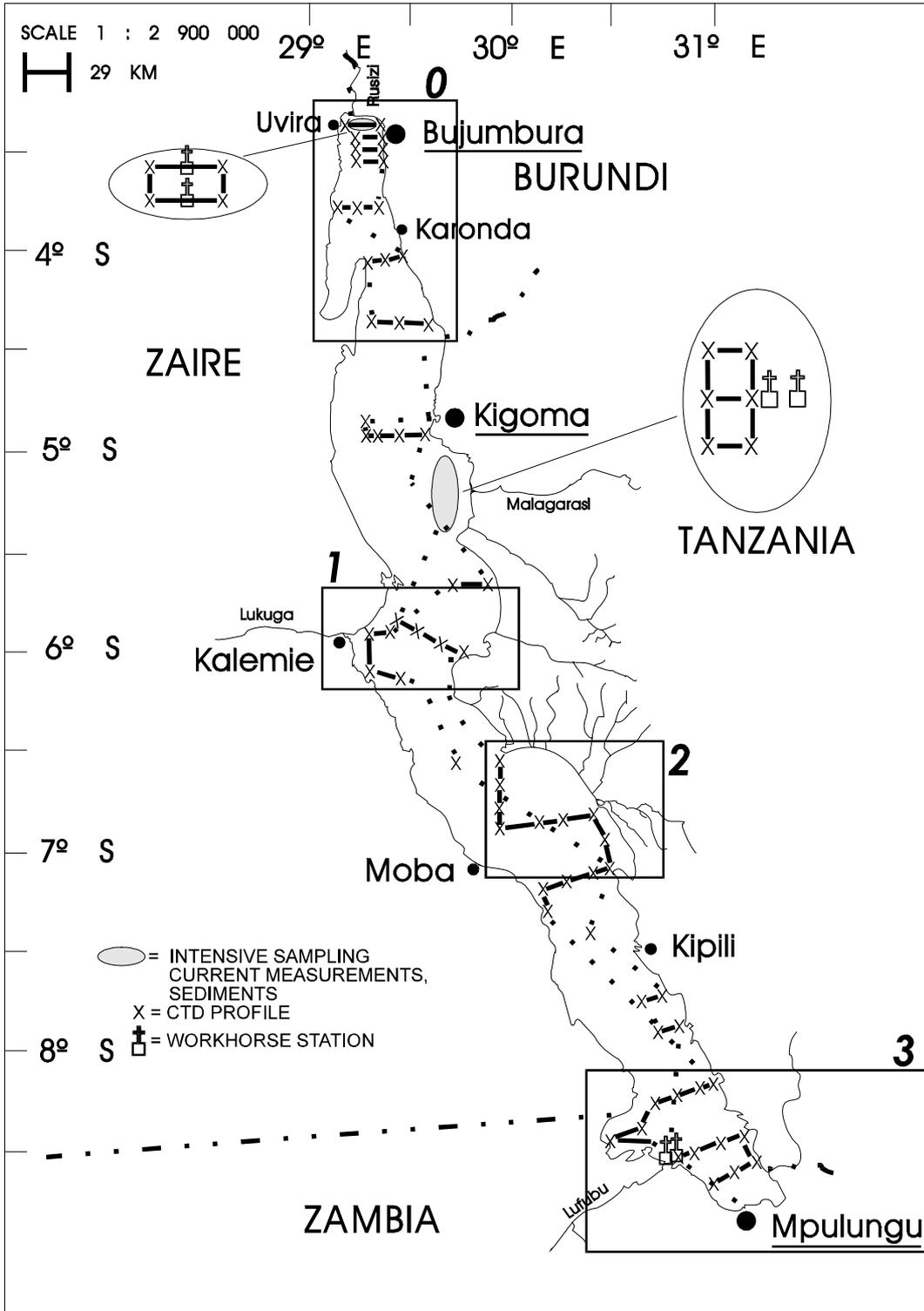
Figure 2.2./5 Schematic map of the transects and CTD profiles measured during the expedition 16 (21.8. - 4.9.97) on R/V TANGANYIKA EXPLORER. Data from the areas surrounded with boxes are discussed in results.
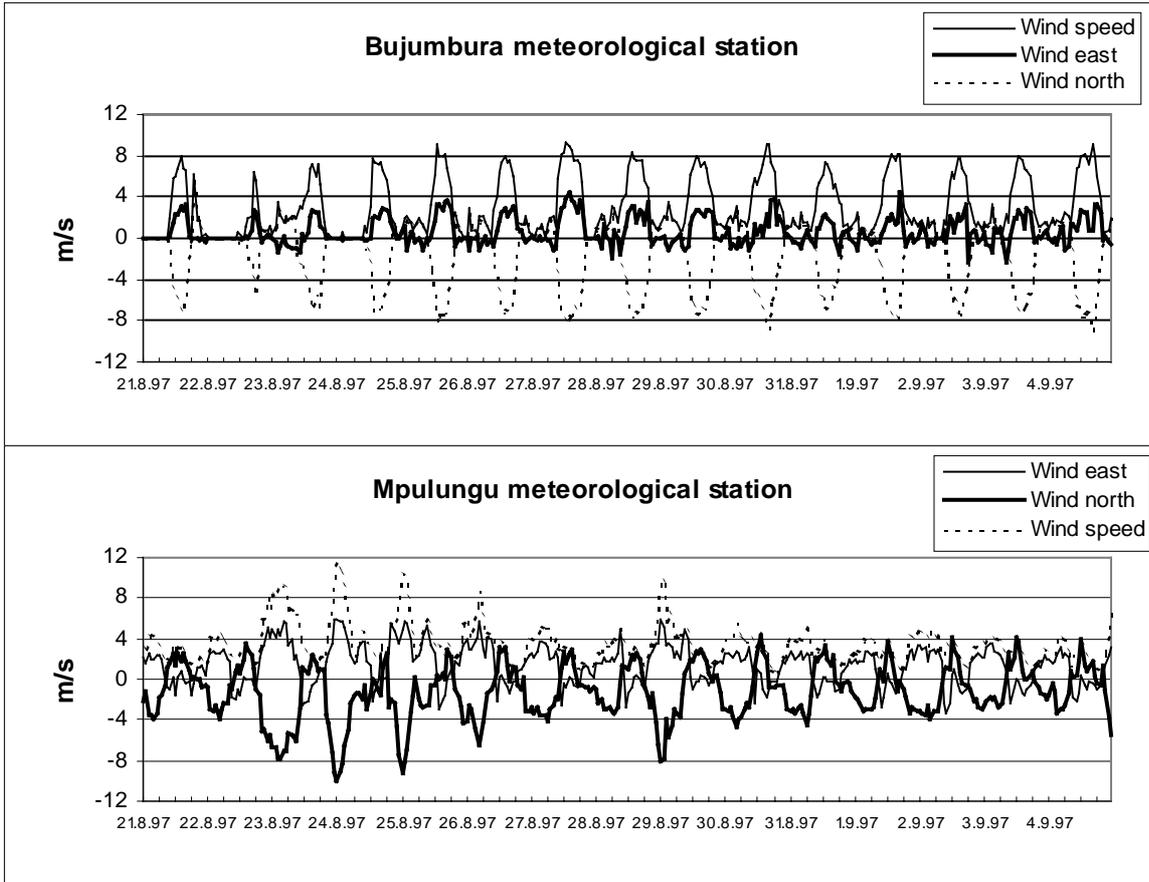
Figure 2.2./6 Hourly means of wind speed and wind components at LTR stations during expedition 16.

2.3 Statistical analysis

Automatic recorders used in LTR have a memory unit where recorded data are stored. The memories have a limited capacity which depends on present recording intervals and the number of recorded variables. Therefore, the capacity of a memory varies from 1 to 9 months. Recording intervals and the memory capacity of each station are presented in Table 2.3./1. Recorders need frequent inspection and maintenance so, in practice, their full capacity is seldom used.

The meteorological stations on land and lake stations were unloaded using Aanderaa Instruments P3059 software and water level recorders with Telog Inc. software. CTD-probe and ADCP's are unloaded using their own software. The procedures are given by Huttula, Peltonen, Nieminen (1993) and Kotilainen (1994). Further data processing has mainly been done using EXCEL.

Table 2.3./1. Automatic recording stations of LTR, their recording intervals, number of channels and memory capacity.

STATION	Recording interval	Number of channels	Capacity of the memory
Weather station at Bujumbura	10 min	12	37 days
Wind station at Kigoma	10 min	3	150 days
Wind station at Mpulungu	10 min	3	150 days
Lake buoy station off Kigoma	30 min	16	85 days
Lake buoy station off Mpulungu	60 min	16	170 days
Water level stations	60 min	1	270 days

The **meteorological data** was processed as 60 min, daily, weekly and monthly means (solar radiation, air temperature, wind speed and gust, air pressure, humidity) and fluxes (precipitation). Wind directions have been divided into 16 main directions and percentages calculated for each direction. In this report the standard meteorological notations for the points of compass are used, e.g. N and NE. Wind was also divided as north/south and east/west components from the raw data and then averaged over a desired time interval. It has to be noted that for wind components denote the coming direction of the wind. The **water temperatures** were averaged over desired time interval.

The **water level observations** have been used in LTR mainly to provide data about surface tilting and seiche oscillations. This data have been used also for water balance estimations. For this the absolute value of water level above M.S.L. was corrected on the basis of staff gauge observations from Kigoma organised by the Tanzanian Railways hydrological service. Results of different stations were compiled to compare changes in water level between stations. Because of the relatively narrow range of the pressure sensor, from 0 to 0.7 m, and the highly varying water level between the dry and the wet season, the sensors had to be lowered or lifted several times during the recording period.

The software within Navarc Integrated **Ship Weather System** (NISWS) recorded meteorological variables, position and velocity of vessel and also date and time. The meteorological variables were: wind speed, gust and direction, air temperature, humidity, solar radiation, sun shine duration, and precipitation. The recording interval was normally 10 minutes.

The **CTD** was programmed and unloaded with AML software by the instrument manufacturer. A typical depth resolution in the measurements was 0.1 m. The data were exported to EXCEL, where values for temperature, oxygen and conductivity were interpolated linearly for each half meter depth. After this data were imported to a GIS software Echobase This program enables the visualisation, and analysis of both the CTD and ship meteorological station and synthesises the results of the data in space and time. For CTD data the calculation of the temperature isolines was done with SURFER-software and then they were plotted with Echobase. For ship meteorological data interpolation was done directly with inverse distance square method within the Echobase. The wind data from the ship were classified to two periods: one for afternoon-evening (12:00 - 20:00) and the other for the night and morning (20:00 - 12:00).

The data from the vessel mounted **ADCP** were analysed by using software called Transect by RD Instruments. The recording interval was set according to the thickness of water layers, usually so that the standard deviation of current velocity was around 1 cms^{-1}. The raw data was averaged from 60 s to 600 s according to the length of the transect. From these averaged values shiptrack figures were drawn. They show in the horizontal plane the track of the ship and the current from a desired depth. Another graphical output was a vertical current projection figure, showing current speed as projected to the chosen direction from the north. The echo intensity output was also used. See Appendix 10 for explanation of transect outputs.

ADCP data from buoy based instruments was analysed using WATCH and BBLIST software by RD Instruments. The recording interval used was 80 s or 120 s. Raw data was averaged to 30 min and time series and profile pictures were produced.

Data from current **measurements by flow cylinders** like current speeds and directions, were calculated in EXCEL. All lines were analysed separately, but different depths for each line were pooled together. The speeds and the directions of each line were plotted as scattered graphs to give a general view.

Each sample taken with the **LIMNOS sediment corer** was sliced and a slice of first 1 cm was taken as a sample for grain size analysis. The analysis was conducted at the Finnish Environment Institute in Helsinki, Finland. The used analyser was SediGraph 500. The sample was analysed as a wet sample. The organic content was first determined as ignition loss (800 °C). If the ignition loss was higher than 2 %, the humic compounds were removed by H_2O_2 treatment. The analysis with SediGraph was done twice for error determination. The soil texture was determined from the grain size according to Finnish geotechnical classification. In the laboratory the total solids of the trap samples was determined as dry weight (105 $^{\circ}$C, for 72 hours). From this the flux was calculated over unit area and time.

2.4 Results

2.4.1. Meteorology and lake water temperature

The **solar radiation** was higher in the south than in the northern part of the lake (Fig. 2.4.1/1). It was in 1996 on average 30 Wm^{-2} higher at Mpulungu than at Bujumbura. After the dry season in October and November 1996 this difference was the highest.
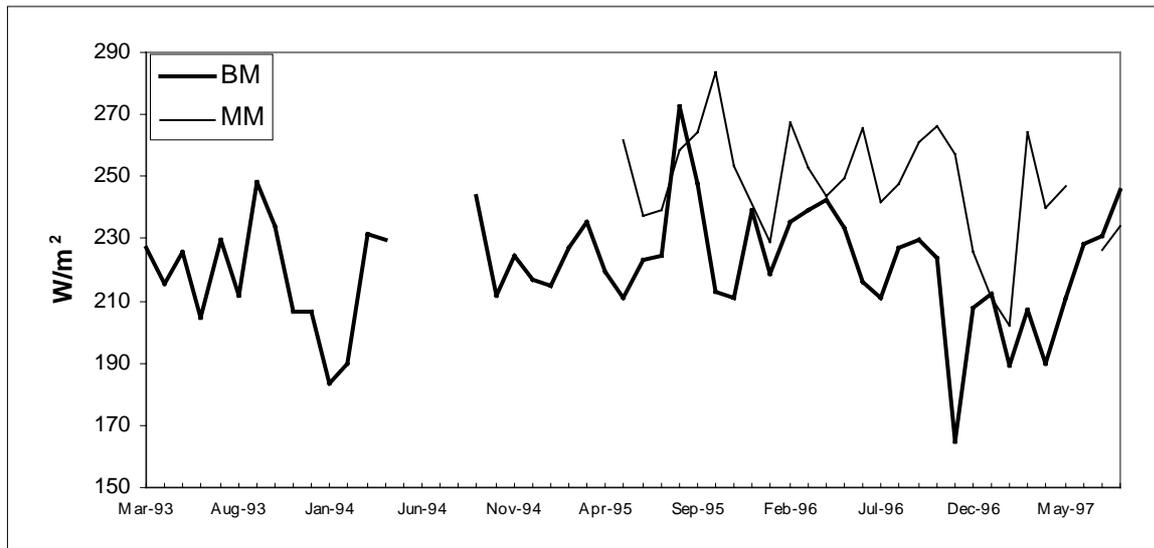
Figure 2.4.1./1 One month averages of solar radiation (Wm^{-2}) at the Bujumbura (BM) and Mpulungu (MM) weather stations.

The seasonal mean values of solar radiation at Mpulungu were almost the same in the dry (251 Wm^{-2}) and wet seasons (254 Wm^{-2}) (Verburg 1997). In the northern part of the lake, at Bujumbura, the solar radiation was higher during the dry seasons (229 Wm^{-2}) than in the wet seasons (218 Wm^{-2}).

In seasonal cycle in 1996 the **air temperature** monthly means were highest in March - May and September - November at all stations. The lowest mean value was reached in July at all stations (Fig. 2.4.1./2). The annual maxima were generally reached in October.

On average, air temperature was highest in the Mpulungu region (either at the buoy or at Mpulungu) and lowest at Bujumbura. During the dry season (June - August) the average air temperature was higher at the Kigoma buoy than in the Mpulungu region. Seasonal variation in the south was high compared to the Kigoma and Bujumbura regions.

When comparing average **air temperatures on land and on the lake** in the Mpulungu region, one can see that only in August - October the air temperature on land was higher (0.2 °C) than at the lake buoy. The average lake surface water temperature was usually higher than the air temperature.
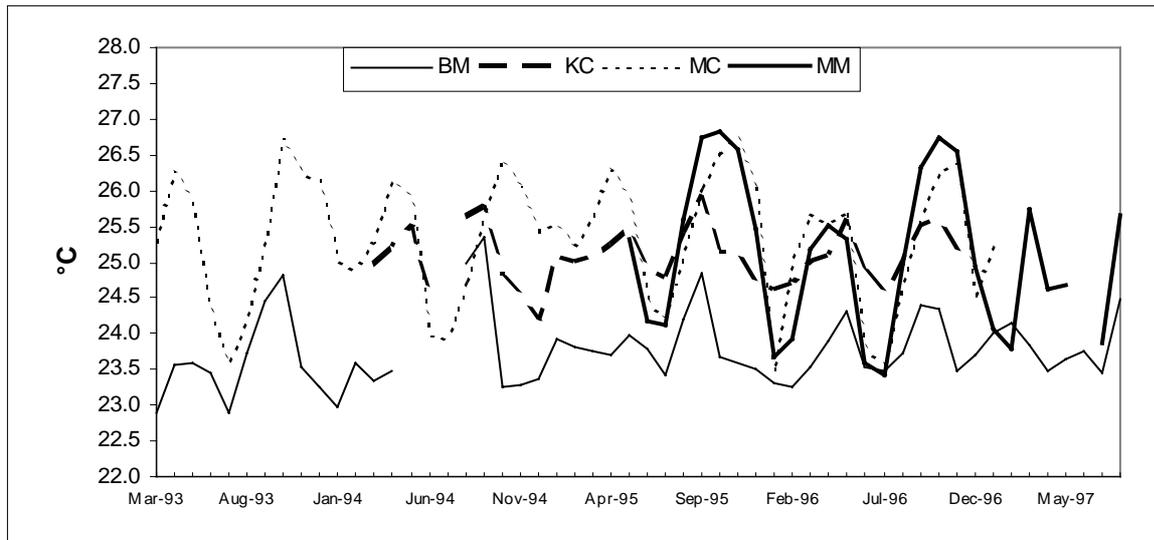
Figure 2.4.1./2 Monthly mean air temperature at Bujumbura (BM) and Mpulungu (MM), and offshore near Kigoma (KC) and Mpulungu (MC).

The annual means for May 1995 - April 1996 and minima and maxima of mean monthly air temperature are shown in Table 2.4.1./1.

Table 2.4.1./1. Annual mean (for May 95 - Apr 96), minimum and maximum values of mean monthly air temperature (^{o}C) Bujumbura (4 m height) and Mpulungu, and off Kigoma and Mpulungu.

	Bujumbura	Kigoma buoy	Mpulungu buoy	Mpulungu
minimum	23.1	24.2	23.6	24.4
maximum	25.5	25.9	26.8	26.8
mean	24.0	25.1	25.5	25.3

In 1996 the air temperature in July at Mpulungu weather station and at the Mpulungu buoy was lower than in 1993 - 1995. Air temperature in January - March 1997 at Bujumbura was higher than in 1996.

The **monthly mean wind speed** was highest in the dry season at all stations (Fig. 2.4.1./3). The highest mean wind speed occurred at Bujumbura in August - September, and in June - August at the other stations. The monthly mean wind speed was usually lowest in January. The values of mean wind speed of each station during 1993 - 96 are shown in Table 2.4.1./2. It was lowest at the Bujumbura weather station at the height of 4 m. At the Mpulungu buoy the wind speeds showed the greatest seasonal variation and were the highest of all stations.

The monthly mean **wind gust** was highest in the wet seasons, at all stations except the Mpulungu weather station. The highest monthly means were 17 to 20 ms^{-1}. At the Mpulungu weather station, the highest average wind gust was 15 ms^{-1}. During the dry season the means were between 13 and 17 ms^{-1}. The highest wind gust was measured in October to December 1995 at the Mpulungu buoy (31 ms^{-1}), the Kigoma buoy (30 ms^{-1}) and the Bujumbura weather station (29 ms^{-1}). At the Mpulungu land weather station the wind gust was highest in January 1996 (19 ms^{-1}).

Figure 2.4.1./3 Mean monthly wind speed for Bujumbura, Kigoma, and Mpulungu meteorological stations (the latter two both on land and offshore) in 1993 - 97.

Table 2.4.1./2. Mean annual wind speeds (ms^{-1}) and the highest daily mean wind speeds at Bujumbura, Kigoma, Mpulungu and at the Kigoma and Mpulungu buoys, in order of increasing annual mean wind speeds. Period 1993 -96.

	Mean wind speed	Maximum daily mean
Bujumbura weather station, 4 m height	2.2	4.1
Mpulungu weather station	2.8	6.8
Bujumbura weather station, 13 m height	3.1	5.9
Kigoma buoy	3.5	5.7
Kigoma wind station	3.6	6.8
Mpulungu buoy	3.9	10.6

In Mpulungu region these maximum wind gusts were observed to occur simultaneously with rapid and **significant decreases in air temperature** during the same hour. A very high decrease occurred in November 18, 1995 between 23:00 - 24:00. Its value was 3.8 °C at land station and 7.2 °C at the buoy. After this decrease the air temperature at the buoy was 5.9 °C lower than at the land station at the same time. This was very interesting, especially since in the same month, at 24:00, the air temperature at the buoy was on average 1.4 °C higher than at the land station (Verburg, 1997b). In May 1995 - April 1996 it was at midnight on average 1.8 °C higher at the Mpulungu buoy (Verburg, 1997b).

In the 1996 - 97 research period, the wind speed was highest in June, except at Bujumbura (August) (Fig. 2.4.1./4). It was lowest in February. Wind speed was on average lowest at the Bujumbura and Mpulungu weather stations and highest at the Mpulungu buoy. At the Mpulungu buoy and weather station the wind speeds showed the greatest seasonality. Variance in the daily mean wind speed was highest at the Mpulungu buoy with maximum daily means of *c.* 8 ms^{-1}. Maximum daily means at Bujumbura, the Kigoma buoy and Mpulungu were *c.* 5, 6 and 7 ms^{-1} respectively.

The highest **wind gusts** were measured between January 5 and February 8, 1996 at the Kigoma buoy (23 ms^{-1}), the Bujumbura weather station (21 ms^{-1}), the Mpulungu buoy (20 ms^{-1}), and the Mpulungu weather station (19 ms^{-1}). These maximum wind gusts occurred again simultaneously with relatively large decreases in air temperature during the same hour (between -2.0 °C at the Mpulungu buoy and -6.0 °C at the Bujumbura weather station).

At the Bujumbura and Mpulungu weather stations the **wind direction** distribution was very similar during the whole year (Verburg 1997). The proportion of the south-east winds increased at all stations during the dry season. Winds from the land were more frequent at all stations during the dry season, except at the Kigoma buoy.
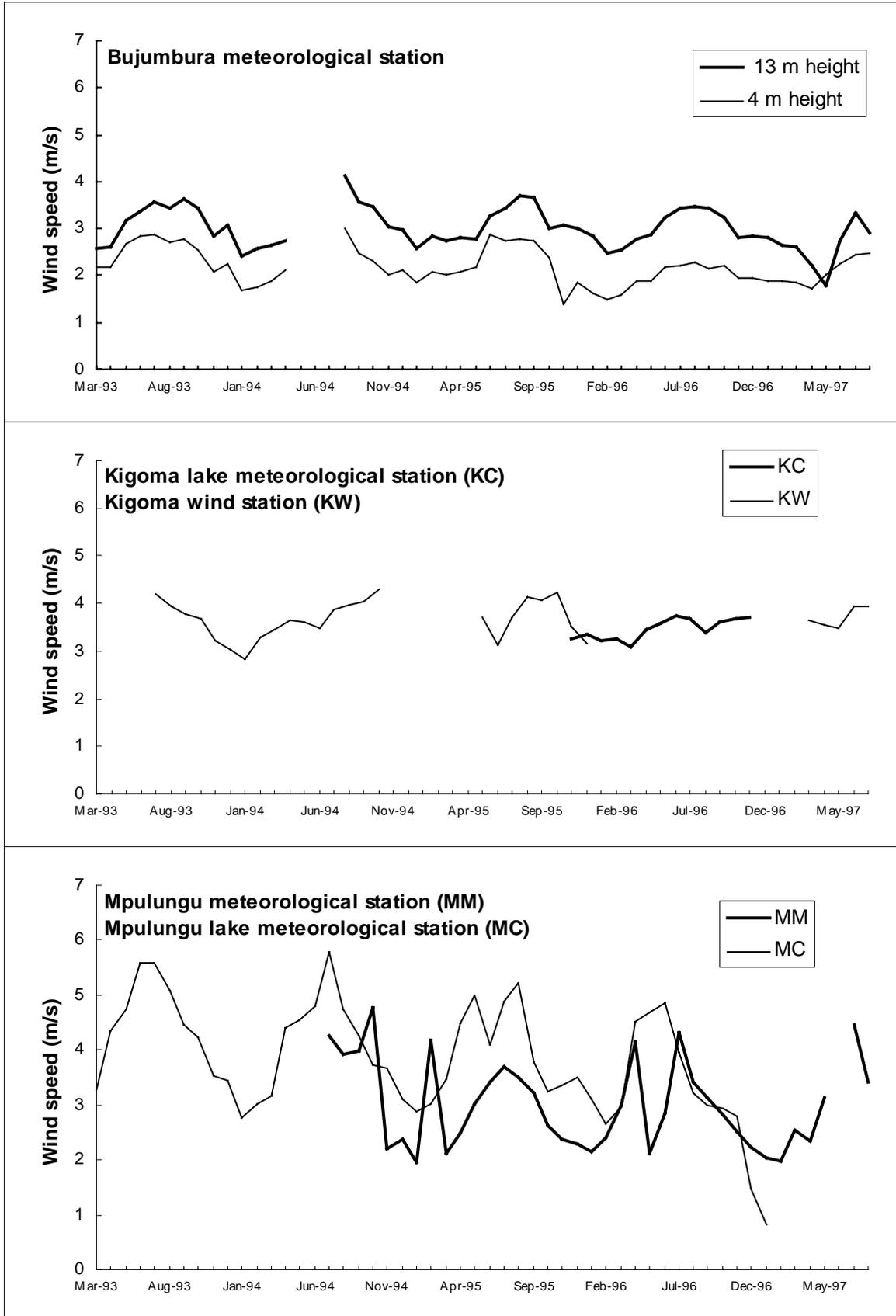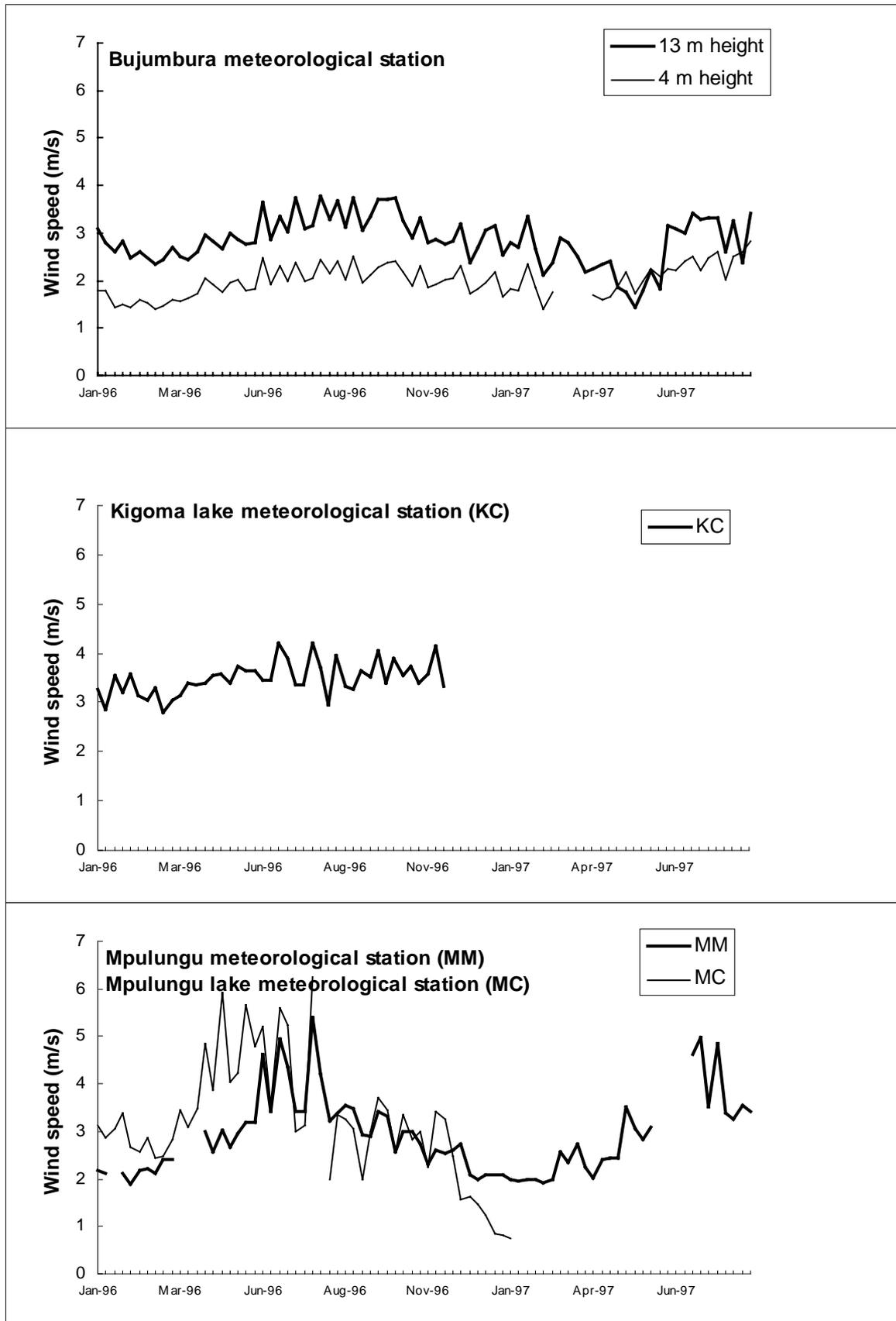
Figure 2.4.1./4 Monthly means of wind speed for Bujumbura, Kigoma, and Mpulungu meteorological stations (the latter two both on land and offshore) in 1996 - 97.

At Bujumbura, the wind direction was primarily from N and there was a slightly smaller S - SE proportion (Fig. 2.4.1./5) the only exception being April 1997 when direction was mainly from NW. At the Kigoma buoy the main wind direction was from S - SE (Fig. 2.4.1./6). In October - November it was mostly from E. At the Mpulungu buoy, the wind came primarily from SE during the dry season (Fig. 2.4.1./7). At the Mpulungu weather station, SE wind was the most common each month (Fig. 2.4.1./8).

The **lake water level** was highest in April - May (maximum of daily measurements was 774.35 m) and lowest in November (Fig. 2.4.1./9a, b). The fall in lake level during the dry season was 0.89 m (between daily means) and the mean lake level was 773.85 m. In Figure 2.4.1./9b the monthly means of lake levels recorded with conventional gauge plates at the Kigoma and Mpulungu harbours are shown. Those at Mpulungu have not been bench marked and the zero reference of the level data was found by comparison with the gauge plates of the Kigoma Department of Hydrology. The data of the conventional gauge plates complied well with the Telog recorder data.

The mean monthly **water temperature** profiles from the buoy stations off Kigoma and Mpulungu are in figs 2.4.1./10 and 2.4.1./11. In Kigoma the vertical stratification was observed during whole year whereas off Mpulungu the profiles from June to August show a very weak vertical stratification. The surface waters in the south heated very rapidly after the dry season. The average surface water temperature increase during August - November 1996 was 0.06 °C d^{-1} .

The upwelling of water below the thermocline can be described with water mass, which has the temperature of 24.50 - 25.00 °C (Fig. 2.4.1./12, 2.4.1./13, and 2.4.1./14). During the wet season this mass lies at the depth of 70 - 80 m. Off Mpulungu this water mass reached the surface and remained there about three months in 1993 from Jun 21 to Sep 22. In 1994 it was impossible to record since May 12. In 1995 the period of this upwelling was shorter than in 1993. It lasted less than two months, Jul 2 - Aug 27 and 1996 it occurred same time as three years before (Jun 20) and lasted two months (Aug 18).

This upwelling has not been observed off Kigoma at all. It is clear there that the upwelling of thermocline waters has happened many times, but there has not been enough wind forcing to bring waters below thermocline to the surface. Off Kigoma the waters, with a temperature from 25.50 - 26.00 °C lie in the upper part of thermocline during the wet season. The depth of this layer varies from 30 - 60 m. This water was observed for the first time on the lake surface in the middle September 1994. Obviously it was brought there already in July. It was brought to the surface twice more during the months of November and December 1994 and again to a large extent in Aug 1995 for more than a month. In 1996 this phenomena was observed for the longest duration from early July to the middle of September. It is interesting to note that the water with same temperature was observed on surface also off Mpulungu during the last half of September 1996.
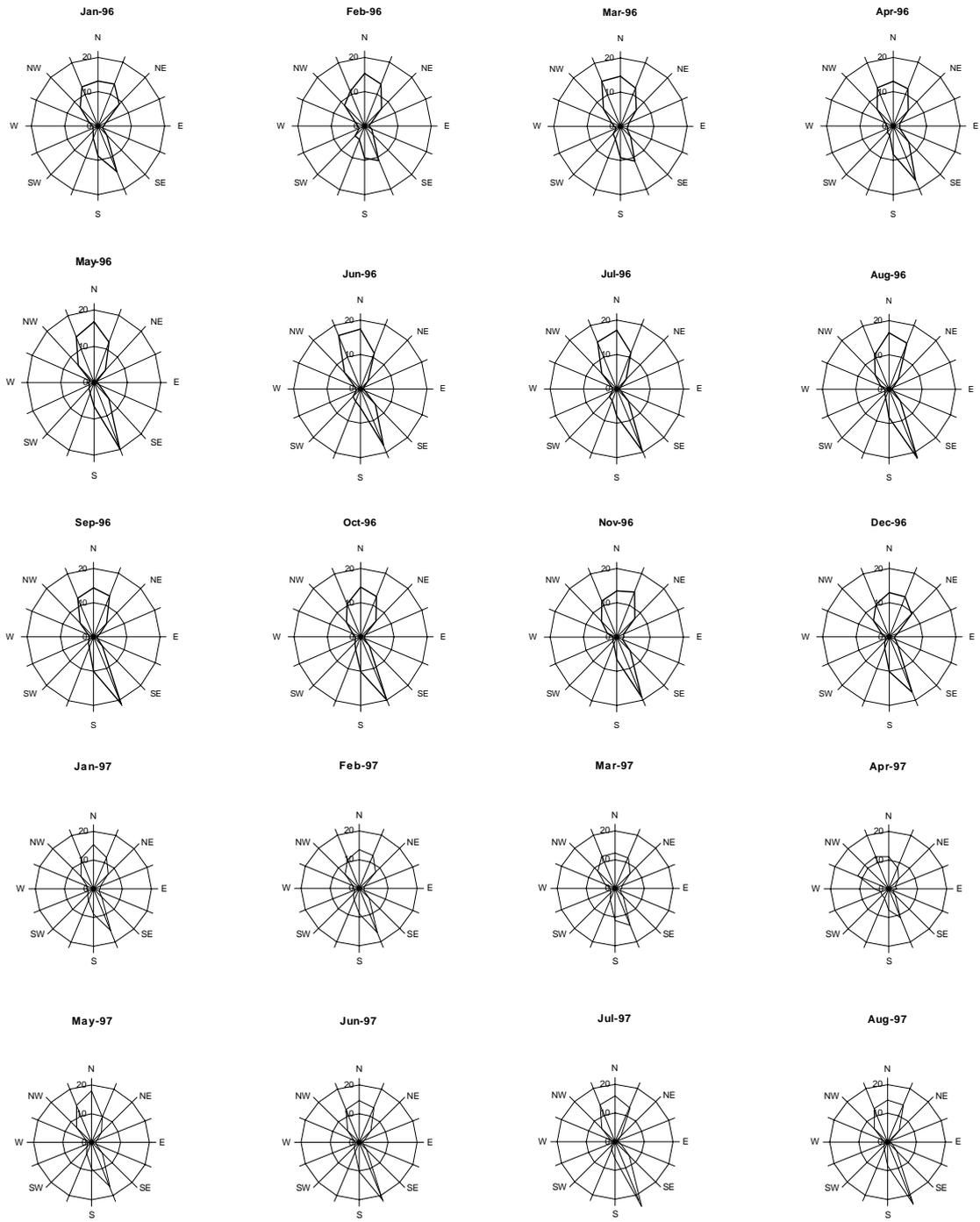
Figure 2.4.1/5 Wind direction distributions (%) on a monthly basis, at Bujumbura weather station.

Jan-96

Feb-96

Mar-96

Apr-96

May-96

Jun-96

Jul-96

Aug-96

Sep-96

Oct-96

Nov-96
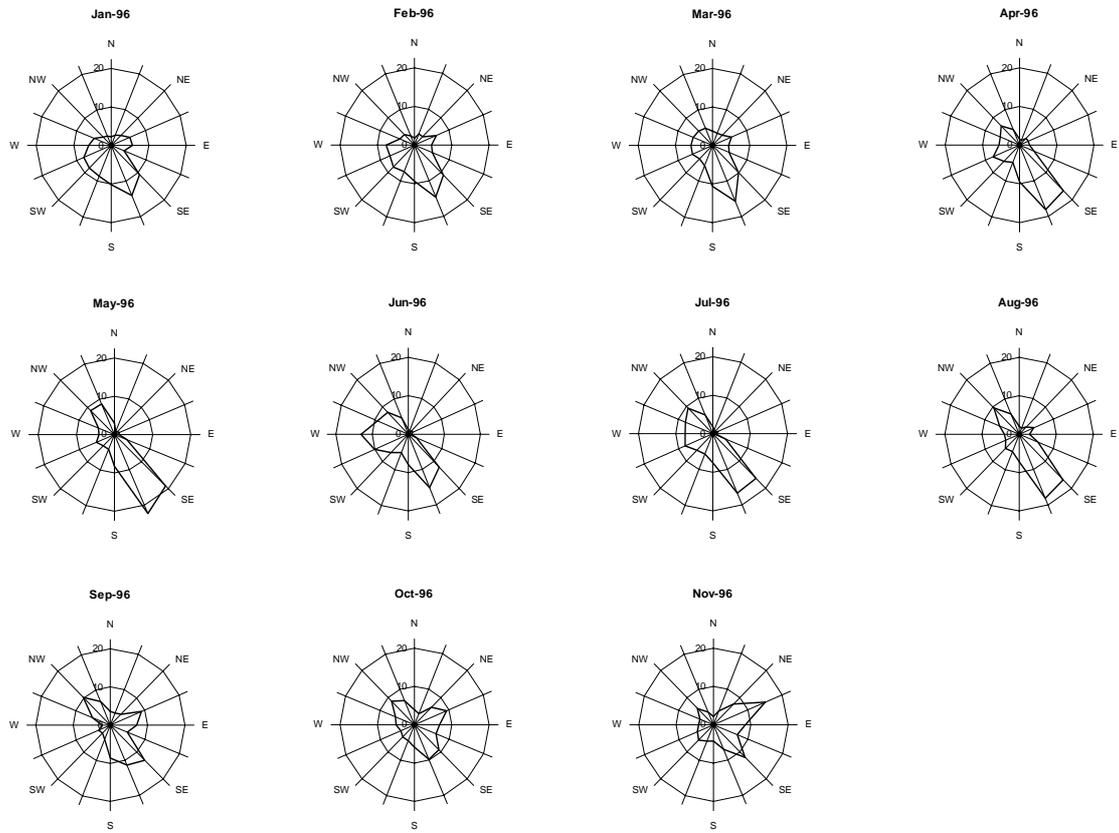
Figure 2.4.1./6 Wind direction distributions (%) on a monthly basis at the buoy off Kigoma.
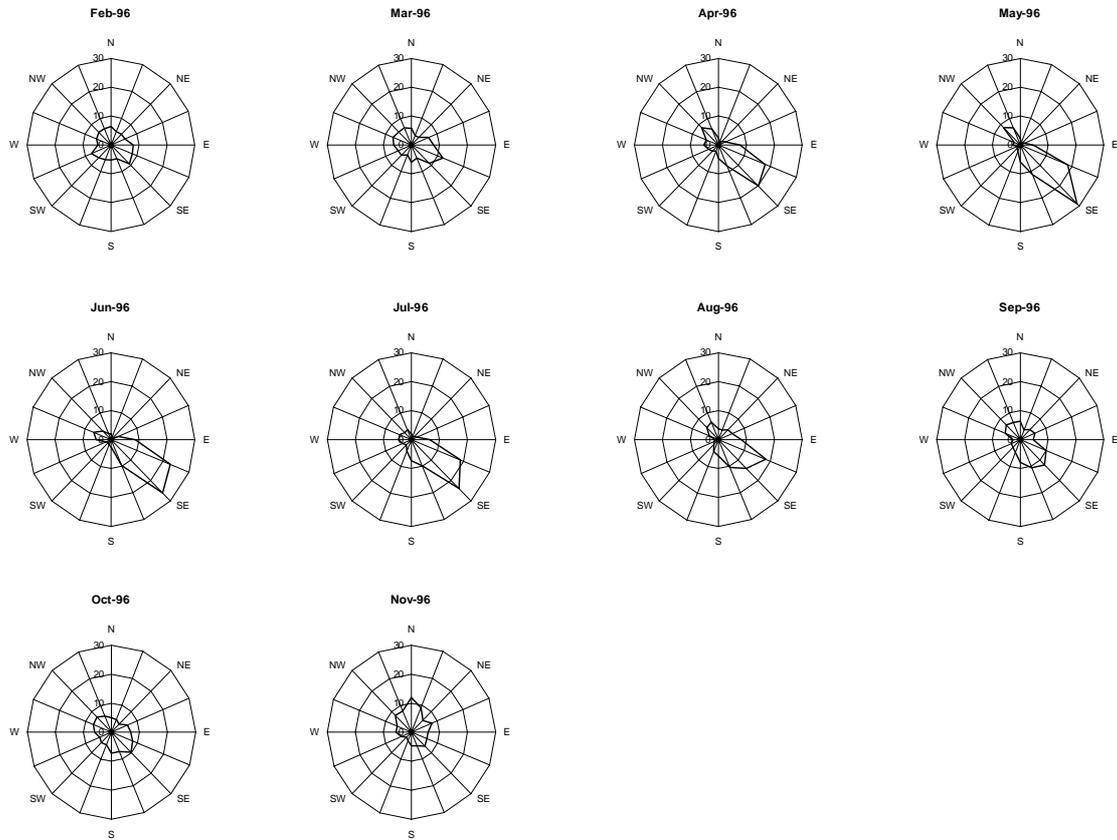
Figure 2.4.1./6 Wind direction distributions (%) on a monthly basis at the buoy off Mpulungu..

Jan-96 Feb-96 Mar-96 Apr-96

May-96 Jun-96 Jul-96 Aug-96

Sep-96 Oct-96 Nov-96 Dec-96

Jan-97 Feb-97 Mar-97 Apr-97

May-97 Jul-97 Aug-97
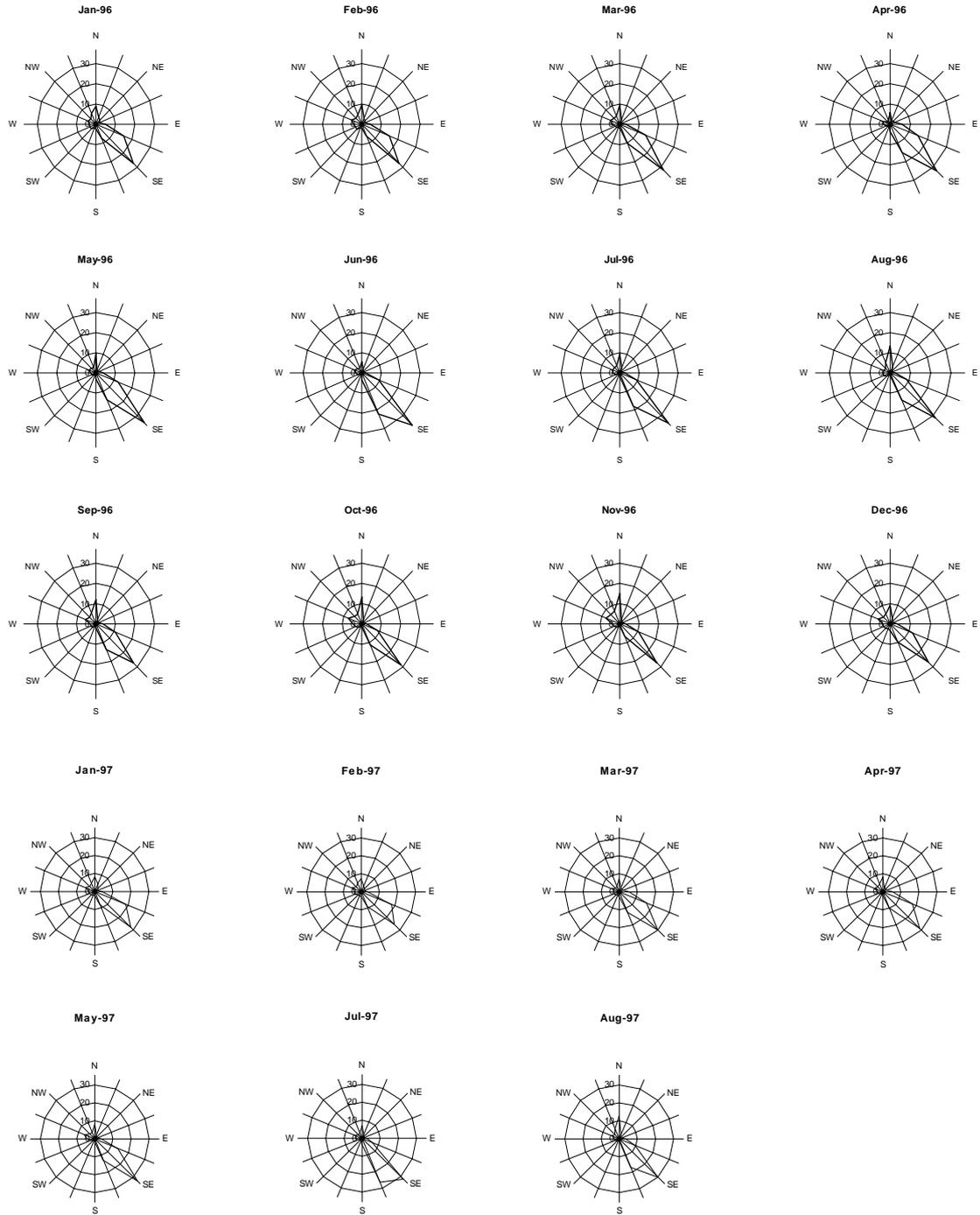
Figure 2.4.1./6 Wind direction distributions (%) on a monthly basis at Mpulungu weather station.
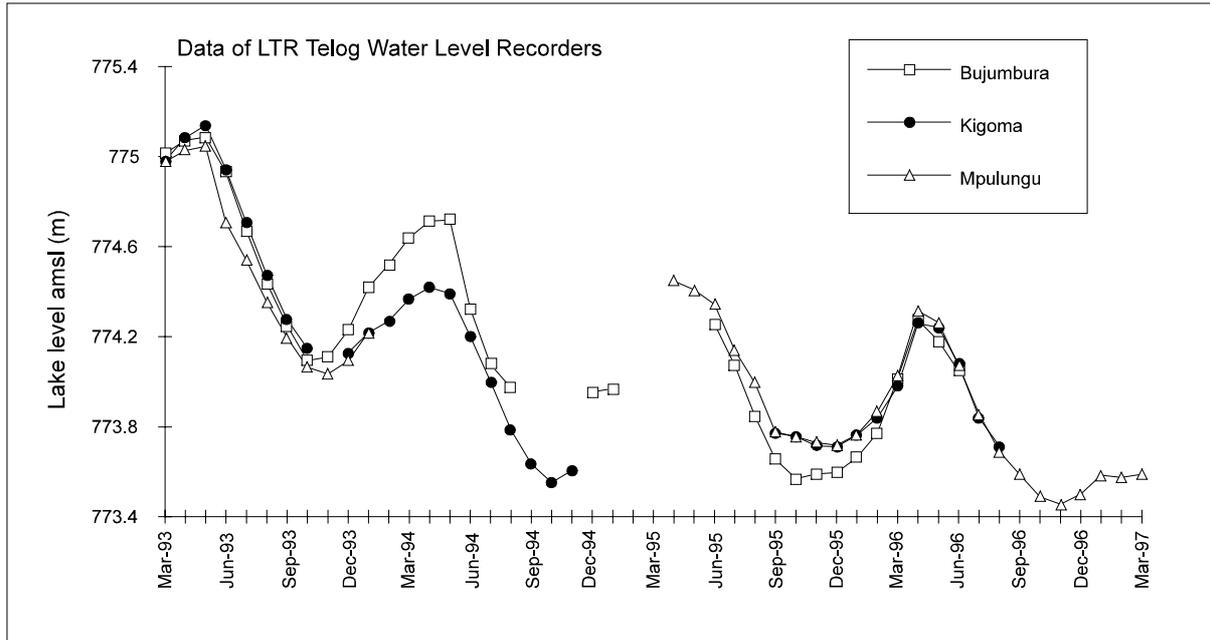
A
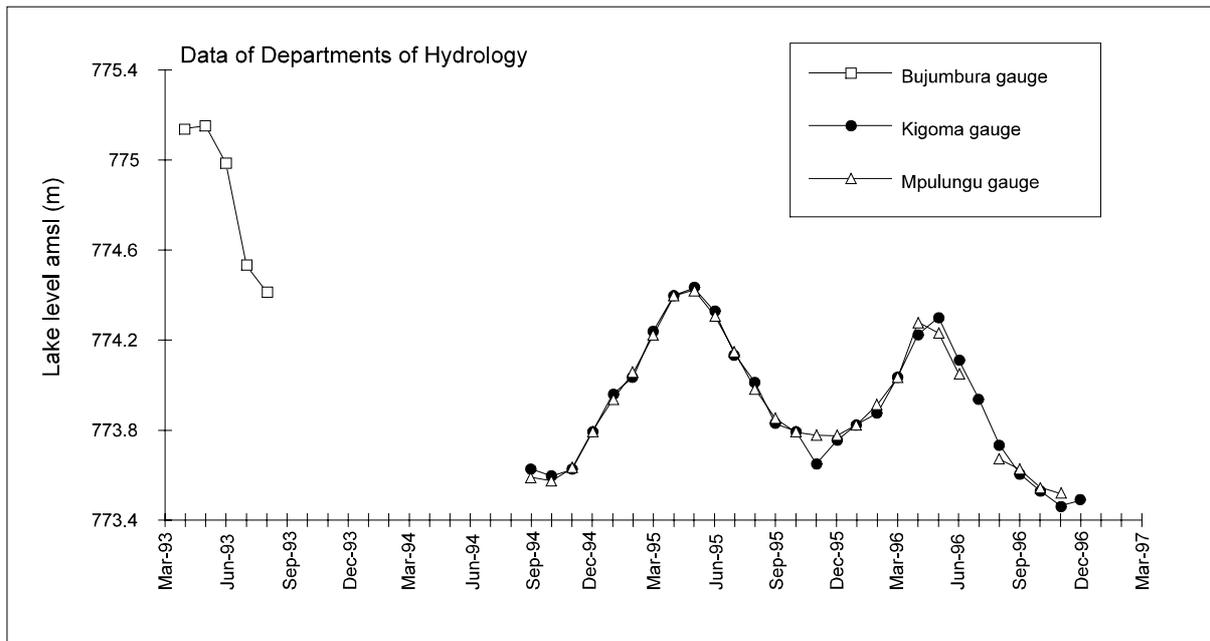
B

Figure 2.4.1./9 Monthly means of lake water level at Bujumbura, Kigoma and Mpulungu harbours. Data from the conventional gauge plates (A) and gauge plates of the Kigoma Department of Hydrology (B).
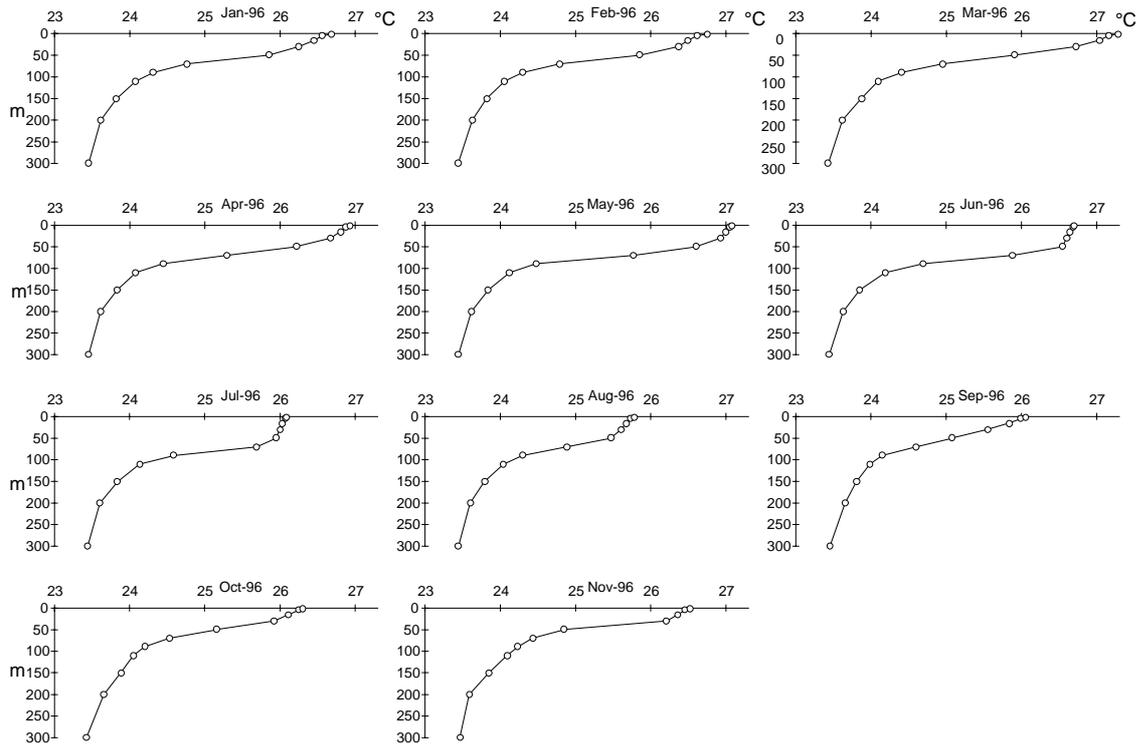
Figure 2.4.1./10 Monthly mean water temperature at the observation depths at the Kigoma buoy.
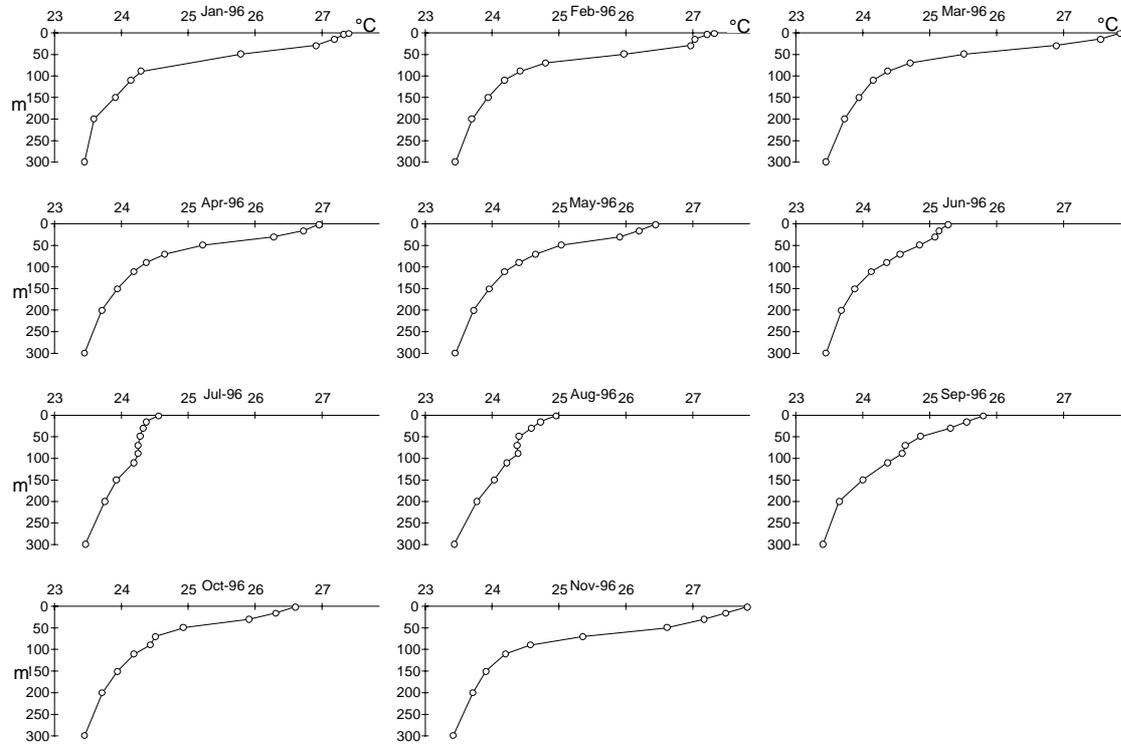
Figure 2.4.1./11 Monthly mean water temperature at the observation depths at the Mpulungu buoy.
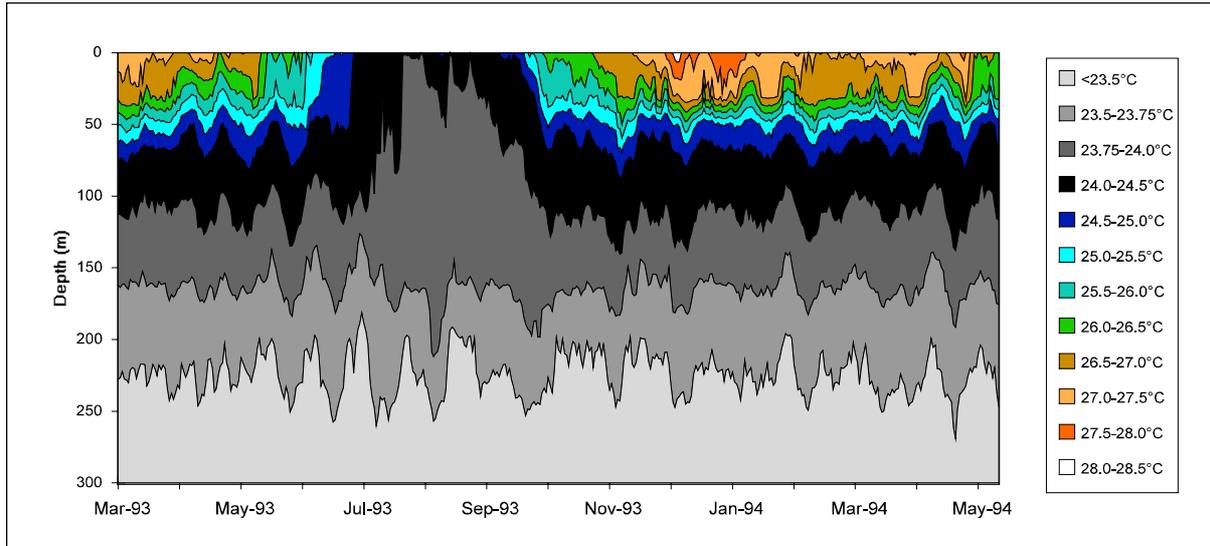
Figure 2.4.1./12 Water temperature isolines (°C) based on daily means. Period from March 1993 to May 1994 at the Mpulungu buoy.
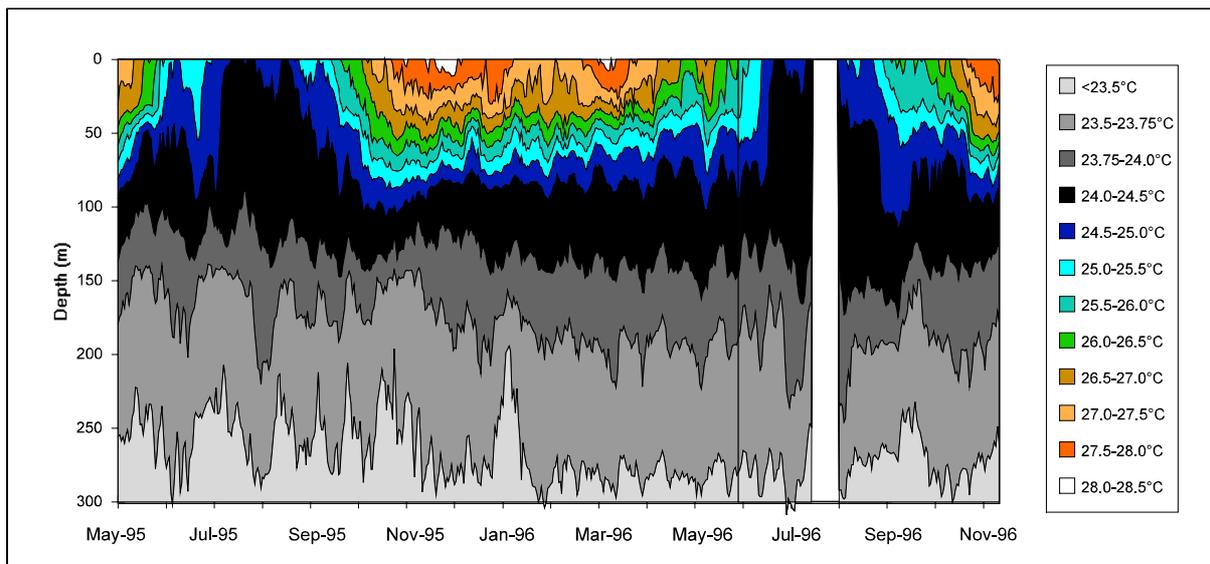
Figure 2.4.1./13 Water temperature isolines (°C) based on daily means. Period from May 1995 to November 1996 at the Mpulungu buoy.
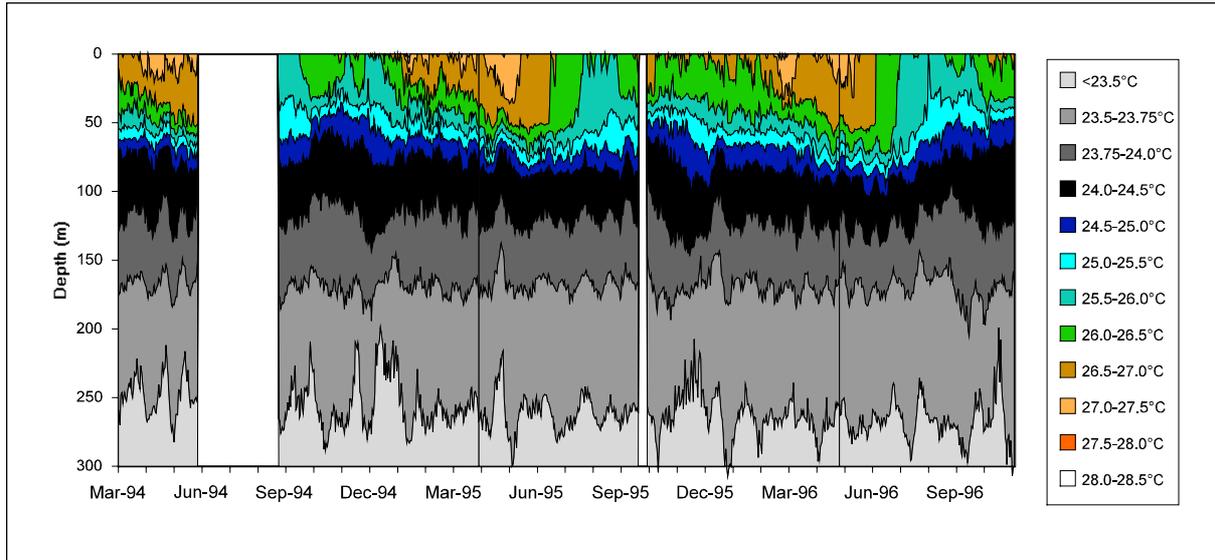
Figure 2.4.1./14 Water temperature isolines (°C) based on daily means. Period from March 1994 to November 1996 at the Kigoma buoy.

2.4.2. Thermal conditions during three expeditions

The thermal regime in the lake varied greatly during expeditions. In the following temperature transects calculated by SURFER-software from CTD results are discussed. The transects are selected along the main axis of the lake in south to north direction. Transects along main transversal axis are also discussed.

For Expedition 10 (Nov 1996) only the results along the main axis from Mpulungu to Kungwe are available (Fig. 2.4.2./1). The thermocline was situated at the depth of 65 m from the south to the region of Karema, where its depth started the increase being in the depth of 45 m near Kungwe. The warm southern waters reached to the region of Kipili (about 160 km from the south end of the lake).
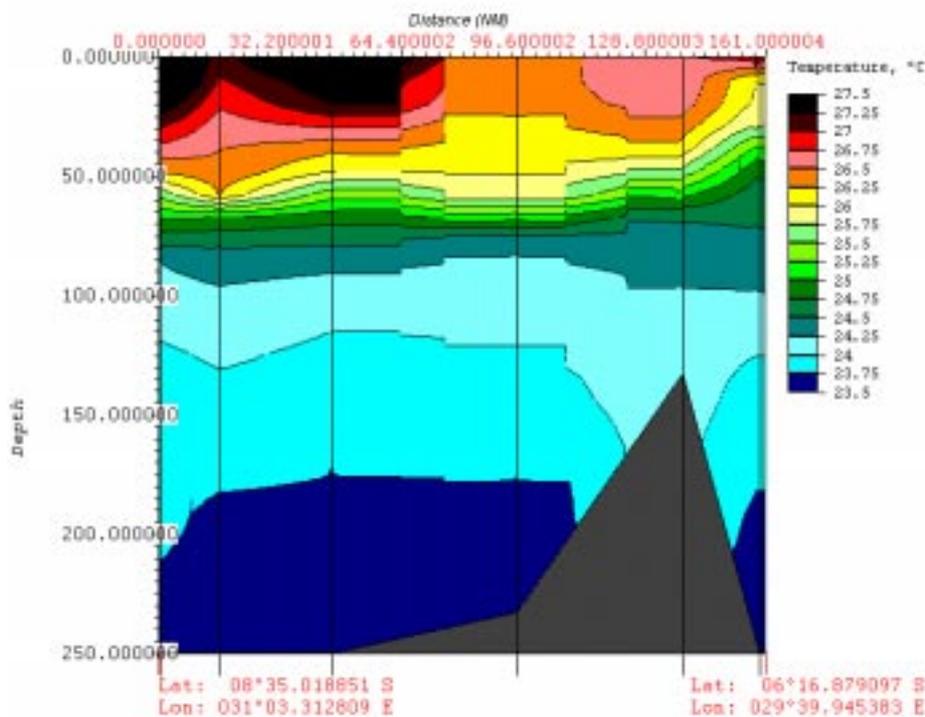
Figure 2.4.2/1. November 1996, temperature isolines along the main axis of the lake.

In April 1997 (Exp 14) the thermocline was also at the depth of 60 m. An internal wave propagating along the main axis was also observed (Fig. 2.4.2/2). No significant tilting along main axis was observed.

The temperature transect along the main transversal axis from Sumbu to Kala showed no significant tilt (Fig. 2.4.2./3). The tilt near the Sumbu bay is not based on the observations but on the interpolation method. A slight SE tilt was found along the transversal axis near Kungwe. (Fig. 2.4.2./4). Further north at Kabogo the thermocline was not tilted (Fig. 2.4.2./5).
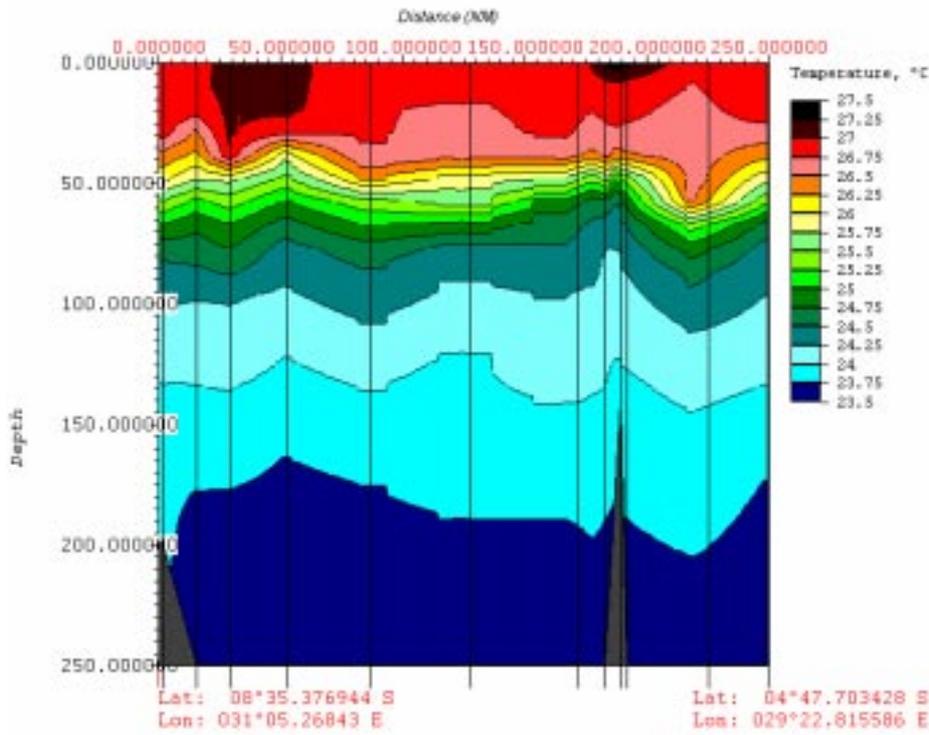
Figure 2.4.2./2. April 1997, temperature isolines based on CTD observations along the main axis of the lake.
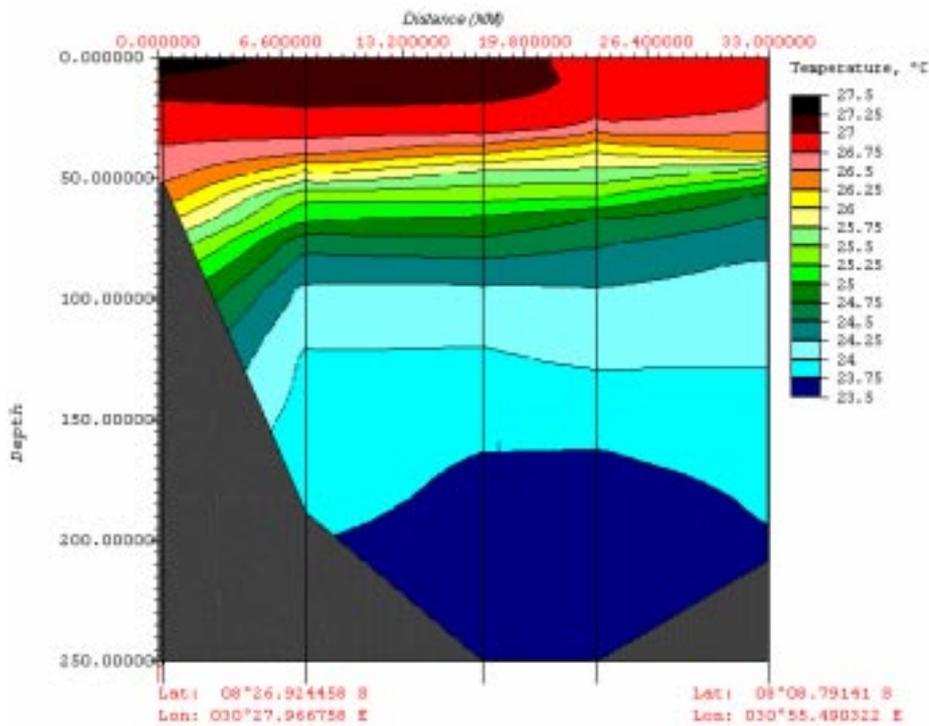
Figure 2.4.2./3. April 1997, temperature transect from Sumbu to Kala.
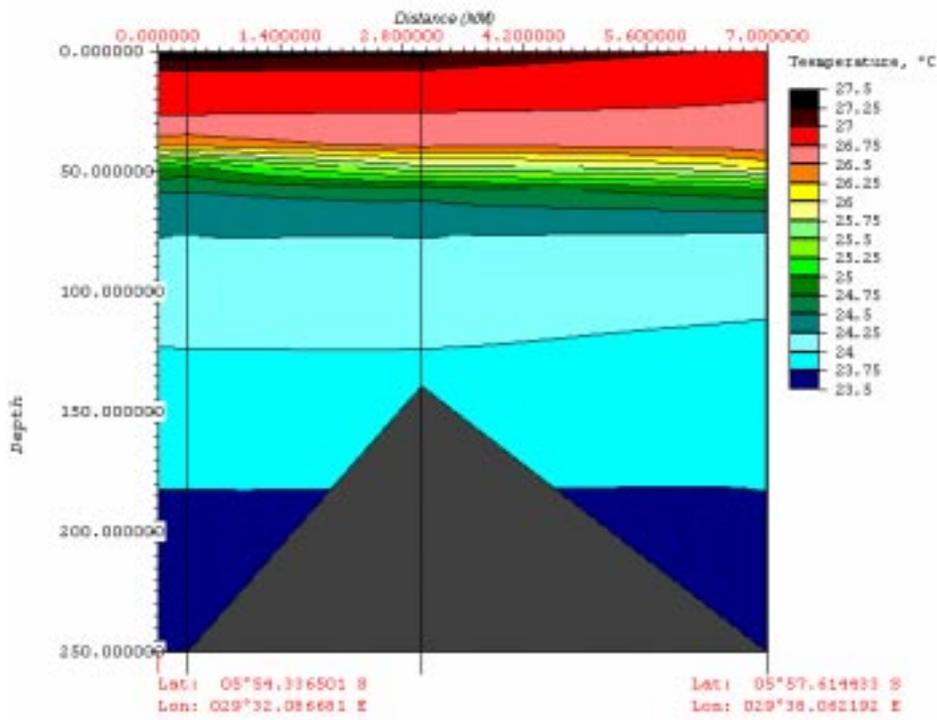
Figure 2.4.2./4. April 1997, temperature transect near Kungwe along transversal axis.
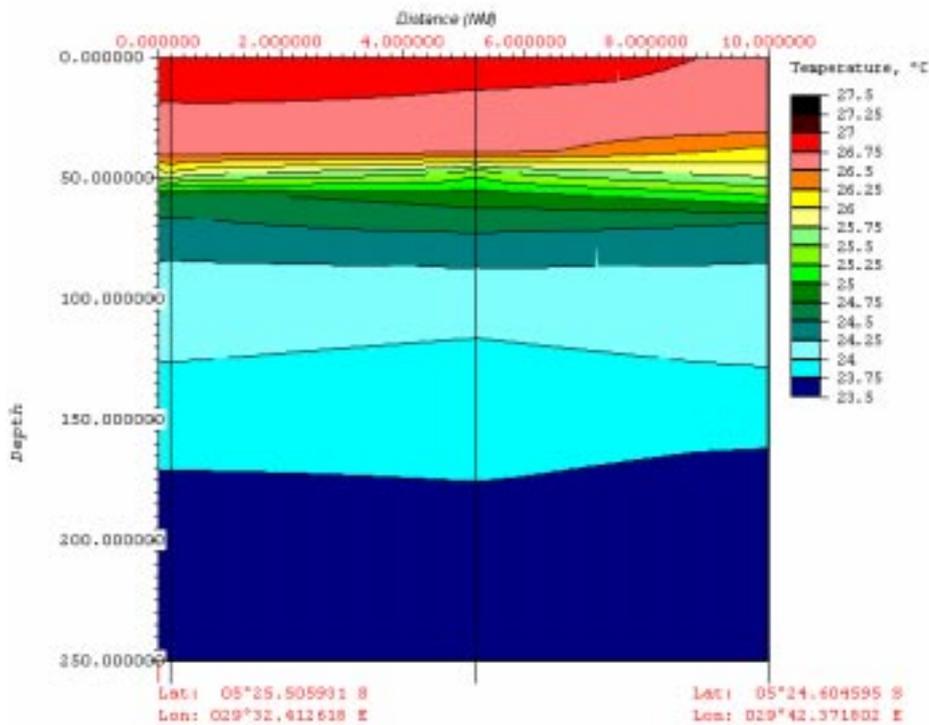
Figure 2.4.2./5. April 1997, temperature transect near Kabogo in west - east direction.

At the end of dry season 1997 during Expedition 16, a clear tilt of thermocline was found along the main axis of the lake (Fig. 2.4.2./6). The water mass 24.75 - 25.00 $^{\circ}$C was at the depth of 25 m near Mpulungu and at 75 m near Rusizi. Also now the waters from the south end to the region of Kipili were very different from the other waters further north with lifted and expanded thermocline waters. This was also the reason why there was no clear transversal tilt of thermocline in the south basin (Fig. 2.4.2./7). This was also the case at the other locations such as near Utinta (Fig. 2.4.2./8), Kungwe (Fig. 2.4.2./9) and Rumonge (Fig. 2.4.2./10) and no transversal tilt of thermocline was found anywhere.
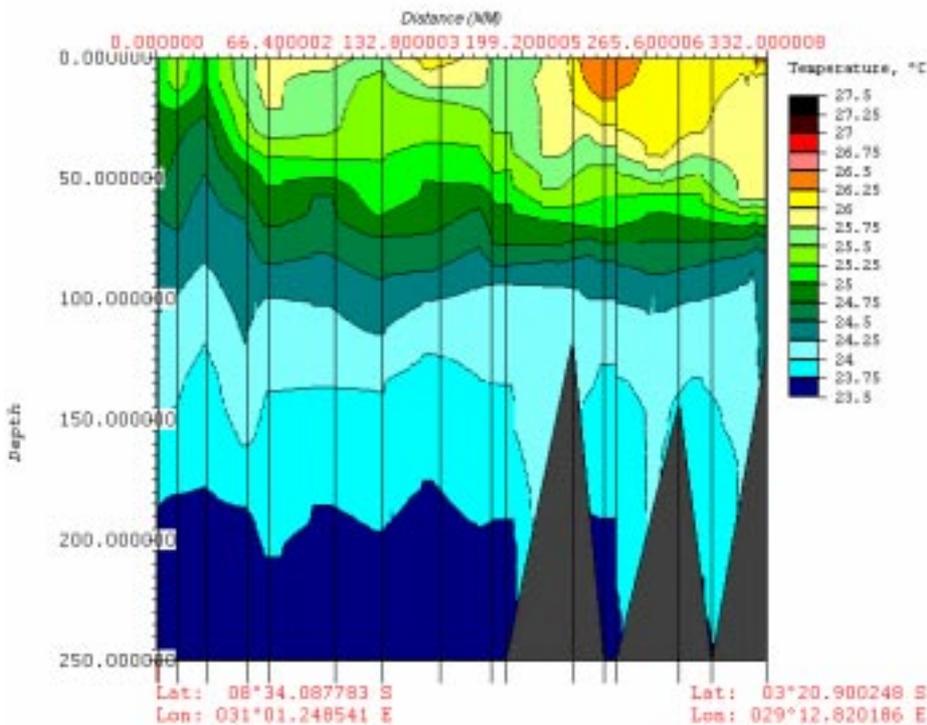
Figure 2.4.2./6. August 1997, temperature isolines along the main axis of the lake.
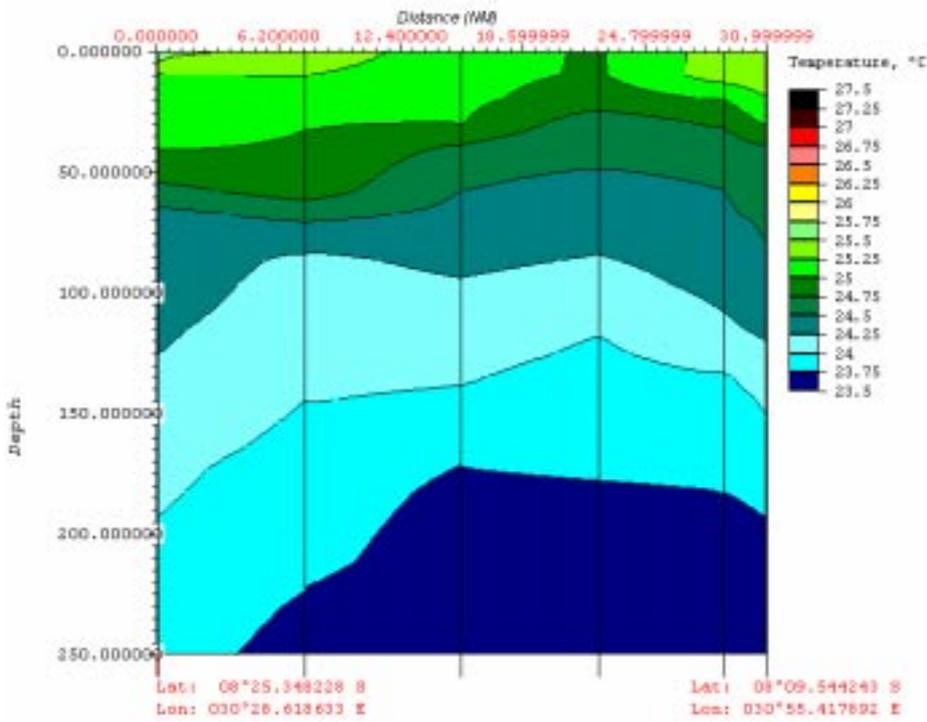
Figure 2.4.2./7. August 1997, temperature transect in the south basin in west - east direction.
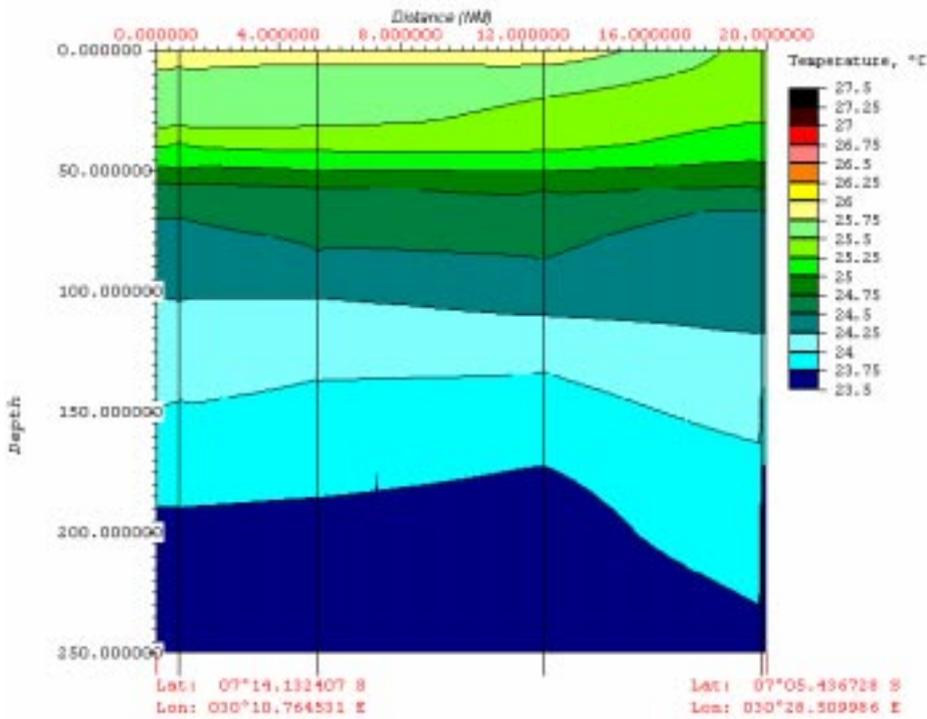
Figure 2.4.2./8. August 1997, temperature transect near Utinta along transversal axis.
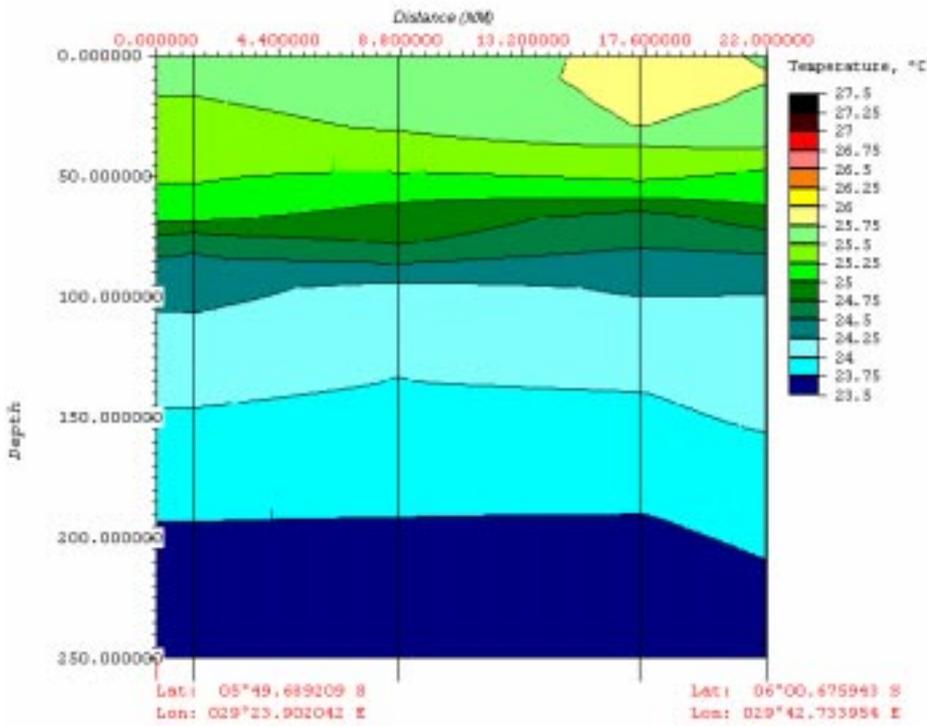
Figure 2.4.2./9. August 1997, temperature transect near Kungwe in west - east direction.
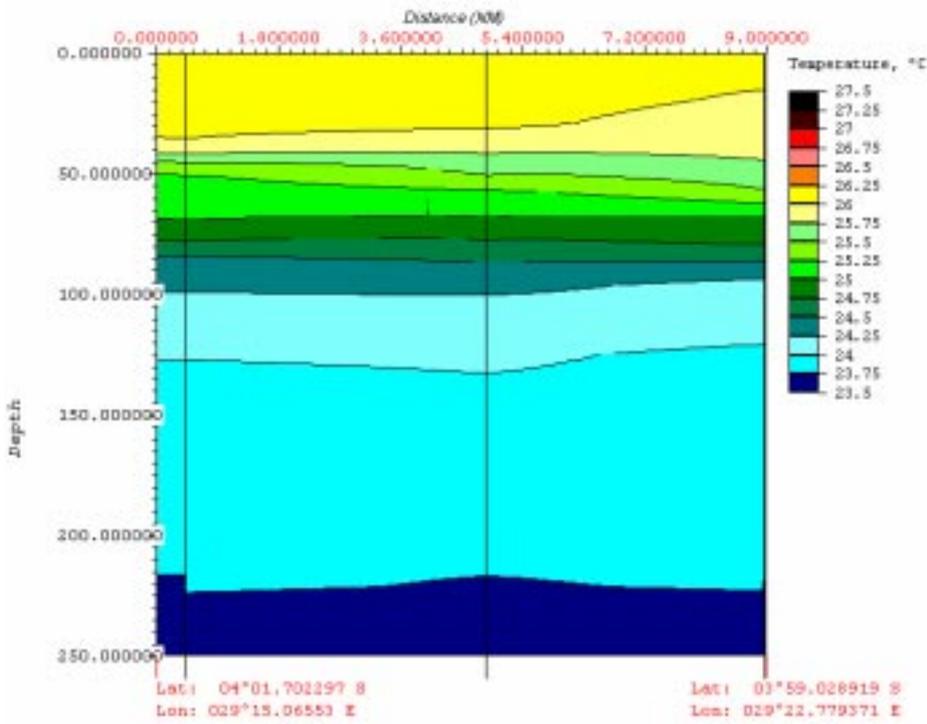
Figure 2.4.2./10. August 1997, temperature transect near Rumonge along transversal axis.

2.4.3. Sedimentation

The **river discharge** measurements were not conducted within the project. It is known that the rivers Malagarasi, Ruzisi and Lufubu have a major share of the inflowing waters to the lake. The sum of their inflow is according Edmond et al. (1993) quoted by Patterson (1996) 334 m^3s^{-1}, which is 58 % of total river inflow. Similarly they obviously contribute most of the suspended solids load to the lake. There is little information about actual measured suspended sediment concentration in the incoming rivers. Patterson (1996) reported about the present status of river monitoring and sediment yield estimations around the lake without doing input estimations of different rivers. Hecky (1992) estimated that the River Rusizi is the main source of salts entering to the lake.

The scope of this study was to find out the dominating flow system and dispersion of river waters in certain main river inlet areas. Since the lake is great in area and volume it can be expected that the incoming waters and substances are mixed rapidly with ambient water and gradient of the suspended solids concentration is great near the river mouths.

The **Malagarasi inlet region** was a natural choice, since there is a large plateau which extends over 40 km in the south-north direction and 15 km in the east-west direction. NORCONSULT conducted a major hydrological programme with Tanzanian authorities at the Malagarasi watershed during the years 1974 to 1980. The river discharge was measured at several locations. The suspended solids flow was monitored in two watersheds near by. From this data it was possible to derive the mean characteristics of the hydrological regime of the River Malagarasi.

For Malagarasi the **river discharge** data was obtained from a NORCONSULT publication (NORCONSULT 1982) for the period of 1975 - 80. The station at 4A9 (Mbelagule) was taken as the outlet of the Malagarasi watershed. The maximum monthly discharge was obtained as 430 m^3s^{-1}. This occurred in April and May (Fig. 2.4.3./1). Great seasonal variation was observed. The mean monthly discharge at the end of the dry season (September) is about 1/10 of the value in the wet season.
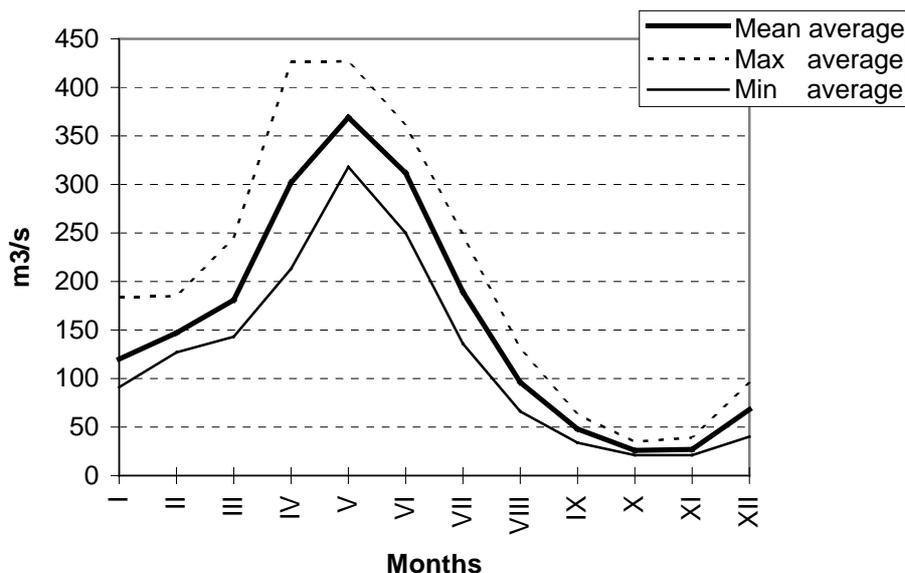
Figure 2.4.3./1 Discharge of the River Malagarasi in 1975 - 80 (NORCONSULT 1982).

The **suspended solids concentration** was estimated on the basis of River Luiche and Lugufu observations. These rivers were monitored during the NORCONSULT Project and a sediment rating curve was formed using these observations. Both rivers are located in the Kigoma region and they collect waters in the same type of climate as Malagarasi. The ratio of mean minimum to mean maximum daily discharge of those rivers is such that the value for Malagarasi is somewhere in the middle when compared with the other two rivers. This indicates the fact that the water storage of these two watersheds is different and that the Malagarasi watershed as water storage type can be taken as an intermediate storage type of these two watersheds. On basis of this the sediment rating curve for Malagarasi was fitted in between the curves of the Luiche and Luguga Rivers. From this rating curve the suspended sediment load was calculated for each month with monthly discharges and averaged for the period of 1975-80 (Fig. 2.4.3./2). Similarly the suspended sediment concentration was obtained by simply dividing the monthly sediment load by monthly river discharge.
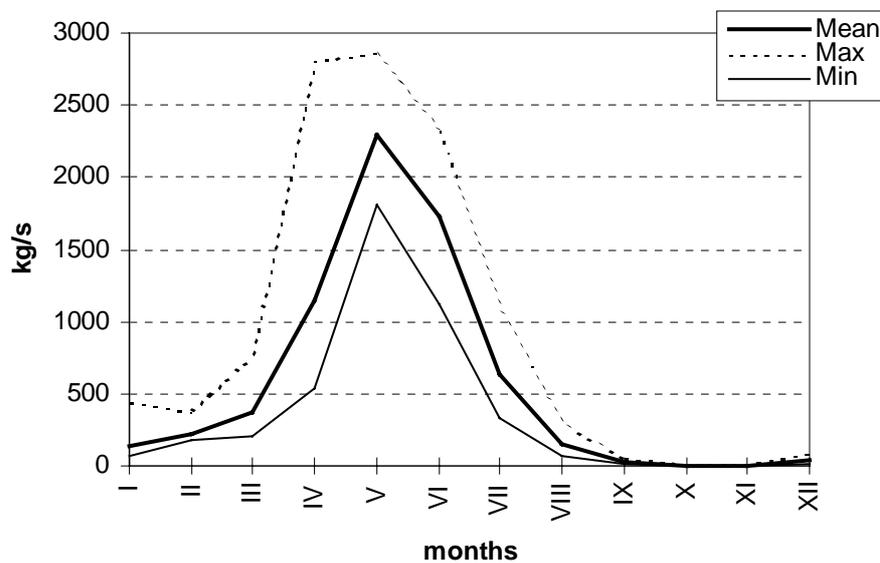
Figure 2.4.3./2 Sediment load of the River Malagarasi in 1975-80.

The **River Lufubu** in Zambia was taken as another example of an incoming river and dispersion of its waters and suspended solids in to the lake were studied. The inlet area of the Lufubu is different to the Malagarasi and the lake bottom slope is quite steep compared to the Malagarasi. Similarly in the north the Ruzisi delta ends in a very steep slope when it reaches the lake. In this way the results from the Lufubu region may also be extended to the Ruzisi region.

Only one set of hydrological data was found from the Lufubu (Table 2.4.3./1). This data comes from the early 1960's by Badenhuizen (1964). He was interested in the migration of certain fish species from Lake Tanganyika to the River Lufubu. Thus he was interested in the high water levels in the river. He reported only six river discharge measurements, but for major peaks in river water level he reported 7 - 14 values for the years 1958 - 64. He reported that the maximum discharge was observed during the wet season in March. From conductivity, pH and secchi depth he concluded that Lufubu waters float on the surface of the lake for a 'considerable distance' before mixing with the lake waters.

From Badenhuizen's (1964) data it was possible to derive a simple state discharge curve. His data, though scarce, adequately covered the whole range of water level observation .

Table 2.4.3./1. River Lufubu hydrological data from period 1958 - 64. Based on data from Badenhuizen (1964). Data given as annual means.

	Value	Unit	Date of occurrence
Mean water level	2.36	m	
Mean high water level	3.06	m	March
Mean low water level	1.21	m	December
Maximum discharge	449	m^3s^{-1}	Jan 13, 1962
Mean maximum discharge	314	m^3s^{-1}	March
Mean low discharge	18.2	m^3s^{-1}	December

Suspended sediment concentration data was available from Lufubu by Badenhuizen (1964).

Grain-size distribution of surface sediments near the river mouths are shown in Table 2.4.3./2. The analysis was made with the SediGraph analyser at the Finnish Environment Institute in Helsinki, Finland. All the samples were treated by H_2O_2 due a high organic content. The results show that the surface sediment structure size is finest near the Malagarasi estuary. The organic content is also highest there as compared to other sites. The coarsest sediment texture is found near the Kalambo river mouth The grain size structure is least dependent on depth at Malagarasi.

Table 2.4.3./2. Grain size distribution of the surface sediment samples taken during expedition 14 in April 1997 from Lake Tanganyika.

Sample slice	River mouth	Latitude	Longitude	Depth m	Ignition loss %	Humus content %	d50 microns	d10 microns	d90 microns
1-2 cm	Malagarasi	05°11.09	29°43.12	30.3	8	5.8	13	<2	110
0-2 cm	Malagarasi	05°10.88	29°44.12	39.2	15.2	13.4	21	2	60
1-2 cm	Malagarasi	05°11.09	29°45.12	50.3	13.9	11.6	13	<2	45
0-2 cm	Kalambo	08°35.91	31°10.10	20.0	3.1	3.1	85	28	135
0-2 cm	Kalambo	08°35.91	31°10.10	41.9	5.3	5.3	70	22	135
0-2 cm	Kalambo	08°35.91	31°10.10	60.0	5.7	5.7	55	22	123
0-2 cm	Lufubu	08°33.71	30°44.67	26.5	3.9	3.9	38	15	120
0-2 cm	Lufubu	08°33.42	30°44.66	52.5	3.7	3.0	48	8	140

Sedimentation to traps near Malagarasi and Lufubu was fairly small during measurements in Aug 1997. The flux of suspended sediments to traps was 16.3 $gm^{-2}d^{-1}$ at the Malagarasi observation site and 23.2 $gm^{-2}d^{-1}$ near the Lufubu river mouth. The low values correspond to expected low seasonal values of the river load.

2.4.4. Water currents

Two **ADCP systems** were used for data collection: 1) a moored ADCP (300 kHz), which was stationary fixed to a buoy and 2) a ship-based instrument (150 kHz) was used to obtain data in space. Moored ADCP's were used to obtain data of current variation at a certain location. They had a measuring range down to a maximum of 120 m. The ship based ADCP was more powerful and had a lower operation frequency than moored ADCP's. It could track the bottom most often at the depth of 600 m. The nominal range for bottom tracking is 450 m for this frequency (150 kHz), but due to the low density of the water it was possible to track the bottom even at the depth of 800 m on some occasions. One drawback was that the DGPS reference station, planned to be used in deep water measurements, was not fully capable of giving an accurate enough reference velocity for the ship. For this reason the measuring efforts were concentrated on areas with water 600 m or less, where it was certain that, the ADCP was able to track the bottom and this way the needed reference ship velocity was obtained. In terms of current speed measurement accuracy by both ADCP systems, one major factor is the amount of reflectors (i.e. zooplankton) in the water. Below oxycline, which varied in space and time, measured currents were often considered inaccurate due to small amount of reflectors.

It was not safe to leave the very expensive moored instruments on the lake for extended periods of time. So they were used in connection with other activities on certain limited area during expeditions. The ship was collecting spatial ADCP and meteorological data together with CTD profiles from the same area where moored ADCP current meters were deployed

Current **measurement regions were selected on the basis of LTR circulation model results** and experience from other lakes (e.q. Podsetchine and Huttula, 1996). Within the present project it was not possible to cover the whole lake. Furthermore the political uncertainties, especially in Burundi and Zaire, made it difficult and unsafe to conduct scientific expeditions in the north part of the Lake. This chapter deals with the results from the three major expeditions. The discussion is done according to geographical areas of the lake. Some other experimental expeditions were also conducted, but the results from these have not been included here since the measurements covered only minor regions. The discussion is mostly based on 30 min. averages of ADCP-buoy-data. The accuracy of this data is 1 cms^{-1}. The amount of collected data is extremely large and the space limited in the report. The scope of this report is the advection of river waters. Due to these reasons the following discussion was limited to the most important data and aspects. It means from ship based ADCP all results are presented and illustrated from the uppermost observation layers. The bottom depth of this layer was between 5 - 12 m depth depending on ADCP layer thickness settings. Nevertheless in the text some more information about deeper currents has been added occasionally. The results near river mouth are discussed more widely as well as the results from moored ADCP's.

Only during the dry season expedition (16) was it possible to carry out **measurements in the northern part of Lake Tanganyika** in **Area 0** (Fig. 2.2/5). Along with the intensive measurements outside the Rusizi river mouth 24 transect lines were measured in the region extending down to Nyanza in the south during 21. - 22.8.97 (Fig 2.4.4./1).
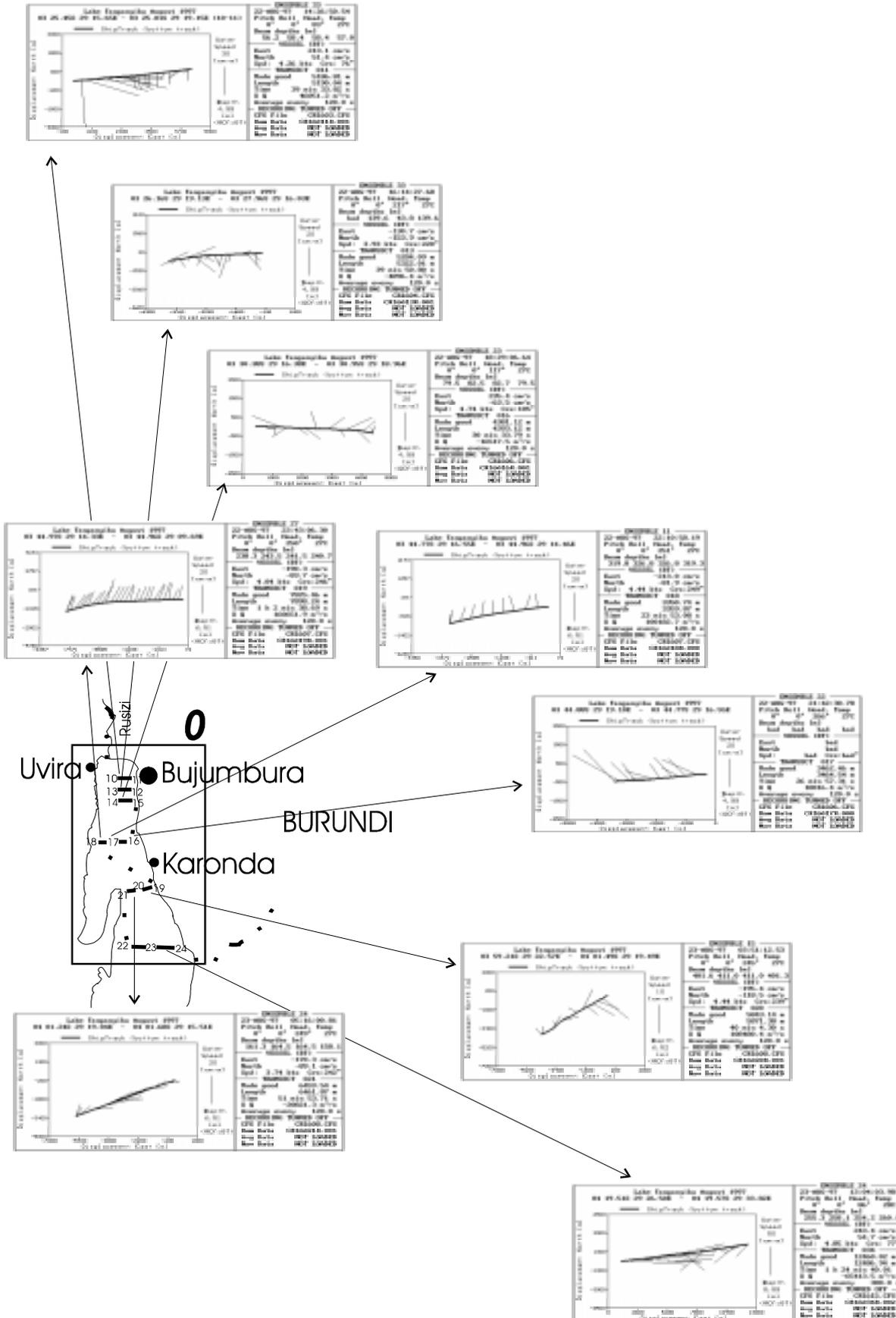
Figure 2.4.4./1 The currents from the uppermost observation layer as 120 s mean values along transects in the north end of Lake Tanganyika. Expedition 16, August 1997.

Two ADCP buoy stations were deployed for 20 hours near Ruzisi. The ship was moving along a rectangular with sides of 5 km (along the northern shore) times 4 km. One lap with ship ADCP measurement took about 3.5 hours. The two ADCP buoy stations were installed in the middle of long sides of the rectangular. The water depth at deployment sites was 46 and 108 m. Altogether 10 CTD profiles were taken.

On the afternoon of August 21, wind observed at Bujumbura harbour blew from the SE with a maximum speed of 8 ms^{-1}. During the afternoon the wind ceased. In the evening (between 19:00 and 21:00 hours) a very strong local thunder storm occurred with N-NW winds. The wind speed on the lake exceeded 20 ms^{-1}. The storm ceased at midnight. The wind increased again on the following morning. The primary thermocline was situated at the depth of 70 m (Fig. 2.4.4./2).

The current data from the buoy in the shallow waters showed that the water was flowing as one mass with very similar speed at all depths. During the afternoon (Aug 21) the waters were flowing NE with the wind. Later in the evening, night and following morning the currents were headed E. The maximum current speeds were observed in the evening of Aug 21 during the local storm (Fig. 2.4.4./3).

At the deeper ADCP site, the instrument gave data only to the depth of 12 m. The reason for this was a programming failure. The currents were stronger than near the shore. They also had a somewhat different direction. Here, the velocity of the current also ceased, as in the shallow waters, during the late evening and night. The currents were then oscillating especially on the east-west axis. The period, about 3 hours, was found in the data.

The ship ADCP transect data was collected during two full laps in the evening and night as the vessel moved with ADCP along the rectangular. The data showed spatial variation in both echo intensity and current velocity.

On the shallow transect along the north coast during both passes with a clear front different water masses were found. This is based on the echo intensity results ADCP. The maximum intensity was observed at the shallowest site (Fig. 2.4.4./4), clearly indicating the river water plume. It was dispersed more to the E than to the W direction.

The location of the masses was almost identical during both passes. The echo intensity also showed that in the westernmost transect the most intensive echoes were coming from the depths of 0 - 74 m (Fig. 2.4.4./5). This was also observed during both passes of the ship. Maximum intensity was recorded at the depth of 68 - 75 m on the steepest slope during both passes. During the early evening pass a S current was observed. It extended from the river mouth in the whole water column down to the thermocline surface. After that further south it was observed in the thermocline. Near midnight after the strong N wind this current occurred only very near the bottom having a fairly thin vertical structure. At the southernmost transect a similar stratification in echo intensity was found. There the boundary was around the depth of 75 m. Also along the easternmost transect there was a clear spatial differences in echo intensity showing a strongly echoing mass nearshore but extending only about 1 km from the shore (Fig.2.4.4./6). A local water mass flowing at a fairly high speed SW was found at the depth of 40 to m about 1 km offshore. After the storm in the evening the echo intensities there increased considerably. It seems that the storm mixed waters and mobilised particles from the nearshore bottom. The eastward current speed was highest fairly near the shore just above the thermocline.
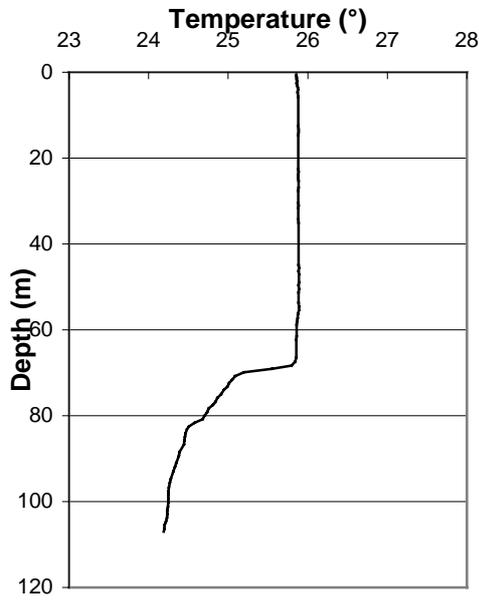
Figure 2.4.4./2 Water temperature profile near Ruzisi in the evening during August 1997 measurements.
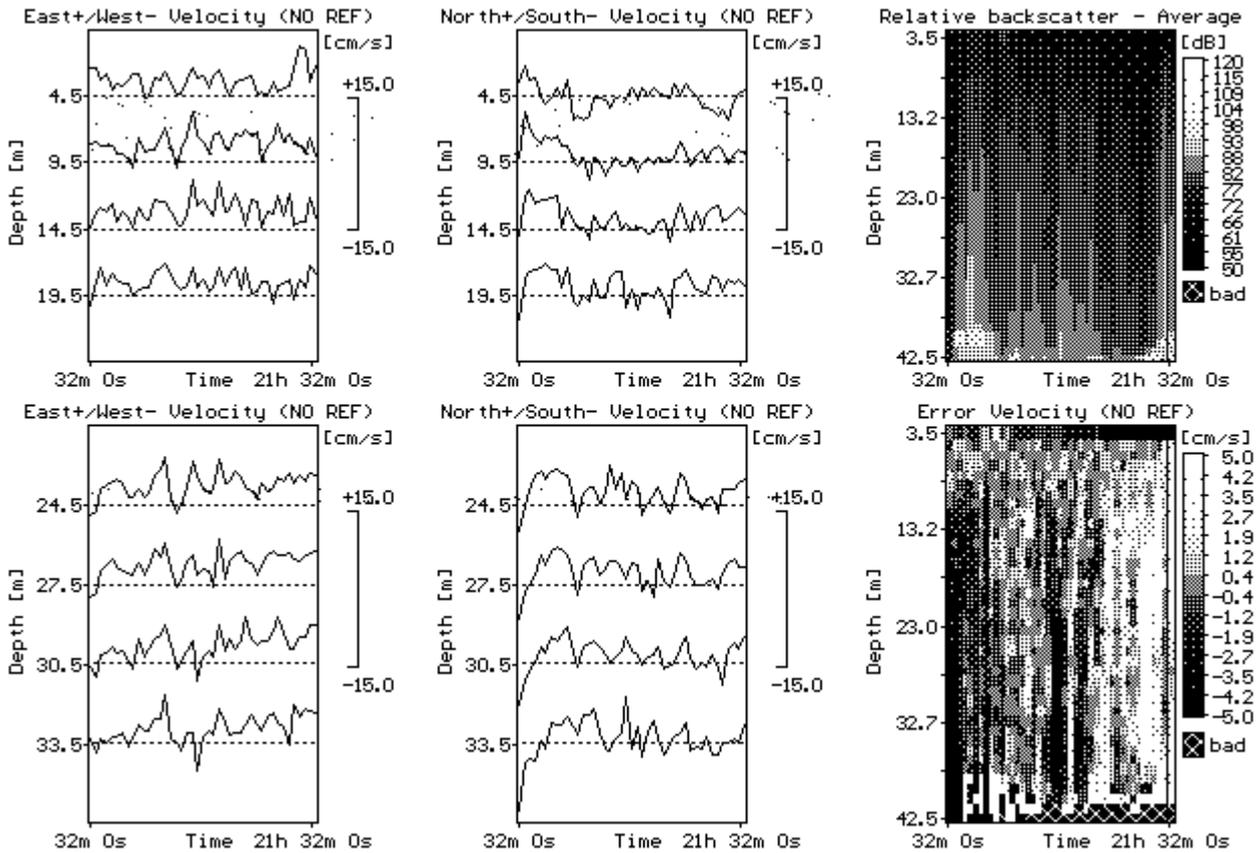
Figure 2.4.4./3 Time series of currents near Ruzisi during August 1997 Measurement period was 21.8. 14:43 - 22.8. 12:26. Water depth at the observation site was 46 m.
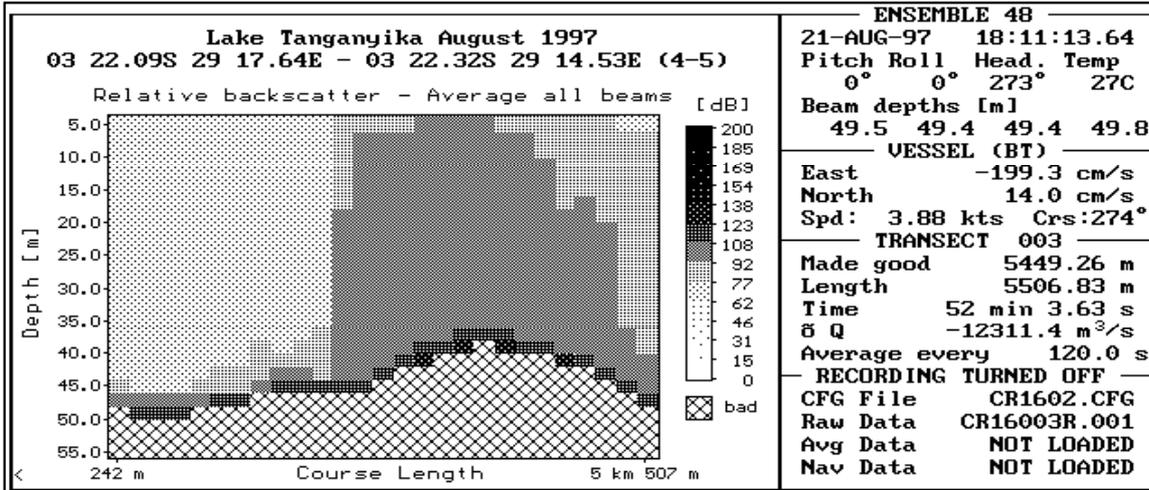
Fig. 2.4.4./4 Echo intensity as recorded by ship ADCP on a transect along the northern shore of the lake in the evening of August 21 (northern side of measurement rectangular).
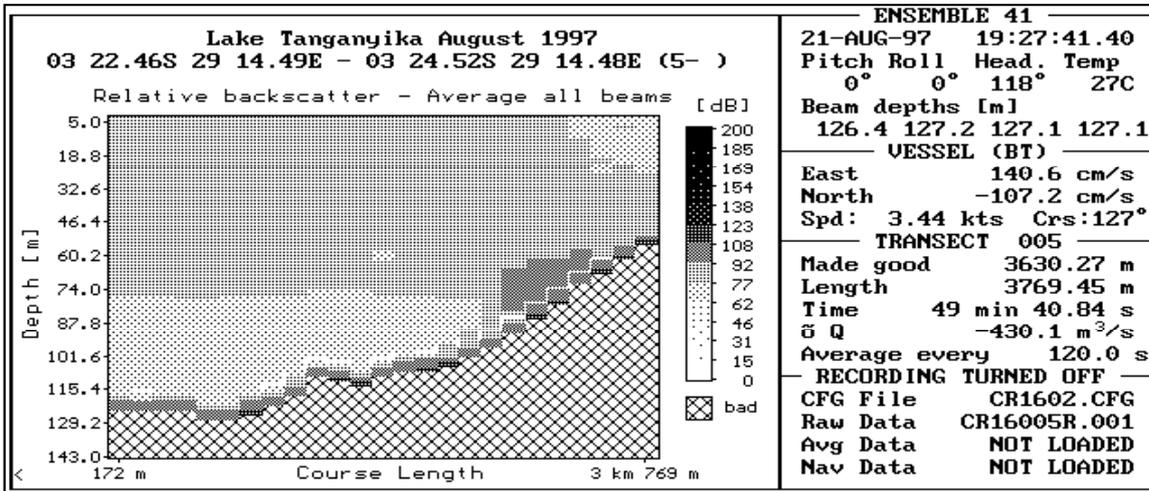
Fig. 2.4.4./5 Echo intensity as recorded by ship ADCP on a transect extending south from the northern shore of the lake (western side of measurement rectangular).
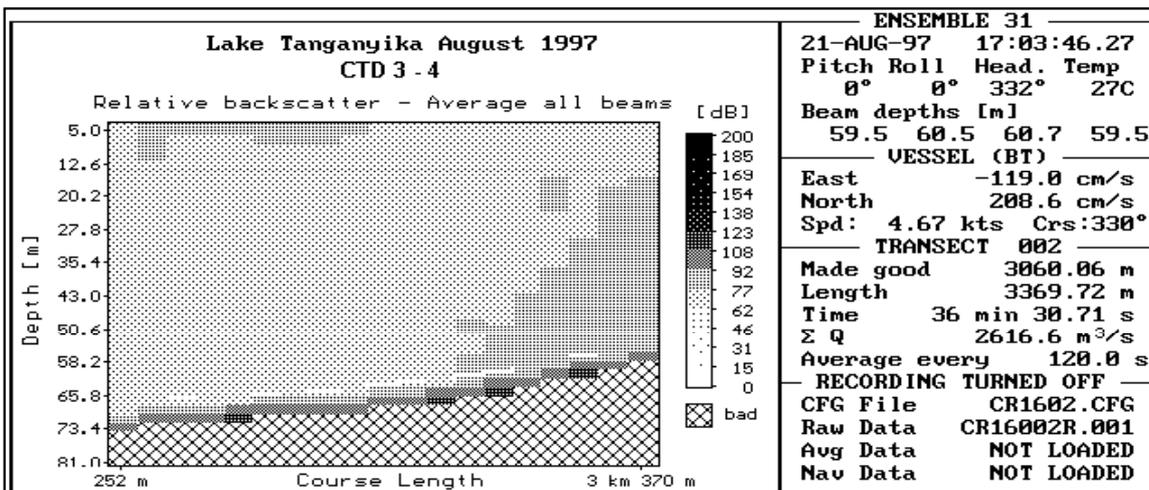
Figure 2.4.4./6 Echo intensity as recorded by ship ADCP on a transect extending south from the northern shore of the lake (eastern side of measurement rectangular).

As the ship moved south from Rusizi measurements were conducted mainly in the Burundian waters near the eastern side of the lake (Fig. 2.4.4./1). In the two northern transects (10 - 11, 12 - 13) the near surface flow was S and SE at the surface (0 - 10 m) but some deeper NW flows were also found. In the next transect (14 - 15) more flows N and NE were found at the surface, the main flow deeper was still S. During these measurements wind velocities were quite high (8 - 10 ms^{-1}). The same trend continued in the next transect (16 - 17 - 18), which crossed almost whole lake. There at the surface (0 - 30 m) the flow was towards the N, deeper (30 - 60 m) towards the S and still deeper (below 60 m) again towards the N (Fig. 2.4.4./7). The same pattern continues in the next transect (19 - 20 - 21) although not as clearly.
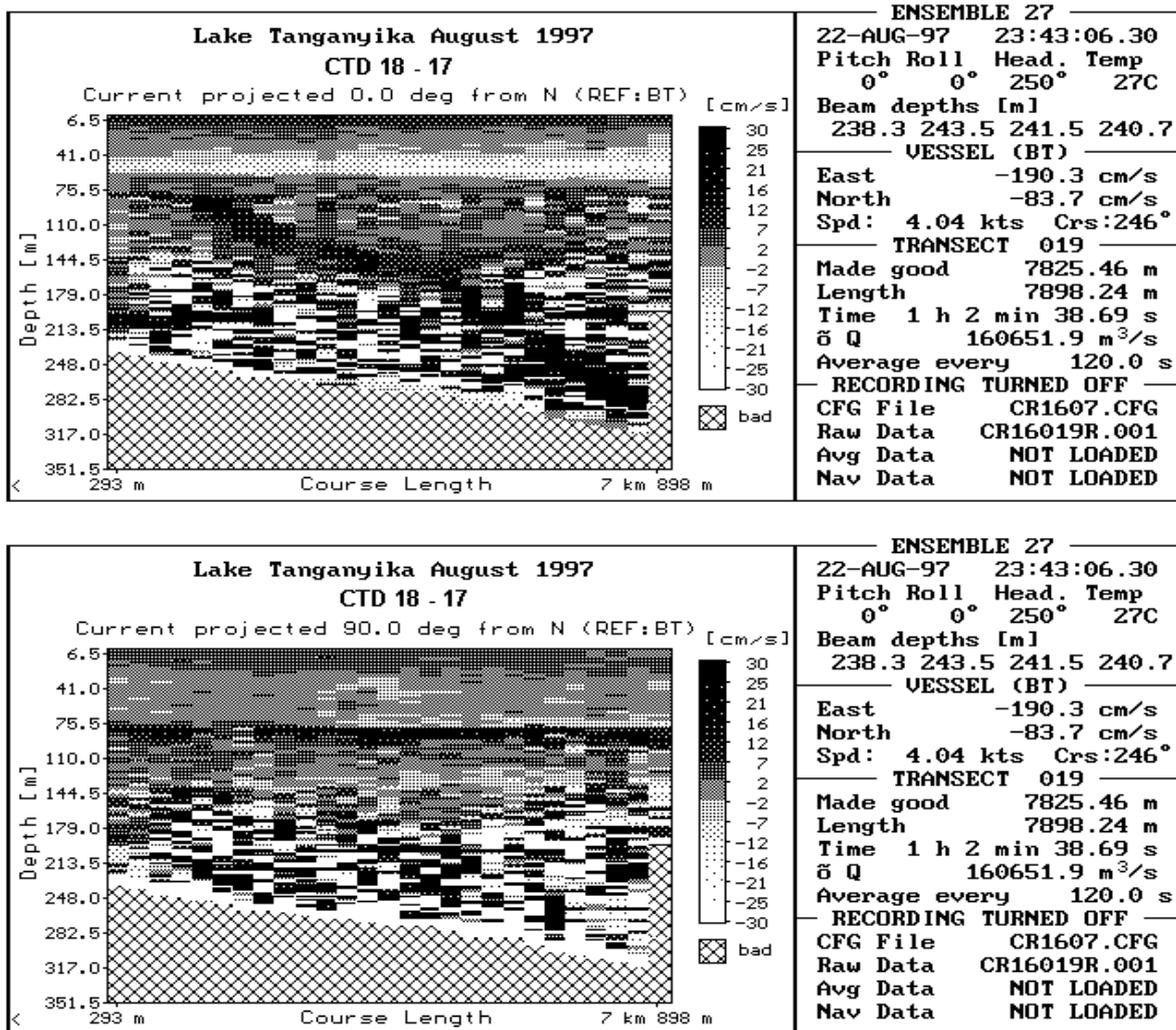
Figure 2.4.4./7 Currents along the transect 17-18 in the northern part of the lake. The currents are presented in the component form. The upper panel shows the north component, the lower one the east component. A major part of data below 76 m is biased and show unrealistically high values.

The most extensive current measurements were carried out near the **River Malagarasi**. Data was collected there during each expedition.

The first measurements **during the wet season** near Malagarasi were conducted on Nov 25 and 26, 1996. Two ADCP buoy stations were deployed (Fig. 2.2/1). They were installed during the afternoon on Nov 25 at 47 and 127 m depths and lifted up early in the morning of Nov 27. During the deployment current transects with the ship ADCP were recorded in the area. The vessel was moving along a rectangular of 29 km (along the shore) times 7 km. In each corner and in the middle of the longer transects a CTD profile was taken. It took about 16 hours to complete a lap. The sailed ADCP transects, CTD profiles and ADCP buoy stations have been described earlier in chapter 2.2.

CTD profiles showed that primary thermocline was situated at the depth of 38 m (Fig 2.4.4/8).
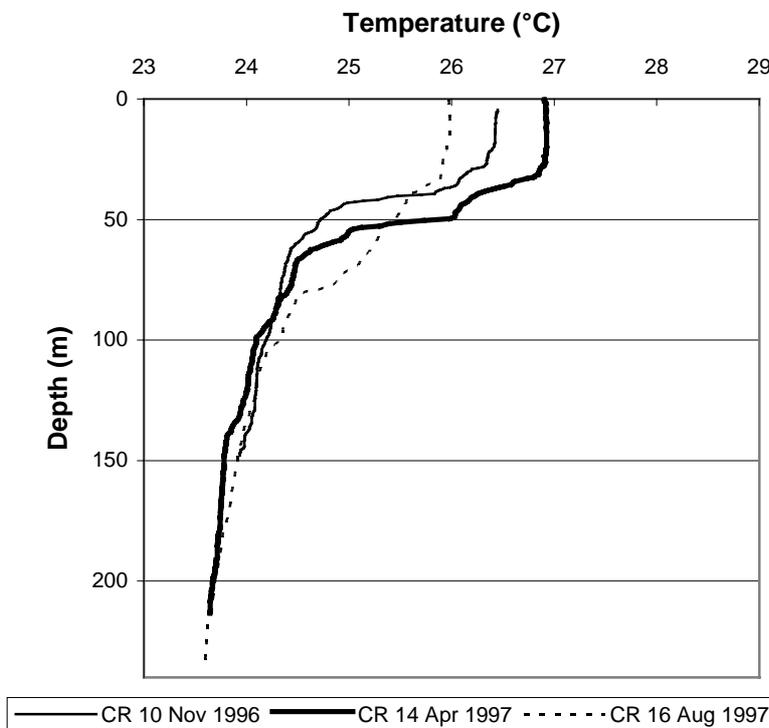
Figure 2.4.4./8 Water temperature profiles near Malagarasi during expeditions 10, 14 and 16 measurements.

The data from the buoy station in the shallow waters showed that at the depths of 0 to 25 m waters were flowing SE most of the time (Fig. 2.4.4./9). The current structure remained fairly constant during the observation period. The current velocity was less than 10 cms^{-1}. Below that layer current velocity was even slower and was in the opposite direction. The maximum velocities in the upper layer occurred during the late afternoon on Nov 25 and early evening on No 26. During the early morning hours on Nov 27 a well developed velocity maximum was at the depth of 22 m as the whole upper layer was flowing steadily S.
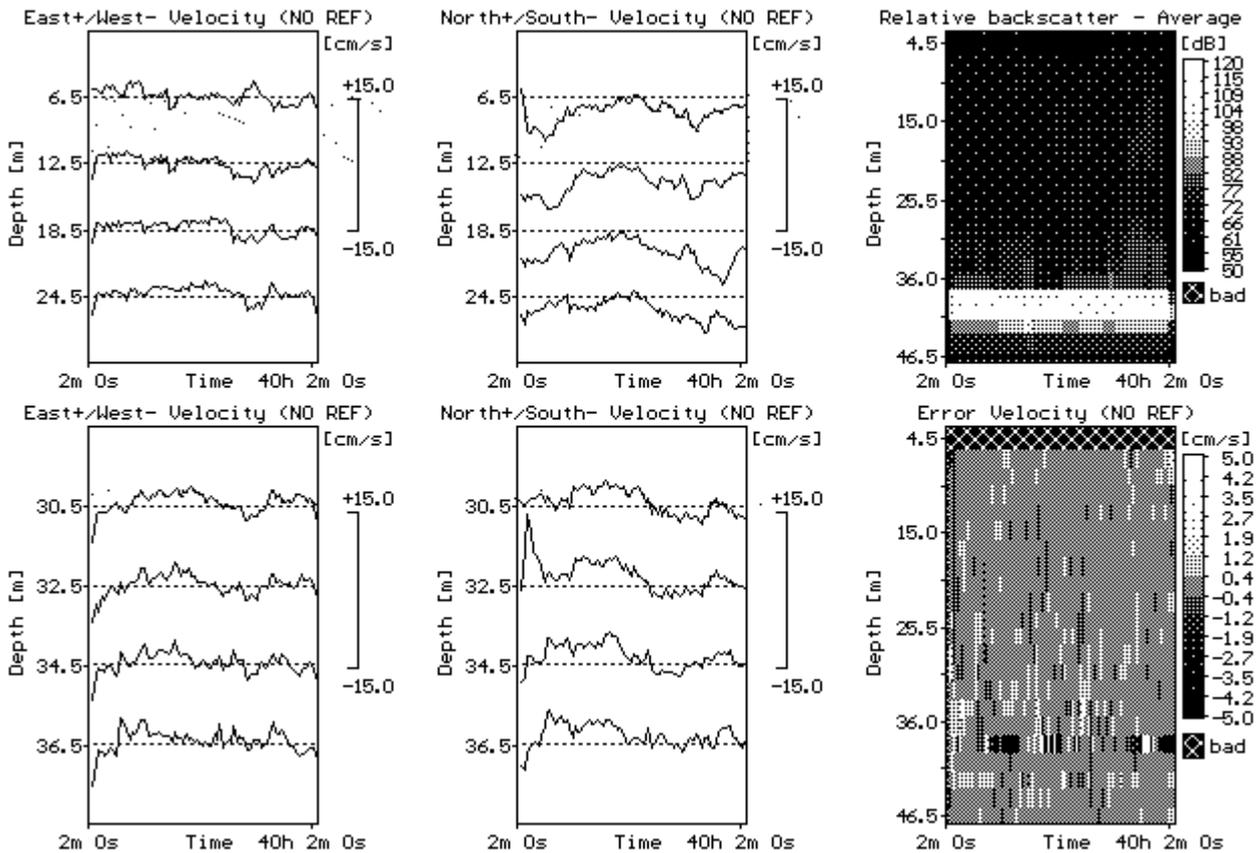
Figure 2.4.4./9. Time series of currents near Malagarasi in November 1996. Measurement period was 25.11. 14:15 - 27.11. 06:14. Water depth at the observation site was 47 m.

At the deeper observation site 5 km to west from the shallow one, currents were recorded down to 60 m. Below the depth data was biased. The currents in the eplimnion were stronger than near the shore. They seemed to correspond fairly quickly with wind speed changes compared to the layers below. During the first 24 hours the currents were heading NW. Later the flow direction of the epilimnion turned SE. The currents between the epilimnion and 45 m depth were NW. Under this layer down to 60 m they flowed SE. Maximum velocities were observed during late afternoon of Nov 25 (Fig. 2.4.4./10).

Another wet season measurement was made in April 1997. During the expedition the ADCP buoy stations were deployed in the region for 40 h starting in the evening of Apr 8. Simultaneously a rectangular of 27 km (along the eastern shore) * 9 km were sailed in the area to measure currents (Fig. 2.2./3). It took about 13 hours to sail one lap. Three laps were completed. The two ADCP buoy stations were installed at 38 m and 127 m depths in the middle of the sailed rectangular. Additionally 11 CTD profiles were taken in the region.
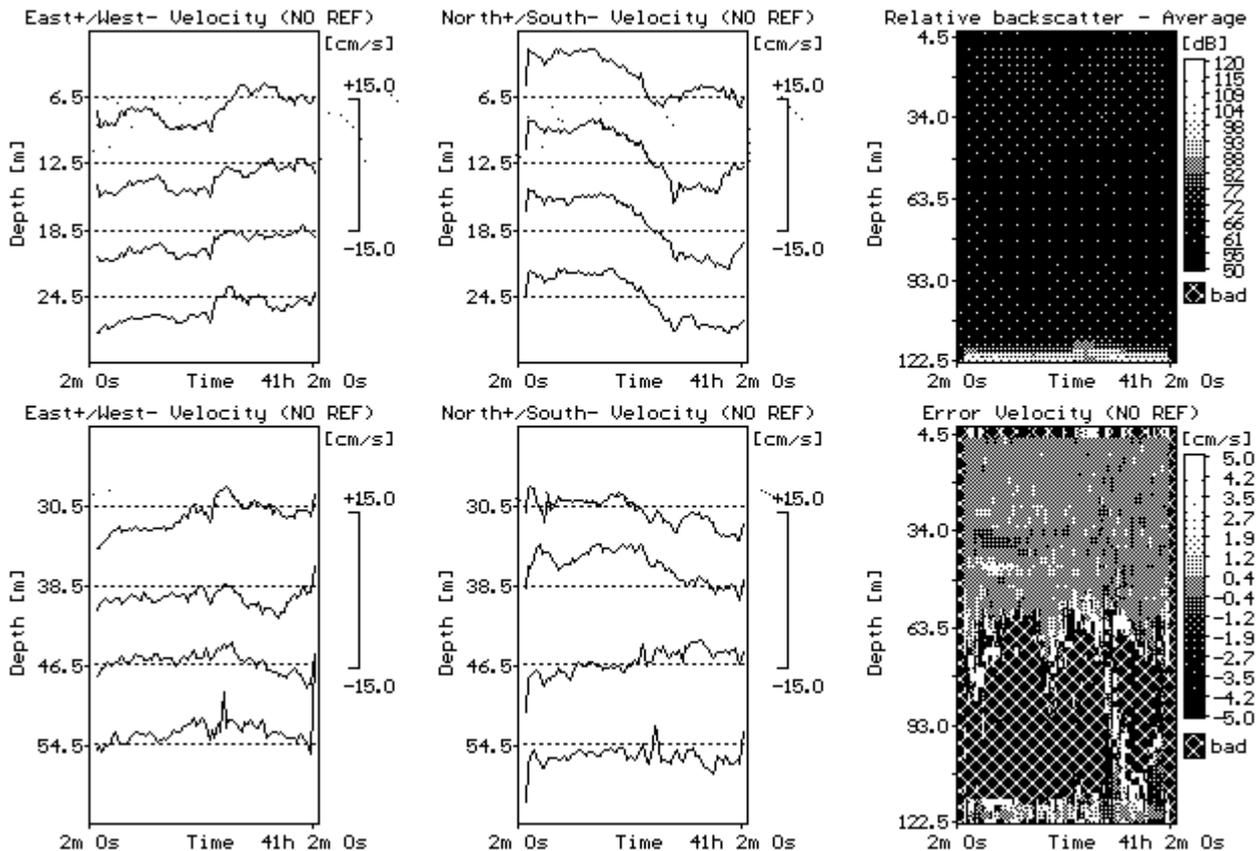
Figure 2.4.4./10. Time series of currents near Malagarasi in November 1996. Measurement period was 25.11. 14:58 - 27.11. 06:45. Water depth at the observation site was 125 m.

The wind data from Kigoma was showing a normal diurnal wind distribution with maximum values at noon except on Apr 9, when the highest wind speed of 6 ms^{-1} (hourly mean) was already recorded at 06:00 (Fig. 2.2./4).

The winds on the lake had a clear diurnal variation both in direction and velocity (Fig. 2.4.4./11). During the afternoon hours, a south westerly lake breeze prevailed with higher velocities than the easterly land breeze during the night and early morning.

A temperature profile in the region showed that in the evening on Apr 8 at the beginning of the current measurements primary thermocline was situated around the depth of 55 m (Fig. 2.4.4./8). A secondary thermocline was found around in the depth of 40 m.
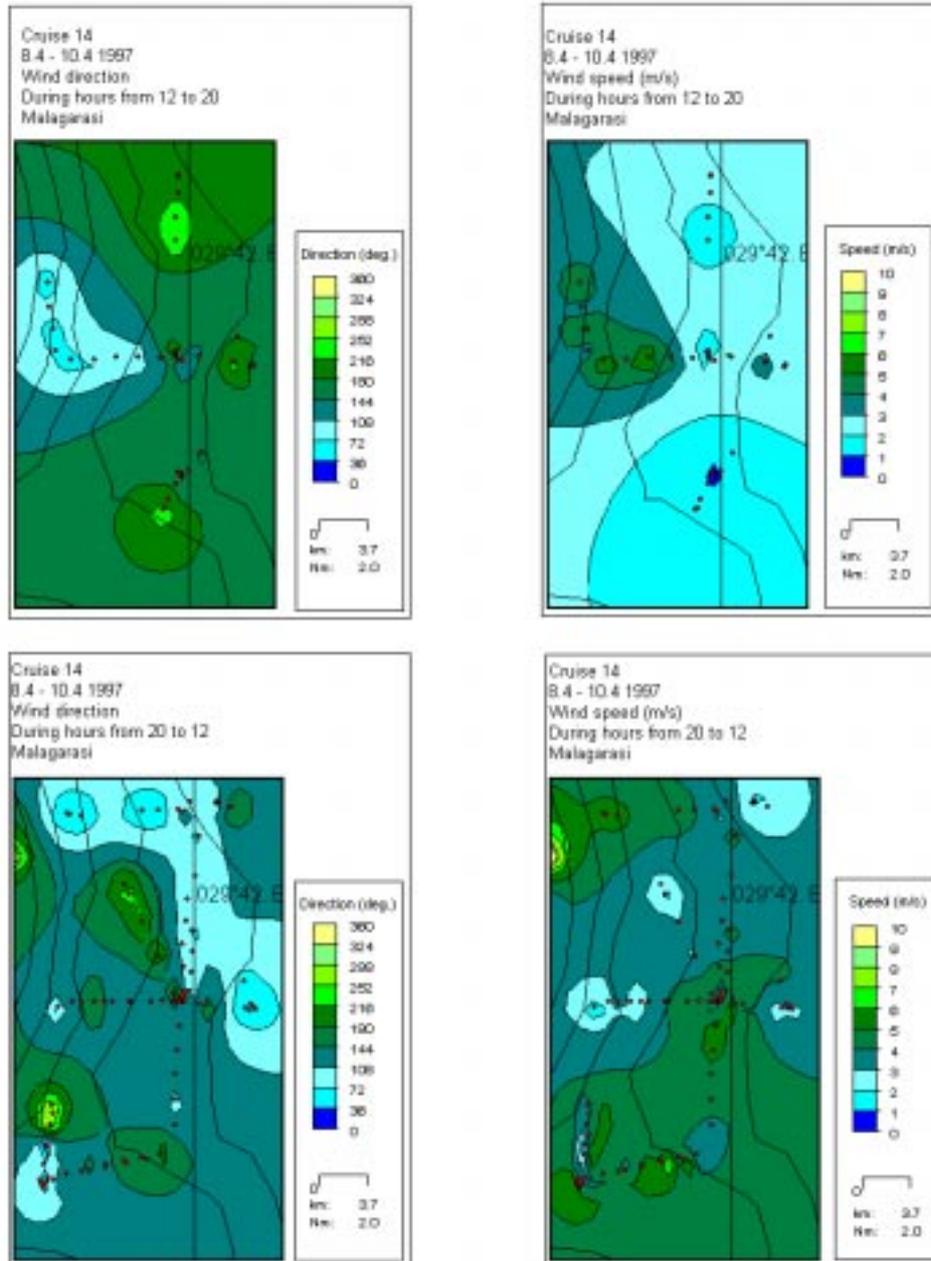
Figure 2.4.4./11 Spatial distribution of wind speed and direction near Malagarasi during April 1997 expedition. Upper figures afternoon and evening winds (noon - 8 p.m.) and lower figures night and morning winds (8 p.m. - noon).

The waters at the buoy station in the shallow waters were flowing in the two layer system (Fig. 2.4.4./12). Echo intensities increased below the depth of 33 m indicating suspended material floating just above the bottom. Recorded currents at the station were fairly slow < 10 cms[-1] throughout the measurement. Apart from the surface layer (4.5 m) they were also fairly similar at all measured depths. During the first night they were flowing W, while the waters below that were flowing S. During the daytime (Apr 9) the upper layer flowed S and the lower layer slowly E. The maximum speeds (about 7 cms[-1]) were recorded during the afternoon. The change in the pattern occurred in the evening of Apr 9 as the waters started to flow N. This direction prevailed during the following night, with maximum speeds recorded at the depth of 27 m before the sunrise.
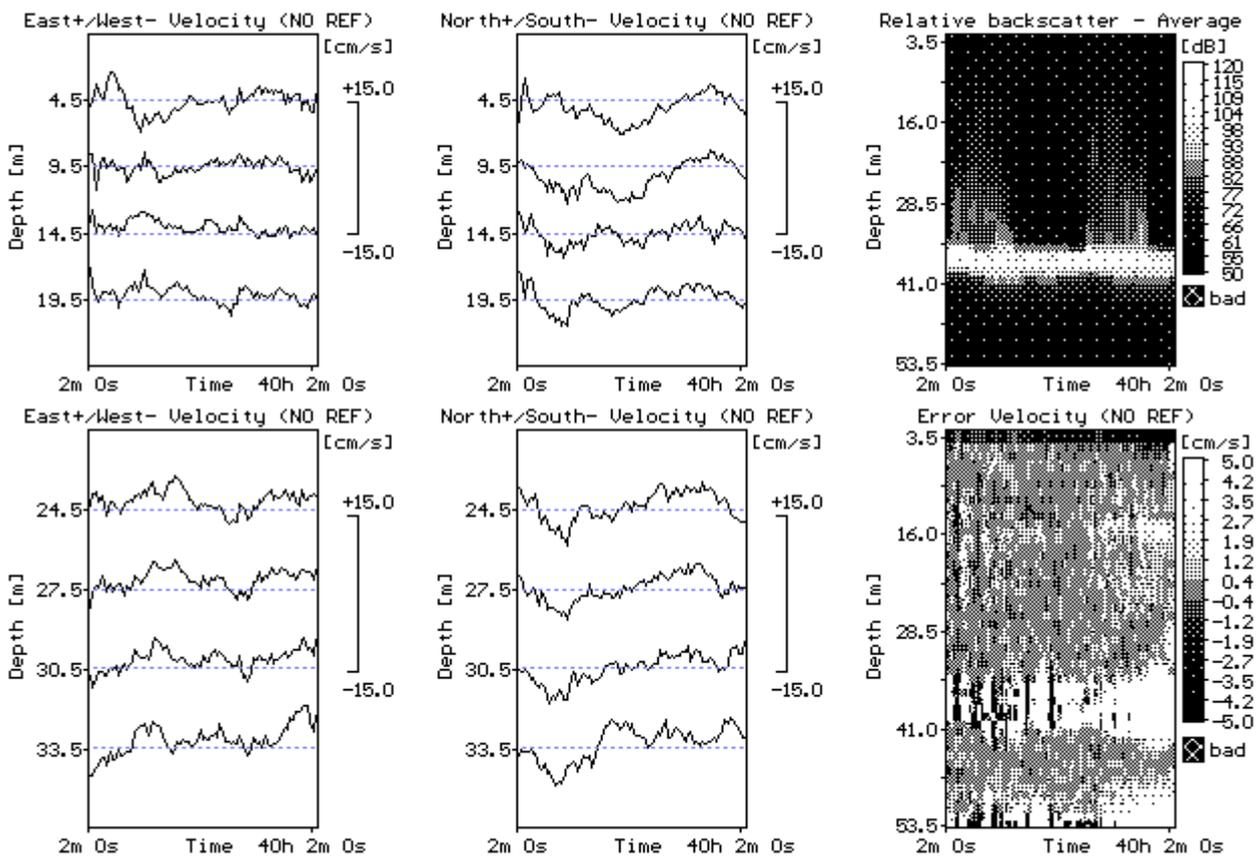
Figure 2.4.4./12 Time series of currents near Malagarasi in April 1997. Measurement period was 8.4. 18:00 - 10.4. 10:00. Water depth at the observation site was 38 m.

At the other ADCP station (127 m) unbiased data could be recorded only to the depth of 54 m. The velocities were higher than near the shore. Here also a weak two layer system was found. The upper layer (0 - 15 m) was flowing NW with maximum velocities during the afternoon. In the evening of Apr 9 the flow turned NE for a few hours. The deeper layers were flowing N with fairly good velocity (about 15 cms^{-1}). During the morning of Apr 10 the current was turning SE at all measured depths.

The ADCP on the ship was able to collect data deeper than the ADCP buoy stations, but only to 75 - 85 m. This might be due to the low amount of reflectors below these depths. There was often a maximum of reflected echo intensities at the depth of 25 - 50 m in the areas south of the river mouth. On the northern side the whole water column down to the depth of 75 m was giving a fairly even distribution of echo intensity with values corresponding to the maximum values on the southern side (Fig. 2.4.4./13). This indicates the effect of thermocline and accumulation of zooplankton above it. Below this layer it was very difficult to obtain any ADCP data. It also indicates that the river waters were mainly transported towards the north during this observation period.
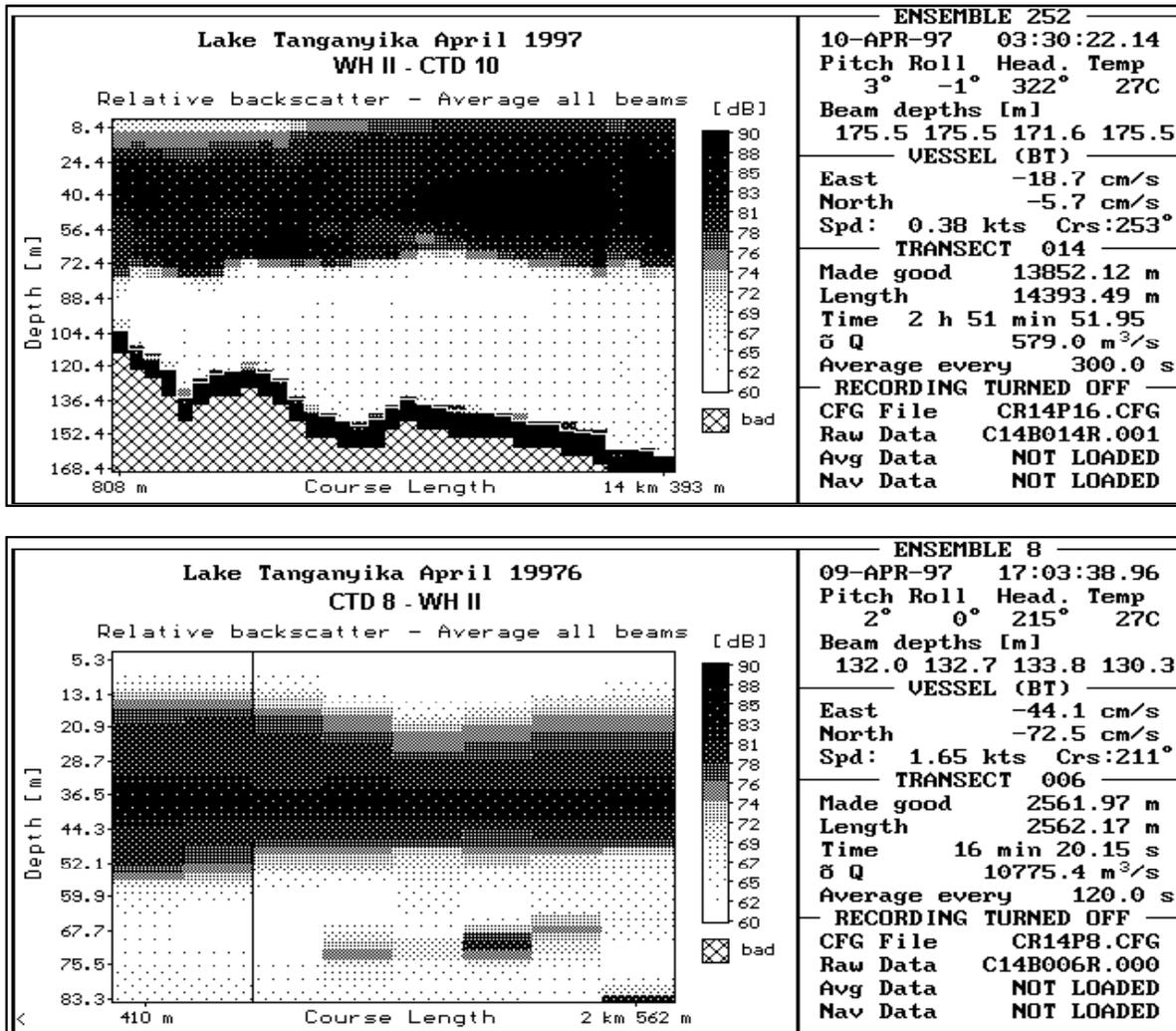
Figure 2.4.4./13 Echo intensity as recorded with the ship ADCP on a transect following the shore extending north from the Malagarasi river mouth (upper picture) and south (lower picture).

The extremely high current speeds were recorded in one afternoon with the ship ADCP in the northern part of the study area. As no reasonable explanation could be found, a possibility that wrong recording settings of the instruments were used, can not be excluded. The prevalent direction of the currents was N. This is consistent with observations from the buoy ADCP at the deeper site.

The **dry season measurements** near Malagarasi were carried out during a period of 53 hours starting from the afternoon of Aug 25, 1997 (Fig. 2.2./5). Two ADCP buoy stations were installed at the depths of 35 and 124 m. During their deployment currents were measured with the ship ADCP in the area. A rectangular of 27 km (along the eastern shore) times 9 km was sailed off the Malagarasi estuary, like during the previous intensive measurement. It took about 12 hours to complete one lap. A total of three laps were sailed and 27 CTD profiles taken during the measurements in the region.

Only vessel's wind data were available as reference wind information of the region during the measurements. The average wind speed (10 min averages) varied from 1 and 9.7 ms^{-1}. Highest

averages were recorded on Aug 26 in the morning. The wind had a diurnal cycle like had been observed during the previous cruise (Fig. 2.4.4./14).
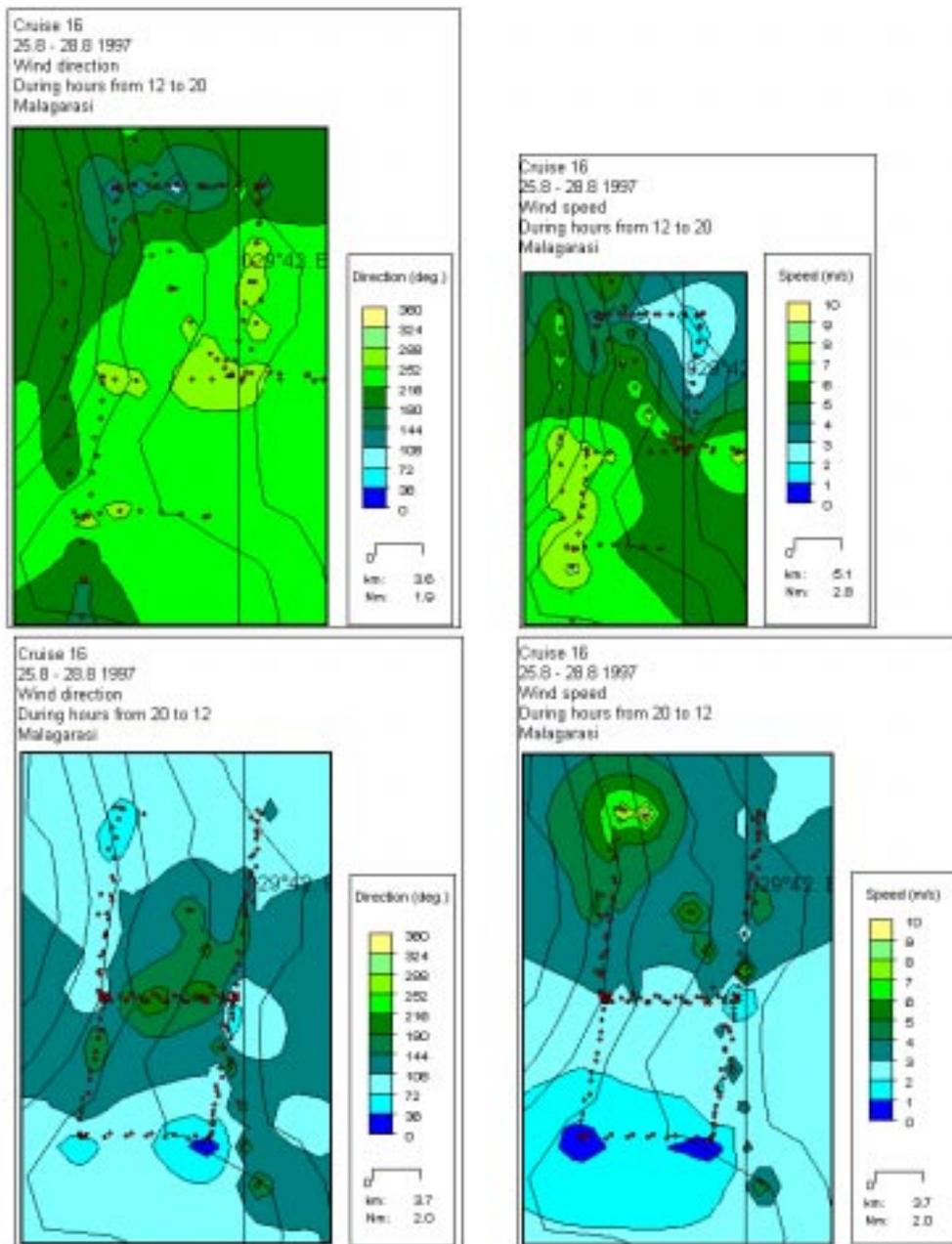
Figure 2.4.4./14 Spatial distribution of wind speed and direction near Malagarasi during August 1997 expedition. Upper figures afternoon and evening winds (noon - 8 p.m.) and lower figures night and morning winds (8 p.m. - noon).

CTD profiles showed that the thermal stratification in the area was less defined than during the wet season (Fig. 2.4.4./8). Some temperature gradients were measured, one at 35 and another one at 80 m depth, but a well-defined thermocline could not be observed.

Data that were collected closer to the shore showed that during the first day in the afternoon there were two different layers of currents (Fig. 2.4.4./15). The boundary between the two layers was at the depth of 15 - 17 m. The upper layer was flowing E and was probably induced by the W wind.

The lower layer flowed W or NW. The maximum velocity in the upper layer was observed around 4 p.m. In the evening the currents in the upper layer shifted to the W - NW and current speed was fairly consistent through the whole column. During the afternoon (Aug 26) the waters were again flowing as a two layer system similar to the previous afternoon. The system changed to a one layer flow later in the evening as in the previous evening.
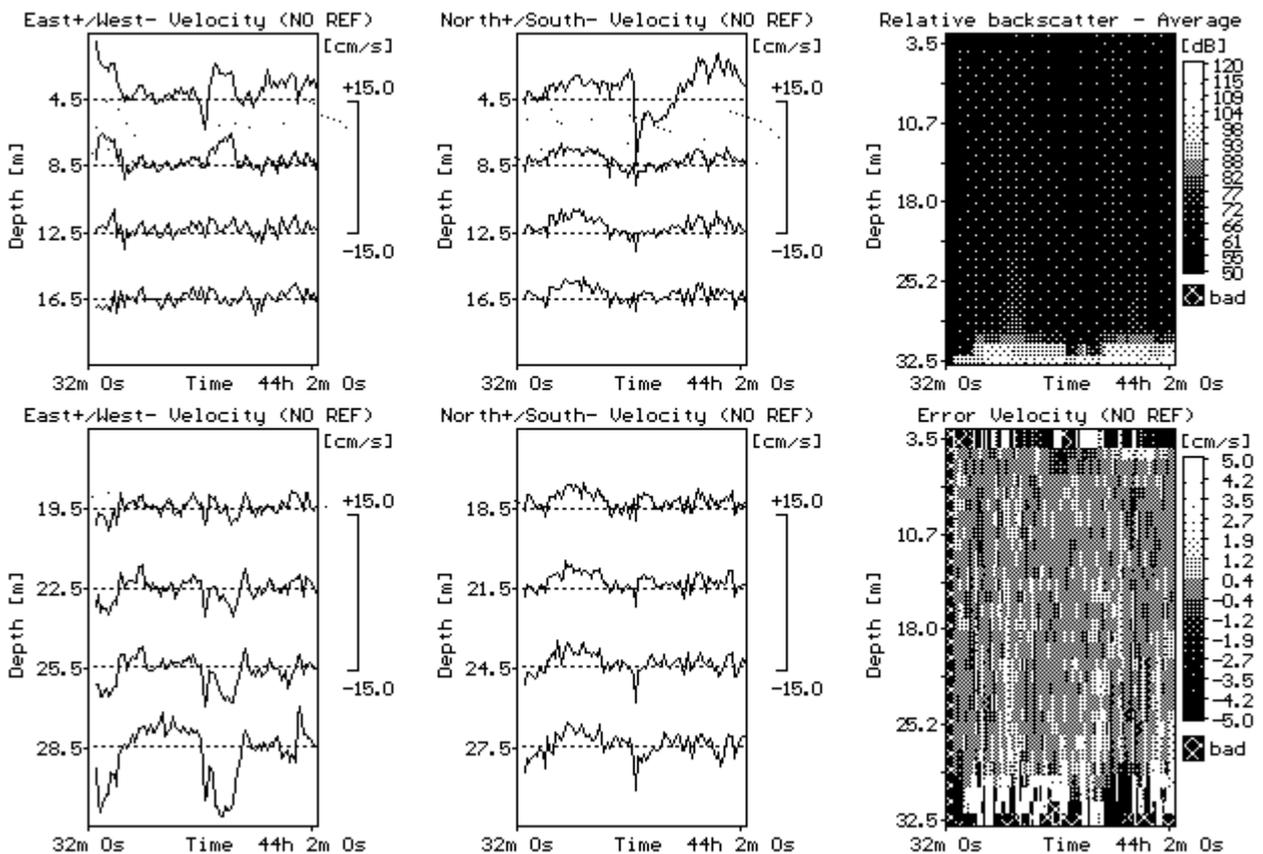
Figure 2.4.4./15 Time series of currents near Malagarasi in August 1997. Measurement period was 25.8. 14:24 - 27.8. 09:52. Water depth at the observation site was 35 m.

At the deeper ADCP station data could be collected down to 50 m. In general current speeds were higher than those close to the shore (Fig. 2.4.4./16), a resemblance between the data of two stations were observed. Also here two different layers could be distinguished. The upper layer reached to 13 m and was flowing NE. The deeper layers flowed slowly NW. The currents in the upper layer shifted NW in the evening. Then the direction turned more and more W with increasing speed until the following noon. At noon there was a short decrease in the current speed and then it turned to flow NE and E.

North+/South- Velocity (NO REF)

East+/West- Velocity (NO REF)
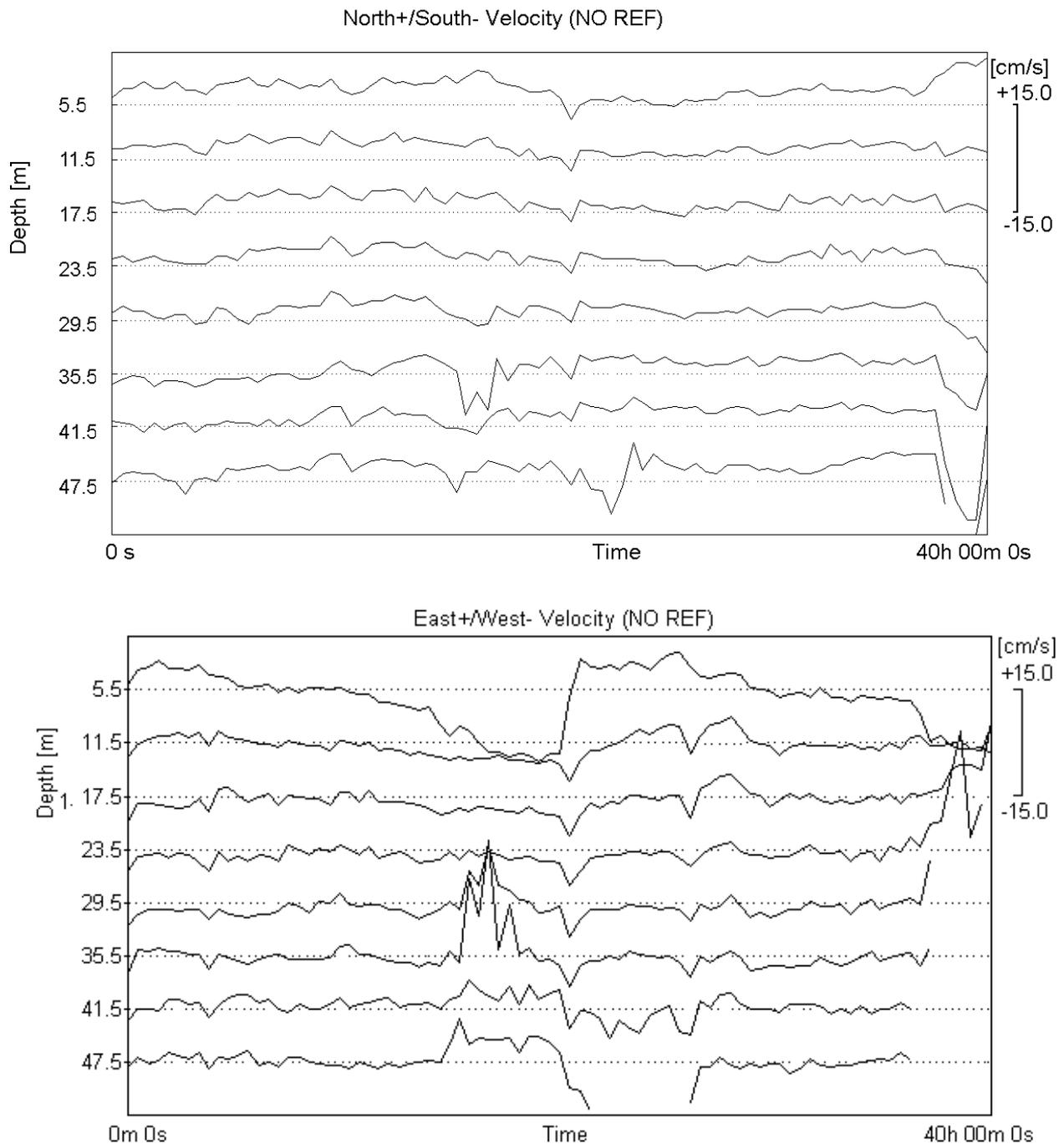
Figure 2.4.4./16 Time series of currents near Malagarasi in August 1997. Measurement period was 25.8. 13:52 - 27.8. 09:26. Water depth at the observation site was 124 m.

In the deeper layers the northerly current prevailed. Quite high current speeds were observed on Aug 26 daytime below the secondary thermocline.

For some reason, maybe bed cable connections, data with the ship ADCP could be gathered only during the nights. Even then only 60 - 70 m depth was reached due to the low amount of reflectors. Therefore, it is impossible to compare the daytime results of the ADCP buoy stations to the results of the ship ADCP. The nighttime data of the ship ADCP showed that the upper layer down to 30 m

flowed N - NW. In the south-western part of the study area was distinguished a layer at the depths at the depth of 30 - 65 m which was flowing SW - SE. On the line along the buoy stations during both nights the waters seemed to flow as one water mass with slightly more westward component near the surface as in the deeper layers. The speed of the currents decreased near the shallow end of the transects. Along the westernmost transects the highest velocities were recorded. The flow was mostly NW-NE in the layer of 0 - 45 m. There were some indications of strong eastward flow above thermocline during the first night but it was not observed during the second night.

The measurements have shown that the currents in this region have a two layer system. The boundary was in the early part of wet season (Nov 1996) at the depth of 25 m. The data from buoy stations showed that this boundary at the end of wet season was situated at the depth of 30 - 35 m as at the end of the dry season 1997. The data from ship ADCP gave the same boundary, at the depth of 30 m. This was the depth of well mixed surface layer.

The upper layer obtained momentum from the local lake land breeze wind and moved accordingly with a relatively high velocity, whereas the lower layer moved slowly with forcing over a longer period. For a short period the diurnal cycle of local winds causes the upper layer to flow in the same direction as the lower one. There was also some spatial distribution in the current pattern. The offshore buoy station and ADCP transects data showed that the velocities were higher offshore than near shore. This was the case for both the wet and dry season.

The **strait between the Kungwe mountains and Kalemie** separates the north and the middle basins of the lake. It is an important area of water exchange between the two areas. Current measurements were conducted in this region during each expedition.

For the first wet season measurements during expedition 10 two transect lines, numbers 78 and 79, were chosen on Nov 23, 1996 early in the morning (Fig. 2.4.4./17). The wind was weak and coming from the NE (speed < 5 ms^{-1}) during the first transect. But during the last hour of this transect (03:00 - 04:10) wind velocities increased to 8 and further to 14 ms^{-1} and blew from the SE until the end of the measurements.

Figure 2.4.4./17 The currents from the uppermost observation layer as 120 s mean values along transects in the strait between Kungwe and Kalemie on Lake Tanganyika. Expedition 10, November 1996.

The ADCP gave reliable data on current speeds down to the depth of 90 m. The flow in transect 78 was S on the eastern shore but turned E more off shore simultaneously with the increasing NE wind. The effect of the wind could still be seen at the beginning of the next transect 79. The wind blew from the SE and pushed the surface waters along. After wind velocity decreased the direction of the main flow turned S.

During another wet season measurement (Apr 11, 1997 around noon) the flow very near the eastern coast (0 - 6000 m) was now directed N with a high speed in a layer from 0 to 50 m (Fig. 2.4.4./18) and with a slow velocity in the layers below. Further along the transect the same flow prevailed up to the region, where the water was more than 400 m deep. There it was observed that the northward flow decreased. When moving further along transect towards Kalemie, the southward flow started to appear.
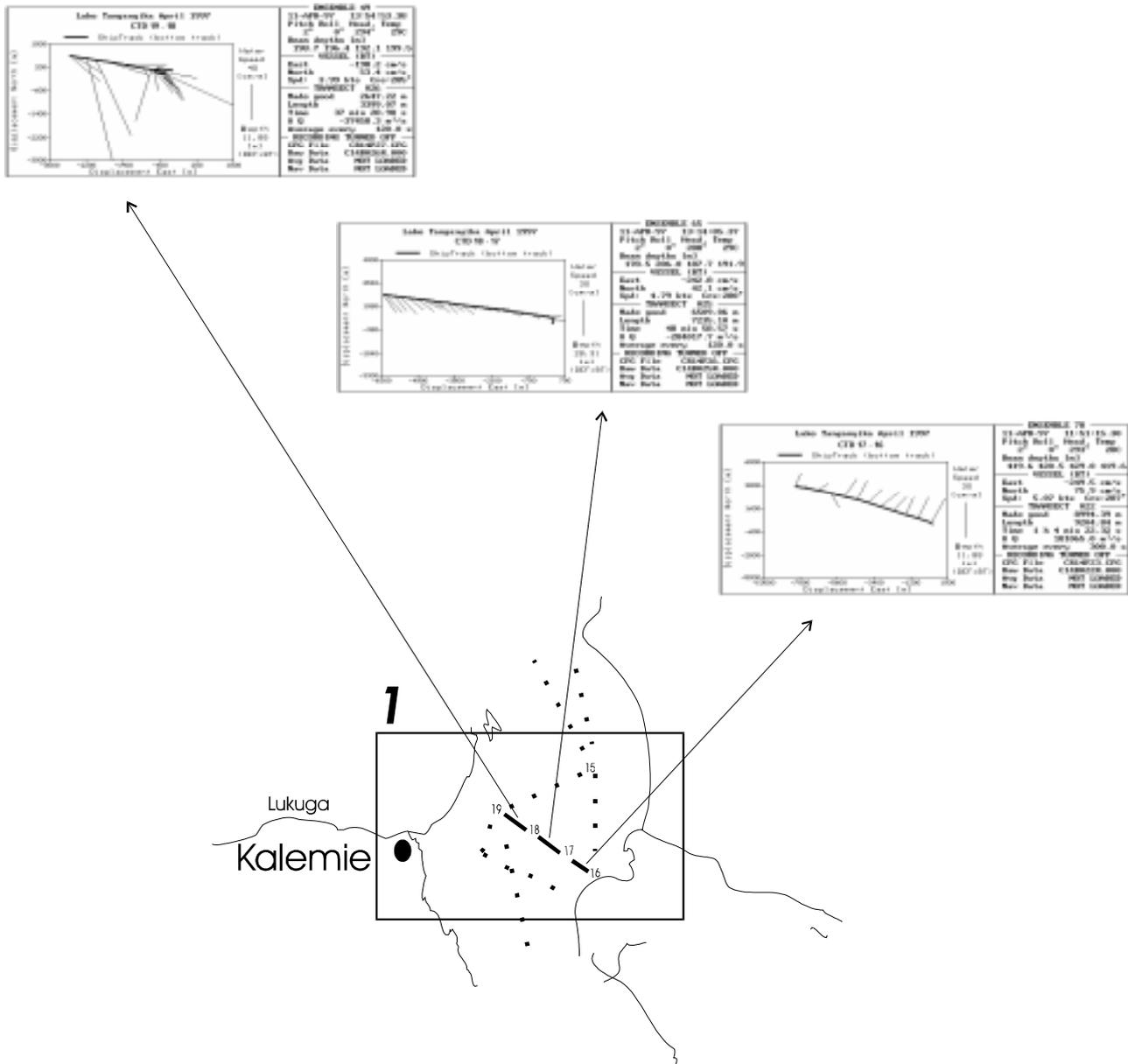
Figure 2.4.4./18 The currents from the uppermost observation layer as 120 s mean values along transects in the strait between Kungwe and Kalemie on Lake Tanganyika. Expedition 14, April 1997.

It has to be noted that in the very early morning on April 11 at Kabogo point a N flow was also measured in the upper part of thermocline. There the epilimnion was moving S.

During the dry season expedition 16 current measurements were conducted in two different time periods (Fig. 2.4.4./19). The first three transects recorded were the same as in April (54 - 57). The measurements were done on Aug 28 during the night and the other three lines a few days later, on Sep 2 - 3, more south (transects 90 - 93).

The wind was weak, < 5 ms^{-1}, during the first measurements. It blew from the SE during the first transect, then shifted to the NE and later again SE. In September wind speed was 2 - 5 ms^{-1} but increased during the second transect up to 11 ms^{-1}. The wind direction was first SW but turned later to blow from the SE.

The flow in the transect 57 - 56 was at the beginning SW, but turned closer Kungwe, the eastern shore, towards the N. In the westernmost transect (55 - 54) the surface waters (0 - 30 m) flowed N as the waters in deep layers, although their velocity was higher. (Fig. 2.4.4./20).

A few days later in the same region the measurements were carried out in the middle of the strait south from Kalemie. The ship first headed towards the shore, then turned N and then W. Measurements along the first transect (90 - 91) gave rather high flow velocities to the N except at the depths below 60 m which flowed slowly, moving S. Flow velocities at the surface were lower in the next transect (91 - 92) but their direction was also N or NW. In the deeper waters flow direction was W. When the ship headed W flow direction was found to be N or NE.

The currents in the region had fairly high speeds both during the wet and dry season, although the winds were not very strong during all the measurements. Therefore, it seems that the local wind can change the surface current pattern for a few hours, but there is no evidence of a persistent strong diurnal cycle of currents in this region.
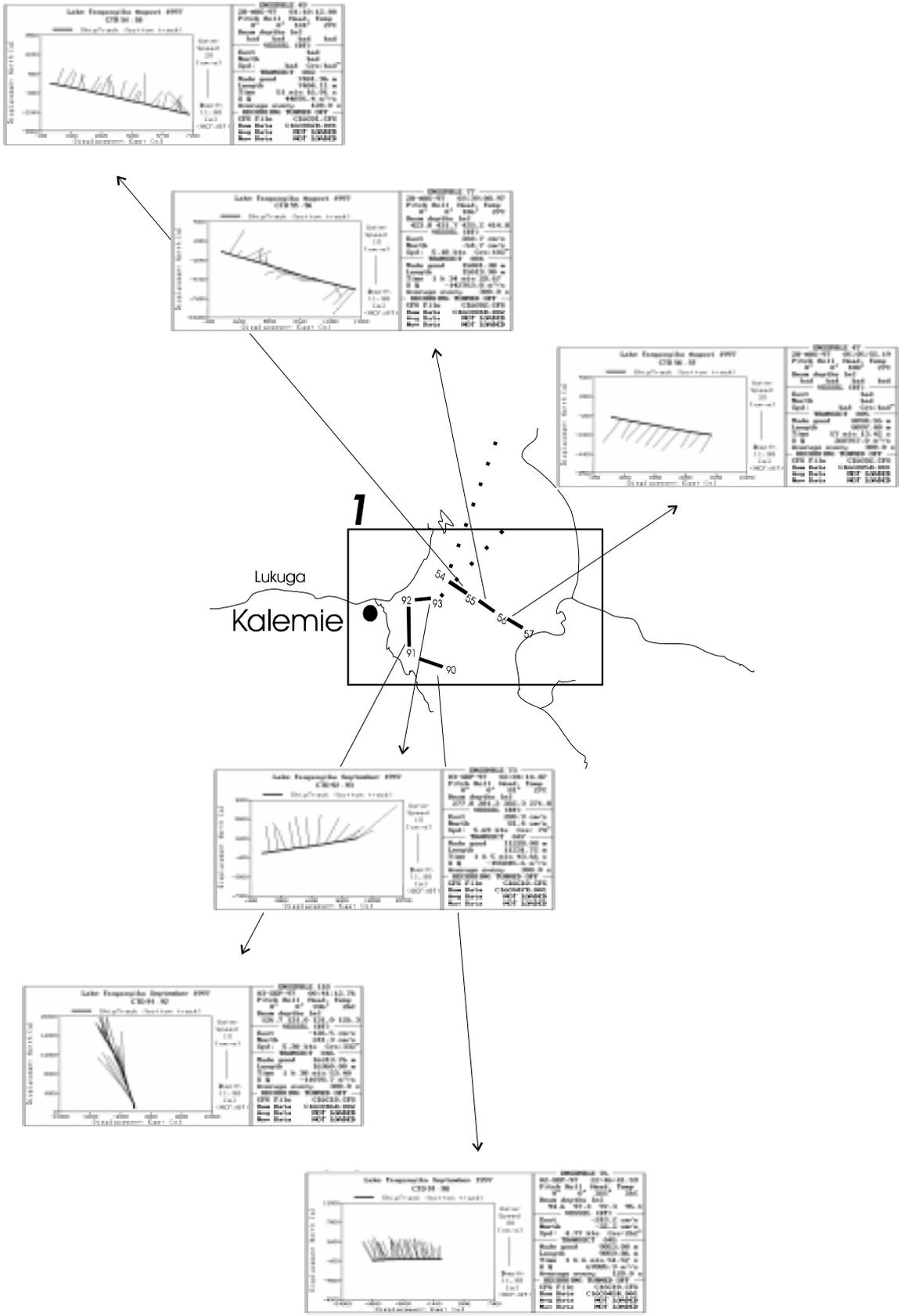
Figure 2.4.4./19 The currents from the uppermost observation layer as 120 s mean values along transects in the strait between Kungwe and Kalemie on Lake Tanganyika. Expedition 16, August 1997.
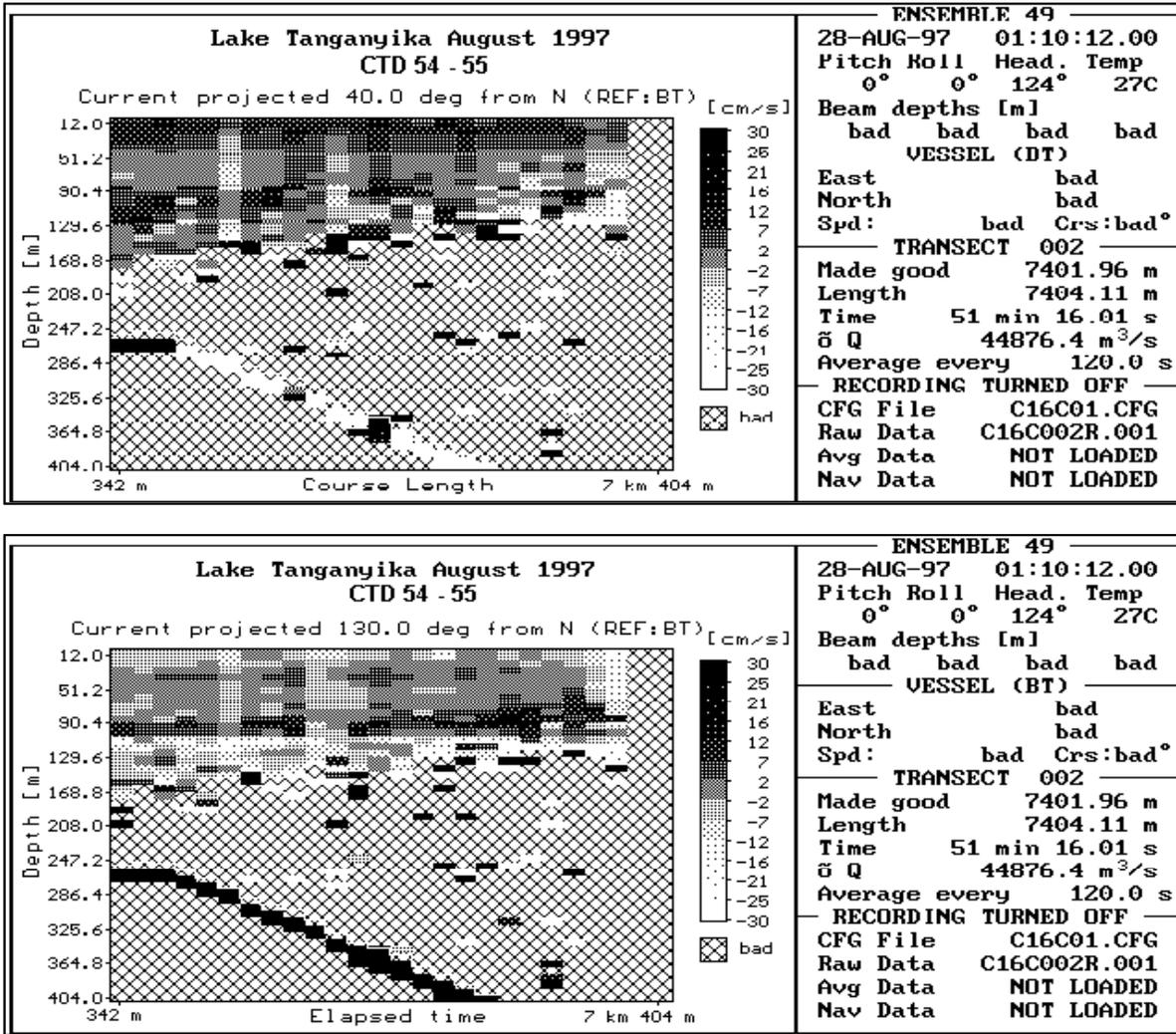
Fig 2.4.4./20 Water currents along the transect 54-55 in the strait between Kungwe and Kalemie on Lake Tanganyika. Expedition 16, August 1997. The currents are presented as components along the coast (upper panel) and components towards the coast (lower panel).

This measurement **area in the middle part of the lake** is dominated by a threshold which between the South Basin and Middle Basin. This region was selected on the basis of the LTR circulation model results. The model showed high current speeds especially along the eastern shore around the Utinta - Karema region (Podsetchine and Huttula, 1996).

The first **wet season measurement** near **Utinta** was carried out in the afternoon of **November 17, 1996** with a buoy ADCP. The water depth at the site was 70 m. A local CTD profile in the morning revealed that epilimnion was well mixed after the nocturnal convection and that the primary thermocline was situated between the depths of 60 - 70 m. At 16:10 a new secondary thermocline at 10 m depth was found. The depth of the primary thermocline was still at 60 m. The wind speed observed on ship was 4 to 6 ms^{-1} and direction from NE.

A short transect was measured in the evening with the ship ADCP. It showed a fairly steady SW current (with speed of 15 cms^{-1}) at all measuring depths. The results coincided very well with the results of the buoy ADCP. Both instruments gave the same current structure: in eplimnion a SW flow and in hypolimnion NE flow.

After the ship returned from south on Nov 22 early in the morning another set of measurements were carried out in this region (Fig. 2.4.4./21). This started near Utinta and continued along the coast to Kibwesa and further towards Kungwe.

In the morning on transect 61 (along the coast from Utinta to Karema) the wind speed varied from 3 to 8 ms^{-1} and the direction was from the NE. It turned SW during the last hour of this measurement. In the evening it turned back NE and velocities increased to 13.5 ms^{-1}.

The buoy ADCP was able to collect data down to the depth of 126 m. In the beginning of the transect 61, north of Utinta, the flow direction was NE down to the depth of 40 m. However at the end of the line, the flow turned NW as the wind blew from the NW. Below 40 m depth the main direction of the flow was SE. After intensive measurements near Kibwesa transects W and then N were covered. In transect 74, the flow at the surface (0 - 15 m) was SE but below that down to 60 m the current velocity was very high and it was directed NW. The effect of growing wind velocities in the evening was clearly seen in the surface current speed as current velocities rose at the end of the line. Current velocities stayed high during the rest of the measurement period. The current was first to the E (75) but turned SE for the rest of the two transect lines (77 - 78).

Between the long transects measurements discussed above the intensive measurements near **Kibwesa** were done with two buoy ADCP's during the afternoon and with the ship (Fig. 2.2/1). The water depth at the buoy sites were 112 and 128 m. The distance between the buoys was about 9 km. The ADCP transects formed a rectangular of 4 km * 7 km.

A CTD was taken on Nov 22 before the ADCP-buoy deployments (Fig. 2.4.4./22). The stratification was not very clear. The thermocline was at the depth of 60 m. Winds recorded on the ship presented W and SW lake breezes, with speeds of 6 - 11 ms^{-1} during the afternoon Nov 22.
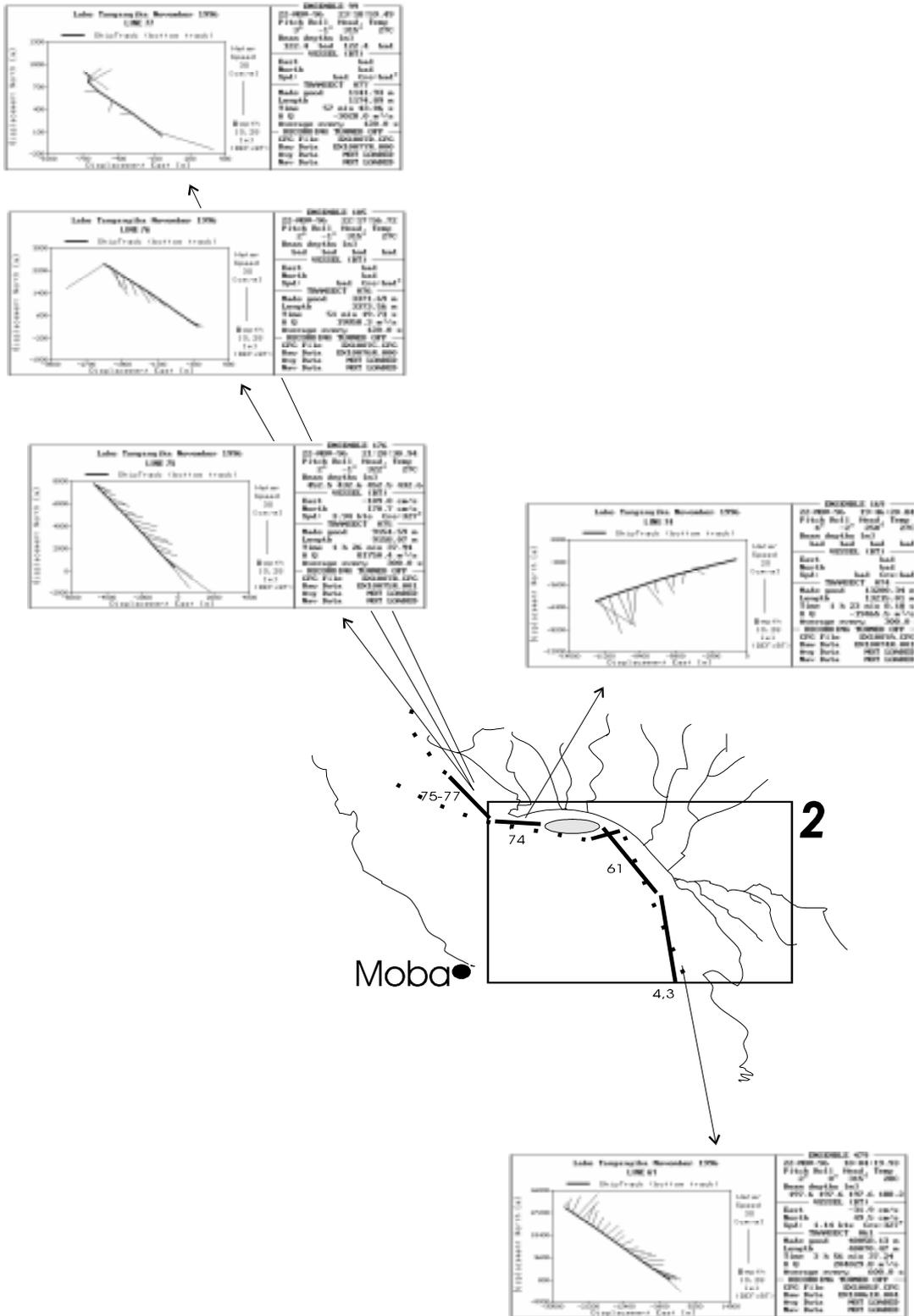
Figure 2.4.4./21 The surface currents along the transects in the Kibwesa - Utinta region of Lake Tanganyika. Expedition 10, November 1996.
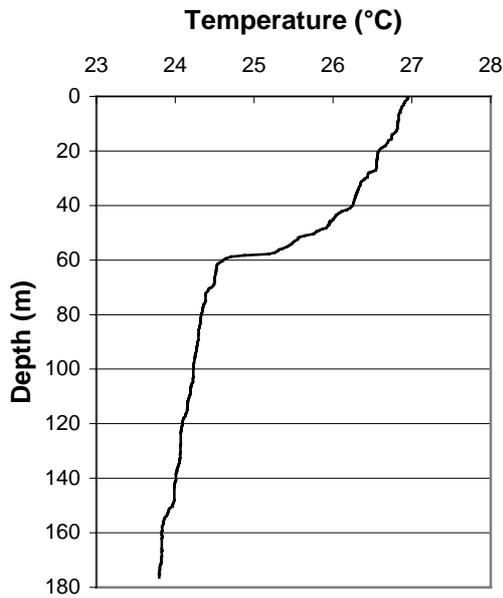
Figure 2.4.4./22 Water temperature profile near Utinta in the morning during November 1996 measurements.

The flow speed below the epilimnion was < 10 ms^{-1}. The boundary of the two layers was at the 55 m at the off shore station and 45 m at the station closer to the shore (Fig. 2.4.4./23).
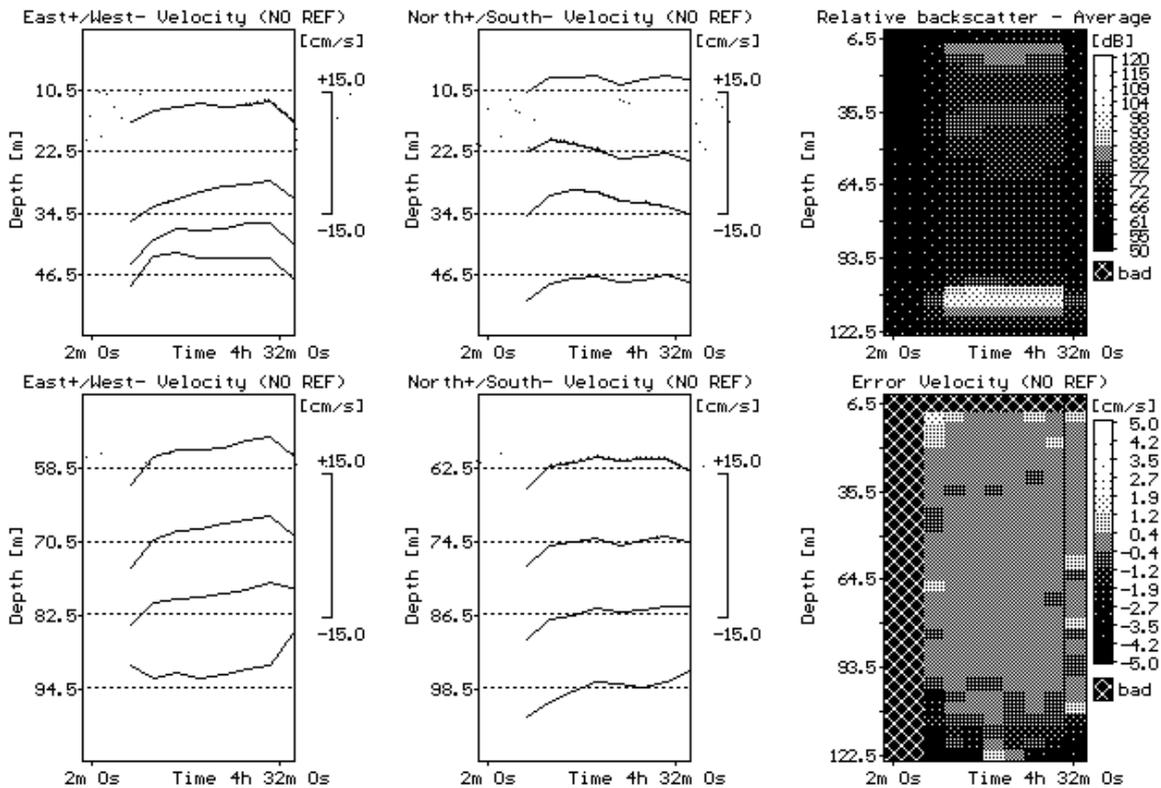
Figure 2.4.4./23 Time series of currents near Kibwesa in November 1996. Measurement period was 22.11. 14:28 - 22.11. 18:02. Water depth at the observation site was 128 m.

More offshore the boundary layer (between the two water masses) was in the thermocline at 60 m. This was recorded with the ship ADCP on R/V Tanganyika Explorer. Near shore close to the surface the flow was to the E, and below the thermocline to the SE. The latter was fairly strong.

In **another wet season expedition** (Exp 14, April 1997) the current measurements in the region were carried out during a period of 17 hours starting south of Kibwesa (Fig. 2.4.4./24). In the previous night a storm had passed the region. Maximum observed SE wind speeds were > 20 ms^{-1}. In the following afternoon moderate winds (5 ms^{-1}) from the S were recorded. Thermocline was situated at the depth of 30 m.

After the storm and due to the shape of the shoreline the SW current was very strong near the Kibwesa point. The maximum current speeds were now about 40 cms^{-1}. Within thermocline the water flow was directed W and NW in the region where water was shallower than 400 m (26 - 27). In the deeper waters the surface flow was directed S (28 - 29) and just above the thermocline waters turned E.

When heading east towards Karema during the early evening, the wind speed increased, turning to blow from the E. The surface current speed was now less than near Kibwesa. It flowed N at the beginning of line and later near the coast it turned W indicating the effect of land breeze (29 - 30 - 31 - 32). The waters in thermocline were flowing at a higher speed N than the waters near the surface. The velocity of the thermocline flow increased as the very northernmost canyon of 750 m was passed. From that region to Karema velocity in the layer remained about the same. The velocity of the near surface layer increased and turned N.

A transect along the shore was sailed after the midnight from Karema to Utinta. The observed current speeds were high and consistent in direction following the coast (e.q. 33 - 34). The direction of water flow was constant down to 70 m. The velocity within the thermocline was less than near surface. The wind ceased during the measurements.

Near Utinta a strong NW current with velocities about 30 cms^{-1} was observed for the whole eplimnion, which was thicker here than near Kibwesa and Karema (35 - 36). Also the waters in thermocline moved with small velocity in same direction.

During the dry season eight transects were measured on Aug 28 - 29, 1997 in a similar manner as in April 1997 in the Kibwesa-Utinta region (Fig. 2.4.4./25). Wind velocities were highest at the beginning of the measurement period (5 - 8 ms^{-1}), but ceased towards the evening and night (1 - 5 ms^{-1}). The wind direction changed from the SE and SW back to the SE and during the evening and night wind blew from the NE. CTD measurements showed that thermocline was situated at the depth of 50 m.

In the first transect 10 km from Kibwesa to south flow velocities were rather high and the direction of surface flow was SE (Fig. 2.4.4./25, 58 - 59). The following two transects (59 - 60 - 61) showed different flow pattern. Velocities were still high but the direction of flow was W or SW. The ship was then turend E towards the coast (61 - 62). Flow velocities were highest below 50 m and directed towards the S. In the transect 62 - 63 S flow continued only in the deeper layers. The surface flowed NW. In the deeper layers the flow direction also suddenly changed NW at the end of the line (Fig. 2.4.4./26). The flow direction changed again when approaching the shore, below 50 m

depth the flow direction was S. For the next two transects along the coastline the velocities were quite high and direction NW except below 50 m where flow was N.
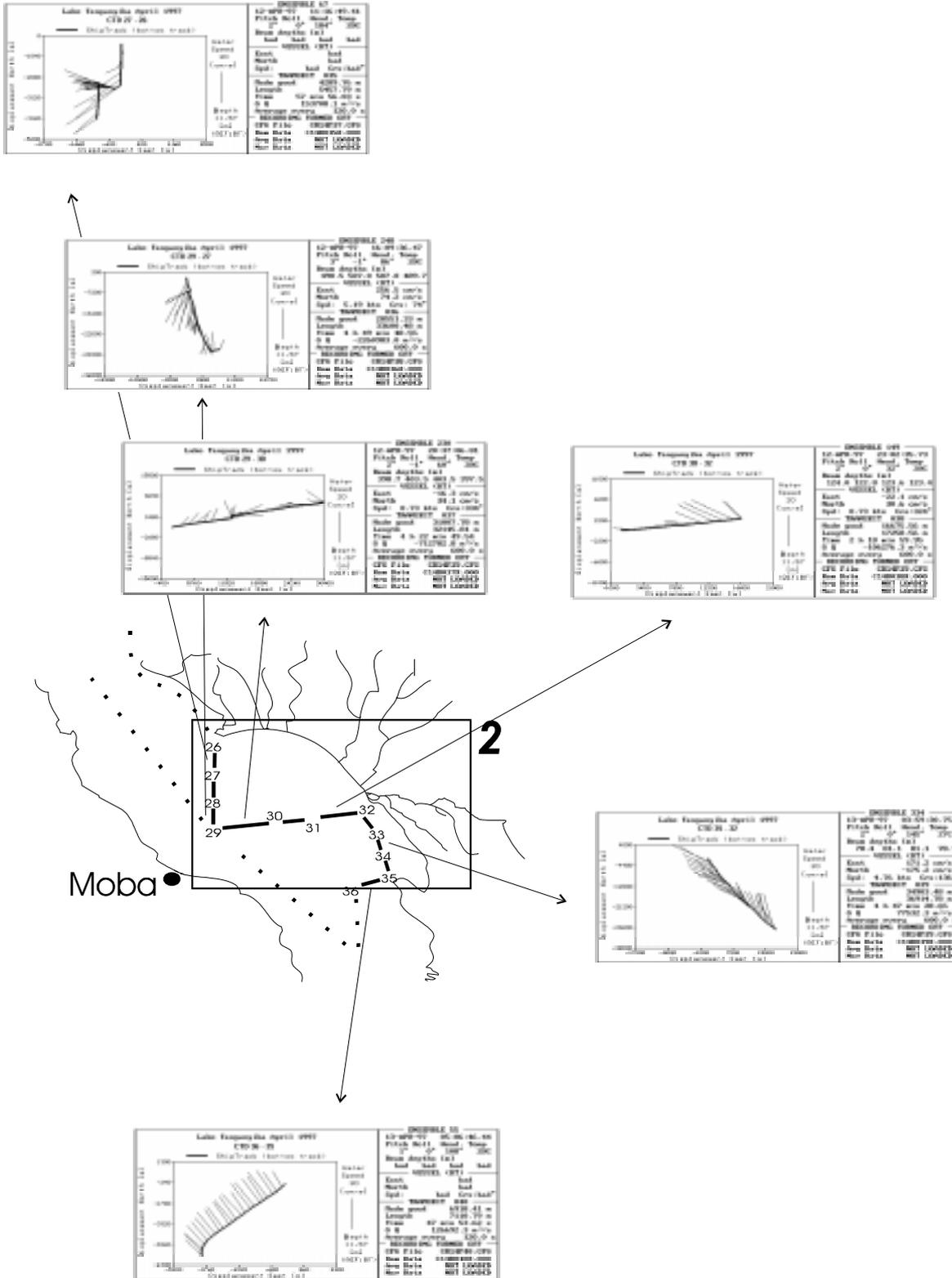
Figure 2.4.4./24 The surface currents along transects in the Kibwesa - Utinta region of Lake Tanganyika. Expedition 14, April 1997.
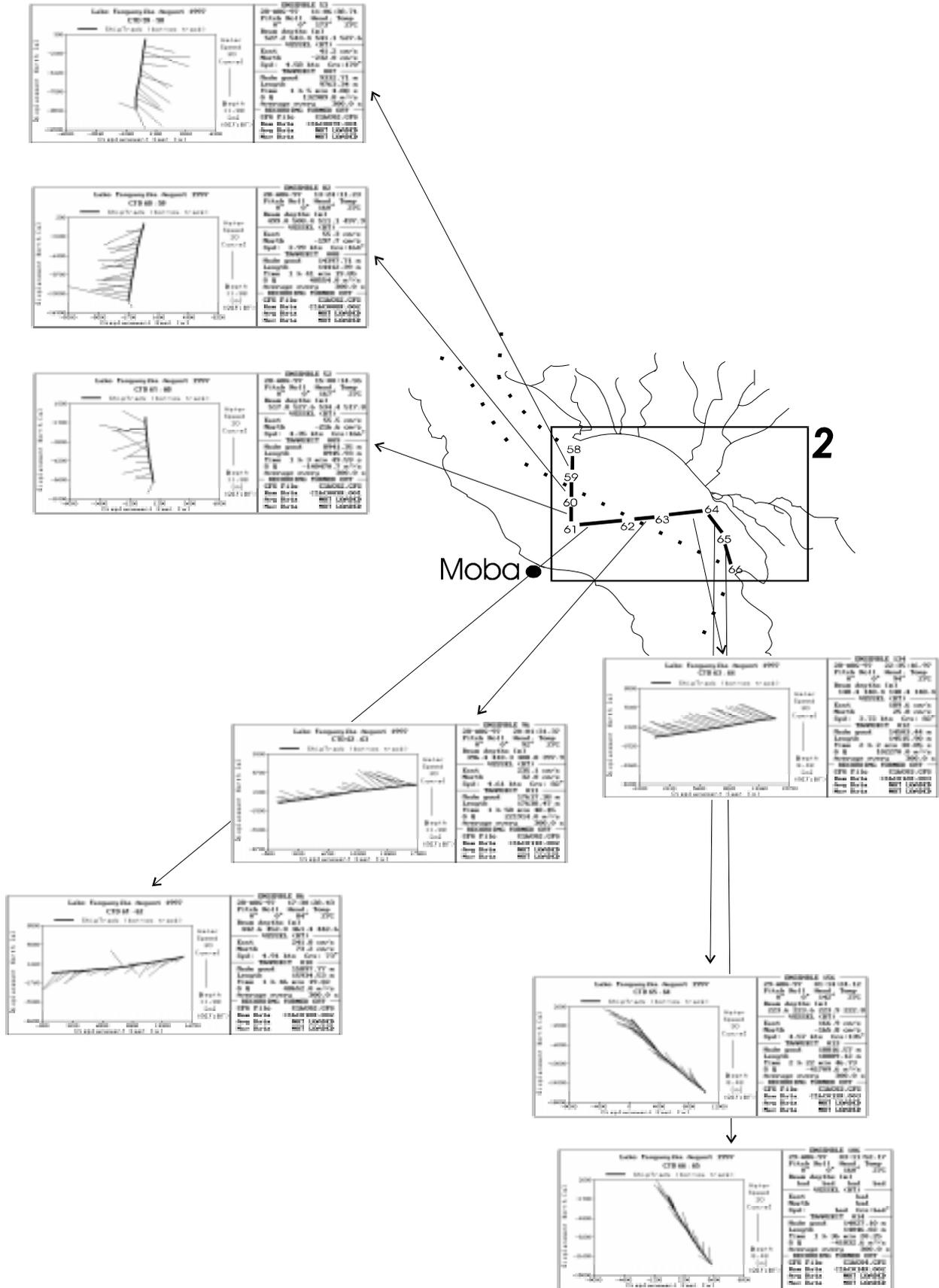
Fig 2.4.4./25 The surface currents along transects in the Kibwesa - Utinta region of Lake Tanganyika. Expedition 16, August 1997.
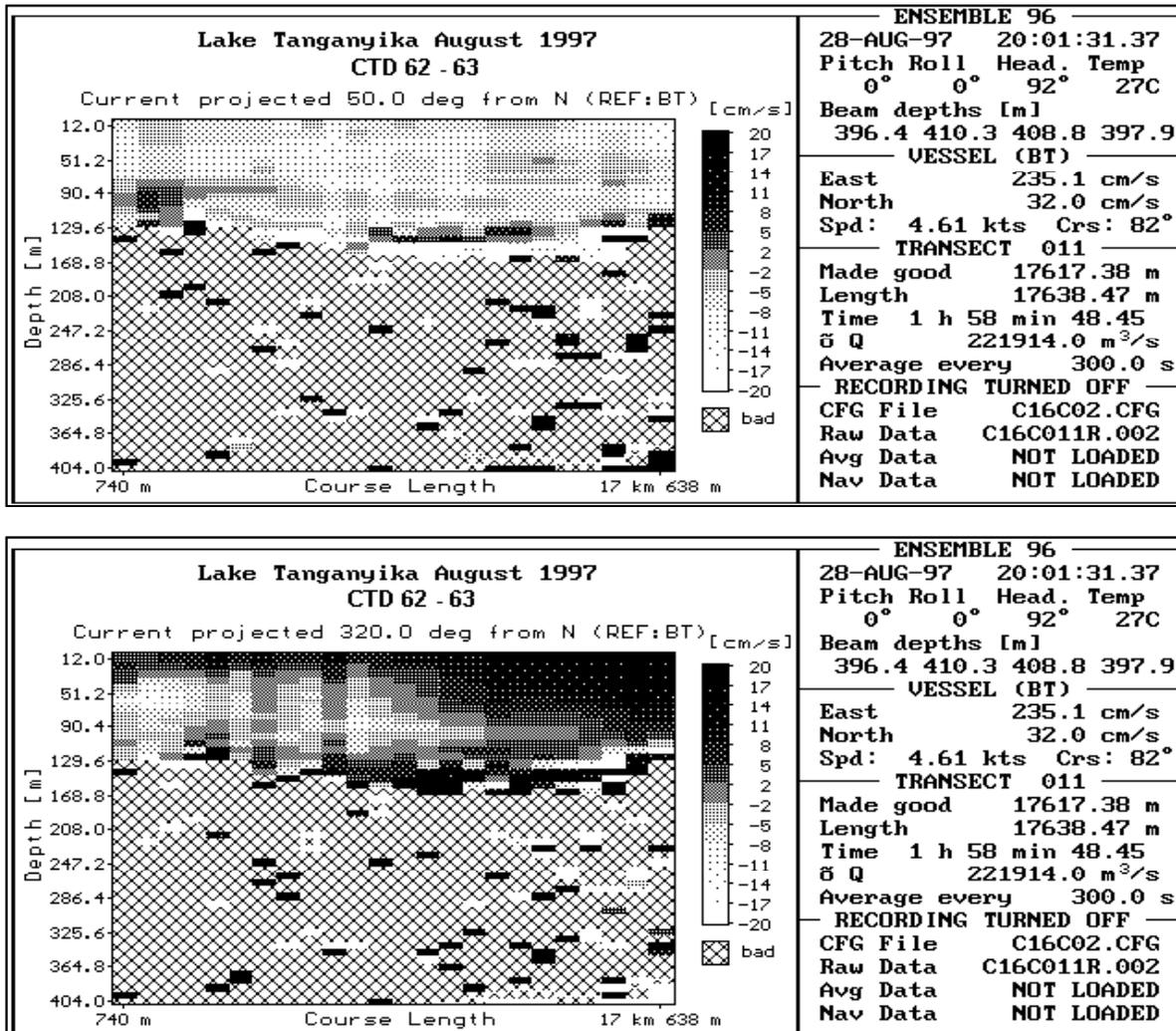
Fig. 2.4.4./26 Water currents in along transect 62 - 63 in Karema region on Lake Tanganyika. Expedition 16, August 1997. The currents are presented as components along the shore (upper panel) and perpendicular to the shore (lower panel).

In general currents in this region had high values both in eplimnion and also in thermocline. It was possible to measure the currents fairly deep. In the region north of Utinta a N flow was observed in the surface layer both at the end of wet season and in the dry season during the night hours. In the early morning hours of November measurements the flow was obviously affected by the lake breeze.

The Kibwesa and Utinta regions revealed a typical current pattern for a steep nearshore region, with a high speed of currents along the shore in the coastal area. Due to the coast it differs from the offshore flow in direction with no or minor coastal effect. This was observed both in the wet and dry season during daytime measurements near Kibwesa.

The **southern part of the Lake** is referred to here as the 'Mpulungu basin' and 'Mplungu region'. This area is known to be the most dynamic. Thus the current measurements were especially concentrated here.

I**n November 1996** five transects were covered on Nov 20 - 21. In addition to the measurements on these lines, intensive measurements were done outside River Lufubu. Quite moderate winds from the N or NE prevailed during the whole measurement period (Fig. 2.2./2). Only at the very beginning of the first line was the wind blowing from the NW. The stratification was very linear. The lower boundary of surface layer was at the depth of 80 m (Fig. 2.4.4./27).
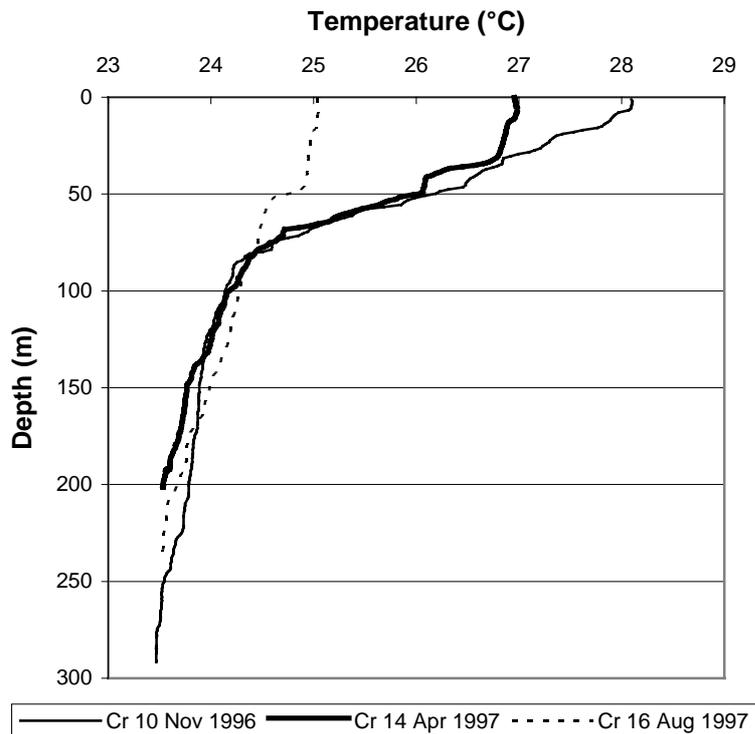
Figure 2.4.4./27 Water temperature profiles in the Mpulungu basin during expeditions 10, 14 and 16 measurements.

The flow direction was NE in the first transect (48) down to 50 m (Fig. 2.4.4./28). Below this the flow direction was S. Velocities there were much lower than near the surface. A NE flow was also found in the uppermost layer of the next transect but the deeper waters flowed W. For the next measurement the ship was headed SW. The flow direction was now NW at the surface but the deeper flow direction changed to the E in the middle of the line. This same direction prevailed during the next short transect when the ship was turned NE.

The ship was then headed N during the last measurement in this area. Flow velocities were quite high and mainly towards the NE, although some W or NW components were found.

In April 1997 measurements were carried out during three days (Apr 13 - 16). Three main cross sectional transects were covered. The longest one reached from the Sumbu bay in the west to Kala on the east coast (Fig. 2.4.4./29).
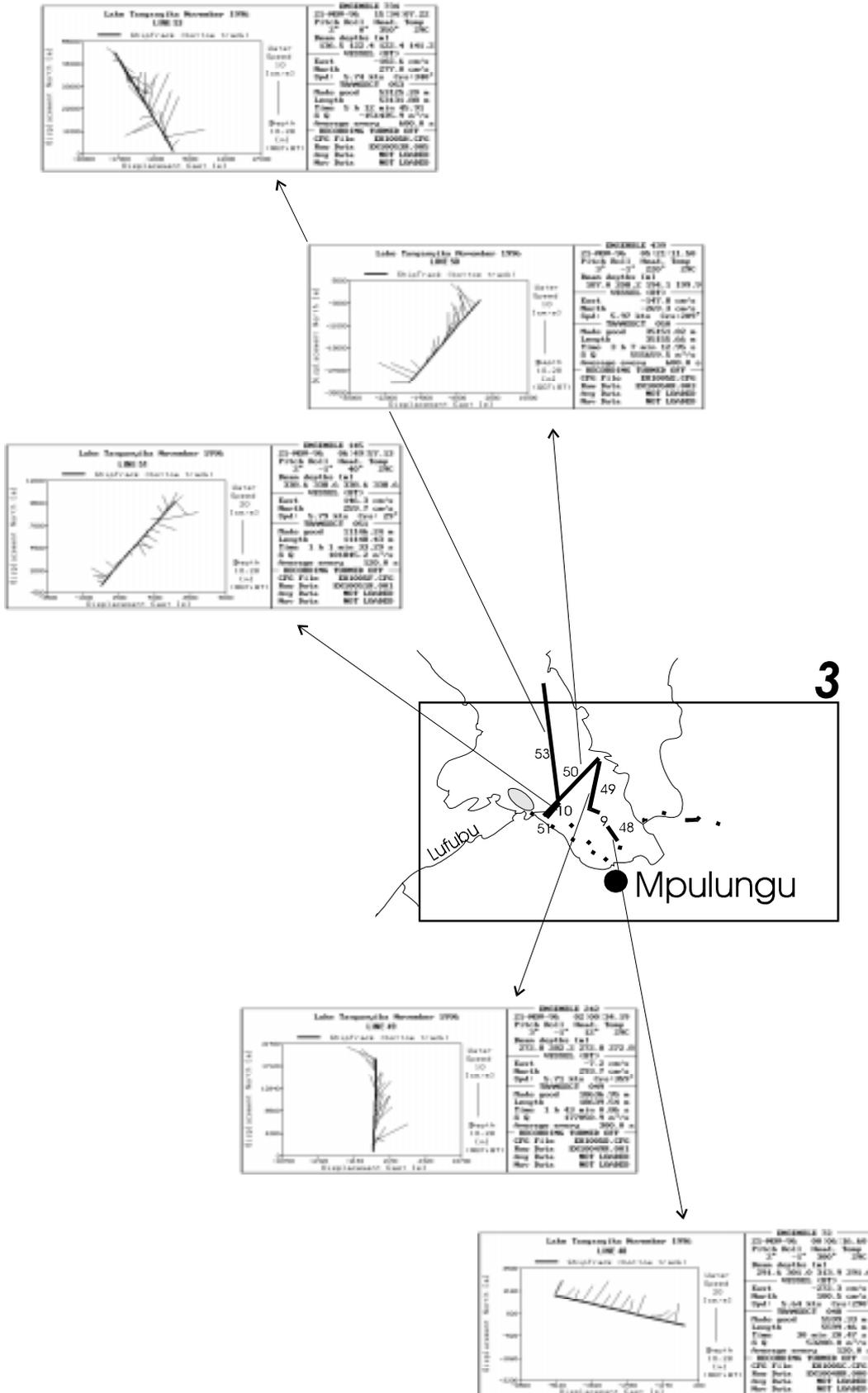
Figure 2.4.4./28 The currents from the uppermost observation layer along transects in the south end of Lake Tanganyika. Expedition 10, November 1996.

Figure 2.4.4./29 The currents from the uppermost observation layer along transects in the south end of Lake Tanganyika. Expedition 14, April 1997.

A time series of currents were also collected with buoy based ADCP's at the Kalambo estuary during 11 hours on Apr 14.

The stratification was now somewhat stronger than in November with a secondary thermocline at the depth of 35 m and the bottom boundary of main thermocline at about the same depth (80 m) as in November 1996 (Fig. 2.4.4./27). Fairly weak winds prevailed in the region during the current measurements (Fig. 2.2./4). The maximum observed 60 min. mean value of wind speed at the Mpulungu water tower was 6 ms^{-1}. However, it seemed that the wind pattern started to change during the measurements. On Apr 11 the maximum wind speed was observed. It was a SE wind around noon and during the afternoon. The wind turned to blow from the NE the following midday (Apr 12) and after few hours turned again SE continuing to blow from there until noon the following day (Apr 13). Again the wind stayed there for a few hours and turned to blow at a weak speed from the SE during the evening and midnight. During the days of 14 to 16 of April, the wind pattern increased in such a way that the north component increased in both directions and the eastern only had a high value at noon.

The transect west from Kala was covered twice: in the evening of Apr 13 and very early in the morning of Apr 16. During both measurements the current was very similar. The general current direction was NW and W (Fig. 2.4.4./29). In the evening the current was weaker than in the early morning. Also in the morning a coastal S flow was found reaching about four 9 km from the shore, where the water depth was about 350 m.

A transect from Kirambo to Crocodile Island was covered during the early morning hours of Apr 14. A slow S flow was detected at the beginning of line in the eplimnium. Below the 30 m depth there was a strong flow to the N up to the level of Kalambo. After leaving the ADCP buoy stations near Kalambo a fairly strong SW flow was observed in the epilimnium with a fairly strong SE flow within the thermocline.

During the night between Apr 14 and 15, a long transect was again covered, first SW from the underwater peninsula towards Katoto (50 in Fig. 2.4.4./29). From there Mpulungu Bay was crossed to Kirambo (53). Data recorded during almost seven hours of measurement showed that at the beginning, at the south-west part of the bay, the currents were fairly weak near the surface. The magnitude of surface current grew along the transect. In the middle of the bay around midnight, a fairly large area with E current was observed. The waters in the deeper layers flowed N at a fairly weak velocity except near eastern coast. Again a strong N current was found there beginning about 16 km south from Kirambo point (54 - 55).

The basin was crossed again from Kirambo SW along a transect via the Lufubu estuary (58) and back to the lake buoy (meteo station with thermistor chain) site. The measurements were conducted during the morning hours of Apr 14. A NW current dominated near the surface down to the 45 m depth in the region extending about 16 km from the beginning of the transect. This result was again consistent with the results from earlier transects near the eastern coast. Near the western end of this transect waters in the same layer were flowing NE. Within the thermocline the current structure was not clear in the open part of the lake. Near the western shore a SE (along coast) current increased.

In the surface layers near the Lufubu estuary a N current was observed (Fig. 2.4.4./29). Within thermocline, the flow was directed SE along the coast. The echo intensity near the Lufubu estuary had higher values than in the nearby areas (Fig. 2.4.4./30). The maximum values were found in the

layer from 10-15 m as well as at the depth of 56 m to 70 m. This indicated the advection of river waters in this layer.
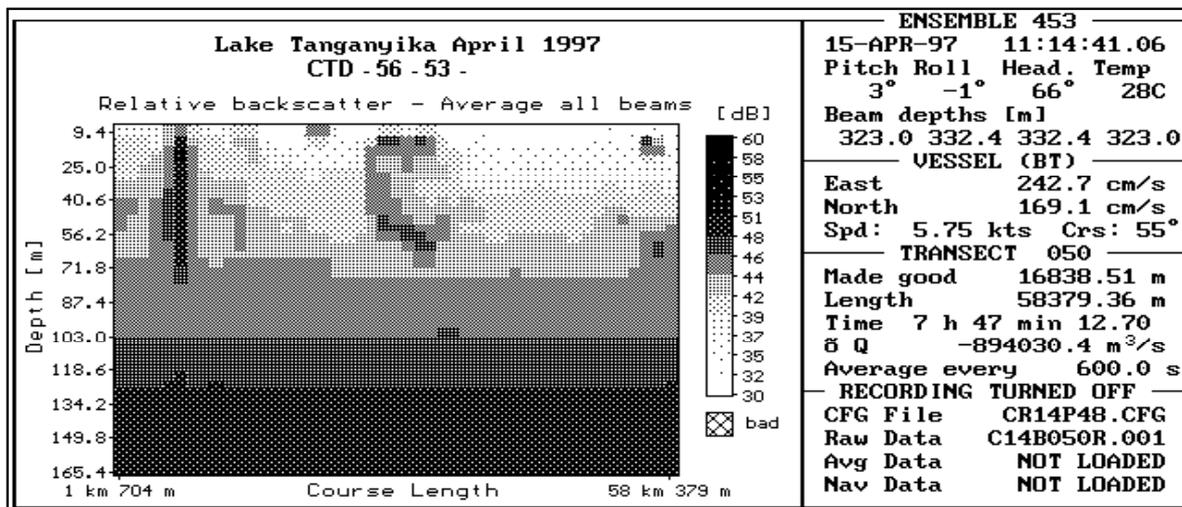
Figure 2.4.4./30 Echo intensity near Lufubu during April 1997 measurements.

The measurements were conducted again near the western shore to Lufubu estuary during the noon and early afternoon (line 52 in Fig. 2.4.4./29). The near surface flow was heading NW as in the morning. But now the magnitude was higher. A SE current was now well developed in the deeper layers and it was found now to cover almost the entire 17 km transect. In the morning it covered only about half of that distance and appeared near the coast.

The NE transect from Sumbu Bay was made along the middle axis of the bay (line 59 in Fig. 2.4.4./29). At the eastern end of the bay (mouth) the ship was headed SE to cover the south side of the Sumbu bay mouth. When the shore was reached near Kasaba Point, the ship was headed again NE. The measurement was carried out during 161 min. in the late evening. The currents varied very much along the transect. The near surface layers were flowing to the SE along the whole transect. The flow velocity was at maximum in the Sumbu bay. This indicates the presence of a land breeze from the mountains on the northern shore of the Sumbu Bay. The flow in the upper part of thermocline was directed NE within the whole transect. A SE flow was found in the Sumbu bay. The magnitude of this flow increased in the deeper layers of thermocline. At the mouth of the bay, the flow was increasingly turned to the left when going to deeper layers of thermocline.

A local maximum echo intensity was found near the middle part of the mouth of the Sumbu bay (Fig. 2.4.4./31). The values in other parts of the water column were also higher here than in the nearby areas. This could indicate a local water mass, which is not well mixed with the other water masses like in the middle of a big gyre. The current structure near this point also supports the existence of such a gyre.

During the night the lake was crossed using ADCP measurements and the transect ended near Kala (lines 60 - 63 in Fig. 2.4.4./29). On the western side of the transect a W current was observed in the epilimnium and a common SE current was present in the lower part of thermocline.

On the eastern side at the level of Kala a fairly strong NE current prevailed in the eplimnium and also within the thermocline. Very near the eastern coast (from the sites with 260 m water depth) a

SE coastal flow was found to prevail. This had not been found three and half days earlier (in the evening of Apr 13) when the transect was ended about 3.5 km further offshore.
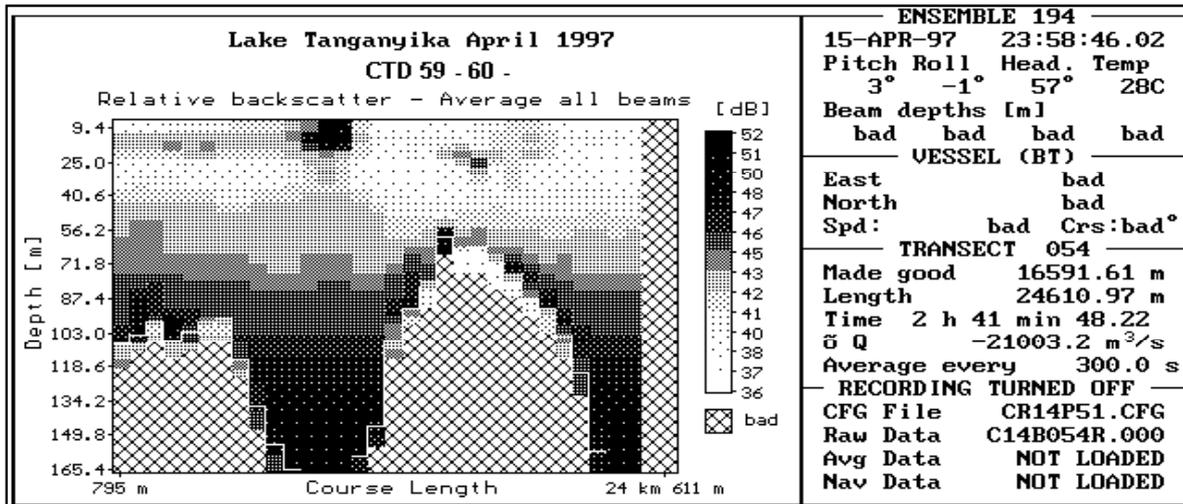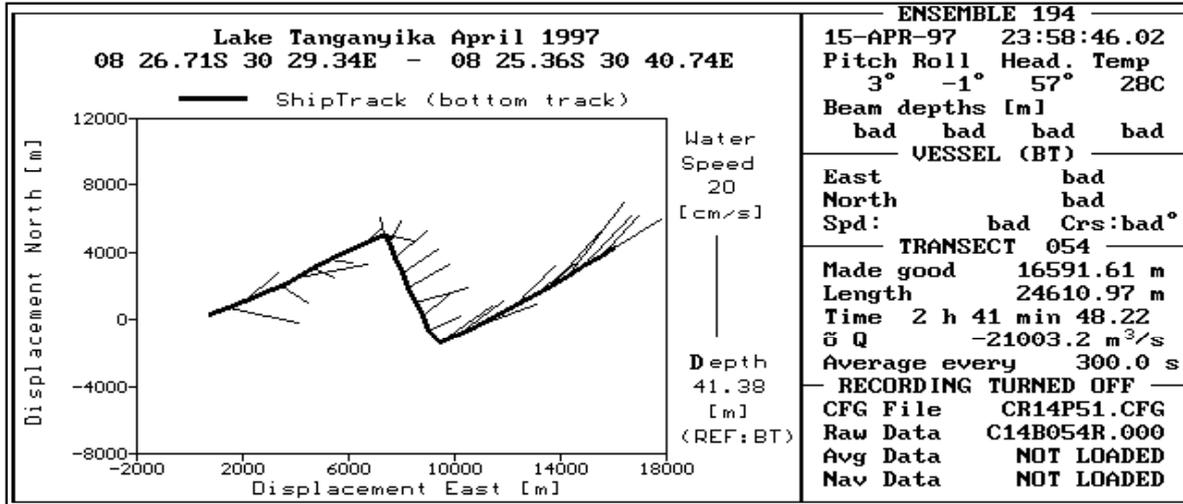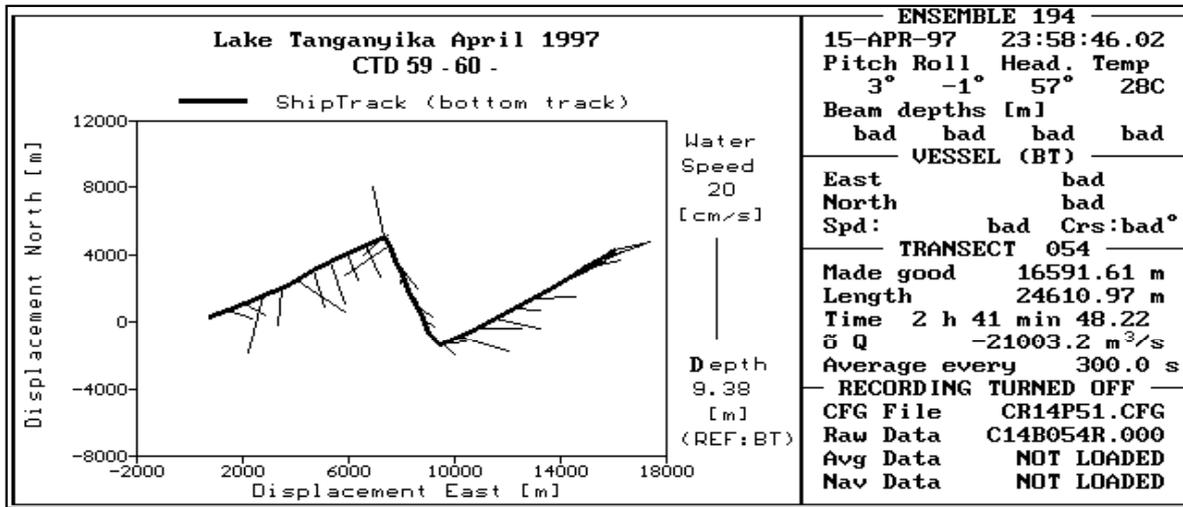
Figure 2.4.4./31 Water currents and echo intensity (lower panel) along the transect in Sumbu bay during April 1997 measurements.

In the dry season (August 1997) measurements were carried out during Aug 30 - 31. Again the transect lines were similar to those of expedition 14th in the same area (Fig. 2.4.4./32). Buoy-based ADCP's were used at the Lufubu river mouth for 48 hours on Aug 30 - Sep 1 to collect time series data of currents.
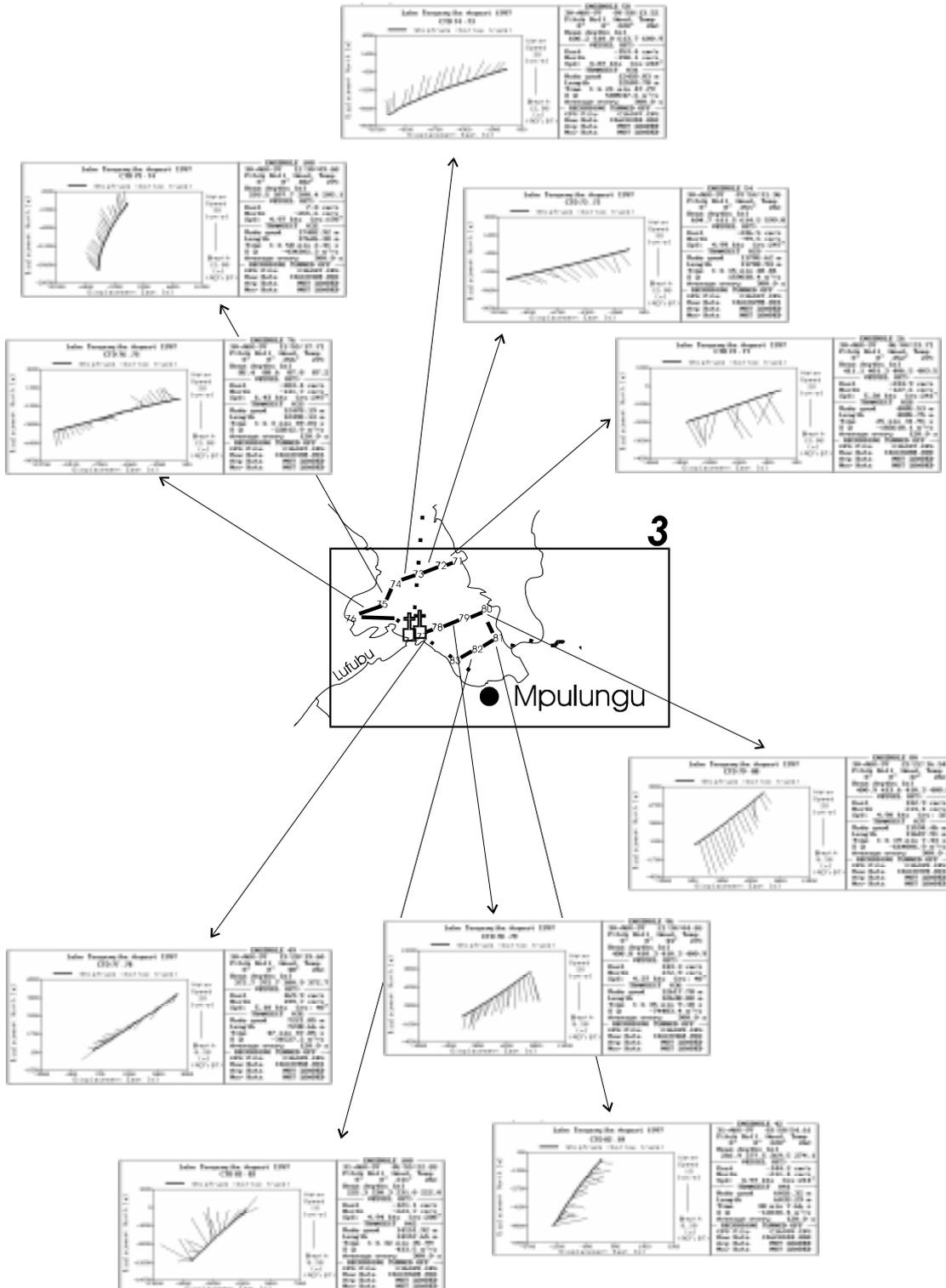
Figure 2.4.4./32 The currents from the uppermost observation layer along transects in the south end of Lake Tanganyika. Expedition 16, August 1997.

During the measurement period wind speed was between 5 and 6 ms^{-1} with the direction mainly from the NE (Fig. 2.2./6). The waters were now quite mixed in the layer of 0 - 240 m. A very weak thermocline was observed at the depth of 50 m.

The transect west of Kala (71 - 72 - 73) was measured on Aug 30 early in the morning (Fig. 2.4.4./32). The general direction of the current was SE. About 16 km from the shore (73 -74 - 75) the current direction turned NE and then NW.

The transect line (75 - 76) from the Sumbu bay mouth to the end of the bay showed a spiral pattern in the current directions. About 5 km from the beginning of the line, the current turned from the NW to the SE. This change in direction could be most clearly seen in the surface layer. The ship was then headed out of the bay along the south coast where the same trend in the current direction was also seen (76 - 77).

The transect started from the Lufubu River (77 - 78 - 79 - 80) in the evening and reached Kirambo on the east coast at midnight. The general direction of the current was S down to 40 m but in the deeper layers it was W. Near the Lufubu river mouth (77 - 78) the echo intensity was similar that of the nearby areas but the maximum values were found only at the surface down to 20 meters instead of 60 - 70 m in the other areas. Further, near the river mouth the direction of the current was W in the layer of 0 to 40 m.

The transect line reaching from Kirambo down to Kasanga (80 - 81) showed NE currents at the surface and SW currents at the depth of 20 - 50 m. Outside Kasanga the ship was turned and headed SW across the lake. The first transect (81 - 82) covered 6 km and showed E currents at all depths. the next transect showed the direction of the currents as being towards the NE (82 - 83).

Two moored ADCP's were deployed at the **Kalambo river mouth** on **April 14, 1997**. Unfortunately due to an operational error only one gave useful data. This instrument was recording currents during daytime about 1 km west from the Mwina point at a site where the water was 39 m deep.

No mesoscale ADCP transects were covered at this time in the vicinity of the buoy stations but the ship made measurements at the very end of south bay and shortly visited Mpulungu harbour.

The wind was fairly weak as observed on the hilltop site in Mpulungu. The maximum observed velocities were about 4 ms^{-1}. They were observed during the early afternoon.

A CTD profile taken in the early morning of Apr 14 showed that primary thermocline was situated at the depth of 80 m and the secondary thermocline was at the depth of 35 m. (Fig. 2.4.4/27).

The currents at the mooring site were heading S at all observation depths during the day (Fig. 2.4.4/33). The velocities were about 10 cms^{-1}. Very high short term current velocities were observed at the depth of 9 - 14 m during the morning hours. It is not clear were these real observations or did some errors occur during observations (instrument malfuction or a disturbance by fishermen). The magnitude of velocities increased during the late afternoon as the wind speed also slightly accelerated. The echo intensity was uniformly distributed in the vertical. The increase of echo intensity recorded by ship ADCP was also very clear as the ship was moving towards Mpulungu away from the deployment site (Fig. 2.4.4./34). This means that the waters from the Kalambo river are also well mixed in the water column and transported south in the direction of Mpulungu.
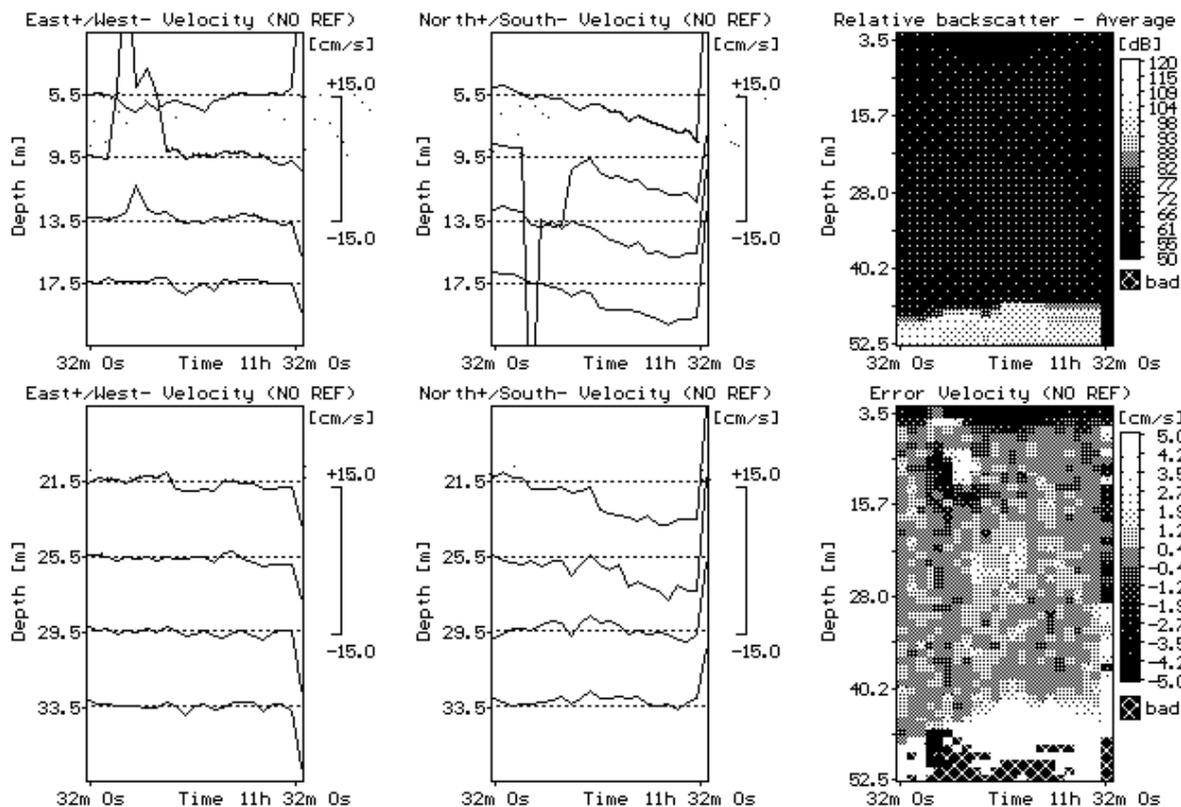
Figure 2.4.4./33 Time series of currents near the Kalambo River mouth in April 1997. Measurement period was 14.4. 06:00 - 17:15. Water depth at the observation site was 39 m.
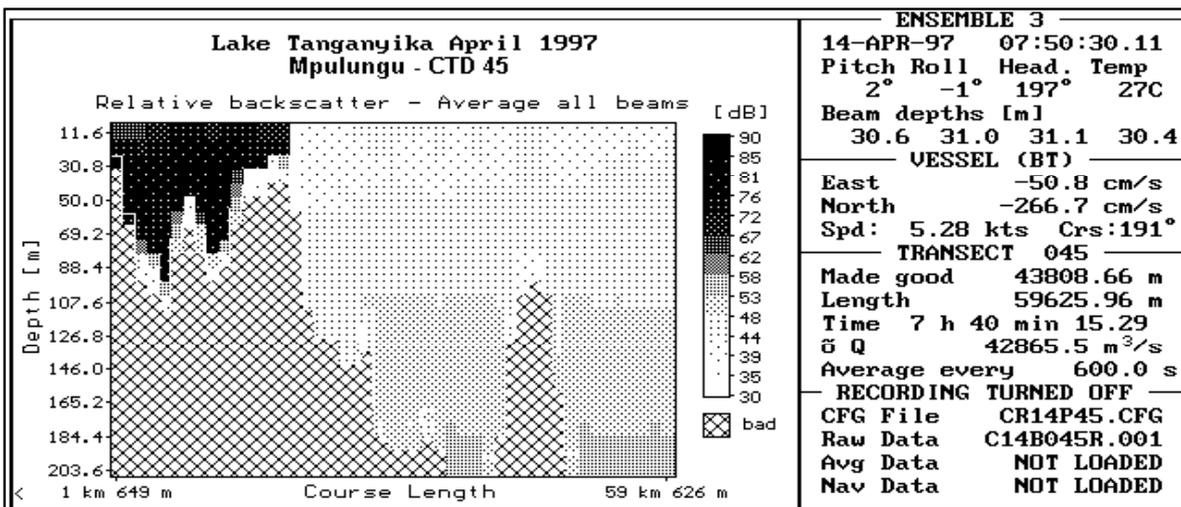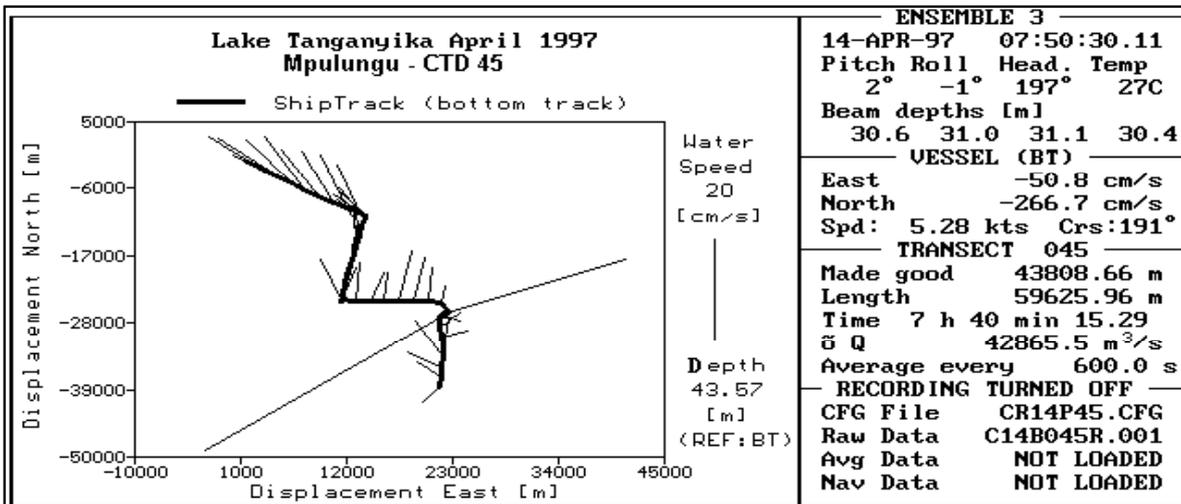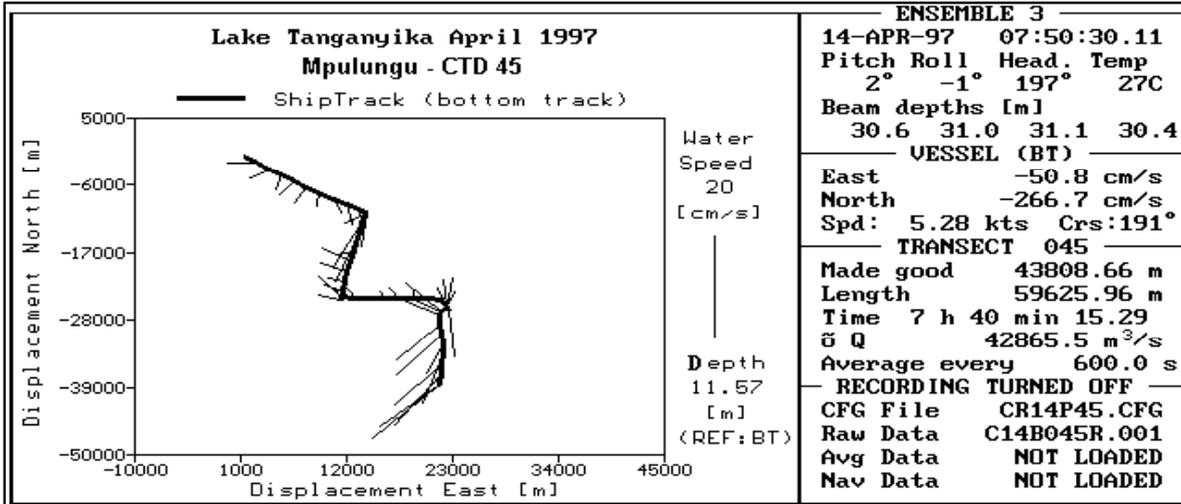
Figure 2.4.4./34 Water currents and echo intensity along the transect from the Kalambo River mouth to Crocodile Island during April 1997 measurements. The currents are presented in shiptrack form from the layers of 11.6 and 43.6 m. The echo intensity along the transect is shown in the lowest panel.

Near **Lufubu** the buoy ADCP's were used twice, in November 1996 and in August 1997. In **November 1996**, the first deployment site had 50 m of water and the other 117 m. The CTD profiles were taken three times (Fig. 2.4.4./35). At midnight on Nov 18 the measurement revealed that primary thermocline was situated between the depths of 40 and 75 m. A secondary thermocline was found at the depth of 10 m. It had vanished, when the next profile was taken in the early hours of the morning (04:22). The cause for this was the nocturnal convection. Still the depth of primary thermocline had not changed. In the evening of following day the temperature of eplimnium was higher than in previous measurements, and the epilimnium was very linearly stratified with little vertical mixing.
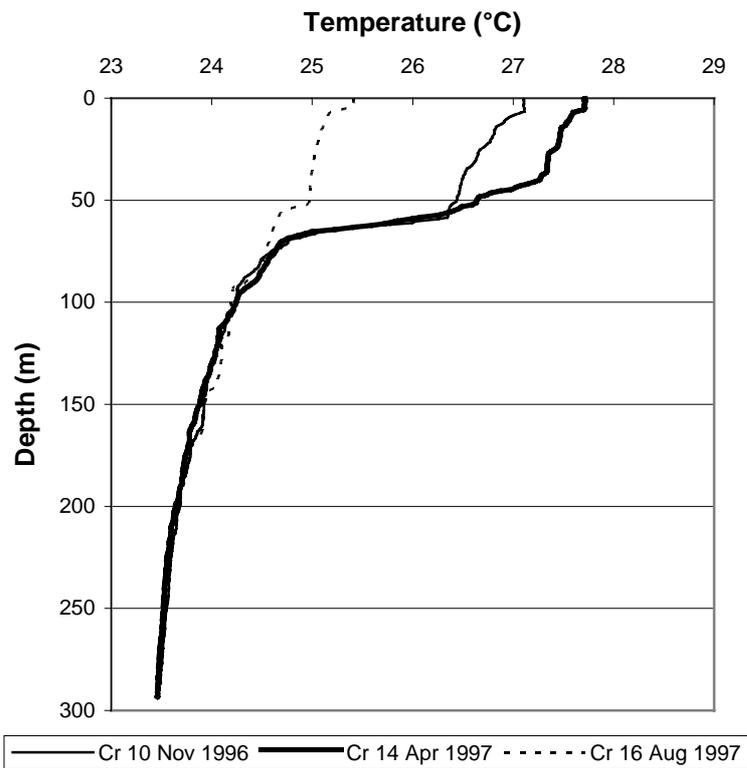
Figure 2.4.4./35 Water temperature profiles near the Lufubu River mouth during expeditions 10, 14 and 16 measurements.

The winds on the lake, as recorded by the ship and at the buoy, were weak and from south east.

Two ADCP-buoy stations were deployed for recording currents during the night between Nov 18 and Nov 19, 1996. During the time of deployment, the ADCP on the Tanganyika Explorer was used for measuring the currents in the region. The measurements were conducted along rectangular with sides of 10 km * 8 km. Total of two laps along the rectangular were made during the ADCP buoy deployments. Each lap took about 6 hours.

The current structure remained fairly stable during the night. On the most offshore transects during both passes the water in eplimnium was flowing W and water in the hypolimnium towards the SE. The magnitude of currents recorded by the ship ADCP and the moored ADCP's was very similar.

On the transects closest to the shore the waters were flowing slowly N for both in eplimnium and hypolimnium during both passes of the research vessel .

The two moored buoy ADCP's showed that at the deeper site the current magnitude was stronger especially just above the thermocline. At the shallow site the W current extended only to 25 m (Fig. 2.4.4./36). Also at the deeper site a persistent hypolimnetic flow was moving SE and E.
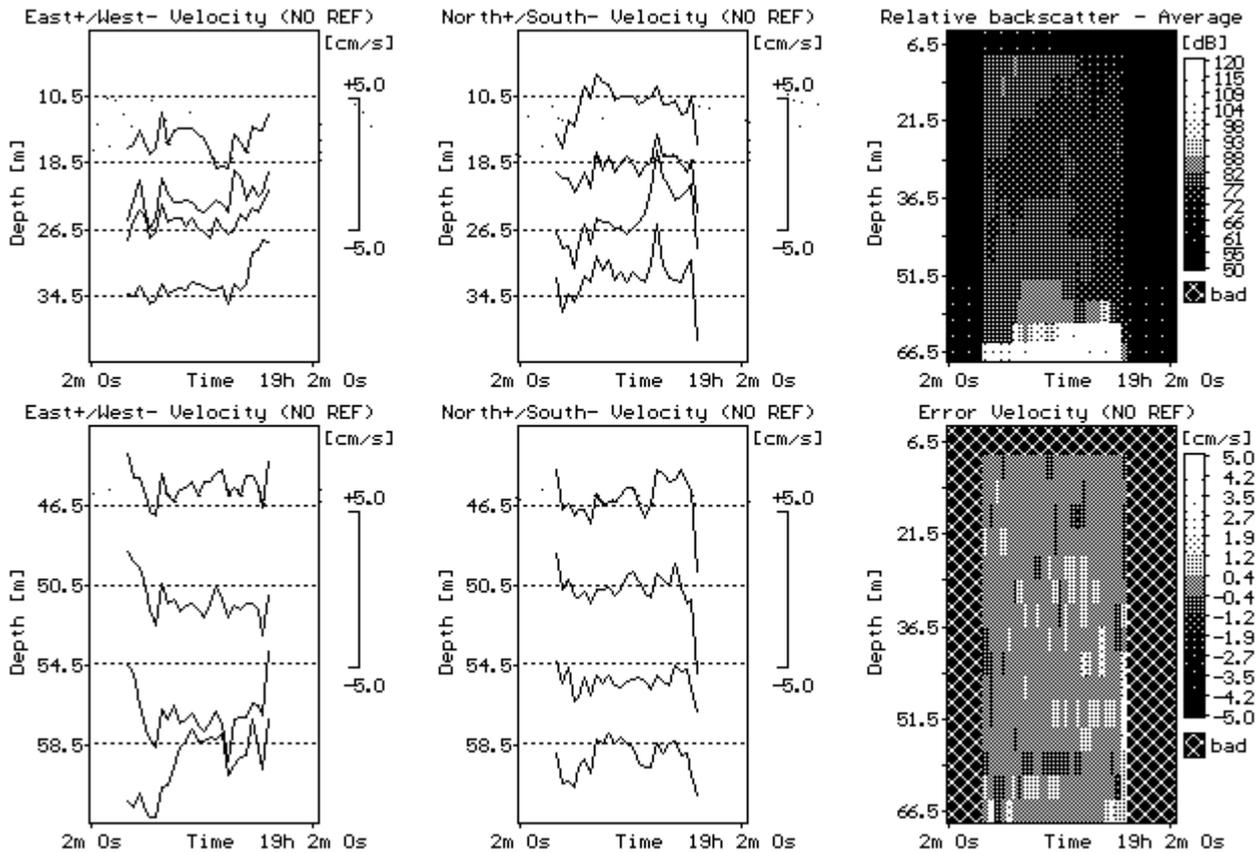
Figure 2.4.4./36 Time series of currents near the Lufubu River mouth in November 1996. Measurement period was 18.11. 20:40 - 19.11.08:55. Water depth at observation site was 50 m.

In the dry season (August 1997) the measurements near Lufubu were carried out during a period of 50 hours starting from sunset on Aug 30. The two ADCP buoy stations were deployed to almost the same position. The deployment site was now 2.5 km NW of the shallowest site used in November 1996.

No mesoscale ADCP transects were collected in the vicinity of the buoy stations. During the recording time of the buoy stations the Tanganyika Explorer made measurements all over the south bay.

The wind observed on land in Mpulungu showed that there was a typical dry season wind pattern, i.e. a SE wind during the evening and night and the morning land breeze (Fig. 2.2./6). The maximum observed velocities in Mpulungu were about 6 ms^{-1}. Similarly on the lake the winds were

weak with a typical dry season diurnal cycle. The maximum recorded wind speed was 9 ms^{-1} from the SE during the early morning hours of Aug 31.

A CTD profile taken in the evening of Aug. 30 (CTD 77) showed weak thermal stratification as in the main south basin. A primary thermocline was situated at the depth of 55 m (Fig. 2.4.4./35). A secondary thermocline was found at the depth of 5 m.

The buoy stations showed fairly weak currents. Their 30 min. values were generally about 4 cms^{-1} (Fig. 2.4.4./37). The water masses in the layers of 0 - 20 m flowed as one mass at a very similar speed. During the early evening (Aug 30) these waters flowed towards the S following the northern wind. The same S flow was observed by the ADCP on the ship earlier in the afternoon as the ship approached the Lufubu region. However, very near the Lufubu river mouth, the ship ADCP revealed N flowing water masses with a slightly high echo intensity, especially near the surface. Later in the evening and during the night, the water at the buoys' site was flowing N and NE. In the uppermost 10 m layer a slight change in current direction occurred in the morning as the lake breeze increased and turned the near surface current to flow NW. In the evening a flow towards the SW was again observed, as during the previous night.
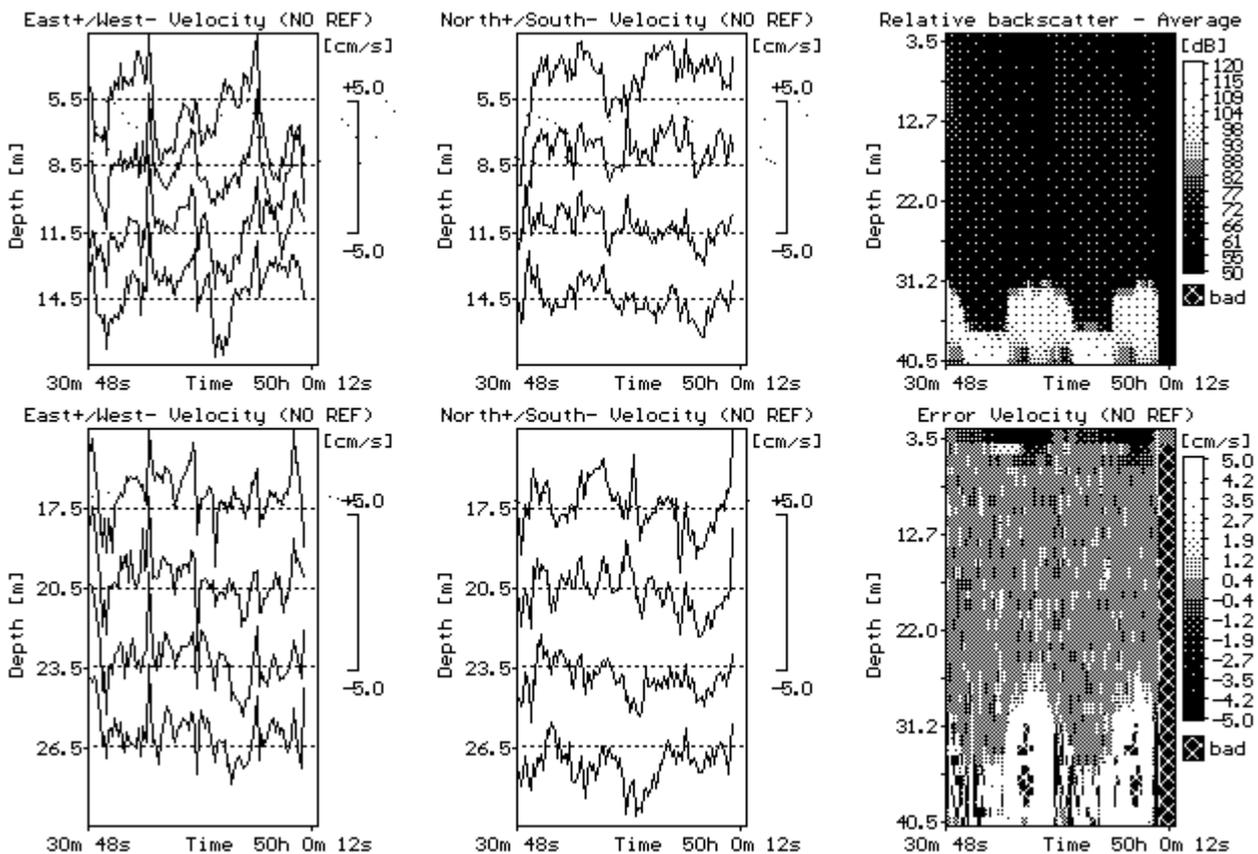
Figure 2.4.4./37 Time series of currents near the Lufubu River mouth in August 1997. Measurement period was 30.8. 17:32 - 1.9. 18:00. Water depth at observation site was 46 m.

The current data showed some short scale oscillations. The variation of N-current component seemed to have a period of 4.5 hours. This indicates the effect of the lake's uninodal seiche. In E-

current component the diurnal variation was clear. However, the effect of uninodal seiche could also be seen especially at the depth of 17 m.

In conclusion, the waters from the Kalambo River flowed south during the daytime wet season measurements. The mixing of these waters was not very efficient as compared to the waters coming from Lufubu.

Transport and mixing of Lufubu waters is affected by diurnal winds. The lake breeze seemed to push the waters NW along the coast in the afternoon. In the evening, the waters flowed along the coast to the south. The velocity of currents during the August observations was somewhat low. This is due to fairly low observed wind velocities. Still the varation of currents was quite high. When higher wind speeds occur in the dry season they produce even higher variation in current speed than now was observed and also higher velocities resulting in higher mixing.

2.5. Discussion

The previous data collected before LTR have been uneven in spatial and temporal coverage, and the sampling was carried out mainly around the few major ports of the lake. Furthermore, as Coulter (1991) pointed out that there has been a great need to use sufficiently accurate recording devices to obtain exact and reliable information on hydrological phenomena in the entire lake. In the report by Kotilainen et al. (1995a,b) the meteorology around and on the lake was discussed together with thermal regime. The water flow discussion was based on the flow cylinder measurements near the field stations in Bujumbura, Kigoma and Mpulungu. **The present report gives first lake wide perspective on the circulation pattern and sediment transport** within the lake using both best possible current measurement technique and modelling.

The results will be compared here to our earlier results and results from other researchers. It is especially interesting to compare the present results to the results of Coulter (1963, 1967, 1968 and 1981) and Coulter & Spiegel (1991). His studies have made the basis of the understanding the hydrodynamics of Lake Tanganyika this far. In 1963 and 1968 in his studies Coulter reported about temperature observation at the outer Mwela station 10 km off Mpulungu and his temperature transects along the main axis of the lake in May and October 1964 and April 1965.

The **results** concerning the seasonal and spatial variations **of meteorological variables** around the lake and on the lake **support the earlier results** by Kotilainen et al. (1995a,b). The timing of these changes varies somewhat between the years (Kotilainen et al. 1995a,b).

The fall in **lake water level** in the dry season in 1996 (0.89 m) was higher than the mean (0.82 m) for the period 1941 - 1959, given by Bultot (1965). In 1996 the lake level reached the lowest level since 1959 (Verburg 1997). The lake outflow calculated by him has been between 160 and 50 m^3s^{-1} during the period 1929 - 1996. The annual mean for 1996 was 93 m^3s^{-1}. This was 5 % of the water budget (the sum of the rainfall on the lake and the river inflow, or of the evaporation and the outflow). Verburg (1997) concludes that in 1996 the lake level was less than 1 m above its lowest possible level, and if the declining trend of the past years persists the lake may be facing a new closed period in the near future, for the first time since 1874 (Camus 1965).

The **offshore winds** in Kigoma are a result of lake-land breeze system, slope and the south-easterly trade winds. This has been observed also in earlier studies (Kotilainen et al. 1995a). Savijärvi (1995, 1997) concluded from an atmospheric model application study in Kigoma region, that the mountain slops contributed about 50 % , trades 25 % of the diurnal variation of winds. The rest 25 % of the wind variation was due to the lake effect. The SE tradewind enhances the lake breeze considerably at daytime and adds on the downslope winds at night time.

The diurnal variation and also values of air temperature and wind speeds during the dry season are highest in Mpulungu (Kotilainen et al. 1995a, Huttula et al. 1994). During the rainy season, the wind forcing was fairly similar in the three observation regions. Occasionally, however, for example in December 1993, the wind forcing was stronger in the Bujumbura region than in the south and in late March 1994, the wind forcing was strongest in the Kigoma region.

The upwelling of hypolimnetic waters in south was observed during the study period (Jan 1, 1996 - Sep 10, 1997) in similar manner than during the earlier observation years. The regional expansion of upwelled waters reached from south to the level of Kipili. Also in this region very warm

water was found during November expedition. It shows that the south part of the lake obtain much solar radiation and in a rapid mode. Coulter (1968) reported the same upwelling of hypolimnetic waters at the outer Mwela station in summer 1964 and 1965. In 1964 these water masses disappeared from surface in late September and in 1965 they came to surface early June and remained there to the middle of September. In this study the upwelling periods were shorter but also the recording site was situated about 30 km more off shore than Coulters observation site. The regional expansion of the southern waters observed by Coulter was greater. His observations show that they were transported in early May 1964 to the region of Karema.

The **surface water temperatures** during the upwelling in the south in June 1993 and 1994 were higher than those recorded by Coulter (1963). In the present study the surface temperatures were > 24.0 ºC, while Coulter measured surface temperatures between 23.50 and 23.75 ºC. Nothing is known about winds and other variables affecting the evaporation at the times when Coulter made the observations. So no comparison about cooling of surface waters due evaporation can be made.

In April 1965 the 24.00 ^{o}C isoline was situated at the depth of 95 m, having amplitudes of internal oscillations of 20 m (Coulter 1968). In April 1997 this isoline was at the depth of 130 m. **This may indicate some heating of water masses due to various reasons like the climatic change.** Terrestrial heat input or adiabatic heat input to deep waters may also have a secondary role. If heating of lake waters is really happening, it will affect the thermal stratification of the lake and stabilise it as Hecky and Bugenyi (1992) discussed in connection of climatic change. This will reduce vertical mixing and affect the lake biota. The maximum surface temperature in April was observed both in this study and by Coulter to locate around Msamba region. The waters were warmer in 1997 as 1965. In 1997 the isoline of 26.75 ^{o}C was located below the surface at the depth of 20 - 40 m for the whole distance from Mpulungu to Kigoma, whereas this isoline existed in the water only in about 2/3 of the stretch from Mpulungu to Kigoma in 1965.

During present study the observed values of **solar radiation in Mpulungu were much higher as compared to the values in the north end of the lake especially during the months of October and November**. This speeds up the restartification in the south, where the upwelling and high evaporation due to the winds have cooled the surface waters. This was observed also earlier. E.g. at the end of August 1993, the thermal stratification began to strengthen while the wind was still quite strong, 5 - 6 ms^{-1}. The stratification intensified in late September when the wind speed decreased.

The vertical mixing of waters in Kigoma takes place only to the depth of upper thermocline. Thus **it is not accurate to talk about upwelling** in the sense of the vertical transport of hypolimnetic waters to the surface. The upwelling of waters **at the Kigoma** has been discussed by Kotilainen et al. (1995a). Beauchamp (1939) reported that in late August and in September, when the stratification was weak, some mixing occurs off Kigoma as late as early October. It has been suggested by Coulter (1991) that the warm surface water from the south, pushed by the trade wind, flows to the north and can be seen as a downward tilting of the thermocline in the northern part of the lake. The fact that the surface water and air temperatures differ by as much as two degrees supports this theory. However, the measurements with flow cylinders off Kigoma were not supporting this as the currents there flow mainly towards the south (Kotilainen et al. 1995a).

The thermal regime in the water at the two locations (Kigoma and Mpulungu) on the lake can be compared for the same period in **March and April** 1994. The isoline 24.50 ^{o}C was on average 9 m deeper near Kigoma than off Mpulungu. This was a result from late wet season (March - April 1994).

The **tilt of thermocline along the lake's main axis** observed in April 1997 during the expedition was very small. The depth of 25.25 $^{\circ}$C varied between 47 (CTD 21) and 67 m (CTD 71), this means a slope of 27 cm/km. The average slope of this isoline from the meteo buoy site in Mpulungu to CTD 1 at Kigoma was only 0.2 cm/km. In May 1993 a higher tilt was found which was approximately 26 m in the 320 km-long region extending from Kabogo to the Mpulungu buoy (Huttula et al. 1994). These values mean a slope of 8 cm/km. This was observed after strong south-easterly winds, which prevailed from May 10 to the last day of the expedition. Coulter (1968) also observed a slight tilt from Mpulungu to Karema in April. After Karema to Kungwe (90 km) the thermocline (25.25 $^{\circ}$C) sank from the 40 m depth to 60 m, which means a slope of 22 cm/km. After that there was no significant tilt. The average tilt form the Mwela station to Kigoma was 11 m, which means a slope of 2 cm/km.

In **November** 1996 the depth of 24 $^{\circ}$C isoline was about 10 - 20 m deeper than in October 1964. The surface waters in south were about 2 $^{\circ}$C warmer as was observed in October 1964. Also the tilt of thermocline now at the end of November was towards the south. The slope of 25.25 $^{\circ}$C isoline was 8 cm/ km. From Coulters data it can be seen that in October 1964 the tilt was clearly towards the north. E.g. for the 25.25 °C isoline there was a slope of 5 cm/km between Mwela and Kigoma. This difference cannot be explained by the one month difference in the observations, there must also be a difference in wind forcing during the dry season, which caused longer tilting of thermocline and stronger cooling in 1964.

The tilt of thermocline **at the end of the dry season in August 1997** was also quite clear. The waters in the south were almost mixed vertically but the isoline of 25.25 °C was observed 130 km north of Mpulungu at the depth of 42 m. Near Bujumbura its depth was 64 m, resulting in an average tilt of 4 cm/km. In early May 1964 Coulter also observed a tilt of 4 cm/km between the two ends of the Lake. The same isoline was at the depth of 43 m at the Mwela station and at the depth of 78 m near Bujumbura.

The **tilt of thermocline along the transversal axis** was very high as compared to the tilt along main axis. A very high tilt was observed in **April** in the strait between Kungwe and Kalemie, where the thermocline was tilted towards Kungwe. For the 25.25 °C isoline this slope was 87 cm/km. Currents observed at the same time were very high and on the Kungwe side they were heading NE and in the middle of the strait S. During the same night a high slope was also observed at Kabogo point (28 cm/km) with southward flows. In **August** the slope at the Kungwe strait was NW with a slope of 10 cm/km. Now also the current pattern was different from the April one. Near Kungwe (0 - 10 km) the waters were flowing SW and near the middle of the strait NE. The tilt of the thermocline and current pattern in the strait follow the theory of inertial flows, where the waters flowing in the southern hemisphere will cause the sinking of thermocline on the left hand side and rising on the right hand side. The strait is situated in the nodal point of the uninodal surface seiche and internal seiche oscillation as discussed by Coulter (1963). He calculated the period of an internal seiche and related transversal slope in the strait. He expected a steady flow in the strait and the location for which he calculated the value was 28 km south from the present observation site. He obtained a slope of 30 cm/km for this situation. This value is lower than the measured value now (87 cm/km), but still the same order of magnitude. The magnitude of flow velocity in the middle strait especially is the result of superposition of flows caused by internal oscillations and wind induced advection. So it is dependent on the observation time and phases of the oscillations.

The **water currents** were measured for the first time on the lake during the expedition in May 1993 (Huttula et al. 1994). The observations were conducted in five areas. Fairly strong lake currents

(maximum speed of 19 cms^{-1}) were found near the eastern shore near Kungwe and also in the south at the lake buoy station. The direction and even magnitude of the flow near Kungwe in May 1993 corresponded very well with present results from the dry season. The same applies to Utinta and results near the lake buoy station. Huttula et al. (1994) discussed the large gyre formation in the lake on the basis of flow cylinder measurements. The **formation of gyres** was confirmed also with the LTR flow model (Podsetchine and Huttula, 1996). From the calculated flow fields 7 - 9 main gyres are found in different wind conditions.

The **diurnal variation of surface currents** has been one of the main results of this study. It has been proven that in certain areas, like in shallow waters near Malagarasi, Ruzisi and even in the deeper inlet area of Lufubu, the lake land breeze system highly dominates the short scale current pattern. On this there is as superimposed the long term variation of the current field. These variations are forced by seasonal winds and regional thermal as well as slope winds and can vary greatly in space and time.

The present flow results together with temperature and echo intensity observations provided good information about transportation of the river waters. Vandelanoote et al. (1995, 1998) have recently discussed the advection and dispersion of **River Rusizi** waters. Their results ware based on long term water chemical data. They conclude that in average the waters mix effectively with the lake waters within a distance of 800 m from the shore and that there is no density current along the bottom. They also state that the waters are mostly carried eastward. The present results show that episodic advection can be both W and E. The observed magnitude of currents and their high variation result to an effective mixing in a fairly limited area near the river mouth and confirms Vandelanoote et al. (1995, 1998) results. The water from the **Malagarasi River** was found to be advected both N and S depending on the current pattern. In April, when the river mass load was at a high level the waters in this region were flowing mostly S along the coast. The waters from the **Kalambo River** were advected very clearly S towards the Mpulungu region. The waters from the **River Lufubu** were transported mostly NW. The strong diurnal character of winds and the surface current also cause high dispersion in this region. There was some evidence that these waters are transported near to the depth of 10-20 m. The observations of Badenhuizen (1965) suggested that the waters are transported practically at the surface of the lake. The same was not observed in the present study.

There was no direct measurements of **river discharges** during the present project. The river discharges were estimated on the basis of literature. The observed grain size distribution at the three river mouth areas showed that the finest sediment enters from Malagarasi. The coarsest was found at the Lufubu river mouth. The sedimentation rates observed at the Malagarasi and Lufubu river mouths during the dry season were quite low compared to the values observed in humid lakes (e.q. Huttula 1994). It seems that the obtained values are realistic. The estimates from NORCONSULT-data give very high values for wet season.

Water exchange of some defined lake areas was also studied. It became evident that the waters in Sumbu bay have a limited water exchange with main basin. Again this was a validation for the numerical model results obtained by Podsetchine and Huttula (1996).

The **lake current results** obtained now can be compared to the observations in 1993 - 94 near the three field stations (Bujumbura, Kigoma and Mpulungu), which were reported by Kotilainen et al. (1995a). The currents were measured twice a month. Comparison of recent current results to flow cylinder results in analogical wind cases provide an interesting insight to the sustainability of current pattern especially in Bujumbura and the south basin. ADCP data was not collected near Kigoma.

In the **Mpulungu basin** from Cape Chaitiga to the Sumbu game reserve in flow cylinder measurements during the middle of the day in Aug 17 - 18, 1994, the waters were flowing NW along the coast with a steady speed of 13 - 20 cms^{-1}. (Fig. 2.5./1) In August 1997 this flow was observed early in the morning near Chaitika but it had an opposite direction in the late evening. Only just near Lufubu was the flow direction the same. On November 24, 1994 the surface flow in this region was headed NE at noon. The waters at the depth of 20 m and 40 m were flowing SE (Fig. 2.5./2-3). The same surface flow was also observed in April 1997 along the ADCP-transect from Lufubu NE.
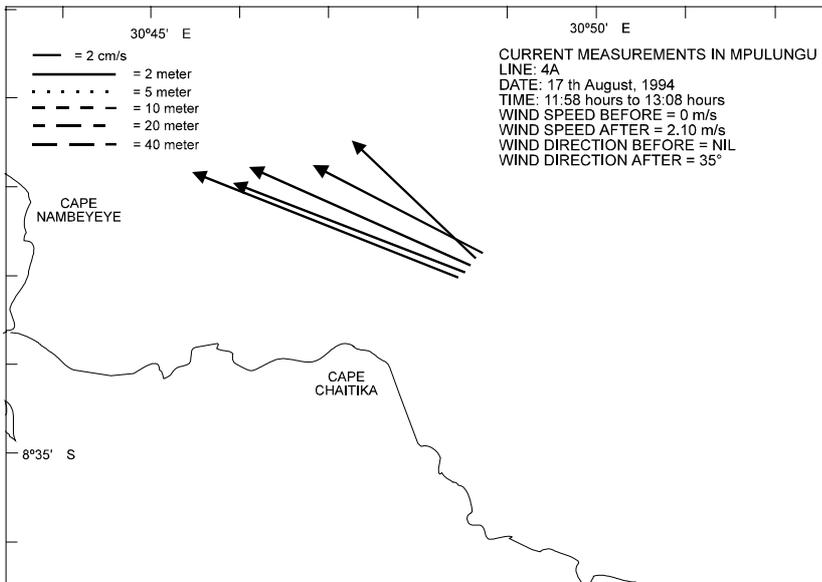
Figure 2.5./1 Water currents measured by flow cylinders in the Mpulungu basin near Cape Chaitiga on Aug 17, 1994. The legend shows wind data before and after the current measurements.
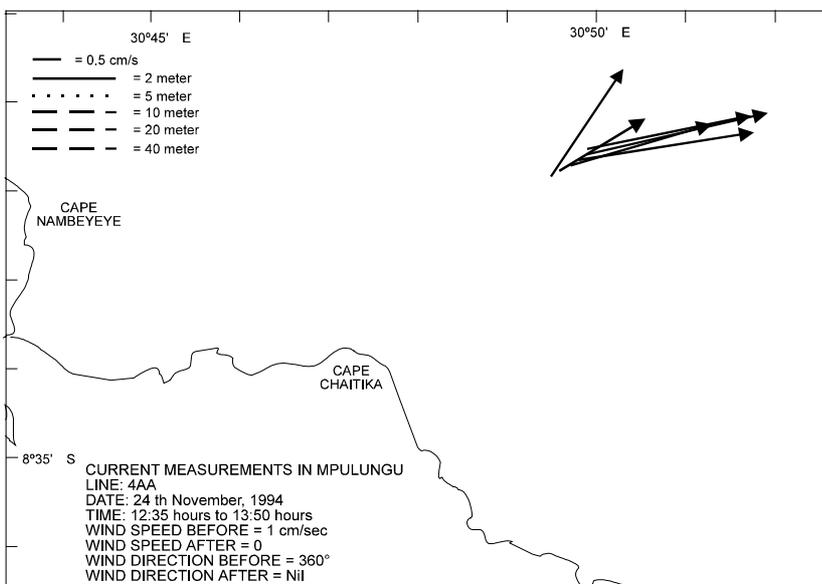
Figure 2.5./2 Water currents measured by flow cylinders (depth 2 m) in the Mpulungu basin near Cape Chaitiga on Nov 24, 1994. The legend shows wind data before and after current measurements.
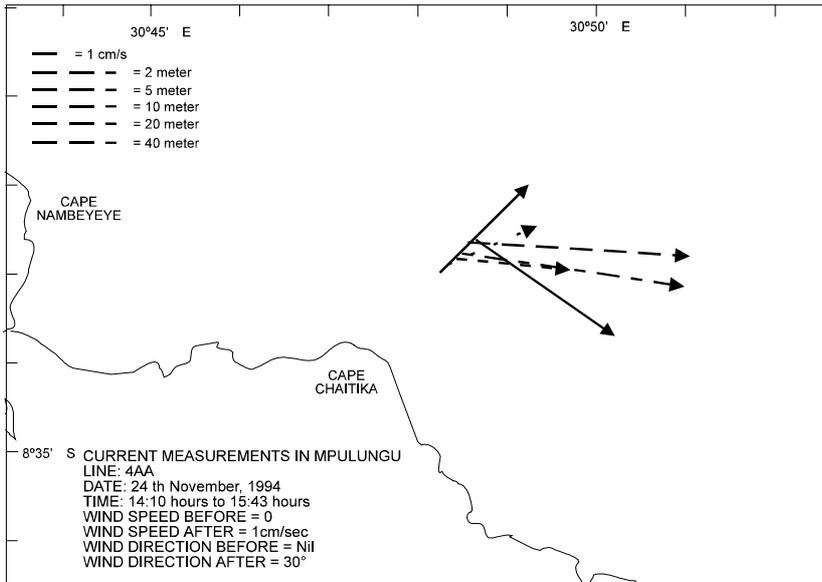
Figure 2.5./3 Water currents measured by flow cylinders (depth 2 m and 5 m) in the Mpulungu basin near Cape Chaitiga on Nov 24, 1994. The legend shows wind data before and after current measurements.

Near **Bujumbura** the current results by ADCP gave somewhat different results as compared to the earlier results from flow cylinders. Two current cylinder measurements of lines 3 and 4 in 1994 present a typical current flow pattern for the late dry season in the region (Figs 2.5./4 and 5). The two measurements were carried out south of Bujumbura on 25.8.1994 and 1.9.1994. Cylinder depths varied from 2 to 40 meters. The measurements started near shore in the morning and ended offshore in the later afternoon. Before noon winds were fairly weak, also the measured currents were slow. In the afternoon, southerly wind grew. Close to the shore before noon currents flowed S or SW, but in the afternoon and more offshore they flew N - NE (Figs. 2.5./4 and 5). In ADCP measurements in 1997 the currents were mostly towards south during the measurement time in the afternoon. A northward flow was detected at a few sites only.
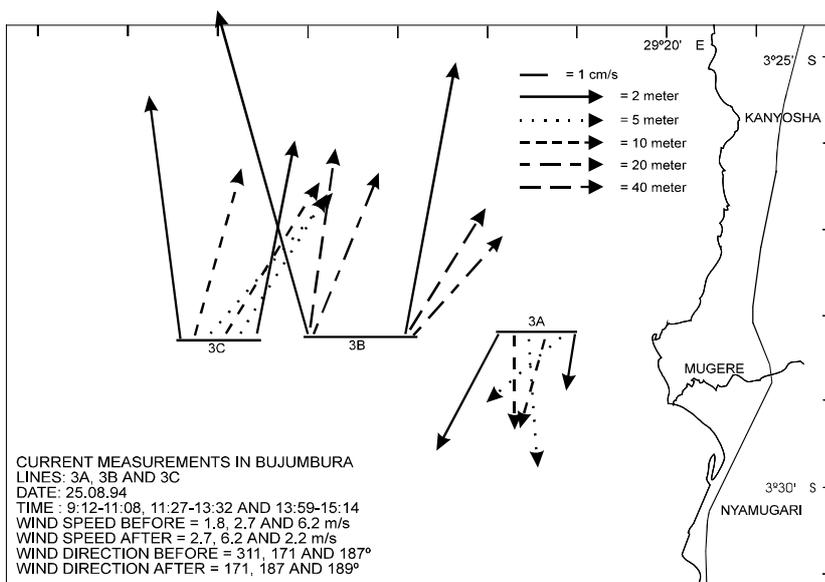
Figure 2.5./4 Water currents measured by flow cylinders (depth 2 - 40 m) near Bujumbura on Aug 25, 1994. The legend shows wind data before and after current measurement on each line.
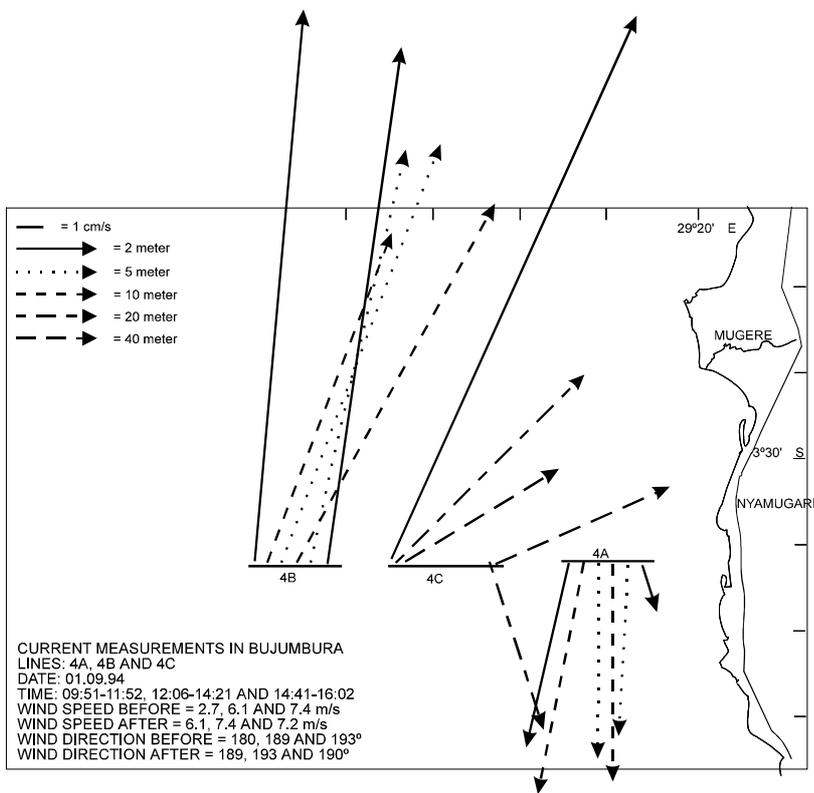
Figure 2.5./5 Water currents measured by flow cylinders (depth 2 - 40 m) near Bujumbura on Sep 01, 1994. The legend shows wind data before and after current measurements on each line.

The great depth (mean value = 572 m) of the lake and the regular forcing of the winds during the dry season result in long and persistent **internal wave motion**. Coulter (1963) has already discussed quite extensively the existence of internal waves. In the present LTR project, the internal waves were recorded for the first time with automatic devices. The periodic oscillations in the thermocline region were discussed both by Kotilainen et al. (1995a) and Plisnier et al. (1996). Their discussion is based on a visual interpretation of time series of temperature. Plisnier used data from the Mpulungu lake station and the water sampling stations near Bujumbura, Kigoma and Mpulungu, and Kotilainen et al. (1995a) used data from the automatic lake stations in Mpulungu and Kigoma. The periods of the internal temperature fluctuations were studied by spectral analysis by Podsetchine and Huttula (1996) from thermistor chain data from Mpulungu and Kigoma buoy stations. The period of internal waves was found to be different during the dry season (23.4 d) and the wet season (34.8 d). Coulter (1963,1968) observed very similar periods. He states that they varied from 23 to 33 days. From his thorough spatial temperature observations he calculated the theoretical values for dry season to be 23 days (May 15), 33 days (October 12) and 26 days (April). The calculations were based on a simple two layer model with a mean depth of 800 m for the hypolimnium. The frequency of these waves supports the hypothesis that they are Kelvin internal waves. The reason for the shorter period during the dry season is the periodic forcing by winds. In the Kigoma data from March-May 1994 the period obtained was also 26.3 d. This is again very much like Coulter's result. A relatively large part of this data represents the dry season. The results now with Coulters observations supports the view that wind forcing causes the long period of internal waves during the dry season. And that by the time they are dissipated by friction.

The results obtained now are unique when considering the Great Lakes of Africa. There is no data from any other African lakes about currents. The thermal regime of other African great lakes has been studied. When the current speed and hydrodynamic pattern of the Lake Tanganyika is compared to the lakes in a humic climate, it can be stated that the warm waters and the persistent forcing and two main season make the lake exceptional as compared to other lakes studied in the world.

3. Numerical modelling

3.1 Flow model - the basic equations

The governing hydrodynamic equations, assuming that **hydrostatic and Boussinesq approximations** are valid, may be written in vector form as follows (Blumberg and Mellor, 1987):

momentum

$$\frac{\partial V}{\partial t} + (\nabla \bullet V)V + f \times V + w\frac{\partial V}{\partial z} = -\frac{\nabla P}{\rho} + \nabla \bullet (\nu_H \nabla V) + \frac{\partial}{\partial z}(\nu_z \frac{\partial V}{\partial z}), \qquad \textbf{(3.1)}$$

(1)   (2)   (3)   (4)   (5)   (6)   (7)

hydrostatic equation

$$\frac{\partial P}{\partial z} = -\rho g, \qquad \textbf{(3.2)}$$

continuity equation

$$\frac{\partial w}{\partial z} + \nabla \bullet V = 0, \qquad \textbf{(3.3)}$$

free-surface evolution

$$\frac{\partial \zeta}{\partial t} + \int_{-h}^{\zeta} (\nabla \bullet V)dz = 0, \qquad \textbf{(3.4)}$$

Here $V=(u,v)$ is the horizontal velocity vector, w is the vertical velocity component, f is the Coriolis parameter, P is the pressure, ρ is the water density, g is the gravity acceleration, ν_H, ν_z are horizontal and vertical turbulent exchange coefficients respectively, z is the water surface elevation, h is the depth from reference level, ∇ is the horizontal gradient operator, t is a time, z is the vertical coordinate positive upward.

Boundary conditions on the free surface and the bottom are:

$$\rho \nu \frac{\partial V}{\partial z}\Big|_{z=\xi} = \tau^s,$$

$$\rho \nu \frac{\partial V}{\partial z}\Big|_{z=-h} = \tau^b \vee V\Big|_{z=-h} = 0 \qquad \textbf{(3.5)}$$

Here τ^s is the wind-induced shear stress and τ^b is the bottom friction stress. Surface shear stress is usually approximated with quadratic law

$$(\tau_x{}^s, \tau_y{}^s) = \gamma\rho_a(W_x{}^2 + W_y{}^2)^{1/2}(W_x, W_y),$$ **(3.6)**

where ρ_a is the air density, (W_x, W_y) are wind velocity components and $\gamma = 2.6 \times 10^{-3}$ is a wind drag coefficient. For bottom stresses either quadratic or linear dependence on water velocity is used:

$$(\tau_x{}^b, \tau_y{}^b) = k_1\rho(u^2 + v^2)^{1/2}(u,v)\big|_{z=-h},$$ **(3.7)**

$$(\tau_x{}^b, \tau_y{}^b) = k_2\rho(u,v)\big|_{z=-h},$$ **(3.8)**

Vanishing velocities near the bottom $(V|_{z=-h}=0)$ are known as "no-slip" boundary conditions.

Together with the equation of state and energy equation the system (3.1-3.4) forms a closed system of equations, describing a wide spectra of motions in real water bodies, such as coastal seas, lakes and oceans.

In many practical applications the system (3.1-3.4) can be further simplified. Let us first examine the role of different terms in momentum equations on the basis of dimension analysis. Introducing non-dimensional variables by expressions: $V^* = V/V_0$, $W^* = w/W_0$, $X^* = x/L$, $Z^* = z/H$, $T = ft$ and so on, where V_0, W_0, L, H are characteristic scales of horizontal and vertical velocity, horizontal and vertical length, the non-dimensional combinations of parameters appear in equation (3.1). Calculated values of these parameters with the characteristic scales of Lake Tanganyika are combined in Table 1 : $L = 600,000$ m, $H = 500$ m, $V_0 = 0.5$ ms^{-1}, $W_0 = 10^{-4}$ ms^{-1}, $f = 1.52 \times 10^{-5}$ s^{-1}, $\nu_{H0} = 100$ m^{2}s^{-1}, $\nu_{z0} = 10^{-2}$ m^{2}s^{-1}.

Table 1. Characteristic values of different terms in momentum equations (3.1).

Term of equation	Non-dimensional parameter	Numerical value
(1)-local acceleration	1	1
(2)-advection	Rossby = $U_0/(fL)$	0.05
(3)-Coriolis term	1	1
(4)-convection	$W_0/(fH)$	0.013
(5)-pressure gradient	$gH/(fLU_0)$	1000
(6)-horizontal diffusion	$\nu_{H0}/(fL^2)$	1.82×10^{-5}
(7)-vertical diffusion	$\nu_{z0}/(fH^2)$	2.60×10^{-3}

Of course, these are rough average estimates, but they clearly demonstrate the dominating role of the pressure gradient term. Relative ratios of different terms vary in time and space, for example, convective terms may be important in shallow coastal zones where high horizontal velocity gradients are observed.

By integrating the hydrostatic equation (3.2) a pressure gradient can be written as a sum of two parts:

$$\frac{\nabla P}{\rho} = -g\nabla\zeta - \frac{g}{\rho}\int_{z}^{\zeta}\nabla\rho d\,z'.$$ (3.9)

       (1)   (2)

The first term is the barotropic forcing, mainly caused by wind induced shear stress. The second one represents the baroclinic forcing due to the internal density distribution related to water temperature horizontal gradients. It is well known that temperature stratification in Lake Tanganyika is rather weak. The difference in temperature between epi- and hypolimnion is about 3 - 4 $^{\circ}$C and can easily be destroyed, especially during a dry season. Observational data (Chapter 2) show that the south part of the lake is almost completely mixed during a dry season. Surface layers are mixed occasionally in other parts of the lake.

On the basis of intensive CTD measurements during IAA expeditions an integral, representing a baroclinic term, was calculated for different parts of the lake. The results of these calculations are summarised in the Table 2.

Table 2. Baroclinic terms estimates using CTD measurements in different parts of Lake Tanganyika. RM - River Malagarasi, RL - River Lufubu. The values should be multiplied by 10^{-7}.

Place	Exp.14				Exp.16					
RM	CTD4	CTD8	CTD6	CTD10C	CTD37	CTD31	CTD33	CTD41	CTD49	CTD51
	CTD5	CTD9	CTD7	TD11	CTD38	CTD32	CTD34	CTD42	CTD50	CTD52
	8.51	-0.387	6.45	-19.2	5.95	2.03	0.29	-11.2	3.43	3.17
RL	CTD56				CTD77					
	CTD58				CTD78					
	-18.8				10.2					

At the same time the barotropic gradient is of the order 10^{-6} - $2*10^{-6}$, according to water level measurements in different parts of the lake performed at LTR stations in Bujumbura and Mpulungu (Kotilainen et al., 1995). On the basis of these estimates it can be concluded that, in our particular case, baroclinic terms are negligible compared to barotropic ones and hence the equations of motions can be reduced to the **barotropic** version. This is especially justified for the case of short-term synoptic scale simulations when the integration period has the order of one week.

3.2 Sediment transport model

In a three-dimensional case the equation of suspended sediments transport takes the following form (Sheng and Lick, 1979):

$$\frac{\partial S}{\partial t} + \frac{\partial uS}{\partial x} + \frac{\partial vS}{\partial y} + \frac{\partial (w-w_s)S}{\partial z} = \frac{\partial}{\partial x}\left(K_x\frac{\partial S}{\partial x}\right) + \frac{\partial}{\partial y}\left(K_y\frac{\partial S}{\partial y}\right) + \frac{\partial}{\partial z}\left(K_z\frac{\partial S}{\partial z}\right),$$ (3.10)

where u, v, w are velocity components, w_s is the settling velocity, K_x, K_y, K_z - are diffusion coefficients in x, y, z directions respectively.

No-flux boundary conditions are imposed on the free water surface:

$$w_s S + K_z \frac{\partial S}{\partial z}\bigg|_{z=\xi} = 0. \tag{3.11}$$

On lateral boundaries either known values of suspended sediments concentration as a function of time (in places of rivers inflow) are used or zero-flux boundary conditions are applied (on solid part of the boundary):

$$S\big|_{\Gamma_1} = S_1(x,y,z,t) \quad \vee \quad \frac{\partial S}{\partial n}\bigg|_{\Gamma_2} = 0. \tag{3.12}$$

3.3 Processes at the water-bottom interface

Complex physical and chemical processes at the water-bottom interface, with different space and time scales, take place in the benthic boundary layer. Strong physical, chemical and biological gradients are found in these layers. Usually scales in the boundary layer are smaller than grid cell size in numerical models and this causes serious difficulties in the selection of a suitable boundary condition. "It requires skill and a correct physical knowledge of bed-load layer" (Tanguy et al. 1991, p. 574) to describe it in a model. Many approaches may be found in literature, but they are all more or less simplifications of the complex phenomena taking place at the water-bottom interface. The following paragraph deals with different types of bottom boundary conditions for suspended sediments in water and their interaction with the bottom. Van Rijn (1984) presented an expression for local equilibrium concentration of suspended sediments at the bottom. He supposed that the bed-load layer maintains a definite value of suspended sediments concentration, the so called equilibrium concentration:

$$S_{z=a} = S_{a,e} = \begin{cases} \dfrac{0.015\, d_{50}}{a}\ \dfrac{T^{1.5}}{D_*^{0.3}}, \ sand \\[3mm] \dfrac{M\,T}{w_s}, \ clay, silt, mud \end{cases} \tag{3.13}$$

where $T = (\tau_b - \tau_{b,cr})/\tau_{b,cr}$ - bed shear stress parameter, $D_* = d_{50}[g(\rho_s-\rho)/(\rho\nu^2)]^{1/3}$ is a dimensionless particle parameter, τ, $\tau_{b,cr}$ are the hydrodynamic and critical shear stresses, ρ_s, ρ - density of sediments and water, ν - kinematic water viscosity, M - material "constant", depending on sediment composition, salinity and other characteristics, a - reference level. The reference level is a fictitious level, for which reference concentration may be calculated and is defined as $a_{min} = 0.01$ H for reasons of numerical accuracy (Van Rijn 1990).

If preliminary estimations show a prevalence of erosion, then the local equilibrium diffusive upward sediment flux on the bottom boundary may be calculated using a similar expression

$$-K_z \frac{\partial S}{\partial z}\Big|_{z=a} = \begin{cases} \dfrac{0.015\, d_{50}\, w_s}{a} \dfrac{T^{1.5}}{D_*^{0.3}}, \; sand \\[2mm] M\,T \,, \; clay, silt, mud. \end{cases} \tag{3.14}$$

A more general form of bottom boundary condition was used by Sheng and Lick (1979)

$$F = -(w_s S + K_z \frac{\partial S}{\partial z}) = -\beta S + E = -\beta(S - S_{eq}) = -D + E. \tag{3.15}$$

Here $D = \beta S$ denotes deposition flux, assumed to be proportional to the local concentration S, E - erosion (resuspension or entrainment) flux due to bottom shear stresses generated by different mechanisms, mainly currents and waves, β - coefficient of proportionality. Under equilibrium conditions when $F => 0$, $t => \infty$, $S_{eq} = E/\beta$. Coefficient β may be considered as the deposition velocity of sediments at the bottom surface. Another interpretation of β as the reflectivity coefficient of the bottom surface stems from the probabilistic point of view (Cheng 1984) i.e., $\beta = 0$ means a perfectly reflecting surface and $\beta => \infty$, a perfectly absorbing surface. Other names for β as the deposition coefficient may also be found in literature.

An approximate analytical expression for β was derived by Lick (1982)

$$\beta = \frac{w_s}{1 - \exp(-w_s / \beta_d))}. \tag{3.16}$$

Here β_d is the limiting value of β when only Brownian and turbulent diffusion is considered. He suggested that settling and Brownian motion are the dominant processes close to the sediment - water interface. For turbulent diffusion proportional to the third power of distance from the sediment-water interface z^3, β_d is given by

$$\beta_d = 0.06\sqrt{\tau / \rho}\,(\rho K_b / \mu)^{2/3}, \tag{3.17}$$

where τ is the shear stress, ρ, μ are water density and molecular viscosity respectively, $K_b = kT/(3\pi\mu d)$ is the Brownian diffusion coefficient, $k = 1.380662 *10^{-23}$ JK^{-1}, is the Boltzmann constant, T - temperature, d - diameter of the particle. The coefficient β converges very quickly to w_s as particle size increases. Only for very small particles ($d < 10^{-6}$ m) when diffusion is prevailing does β equal β_d.

The concept of threshold is commonly accepted for describing processes of particle movement initiation and suspension (Raudkivi 1990; Van Rijn 1990). Initiation of particle motion occurs when disturbing forces of fluid drag and lift acting on particles exceed the values of stabilising weight force. Particles moving along the bed (rolling, jumping, saltating) may go into the suspension phase when bed shear velocities increase to values of the fall velocity (Van Rijn 1990). In numerical modelling, correct parameterization of suspension or erosion flux from the bottom is of crucial importance. As there is no theory of these processes today, empirical relations

from laboratory and field experiments are widely used. Table 3 (Podsetchine and Huttula, 1994) summarises values of critical shear stresses defined by different researchers. For different type of sediments their range is of a three order magnitude.

Table 3. Values of critical shear stresses for different case studies.

AUTHORS	MATERIAL	CASE STUDY	τ, Nm^{-2}
Metha, Partheanides, 1975	mud	laboratory experiments	0.18
Krone, 1976	mud	laboratory experiments	0.06-0.08
Sheng & Lick, 1979	sand,silt	Western Lake Erie	0.05
Huttula, Krogerus, 1982	cellulose fibres	Valkeakoski, Finland	0.008
Lang, Schubert, Markofsky, 1989	fine silt	Weser estuary, W.G.	0.5
Dyer, 1989	mud	laboratory experiments	3.0
Luetich, Harleman, Somlyody, 1990	fine silt	Balaton	0.05
Sheng, Eliason, Chen, 1991	mud	Tampa Bay, Florida	0.001-1.0
Sheng, Eliason, Chen, 1991	mud	Okeechobee, Florida	0.04
Pickens, Lick, 1991	fine sand, clay	California Coast	0.1
Verkfræðistofan Vatnaskil, 1993		Lake Mývatn	0.05-0.4

Based on laboratory experiments with different types of sediments from Lake Erie, Sheng and Lick (1979) selected the following formula for the rate of resuspension E as a function of bottom shear stress

$$E = c_1(\tau - 0.05), \quad \tau \le 0.2 \, N/m^2,$$
$$E = c_2(\tau - 0.1515), \quad \tau > 0.2 \, N/m^2,$$

$$(3.18)$$

where $c_1 = 1.33 \times 10^{-4} \, sm^{-1}$, $c_2 = 4.12 \times 10^{-4} \, sm^{-1}$. No resuspension was observed when the shear stress was less than 0.05 Nm^{-2}. Variation of the deposition coefficient was small for all sets of experiments and an averaged value of $\beta = 8 \times 10^{-5} \, ms^{-1}$ was found.

Field experiments conducted by Lavelle et al. (1984) show that the erosion rate E more than likely has a power law dependence on bottom shear stress τ

$$E = \alpha |\tau|^q.$$

$$(3.19)$$

From the analysis of laboratory and field data they came to the conclusion that the concept of critical shear stress or critical velocity is a very subjective one. Due to the random nature of

turbulent flow there will always be particles in motion. Other researchers argue that threshold value is necessary for practical design purposes (Van Rijn 1990). Results of Lavelle et al. (1984) and other laboratory and field studies show that the erosion rate normalization coefficient α varies from $1.9 * 10^{-8}$ (San Francisco Bay mud, Parthenaides, 1965) to $3.7 * 10^{-5}$ kg m^2 s^{-1} (Lake Erie, Fukuda and Lick, 1980). The value of the power constant q is within the range 1.2 to 5. However, it is very difficult to take into account differences in laboratory and field conditions, mineral content, size and shape distribution of eroding material and biological activity . "This myriad of factors and possibly others yet to be considered make the interpretation of differences among these erosion rates impractical" (Lavelle et al. 1984, p. 6550).

Tests made by Sheng et al. (1991) indicate that in a sediment transport model the erosion rate is the most sensitive term. Since at the moment erosion cannot be predicted accurately, "constants" in these empirical relations must be determined empirically or calibrated numerically with available field data for every case study. In some case studies spatial variation of critical shear stress over lake was taken in consideration (Verkfræðistofan Vatnaskil 1993). This was based on data about composition of bottom and general knowledge that the erosion strength in coastal areas is higher than in deeper areas due to the higher erosion stresses. After numerical calibration, Lake Myvatn was divided into 4 regions with critical shear stresses from 0.05 to 0.4 Nm^{-2} in coastal areas.

3.4 Numerical approximation

The state of the rest (u=v=w=0, ξ=0) is usually used as initial conditions for the three-dimensional hydrodynamic equations (3.1-3.4). Known distributions of suspended sediment concentration are used for equation (3.10).

Numerical realization of the three-dimensional flow and sediment transport models includes:
- the bottom-following vertical coordinate system (σ-coordinate);
- the space-splitting numerical scheme;
- the Galerkin method with linear triangular elements for integration in the horizontal plane
- the upwinding Tabata scheme (Tabata, 1977) for approximation of convective terms;
- the implicit control-volume scheme for integration in the vertical direction.

Schematically the main features of the numerical scheme are as follows. The governing equations can be written in shorthand form as:

$$\frac{\partial \Theta}{\partial t} + A_{x,y}(\Theta) + A_z(\Theta) = 0, \qquad\qquad (3.20)$$

where Θ stands for u, v, ζ, S and $A_{x,y}$ and A_z are operators with horizontal and vertical terms respectively. Approximating the time derivative with a forward difference, equation (3.20) can be split in two:

$$\frac{\Theta^{n+1/2} - \Theta^n}{\Delta t / 2} + A_{x,y}(\Theta^{n+1/2}) = 0, \qquad\qquad (3.21)$$

$$\frac{\Theta^{n+1} - \Theta^{n+1/2}}{\Delta t / 2} + A_z(\Theta^{n+1}) = 0. \tag{3.22}$$

An approximate solution of (3.21) is sought in the form of a finite sum

$$\Theta \approx \sum_{i=0}^{N} \Theta_i \varphi_i, \tag{3.23}$$

where φ_i, i=1,..N, is the set of bilinear interpolation functions. Substituting (3.23) into (3.21), multiplying according to the Galerkin method by weighting functions φ_j^t, j=1,...N and integrating over the solution domain, a system of the algebraic equations is obtained. The Gauss elimination method is used to solve the resulting algebraic system. Equations (3.22) form a set of locally one-dimensional equations. They are solved by the control volume scheme of Patankar (1980).

3.5 Numerical simulations

3.5.1 Application of the HIRLAM operational weather forecast model for the Lake Tanganyika region

In the early stages of Lake Tanganyika Research, it became evident that the wind field over the lake could not be taken as uniform as in many flow model applications for smaller Finnish lakes and even for Lake Ladoga.

The seasonal changes in the surface wind pattern of the Lake Tanganyika region show great variation both in space and time. There are strong seasonal and diurnal variations in wind forcing due to the local and seasonal trade winds. The dry season from May to September has the strongest winds of the year and the flows induced by winds are also strong. The local winds are mainly diurnal mesoscale flow patterns (slope and lake breezes) caused by the strongly varying temperature differences between the rift lake and the strongly sloping shore. These local circulations are quite regular and strong over the shores of lake. They are combined with the large-scale trade winds, which are weak but steady.

With the help of funding from the Academy of Finland, a meteorological mesoscale model was applied along 10 transects across the lake. The mesoscale atmospheric model simulates the diurnal behaviour of near-surface winds due to topography and variations in the temperature between land and lake (Savijärvi 1995). This provides an opportunity to study peculiarities in the lake-wide circulation of an average day during the dry season. The atmospheric model is a two-dimensional hydrostatic moist sigma-co-ordinate model. There are 10 transects across the lake with a horizontal grid cell size of 4 km and with 11 atmospheric sigma levels. The time step is 8 seconds. Further details concerning the parametrization of physical processes, the numerical realisation as well as the initial and boundary conditions and comparisons to observations are given by Savijärvi (1997). The near-surface wind field is obtained as a vectorial sum of a constant south-easterly trade wind of 2.5 ms^{-1} and the varying lake-slope breeze component. These near-surface hourly winds in the weather conditions of an average day in July were then used as a input for the lake circulation model. Although the 2D modelling was successful in simulating diurnal surface wind along the selected transects across the lake, it became evident that a 3D model was needed for seasonal atmospheric modelling in the lake-wide scale.

For this purpose, a second phase of wind modelling was started with funding from the Academy of Finland for the years 1996-1998. In this work, a 3D atmospheric model (HIRLAM = High Resolution Limited Area Model) is being applied to the Lake Tanganyika region. This model is currently used for operational weather forecasting in several European countries. The application of the HIRLAM model to the Lake Tanganyika region was conducted at the Finnish Meteorological Institute (FMI). The production runs needed for the flow model were done at the University of Kuopio. For operational weather forecasting purposes the Finnish Meteorological Institute uses two spatial grid systems of 44 km and 27.5 km (Järvenoja et al. 1997). In Denmark, an experimental model with a 4 km grid is used. An equally high resolution is now used also in the Tanganyika application, since the flow model has a spatial resolution from 2.5 to 5 km.

HIRLAM is a complete system for short-range numerical weather forecasting. It contains an objective analysis scheme for treatment of initial observations, a non-linear initialisation scheme, a forecast model and required pre- and post-processing packages. The main component, the forecast

model, is a primitive equation model using grid point representation for finite differences. The prognostic variables are the horizontal wind components, the temperature, the specific humidity and the surface pressure. The physical part of the model contains parameterization of stratiform and convective precipitation, turbulent transport, short- and long-wave radiation and surface exchange processes. The whole HIRLAM system is described in the HIRLAM Documentation Manual, System 2.5 (Källen 1995).

When applying the HIRLAM model to the Lake Tanganyika region with a 5 km resolution, high resolution physiographic data are needed to prepare the important surface fields such as orography, land/water distribution, roughness length and albedo for the model. The model orography was prepared using the terrain altitude data from the U.S. Geological Survey's Eros Data Center (http://edcftp.cr.usgs.gov/pub/data) in a 3*3 km² grid. The land use data was obtained from UNEP's (the United Nations Environment Programme) Global Resource Information Database. These data were used for determining the fraction of land, fraction of lake, fraction of open land and fraction of forest. These result fields are further used together with the HIRLAM physiographic and climate database (Bringfelt et al. 1995) for determining roughness and albedo.

The model grid consists of 162 by 170 grid points with the grid length of 0.05° (5.5 km) in regular latitude-longitude grid. The forecast model has 31 so-called hybrid levels in the vertical. The very high horizontal resolution requires a short time step of 30 seconds in the model integrations. There are no (or very little) observational atmospheric data available from the Lake Tanganyika area. Therefore the HIRLAM system was run without the atmospheric analysis part. The initial conditions are taken from the ECMWF (European Centre for Medium Range Weather Forecasts) analysis interpolated to the HIRLAM model grid. The lateral boundary conditions (also ECMWF analyses) are therefore the only external forcing. The surface water temperature data was imported from CTD observations conducted during the expeditions. This was done during a so-called 'warm-up' period of one day, when 4 data assimilation cycles (of 6 hours) were carried out. After the 'warm-up' day (the first day of each month), the actual forecasts were run for the following 7 days (2 - 8 for each month). Figure 3.5.1./1 illustrates near-surface winds over Lake Tanganyika at midnight calculated with HIRLAM model. Combined downslope and land breeze winds (Savijärvi 1997) with convergence zone along the main axis of the lake are clearly distinguished.

Although the work is still in progress the comparison of the calculated meteorological characteristics with observed ones is very promising (Pessi 1997). The weather forecasting system is able to reproduce rather accurately diurnal variations of air temperature (Fig. 3.5.1./2), wind direction and magnitude (Fig. 3.5.1./3) and other parameters.
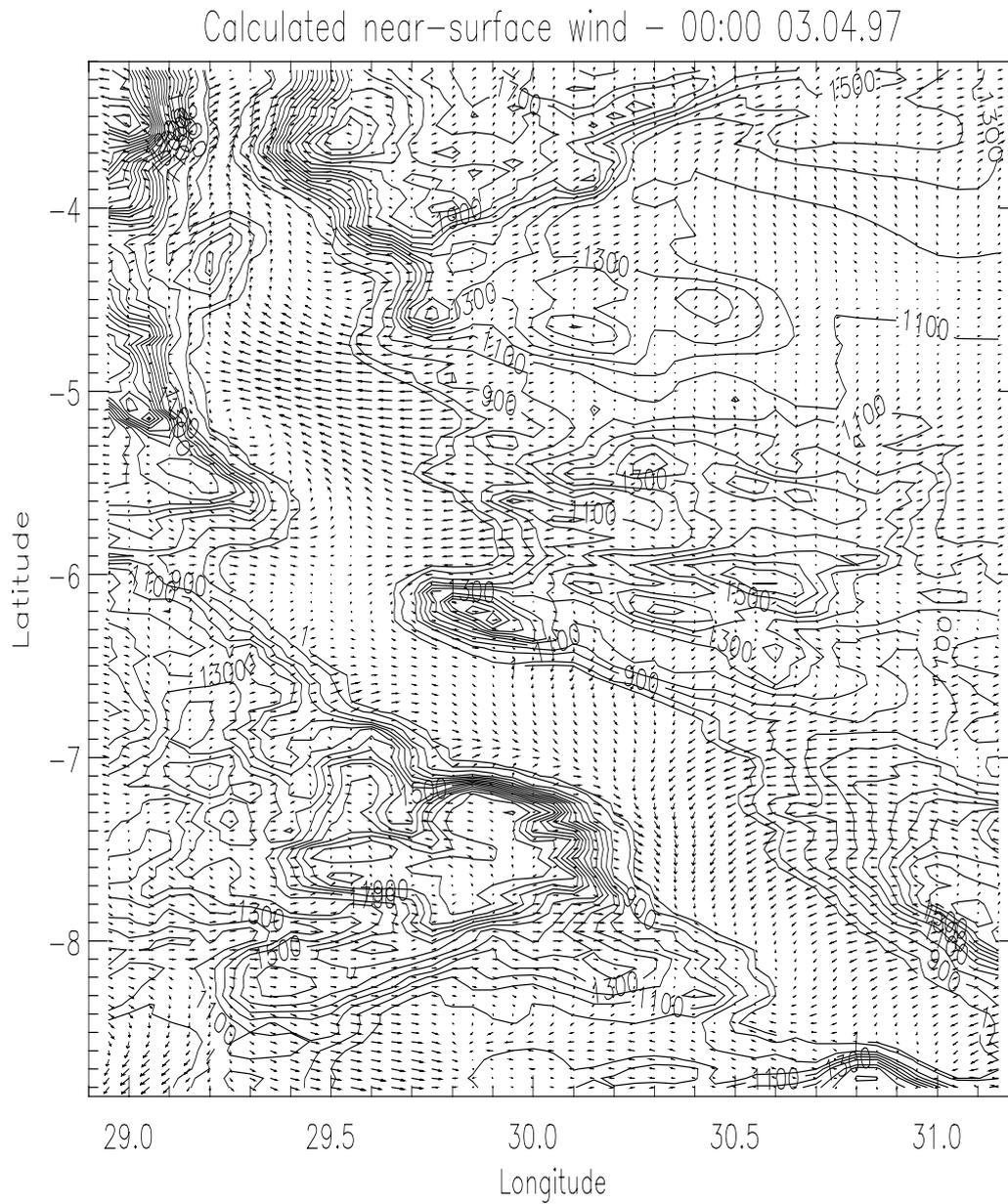
Fig.3.5.1./1 Calculated near-surface wind over Lake Tanganyika region. Isolines show orography in meters above mean sea level (MSL).

Kigoma lake meteo station - 2.7. - 8.7.95
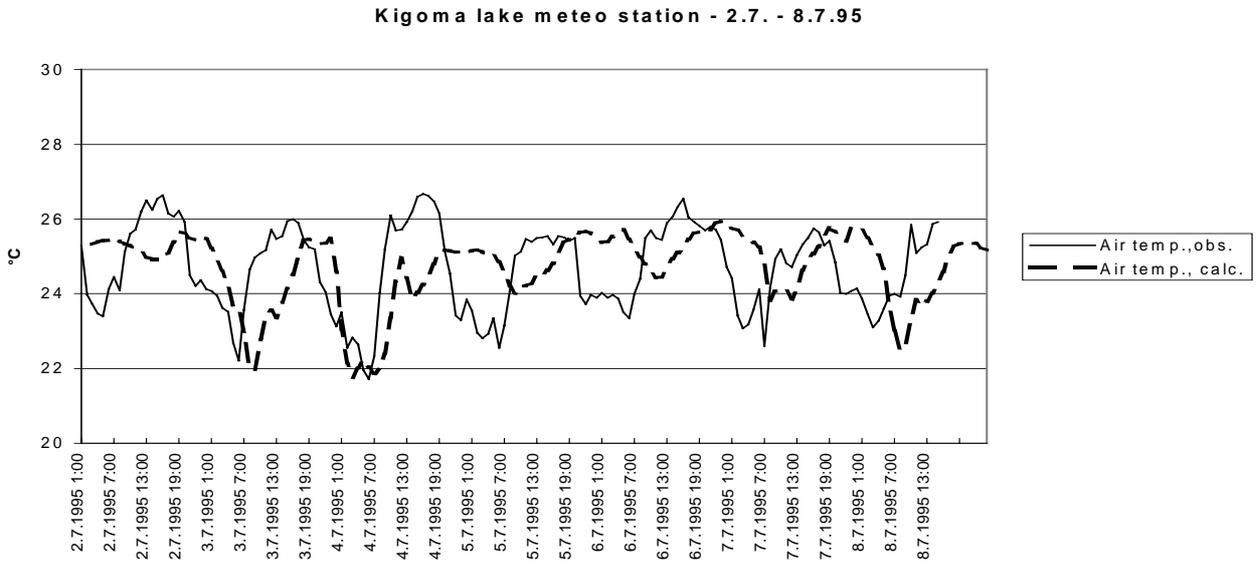
Fig.3.5.1./2. Comparison of one hour mean observed and calculated air temperature at Kigoma lake meteo station.

A

Kigoma wind station - measured wind
03:00 2.7.95 - 02:00 8.7.95
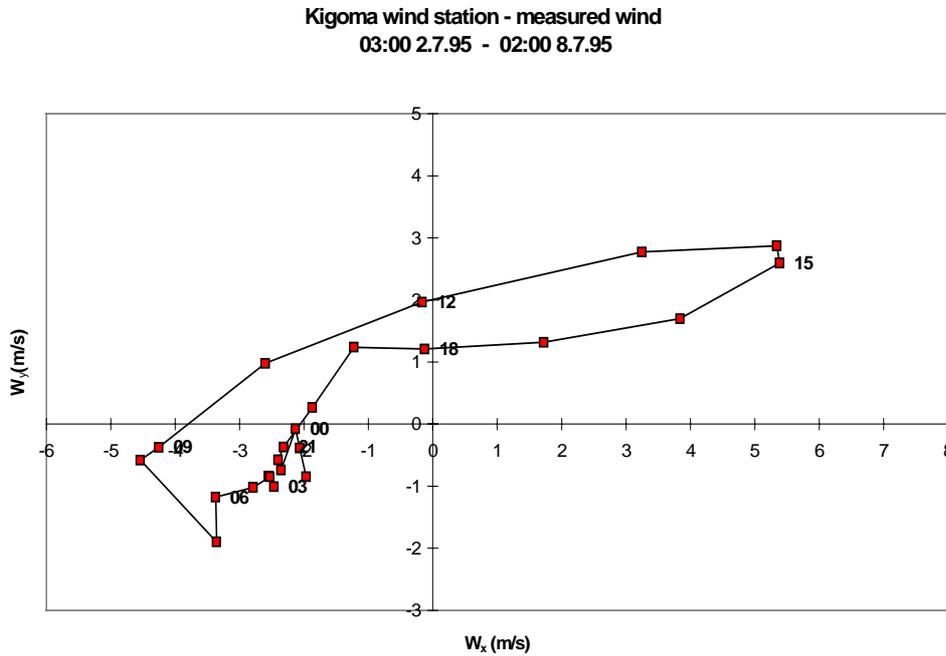
Fig.3.5.1./3A. Observed hodographs at Kigoma wind stations. Numbers near boxes denote a time of the day.

B
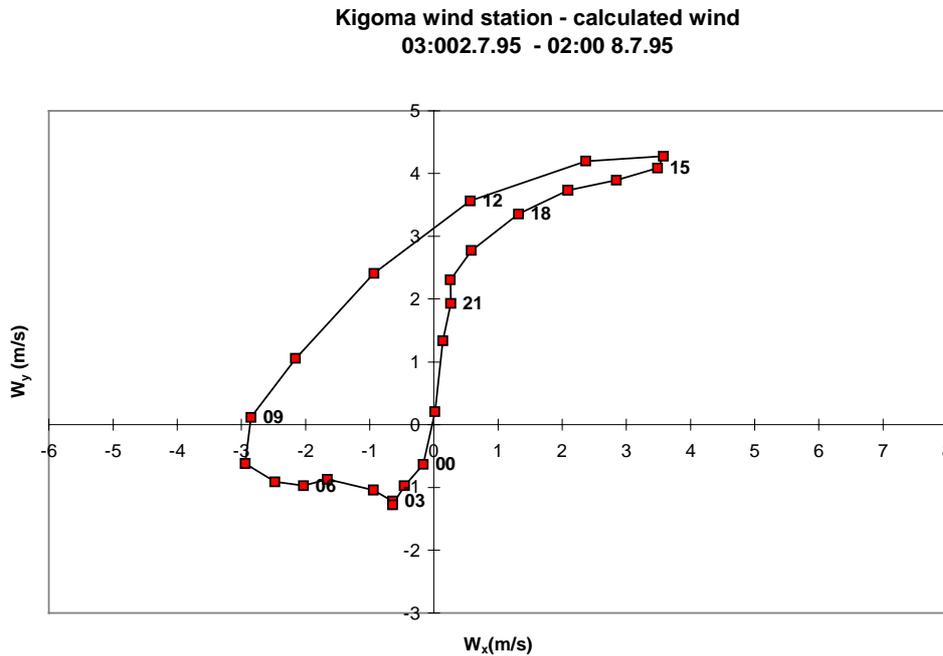
Fig.3.5.1./3B. Calculated hodographs at Kigoma wind stations. Numbers near boxes denote a time of the day.

3.5.2 Flow simulations - calibration of the model, comparison with observations

The HIRLAM simulations provided the necessary wind input data for flow models. Three different flow models were used. The first one is the lake-wide circulation model developed earlier during LTR Project (Podsetchine and Huttula, 1996). It has a spatial resolution from 2.5 to 5 km in the horizontal plane and 10 layers in the vertical direction. Two regional models with higher spatial resolution were developed for River Malagarasi region (Fig. 3.5.2./1) and for the southern part of the lake (Fig. 3.5.2./2).

The computational grid of Malagarasi regional model (Fig. 3.5.2./3) consists of 659 triangular elements with 1219 nodes in horizontal plane with average grid cell size of 1.5 km and 10 vertical layers. The integration time step was equal to 300 s. The other constants were taken to have the following values: $f = -1.26 * 10^{-5}$ s^{-1}, $\nu_H = 0.5$ m^{2}s^{-1}. No-slip boundary conditions were applied at the bottom.

The numerical grid of the south regional model (Fig. 3.5.2./4) has 632 triangual elements with 1095 nodes in horizontal plane and 10 layers in the vertical direction. The grid cell size varies from 0.4 km in the vicinity of River Lufubu mouth to 5 km in the north-eastern part of the domain. The integration time step was equal to 120 s, the Coriolis parameter $f = -2.14 * 10^{-5}$ s^{-1}. Other constants were identical to that of the Malagarasi model. Rivers Malagarasi and Lufubu were introduced in the models as point sources with constant velocities: 0.05 ms^{-1} for wet season and 0.03 ms^{-1} for dry season. These values have been extrapolated from literature (NORCONSULT, 1982). More details about hydrological measurements are provided in previous Chapter 2.4.3. All simulations covered one week period.
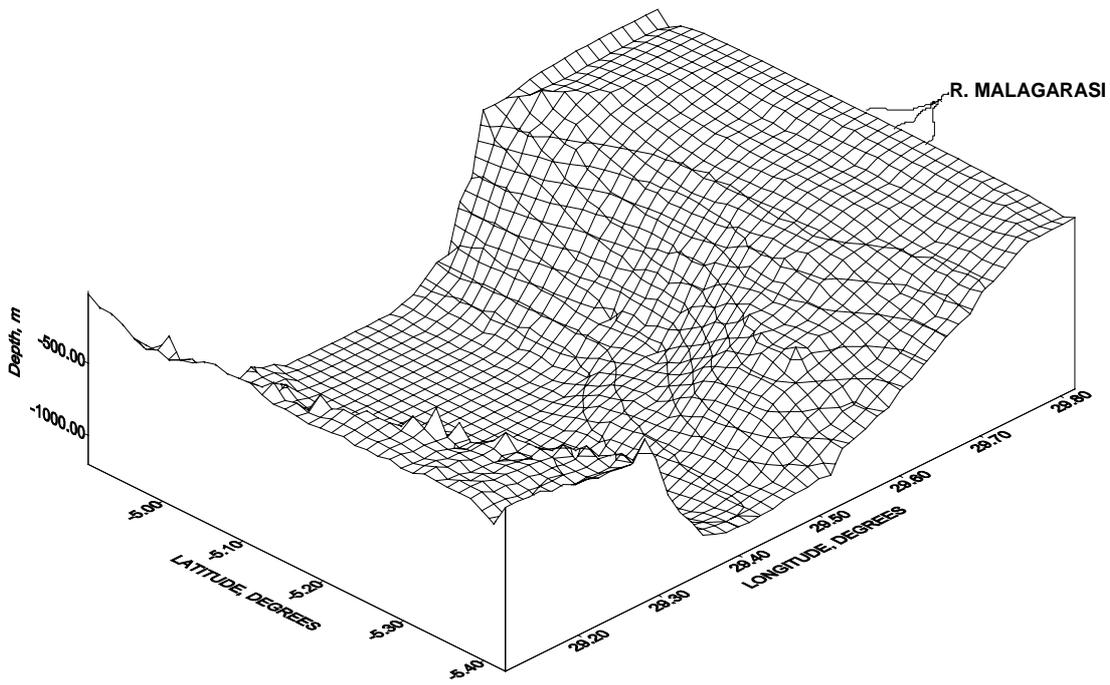
Fig.3.5.2./1 Lake Tanganyika bathymetry near River Malagarasi mouth.
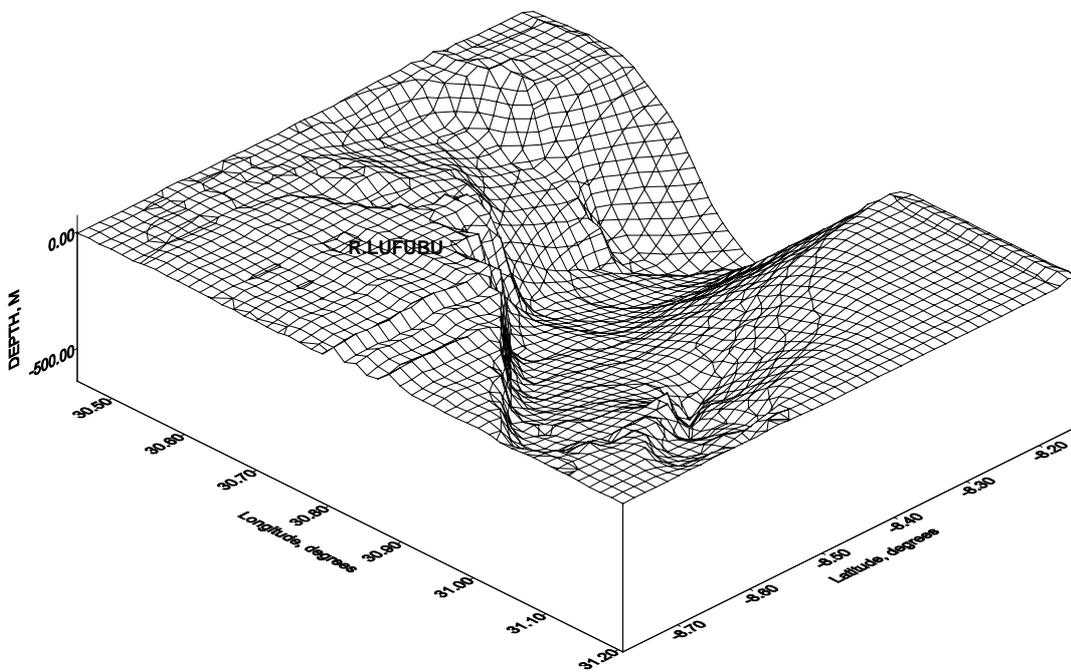
Fig.3.5.2./2 Lake Tanganyika bathymetry in the south part.
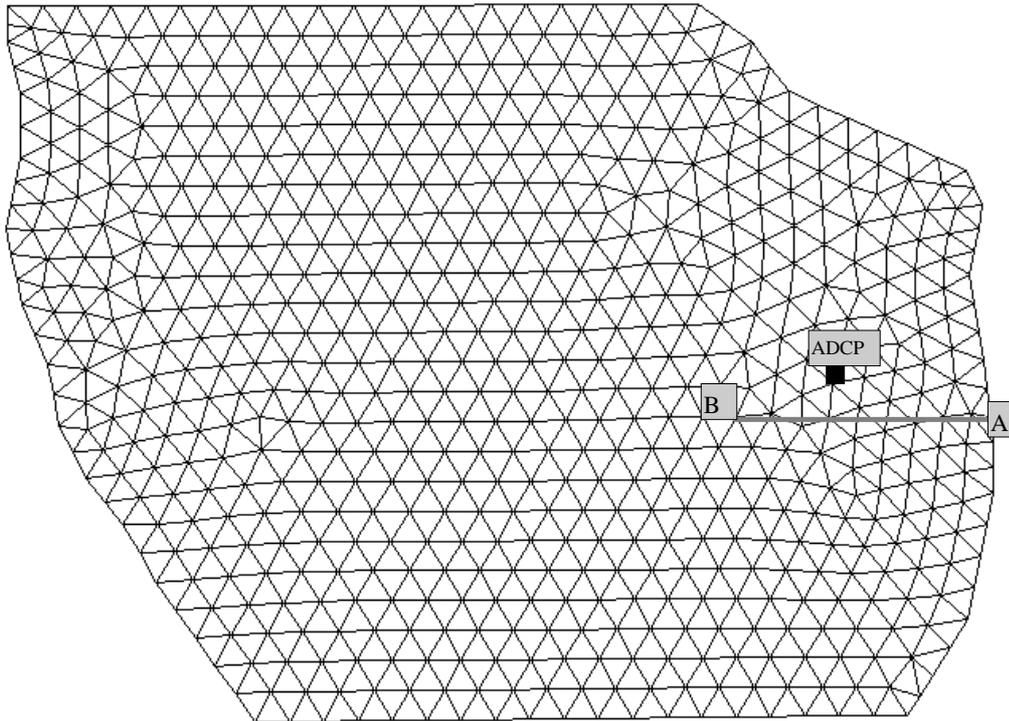
Fig. 3.5.2./3. Triangular grid of the Malagarasi regional model. Black box marks the location of the moored ADCP installed during the last expedition in August, 1997.
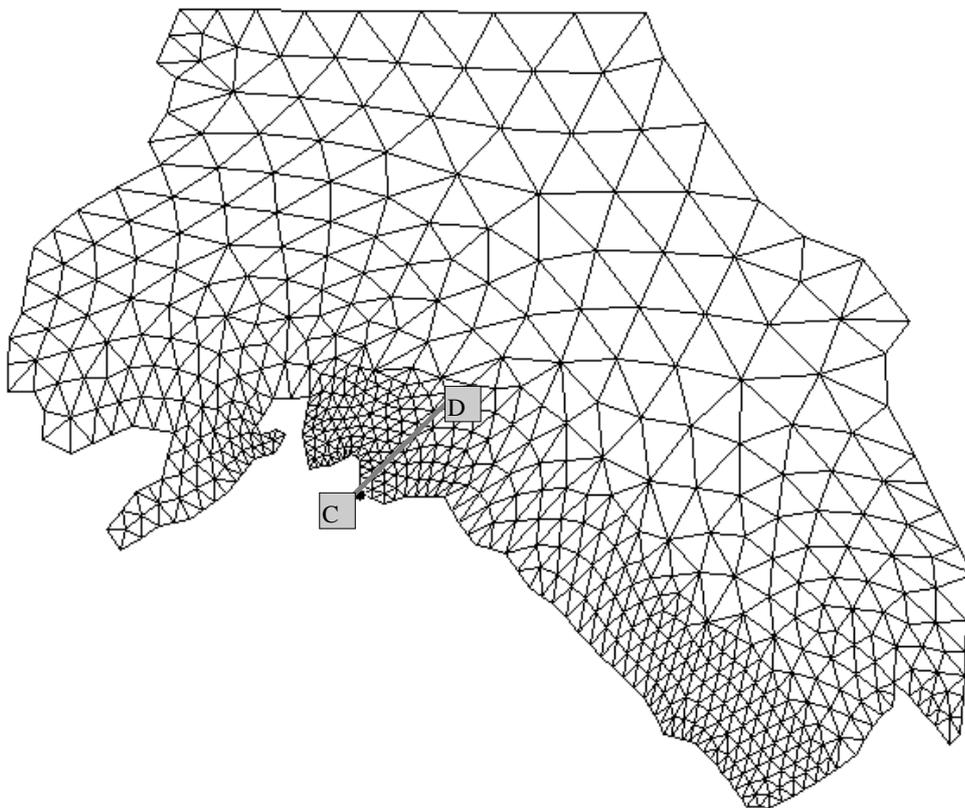
Fig. 3.5.2./4. Triangular grid of the Lufubu regional model.

For comparison with measurements two time periods were selected for numerical simulations: 02.04 - 8.04 1997 and 21.04 - 28.04 1997. They were selected to be coincident with IAA expeditions 14 (April 1997, wet season) and 16 (August - September 1997, dry season). Wind scenarios were also produced by HIRLAM to align with the same periods.

Overall calculations were organised in the following way. First near-surface hourly winds calculated with HIRLAM were interpolated from the regular rectangular finite-difference grid onto non-structured triangular grids of flow models using bilinear interpolation scheme. After that the lake-wide circulation model was run to calculate velocities across liquid boundaries of regional models for selected time intervals. Then regional flow models were used to calculate flow fields which have been stored on a hard disk. And finally transport models were applied to calculate the dynamics of Suspended Particulate Matter (SPM) over the same periods of time.

The calibration of the model was required to define the optimal values of time steps and horizontal diffusion coefficients from the point of view of accuracy, efficiency and numerical stability. Due to the higher spatial resolution of the numerical grid near the river Lufubu mouth the time step of the Lufubu regional model was 2.5 times smaller than that of the Malagarasi model.

A direct comparison of calculated surface flow with measured ADCP transects (Figures 2.4.4./28, 2.4.4./29 and 2.4.4./32) is rather difficult because measurements represent current patterns extended over time interval from 12 to 24 hours. Whereas the calculations produce the flow distribution for a certain instant of time. Due to the huge amount of collected ADCP measurements and simulations results it was not possible to report completely the validation of the model. This work will be published later. In what follows only the most interesting from the authors point of view results are discussed.

It is worth noting that in general both simulated and observed surface currents follow the wind direction. A comparison with point measurements made with moored ADCP at different depths (Fig. 3.5.2./5) near river Malagarasi mouth confirms this fairly obvious conclusion. Simulated currents in the vicinity of river Malagarasi delta fit rather well in direction with observed ones. Turning of the flow with wind is more clearly pronounced in the simulations. The magnitude of the calculated flow is lower than of the observed one. This difference grows as depth increases. While the calculated flow gradually decreases with depth observations show growing dispersion of the signal.

As it was already mentioned in Chapter 2.4 due to presence of a high frequency noise measurements at depth layers below 50 m are unreliable and have been discarded. Underestimation of the flow magnitude by the model may be partially explained by high diffusion properties of the numerical scheme. Both measurements and simulations are consistent in a sense that during dry season prevailing direction of the flow near river Malagarasi mouth is N-NW with regular diurnal cycle. Opposite currents directed towards south are considerably weaker and may be observed during a shorter period of time. Figures 3.5.2./6 - 3.5.2./65 illustrate calculated spatial and temporal variations of currents during 5.04.97 and 24.08.97 (middle of each integration period) in considerable detail. Surface currents, currents at 50 m and 100m depths, wind field (interpolated HIRLAM results) and depth-integrated flow are depicted. Rapid changes in flow patterns are observed within a daily cycle. Because of high hydraulic friction the influence of river plumes on currents is negligible. Winds over the lake are the main driving forces controlling the direction and magnitude of water currents.

121
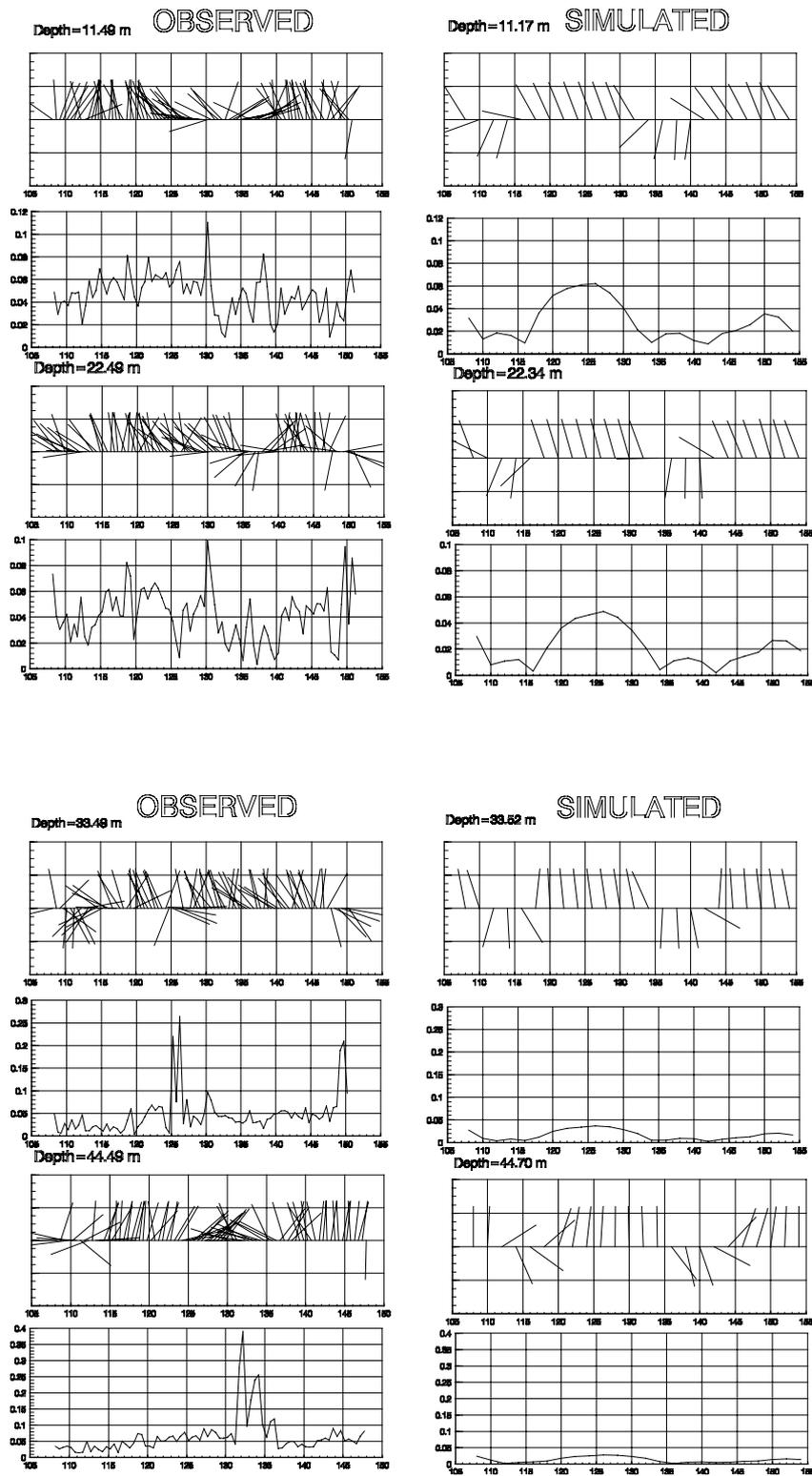
Fig. 3.5.2./5. Observed and simulated currents (ms^{-1}) near River Malagarasi mouth at different depths vs. time (hours) from 14:00 25.08.97 till 10:00 27.08.97. The site represents the deeper of two ADCP moorings.

The zone with highest velocities is located in shallow region adjacent to river Malagarasi mouth. Maximum calculated velocity of 0.13 ms^{-1} was at 04 hours in August when strong land breeze intensified by large scale trade winds blew (Figures 3.5.2./21 and 3.5.2./24). As it was noted already flow in surface layers follows the wind. As the depth increases more complex flow structures are revealed with compensational return currents directed against the wind

Among interesting features is the existence of rather stable eddy during the whole day of wet season in the region of river Malagarasi (Figures 3.5.2./12 and 3.5.2./17). It disappears in August when stronger winds blow.

The flow pattern in the south is more complicated than in the Malagarasi region. It was known also from previous numerical experiments (Podsetchine and Huttula, 1996) and ADCP measurements (Chapter 2). The gyre in Sumbu bay was observed earlier. Present calculations with higher spatial resolution reveal eddies formation in several places. It is strongest during night time (04 h) in August (Figures 3.5.2./40 and 3.5.2./55). The direction of calculated water currents along the NE coast of south region near Kala and Kalambo (Fig. 3.5.2./40) fits closely with the observations in April (Fig. 2.4.4./29). Near Kala the discrepancy between calculated (04:00 h, Fig. 3.5.2./55) and observed (05:40 - 06:40 h, Fig. 2.4.4./32) currents in August may be due to the time shift. The clockwise eddy in the SW corner of the region pronounced on the picture of the depth averaged flow (Fig. 3.5.2./41) can be also found in the measurement results (Fig. 2.4.4./29) along the transect CTD 49 - 52. The larger extent of the same gyre was predicted correctly with the model in August at 04:00 h (Figures 2.4.4./29 and 3.5.2./55).

The currents on the western shore vary considerably both in calculations and observations. This can be explained by daily variations of the wind over this region. The gyre in Sumbu meets the middle lake eddy with opposite rotation near the western coast along Kasaba point - Lufubu - Cap Chaitika. The transport of substances from the shore is substantially dependent on these flow structures. At night hours this circulation is the strongest one. In August the rotation of Sumbu eddy is clockwise and the middle one rotates anti-clockwise (Figures 3.5.2./55 and 3.5.2./65). During the night as a result of their interaction the small local gyre just near the river Lufubu mouth is generated. It means that river Lufubu waters are carried by ambient strongly varying flow either along the coast towards NW or SE depending on the time of the day. This type of variation was found in observations also (Figures 2.4.4/36 and 2.4.4/37).

Results of suspended sediments transport simulations presented in the next paragraph will show the important role of currents in the distribution of SS carried out by inflowing rivers.
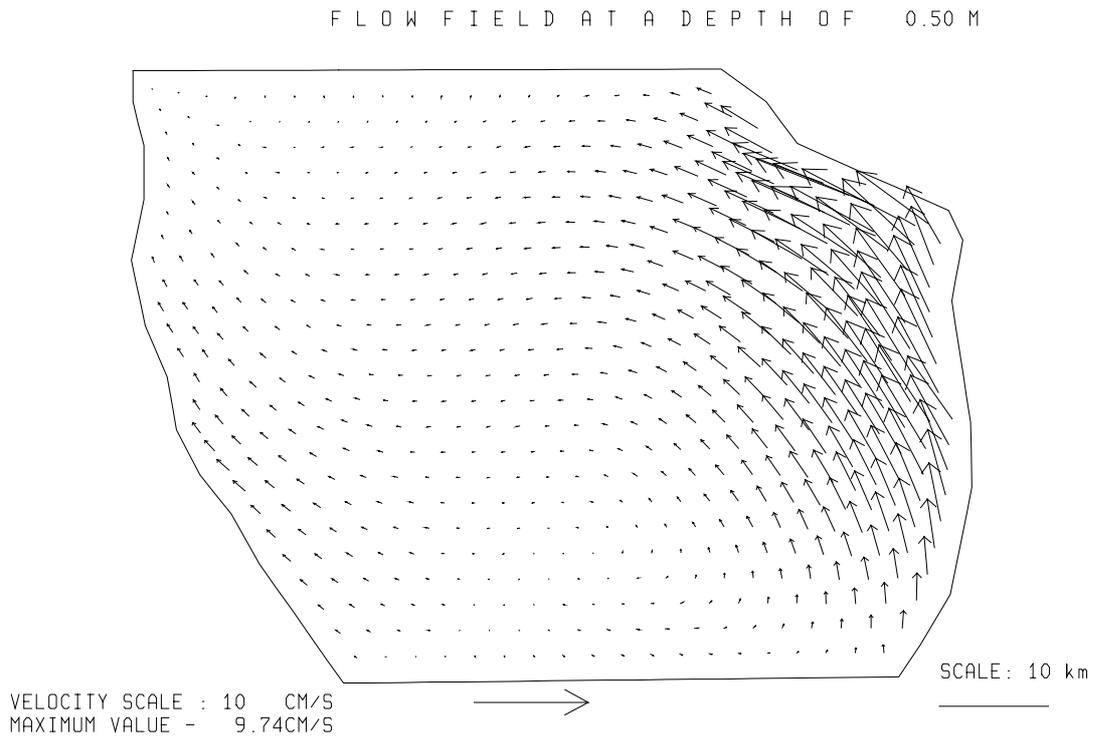
FLOW FIELD AT A DEPTH OF 0.50 M
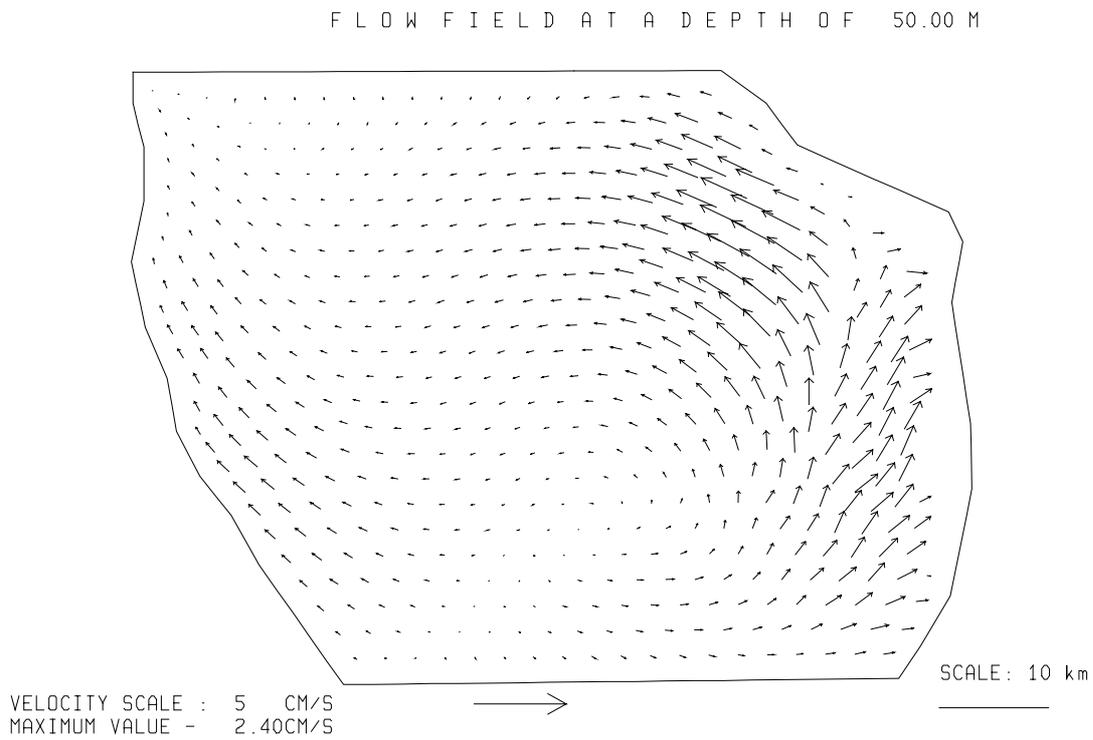
VELOCITY SCALE : 10 CM/S
MAXIMUM VALUE - 9.74CM/S

SCALE: 10 km

Fig.3.5.2./6 Calculated flow at a depth of 0.5 m. Local time 04 h 05.04.97.

FLOW FIELD AT A DEPTH OF 50.00 M

VELOCITY SCALE : 5 CM/S
MAXIMUM VALUE - 2.40CM/S

SCALE: 10 km

Fig. 3.5.2./7 Calculated flow at a depth of 50 m. Local time 04 h 05.04.97.

FLOW FIELD AT A DEPTH OF 100.00 M

VELOCITY SCALE : 5 CM/S
MAXIMUM VALUE - 1.50CM/S

SCALE: 10 km

Fig. 3.5.2./8 Calculated flow at a depth of 100 m. Local time 04 h 05.04.97.

NEAR-SURFACE WIND FIELD

VELOCITY SCALE : 100 CM/S
MAXIMUM VALUE - 243.02CM/S

SCALE: 10 km

Fig. 3.5.2./9 Simulated near-surface wind. Local time 04 h 05.04.97.

DEPTH-AVERAGED FLOW FIELD

SCALE: 10 km

VELOCITY SCALE :   5   CM/S
MAXIMUM VALUE -   3.77CM/S
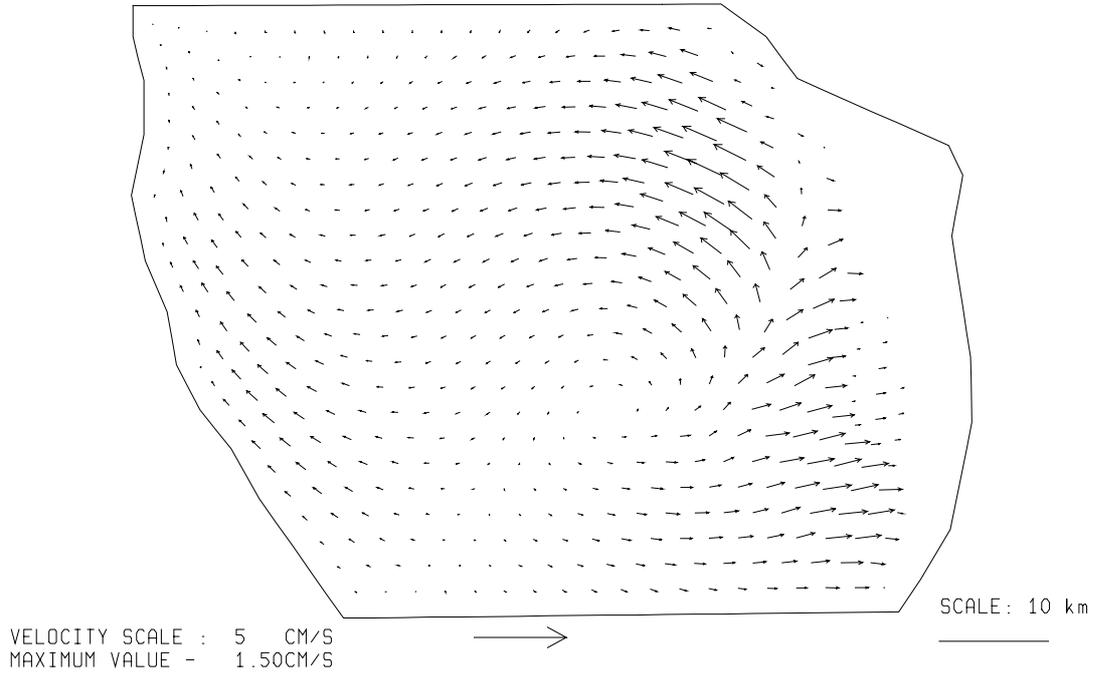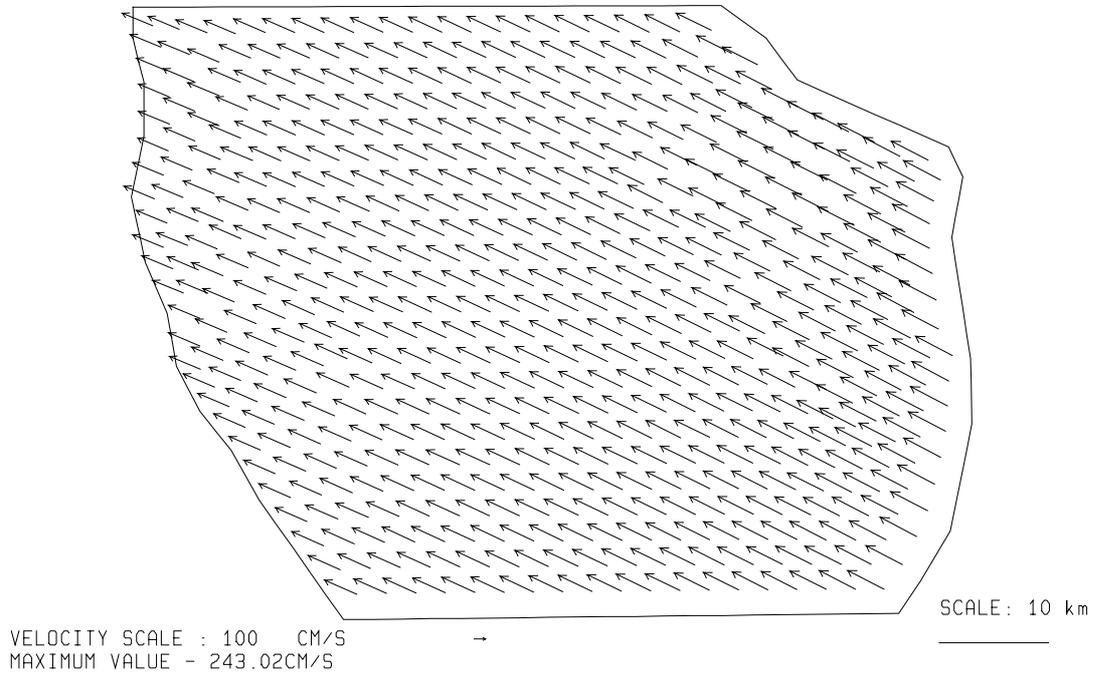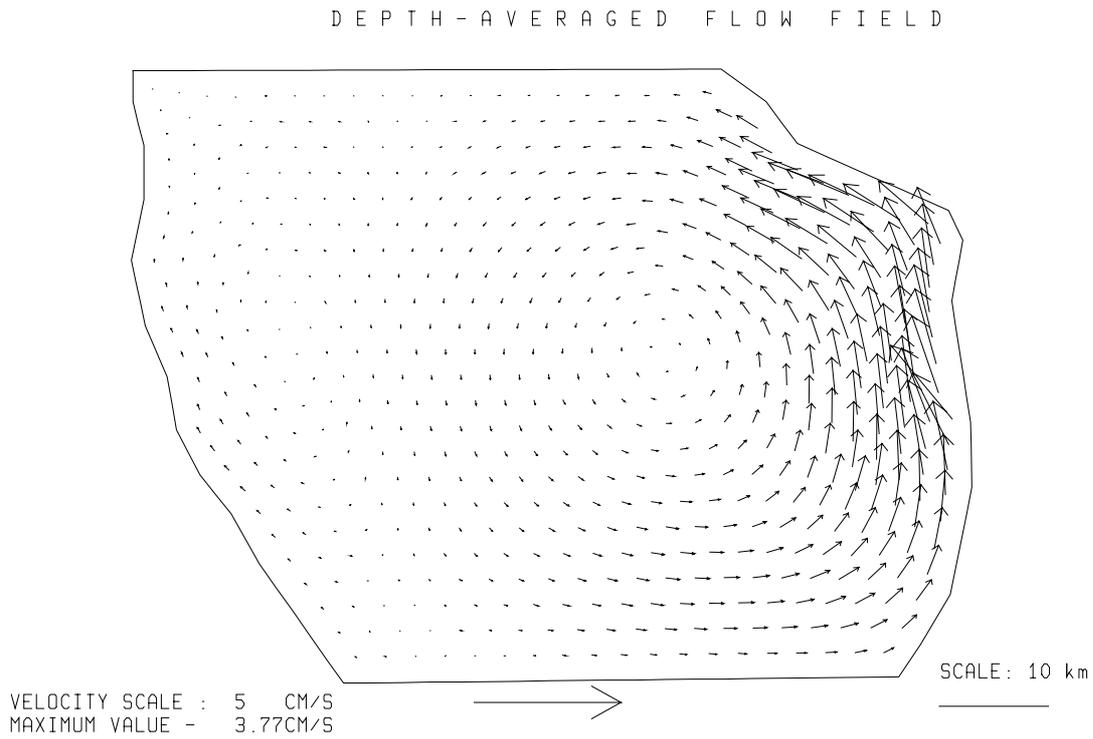
Fig. 3.5.2./10 Calculated depth-averaged flow. Local time 04 h 05.04.97.

FLOW FIELD AT A DEPTH OF   0.50 M

SCALE: 10 km

VELOCITY SCALE :   5   CM/S
MAXIMUM VALUE -   3.33CM/S
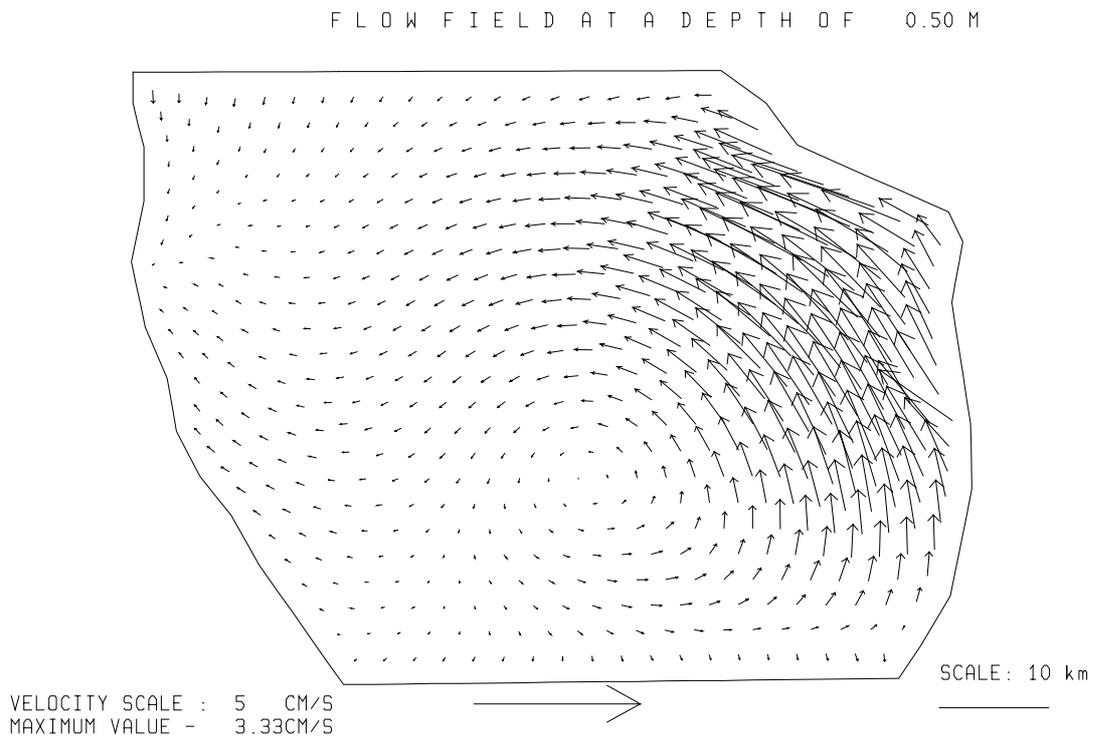
Fig. 3.5.2./11 Calculated flow at a depth of 0.5 m. Local time 12 h 05.04.97.

FLOW FIELD AT A DEPTH OF 50.00 M

VELOCITY SCALE : 5   CM/S
MAXIMUM VALUE -   1.68CM/S

SCALE: 10 km
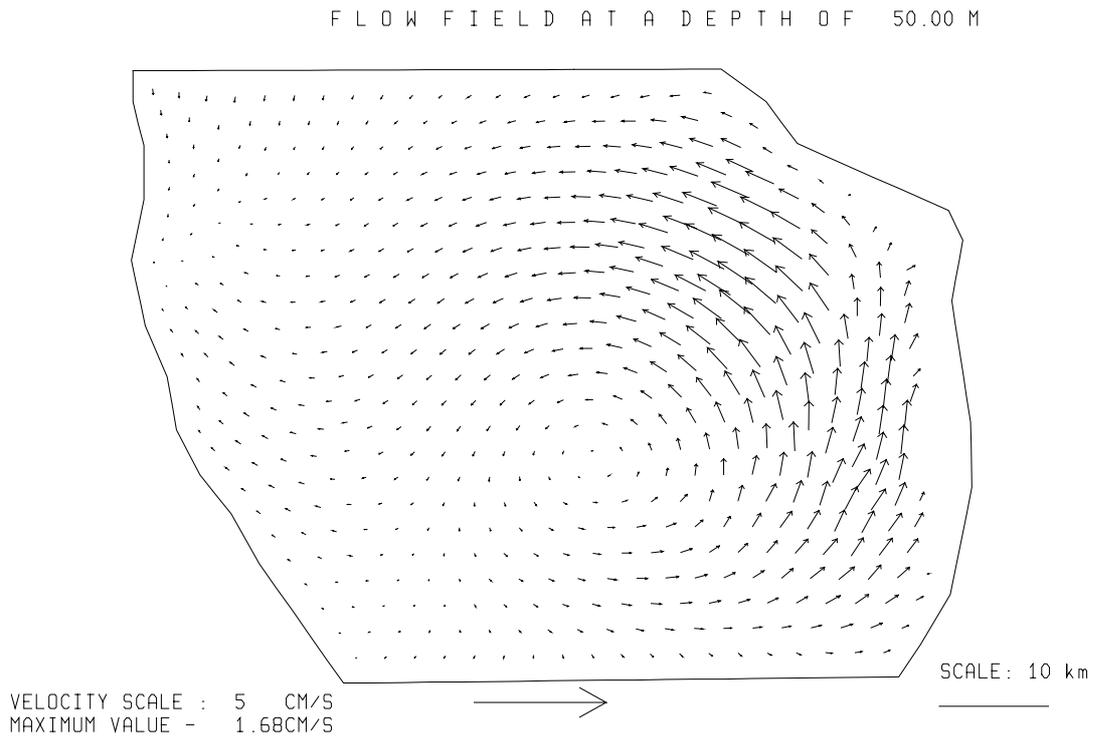
Fig. 3.5.2./12 Calculated flow at a depth of 50 m. Local time 12 h 05.04.97.

FLOW FIELD AT A DEPTH OF 100.00 M

VELOCITY SCALE : 5   CM/S
MAXIMUM VALUE -   1.21CM/S

SCALE: 10 km
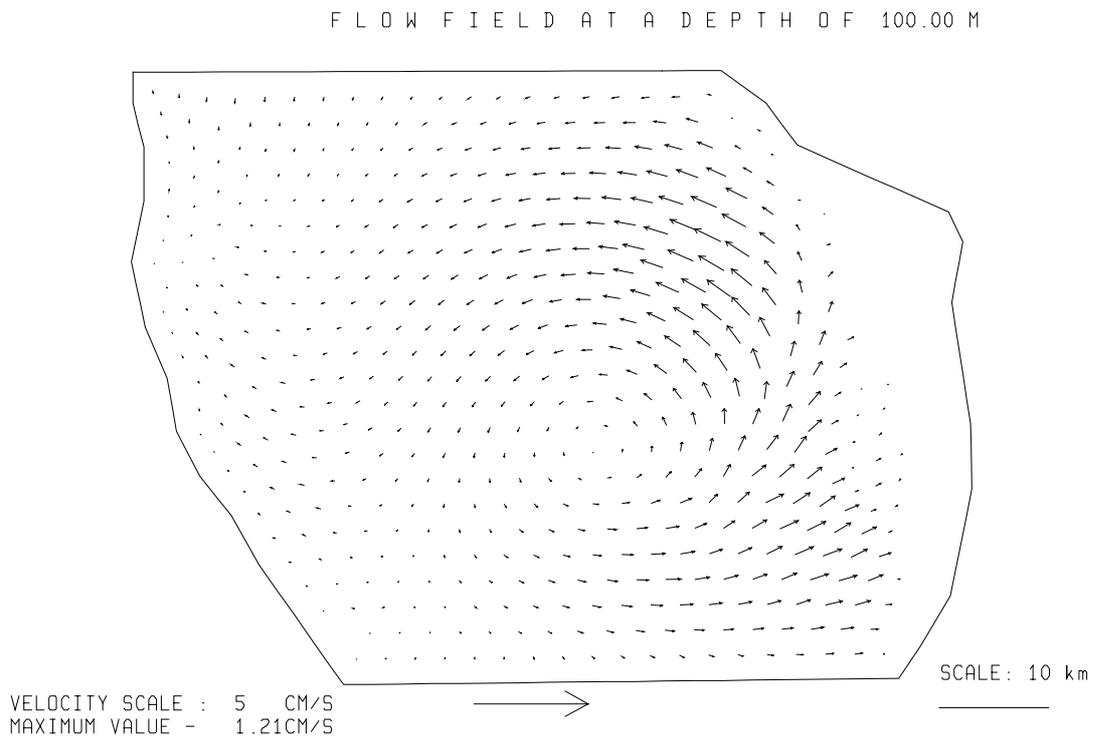
Fig. 3.5.2./13 Calculated flow at a depth of 100 m. Local time 12 h 05.04.97.

NEAR-SURFACE WIND FIELD

SCALE: 10 km

VELOCITY SCALE : 50   CM/S   →
MAXIMUM VALUE - 99.22CM/S
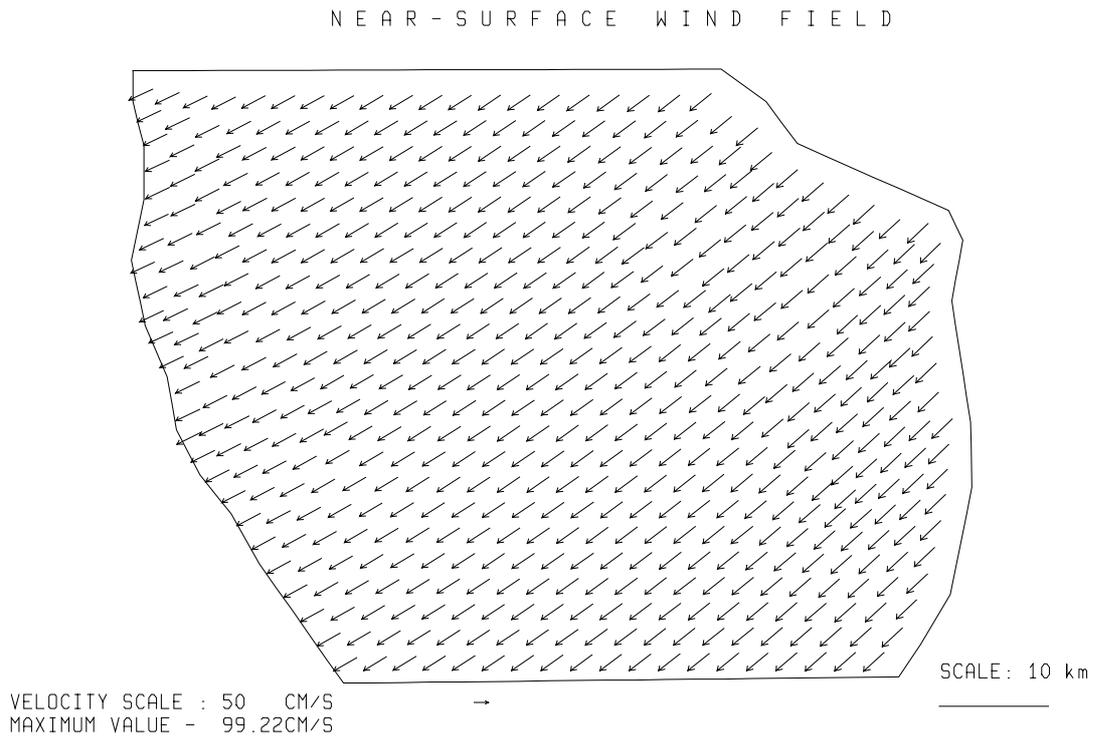
Fig. 3.5.2./14 Simulated near-surface wind. Local time 12 h 05.04.97.

DEPTH-AVERAGED FLOW FIELD

SCALE: 10 km

VELOCITY SCALE : 5   CM/S
MAXIMUM VALUE - 1.93CM/S
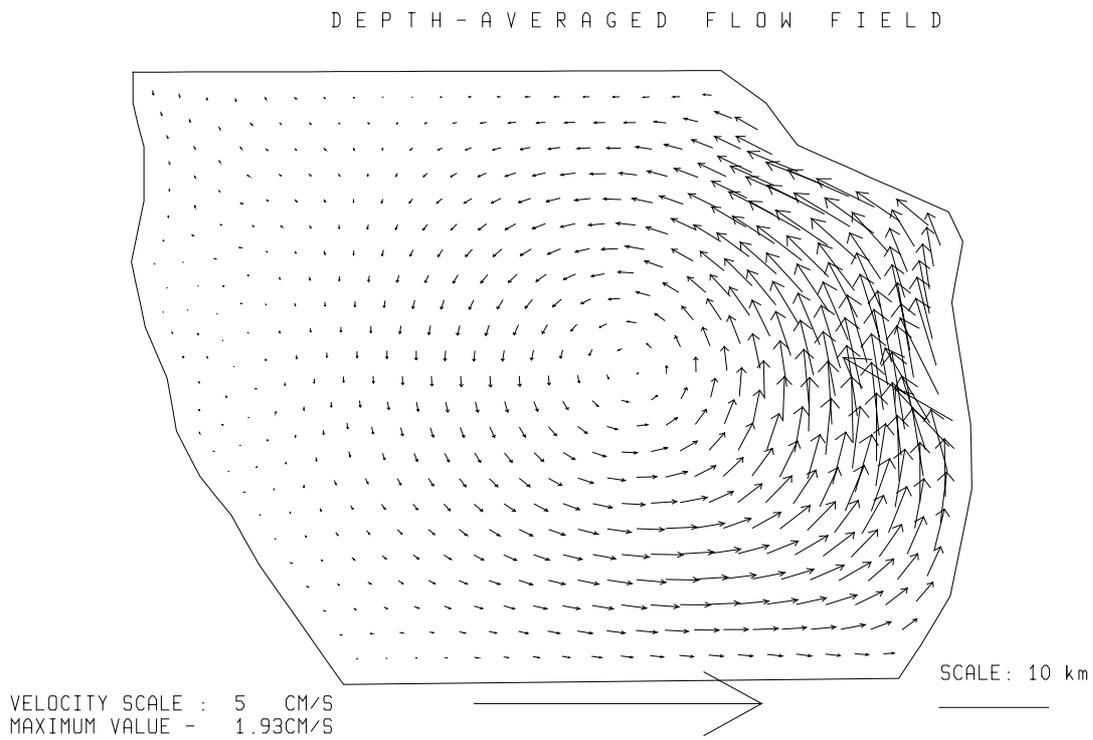
Fig. 3.5.2./15 Calculated depth-averaged flow. Local time 12 h 05.04.97.

FLOW FIELD AT A DEPTH OF 0.50 M

VELOCITY SCALE : 5 CM/S
MAXIMUM VALUE – 2.34CM/S

SCALE: 10 km
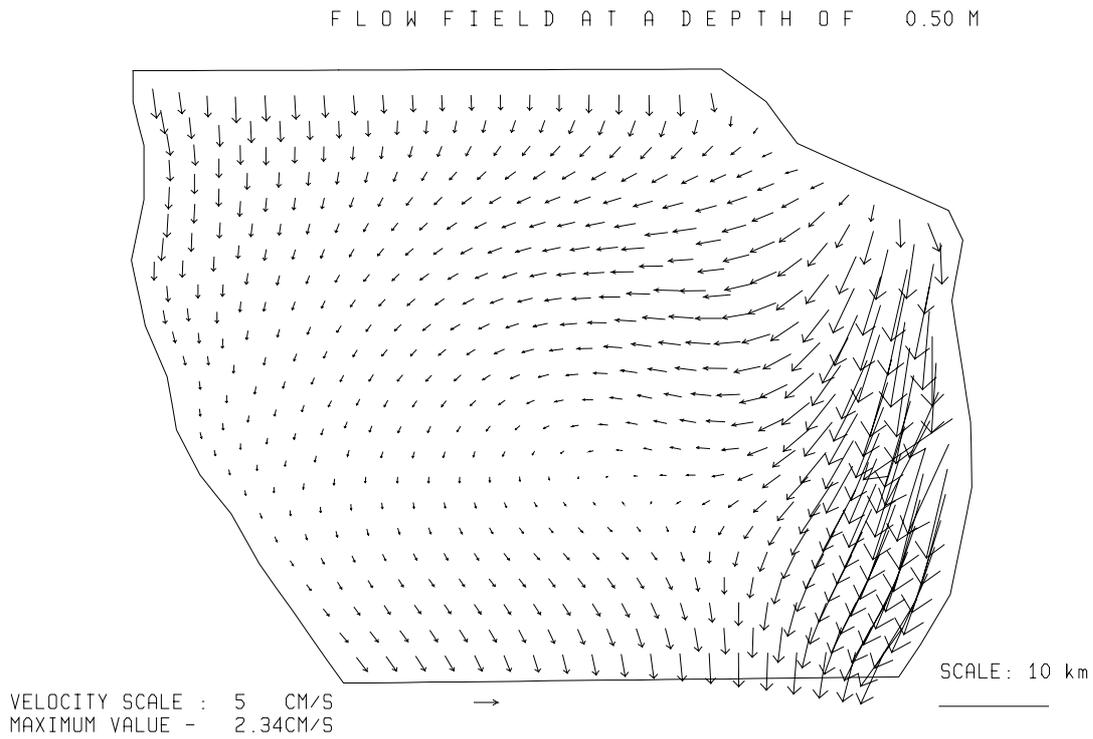
Fig. 3.5.2./16 Calculated flow at a depth of 0.5 m. Local time 20 h 05.04.97.

FLOW FIELD AT A DEPTH OF 50.00 M

VELOCITY SCALE : 1 CM/S
MAXIMUM VALUE – 0.64CM/S

SCALE: 10 km
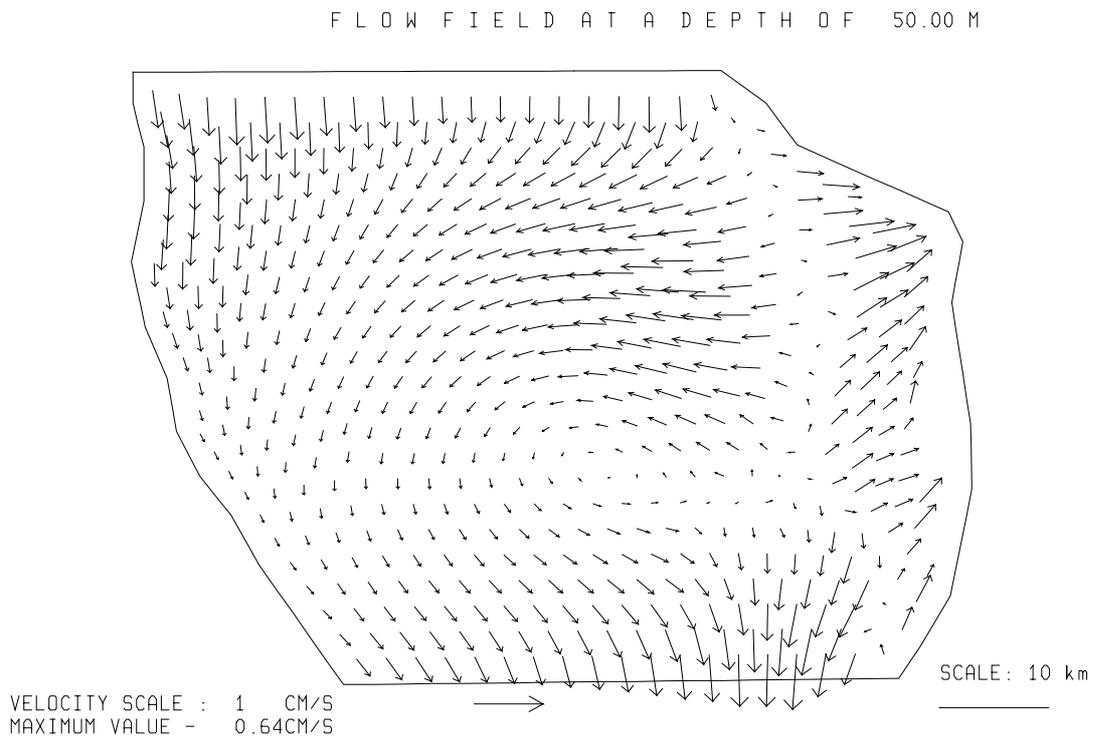
Fig. 3.5.2./17 Calculated flow at a depth of 50 m. Local time 20 h 05.04.97.

FLOW FIELD AT A DEPTH OF 100.00 M

SCALE: 10 km

VELOCITY SCALE : 1 CM/S
MAXIMUM VALUE - 0.45CM/S
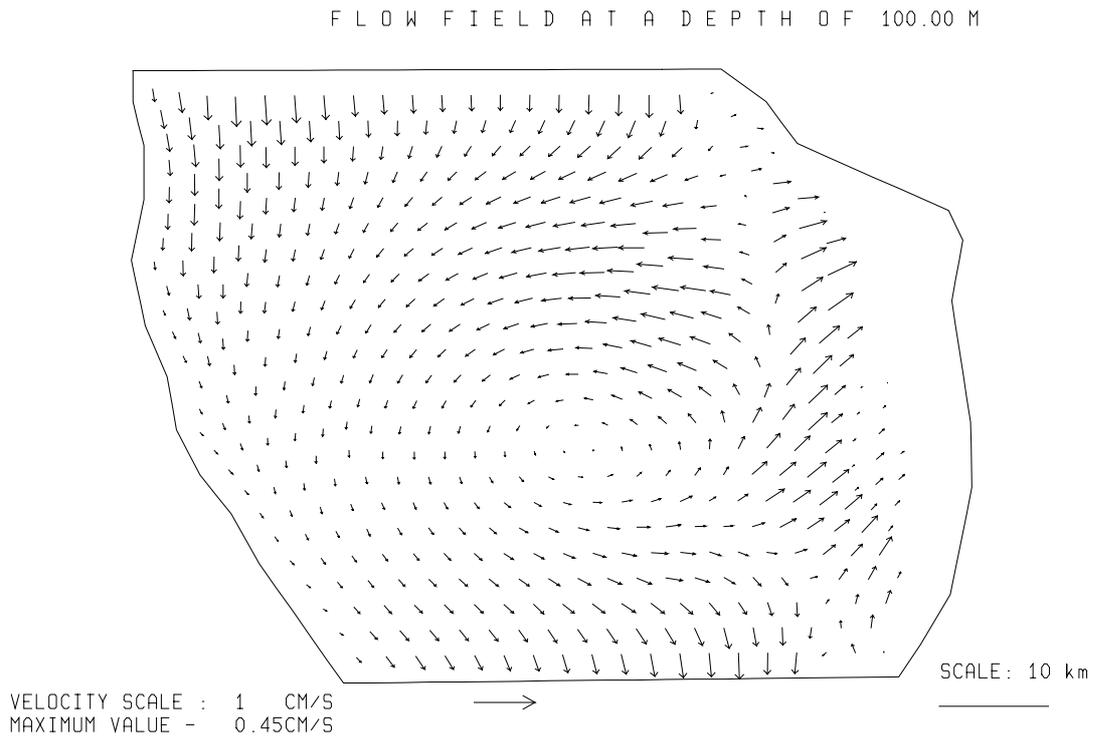
Fig. 3.5.2./18 Calculated flow at a depth of 100 m. Local time 20 h 05.04.97.

NEAR-SURFACE WIND FIELD

SCALE: 10 km

VELOCITY SCALE : 50 CM/S
MAXIMUM VALUE - 63.55CM/S
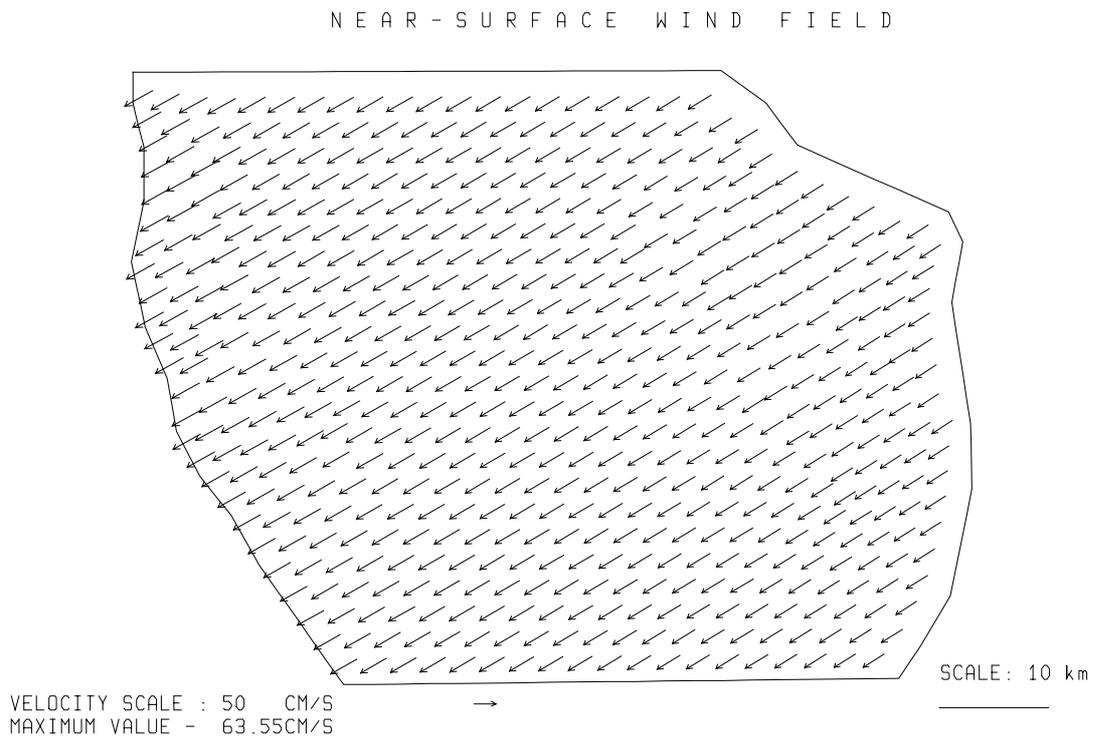
Fig. 3.5.2./19 Simulated near-surface wind. Local time 20 h 05.04.97.

DEPTH-AVERAGED FLOW FIELD

SCALE: 10 km

VELOCITY SCALE :   5   CM/S
MAXIMUM VALUE -   1.33CM/S
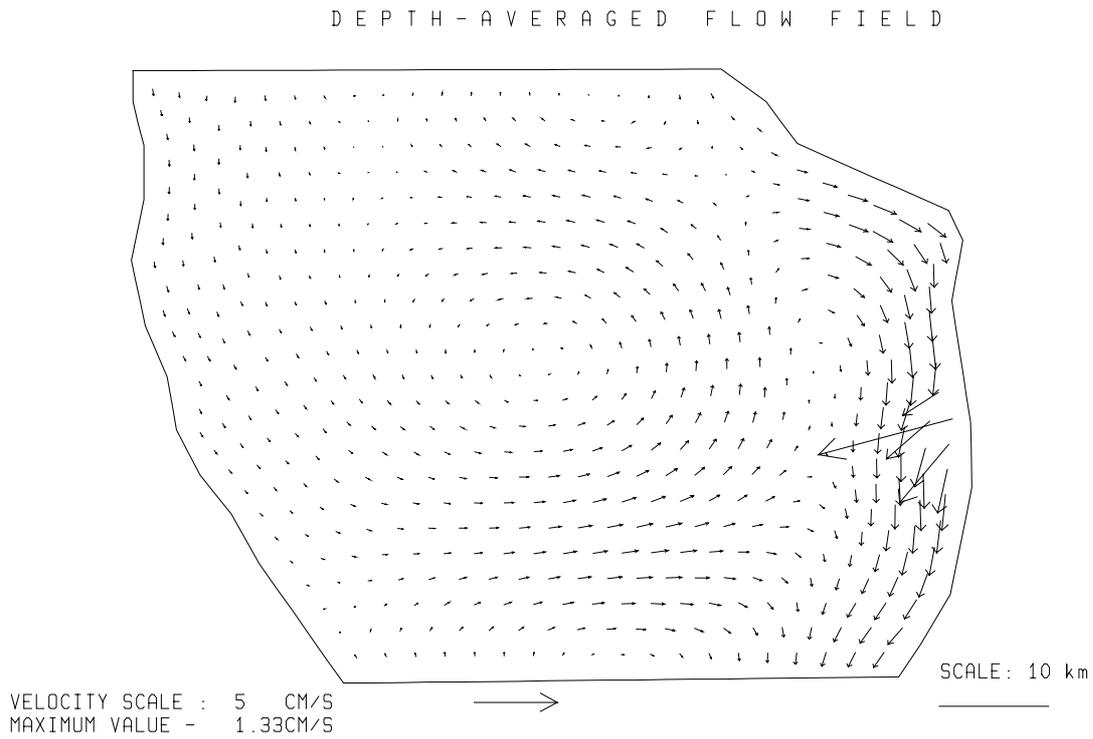
Fig. 3.5.2./20 Calculated depth-averaged flow. Local time 20 h 05.04.97.

FLOW FIELD AT A DEPTH OF   0.50 M

SCALE: 10 km

VELOCITY SCALE : 10   CM/S
MAXIMUM VALUE -   13.43CM/S
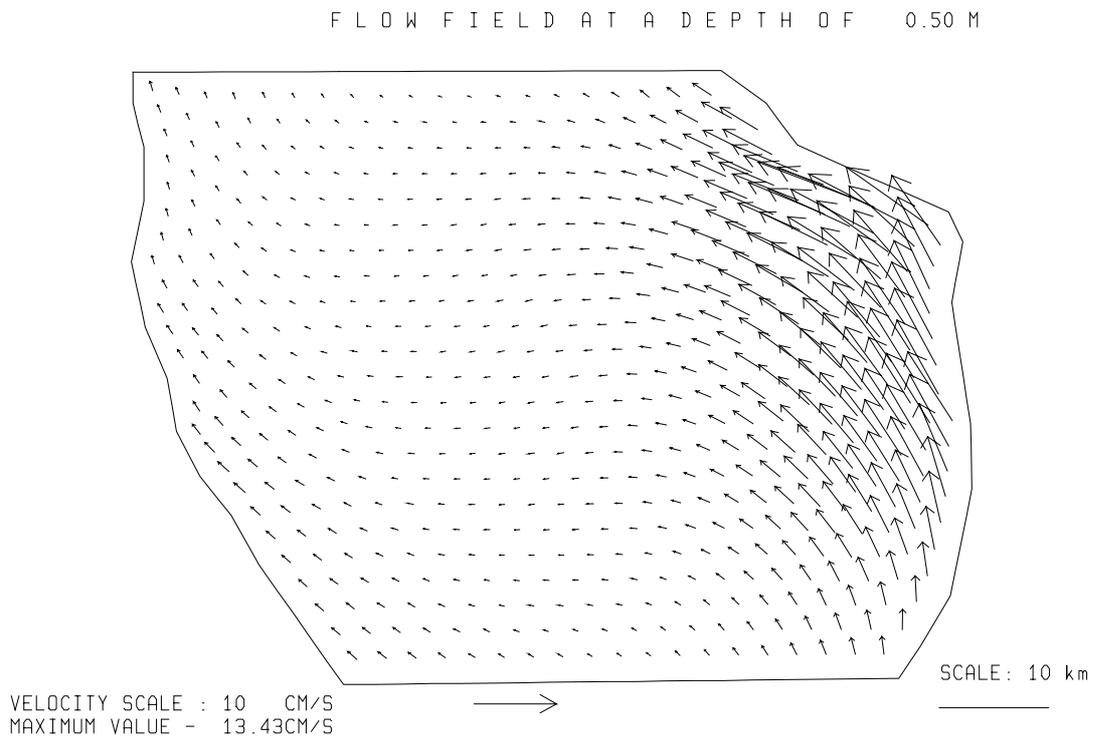
Fig. 3.5.2./21 Calculated flow at a depth of 0.5 m. Local time 04 h 24.08.97.

FLOW FIELD AT A DEPTH OF 50.00 M

VELOCITY SCALE : 5 CM/S
MAXIMUM VALUE - 3.55CM/S

SCALE: 10 km
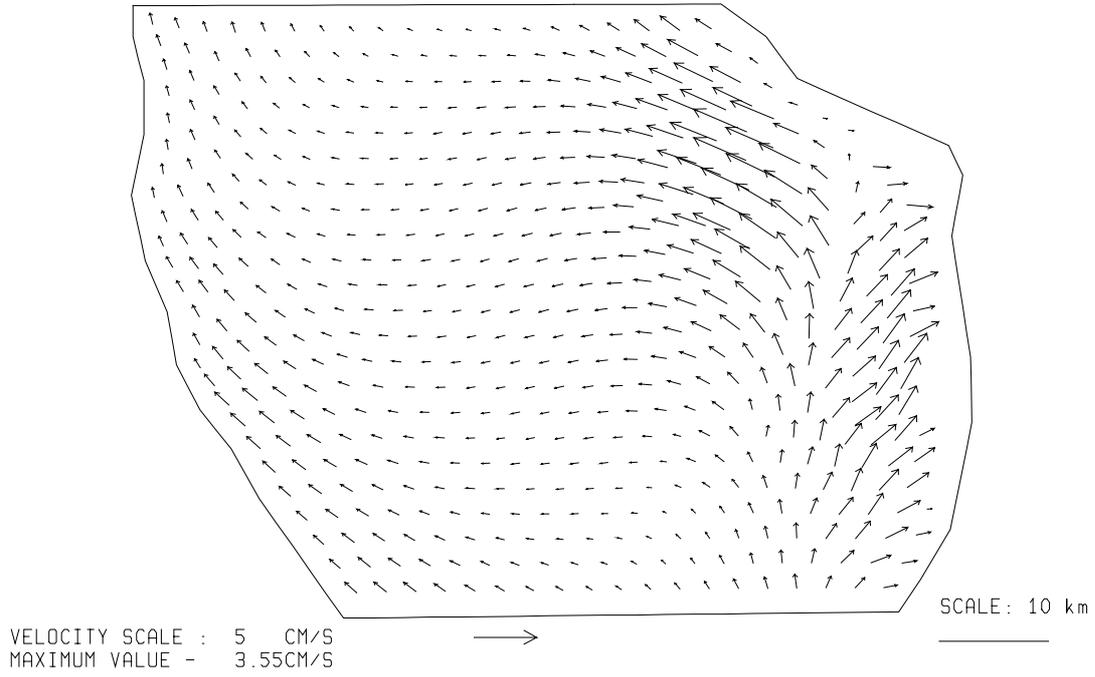
Fig. 3.5.2./22 Calculated flow at a depth of 50 m. Local time 04 h 24.08.97.

FLOW FIELD AT A DEPTH OF 100.00 M

VELOCITY SCALE : 5 CM/S
MAXIMUM VALUE - 2.12CM/S

SCALE: 10 km
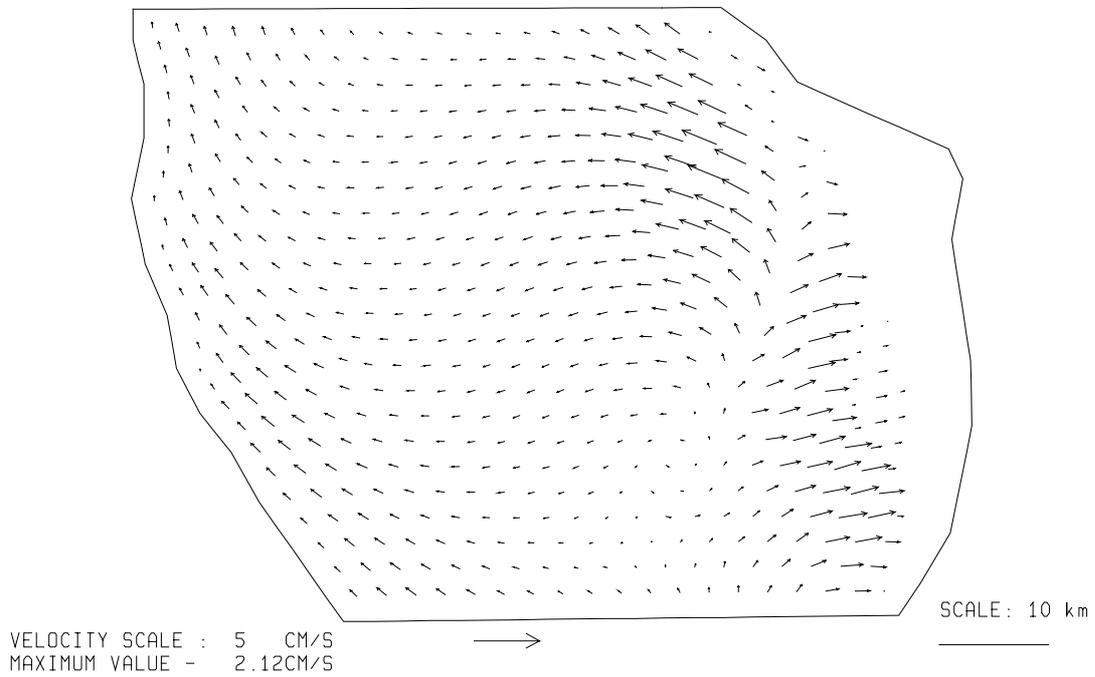
Fig. 3.5.2./23 Calculated flow at a depth of 100 m. Local time 04 h 24.08.97.

NEAR-SURFACE WIND FIELD

SCALE: 10 km

VELOCITY SCALE : 100   CM/S
MAXIMUM VALUE – 338.40CM/S
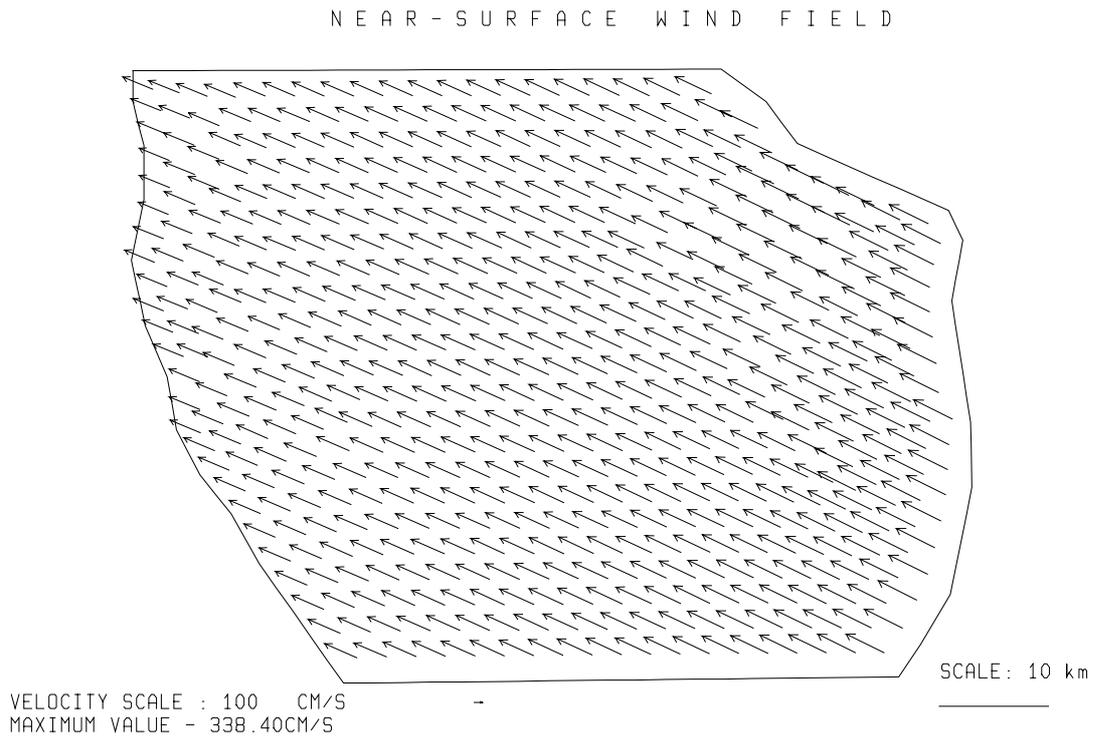
Fig. 3.5.2./24 Simulated near-surface wind. Local time 04 h 24.08.97.

DEPTH-AVERAGED FLOW FIELD

SCALE: 10 km

VELOCITY SCALE : 5   CM/S
MAXIMUM VALUE –   4.86CM/S
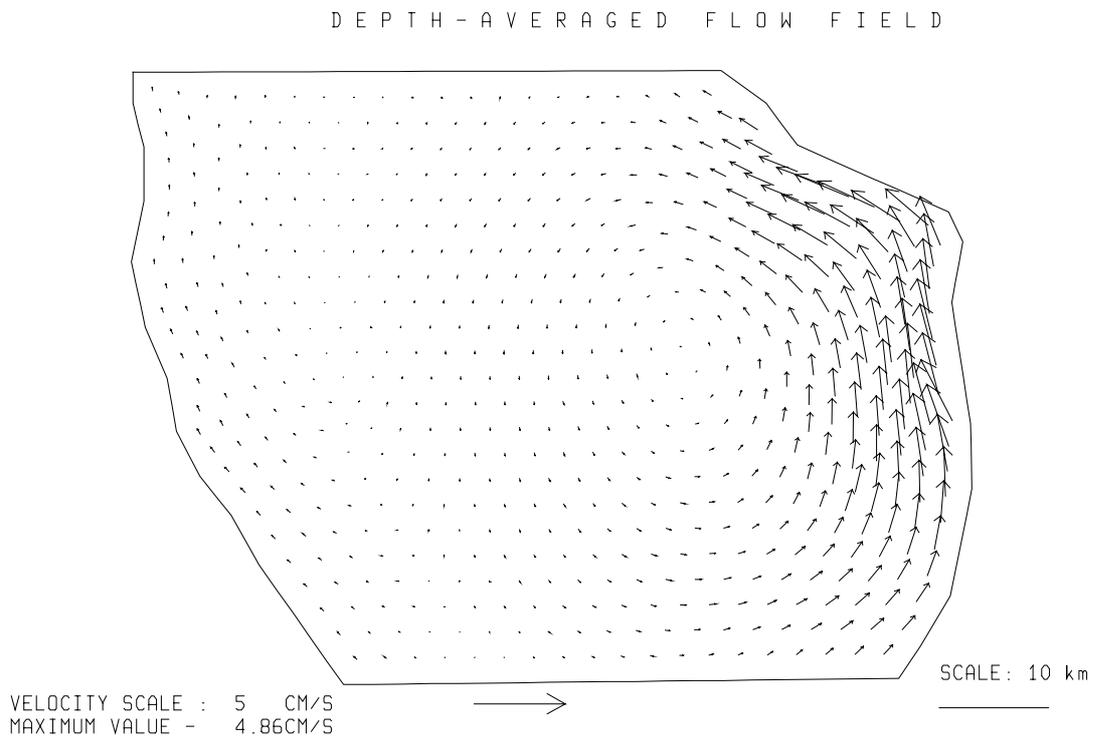
Fig. 3.5.2./25 Calculated depth-averaged flow. Local time 04 h 24.08.97.

F L O W   F I E L D   A T   A   D E P T H   O F   0.50 M

SCALE: 10 km

VELOCITY SCALE : 10   CM/S
MAXIMUM VALUE -   8.66CM/S
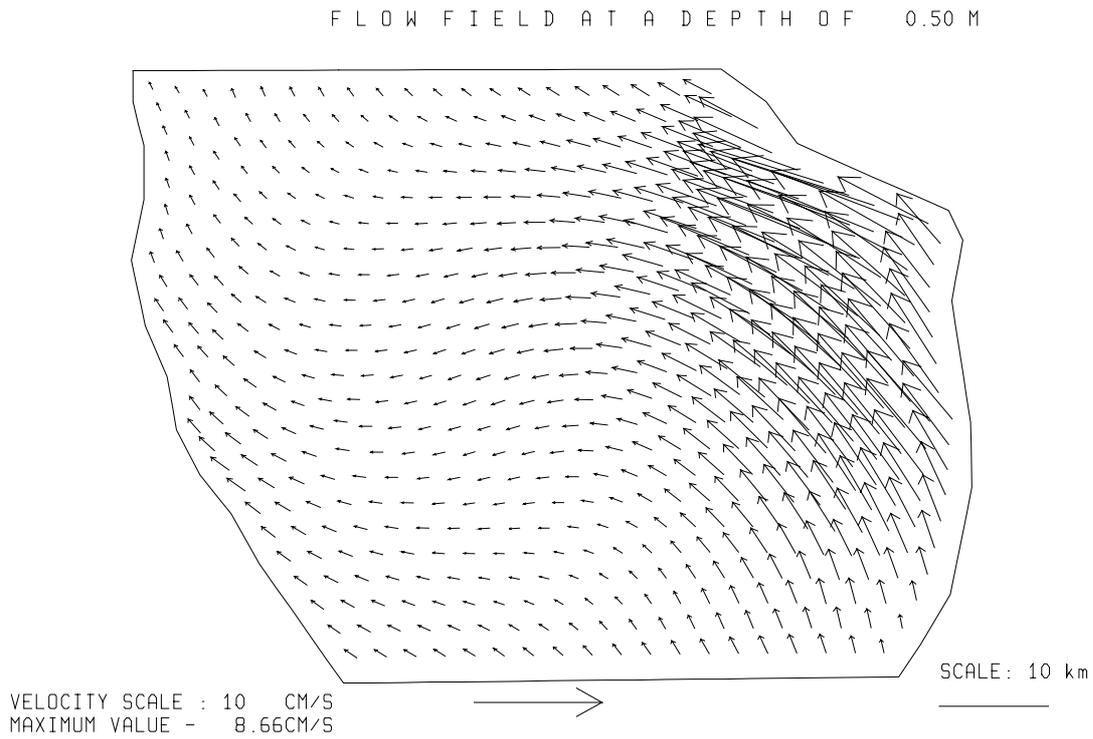
Fig. 3.5.2./26 Calculated flow at a depth of 0.5 m. Local time 12 h 24.08.97.

F L O W   F I E L D   A T   A   D E P T H   O F   50.00 M

SCALE: 10 km

VELOCITY SCALE : 5   CM/S
MAXIMUM VALUE -   3.27CM/S
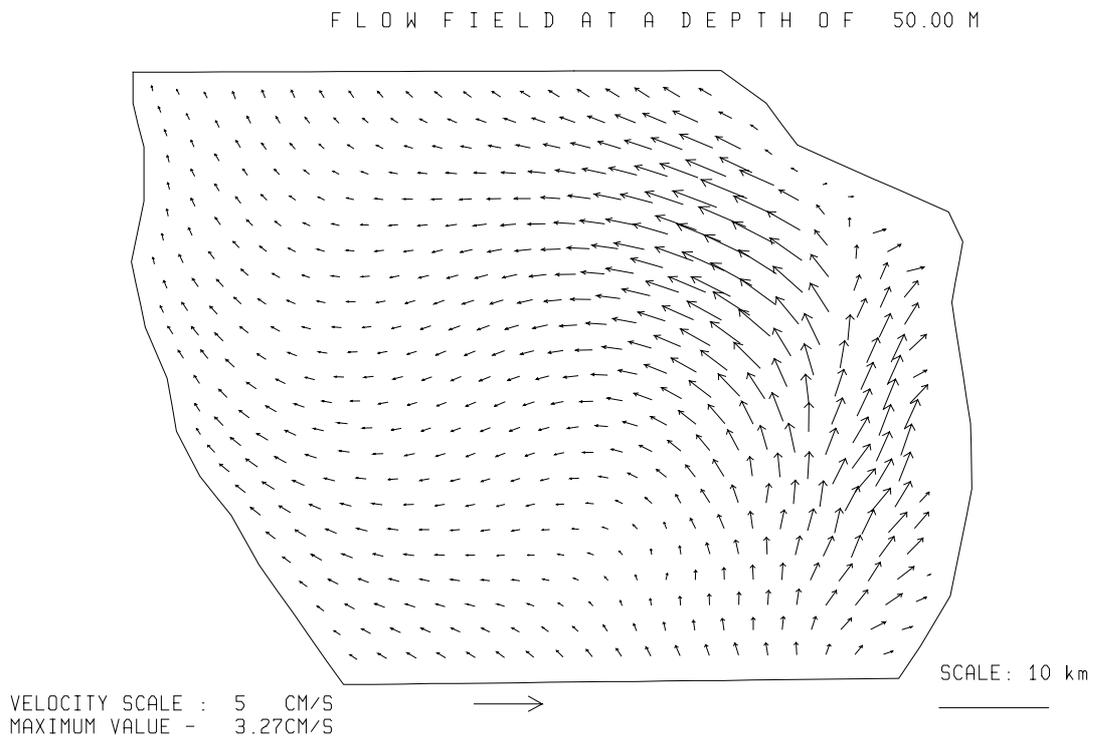
Fig. 3.5.2./27 Calculated flow at a depth of 50 m. Local time 12 h 24.08.97.

F L O W   F I E L D   A T   A   D E P T H   O F   100.00 M

VELOCITY SCALE :   5   CM/S
MAXIMUM VALUE -   2.27CM/S

SCALE: 10 km
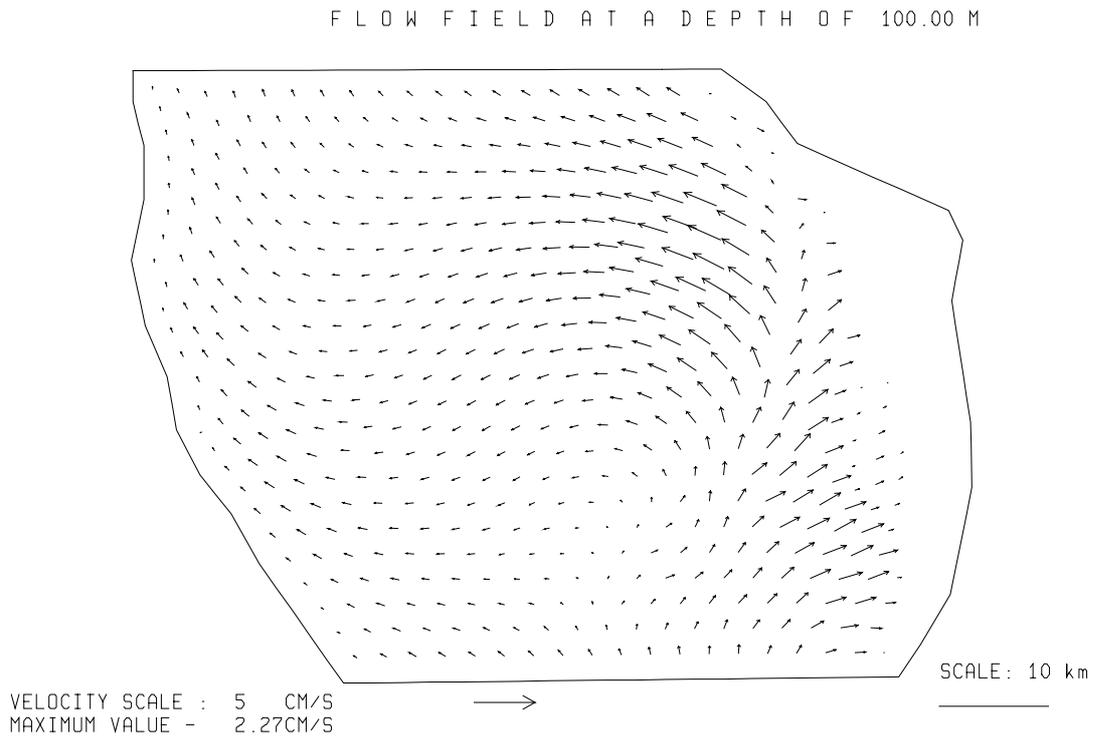
Fig. 3.5.2./28 Calculated flow at a depth of 100 m. Local time 12 h 24.08.97.

N E A R - S U R F A C E   W I N D   F I E L D

VELOCITY SCALE : 100   CM/S
MAXIMUM VALUE - 177.82CM/S

SCALE: 10 km
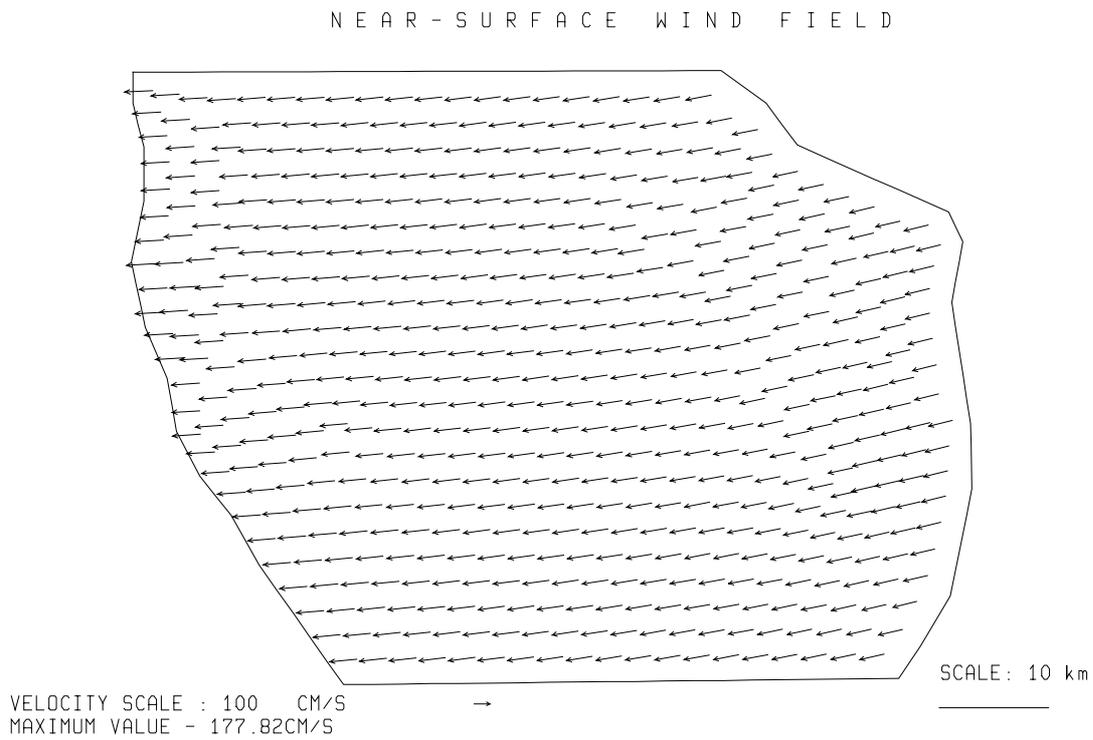
Fig. 3.5.2./29 Simulated near-surface wind. Local time 12 h 24.08.97.

DEPTH-AVERAGED FLOW FIELD

VELOCITY SCALE : 5 CM/S
MAXIMUM VALUE – 3.02CM/S

SCALE: 10 km
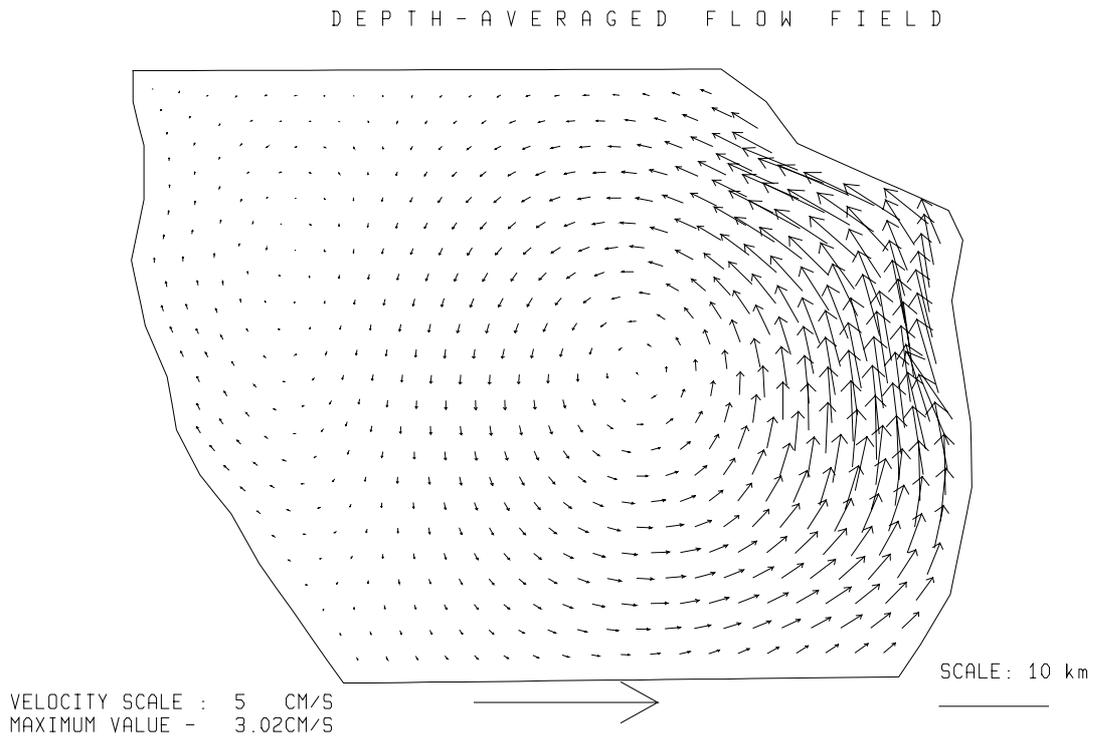
Fig. 3.5.2./30 Calculated depth-averaged flow. Local time 12 h 24.08.97.

FLOW FIELD AT A DEPTH OF 0.50 M

VELOCITY SCALE : 5 CM/S
MAXIMUM VALUE – 3.39CM/S

SCALE: 10 km
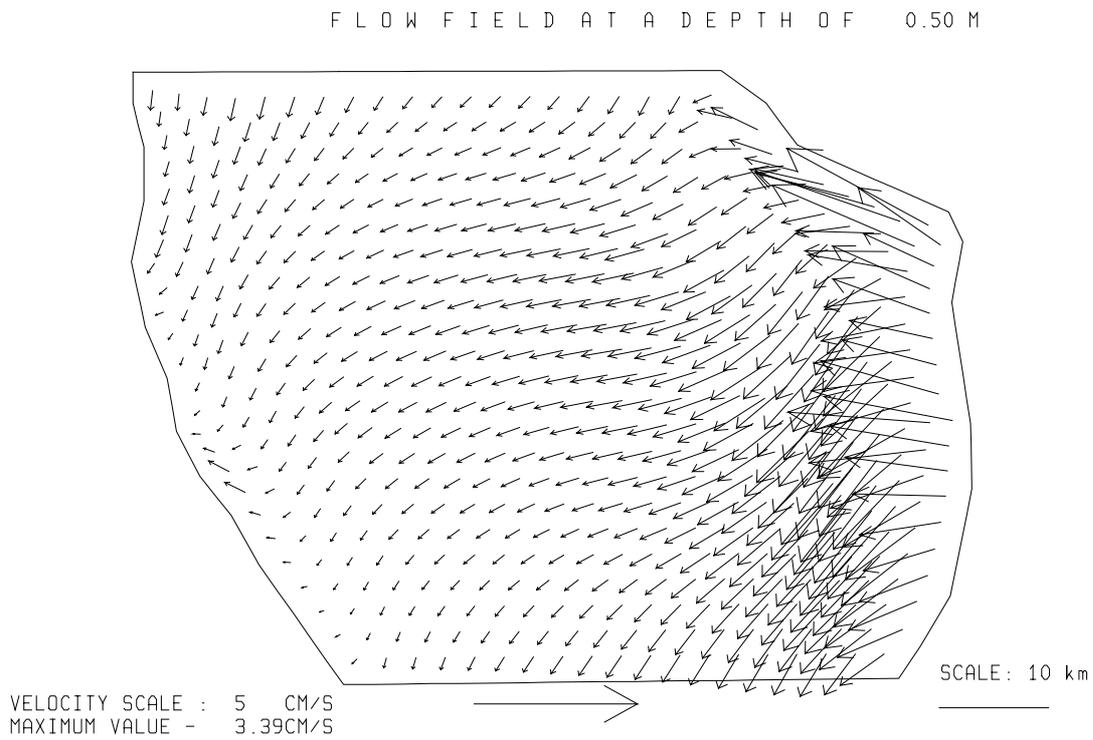
Fig. 3.5.2./31 Calculated flow at a depth of 0.5 m. Local time 20 h 24.08.97.

FLOW FIELD AT A DEPTH OF 50.00 M

SCALE: 10 km

VELOCITY SCALE : 1   CM/S
MAXIMUM VALUE -   0.83CM/S
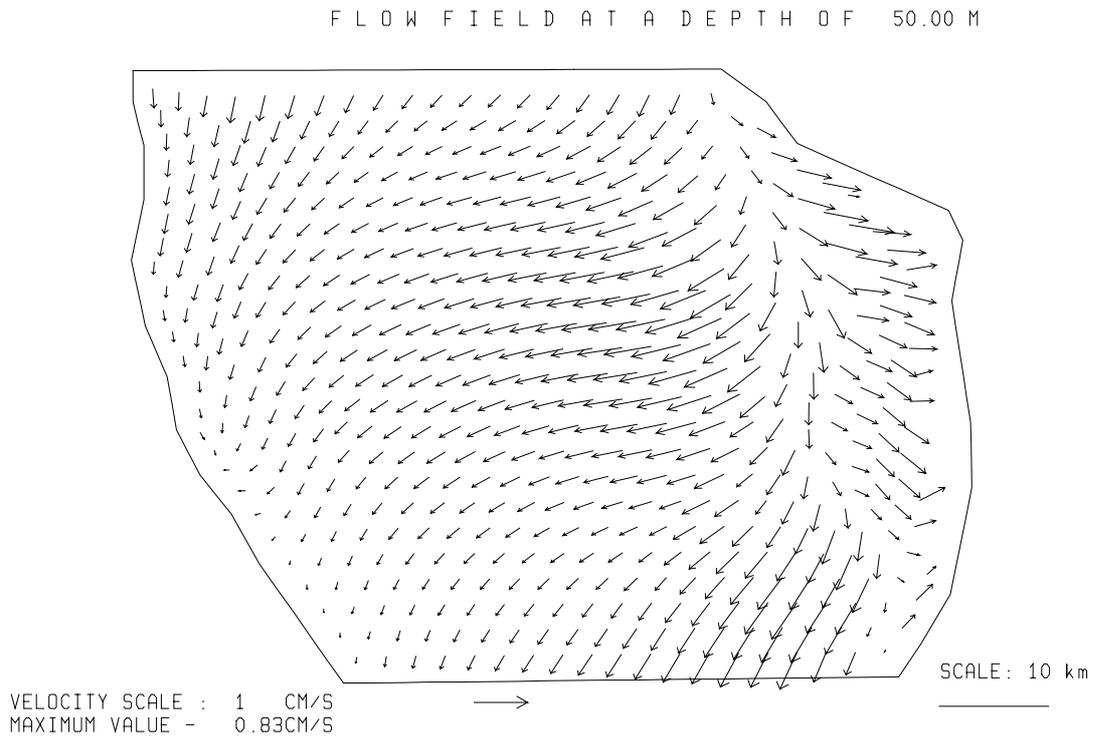
Fig. 3.5.2./32 Calculated flow at a depth of 50 m. Local time 20 h 24.08.97.

FLOW FIELD AT A DEPTH OF 100.00 M

SCALE: 10 km

VELOCITY SCALE : 1   CM/S
MAXIMUM VALUE -   0.58CM/S
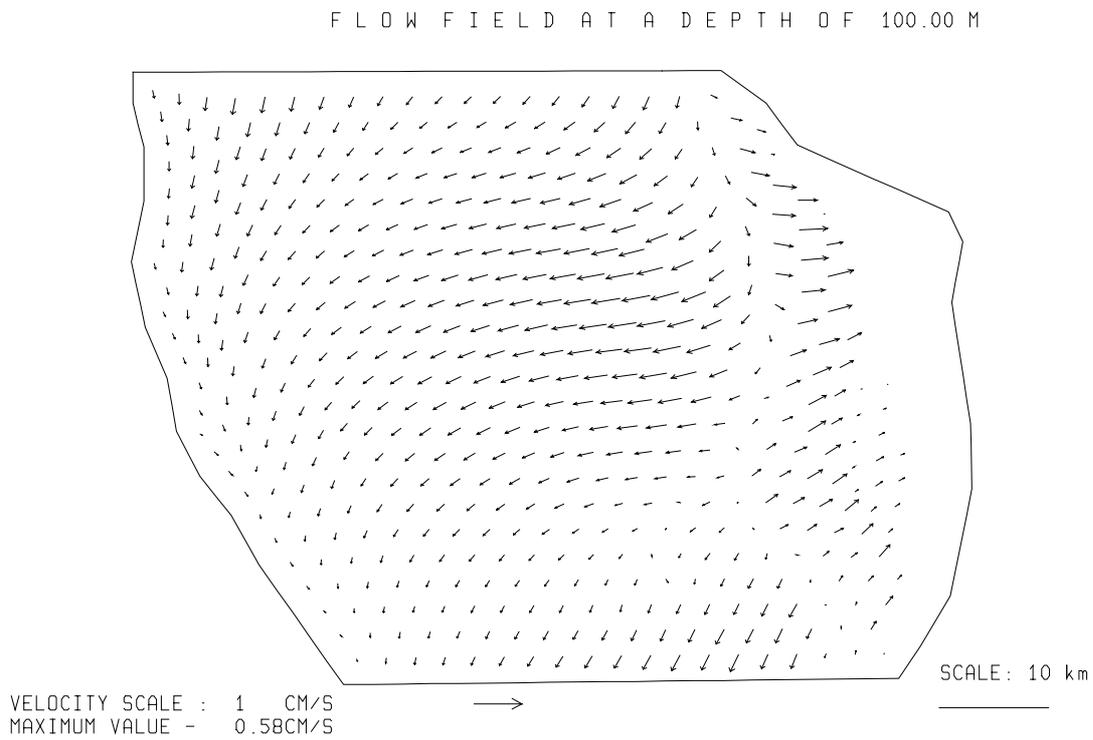
Fig. 3.5.2./33 Calculated flow at a depth of 100 m. Local time 20 h 24.08.97.

NEAR-SURFACE WIND FIELD

SCALE: 10 km

VELOCITY SCALE : 100 CM/S   →
MAXIMUM VALUE – 244.47CM/S
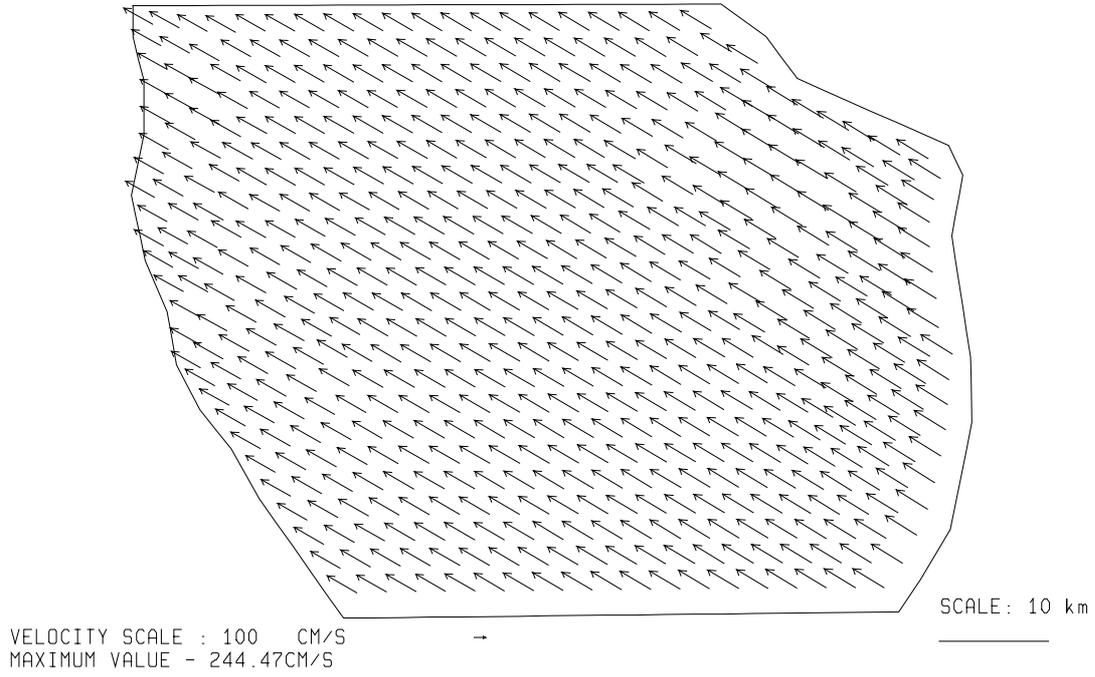
Fig. 3.5.2./34 Simulated near-surface wind. Local time 20 h 24.08.97.

DEPTH-AVERAGED FLOW FIELD

SCALE: 10 km

VELOCITY SCALE : 5 CM/S
MAXIMUM VALUE –   1.06CM/S
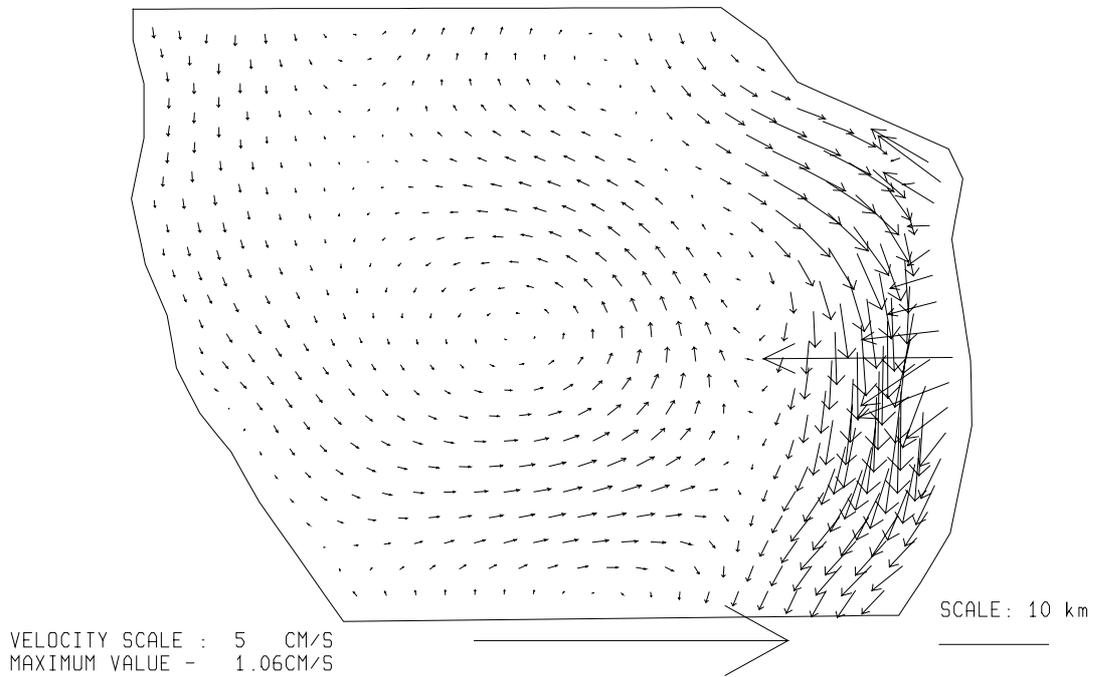
Fig. 3.5.2./35 Calculated depth-averaged flow. Local time 20 h 24.08.97.

FLOW FIELD AT A DEPTH OF   0.50 M

SCALE: 10 km

VELOCITY SCALE : 10   CM/S
MAXIMUM VALUE -   5.92CM/S
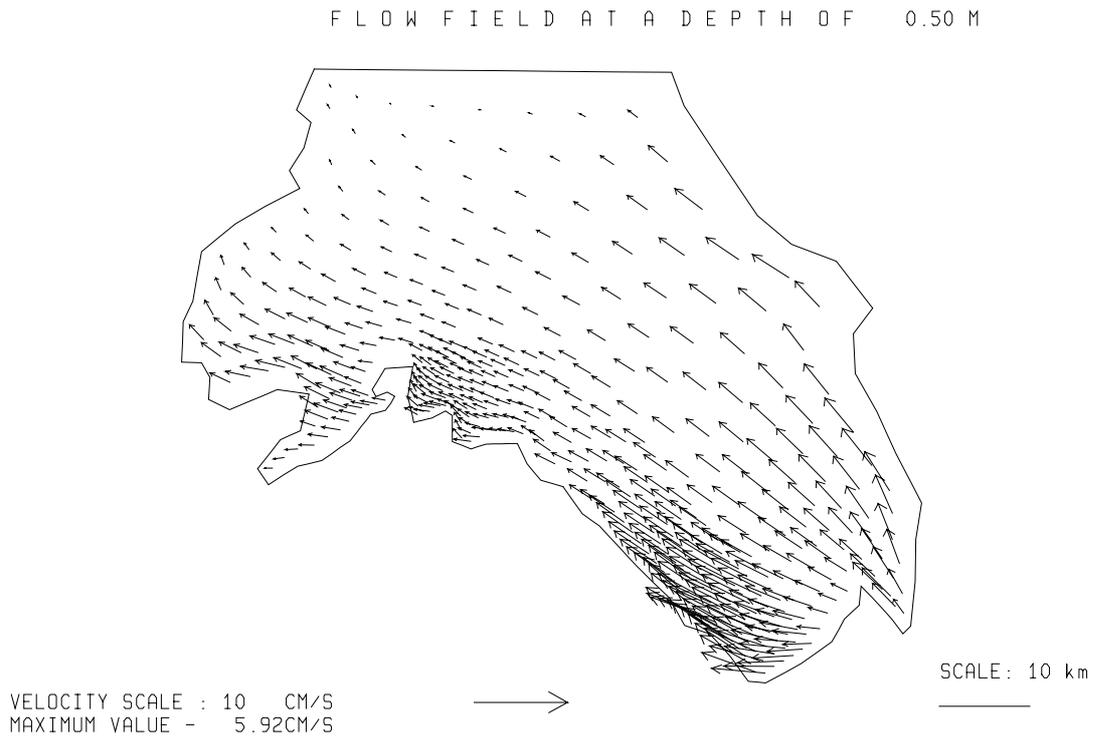
Fig. 3.5.2./36 Calculated flow at a depth of 0.5 m. Local time 04 h 05.04.97.

FLOW FIELD AT A DEPTH OF 50.00 M

SCALE: 10 km

VELOCITY SCALE : 5   CM/S
MAXIMUM VALUE -   1.50CM/S
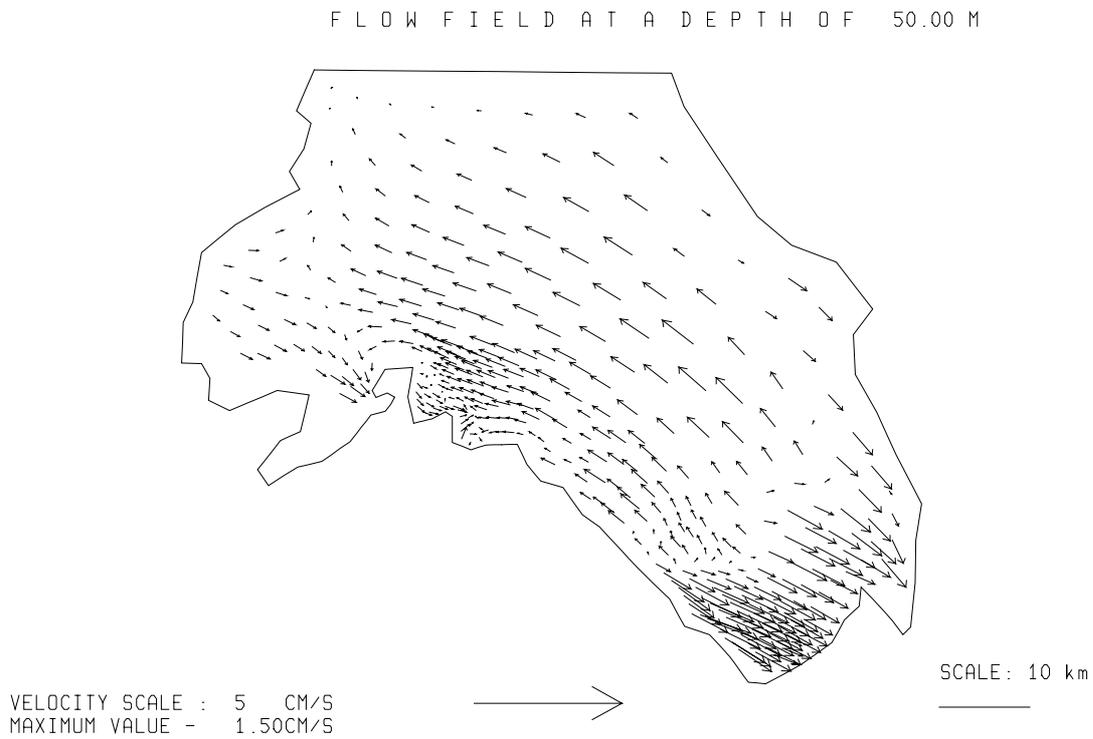
Fig. 3.5.2./37 Calculated flow at a depth of 50 m. Local time 04 h 05.04.97.

FLOW FIELD AT A DEPTH OF 100.00 M

VELOCITY SCALE : 5 CM/S
MAXIMUM VALUE - 1.55CM/S

SCALE: 10 km

Fig. 3.5.2./38 Calculated flow at a depth of 100 m. Local time 04 h 05.04.97.

NEAR-SURFACE WIND FIELD

VELOCITY SCALE : 100 CM/S
MAXIMUM VALUE - 357.77CM/S

SCALE: 10 km

Fig. 3.5.2./39 Simulated near-surface wind. Local time 04 h 05.04.97.

140

DEPTH-AVERAGED FLOW FIELD

SCALE: 10 km

VELOCITY SCALE :   1   CM/S
MAXIMUM VALUE -   0.63CM/S
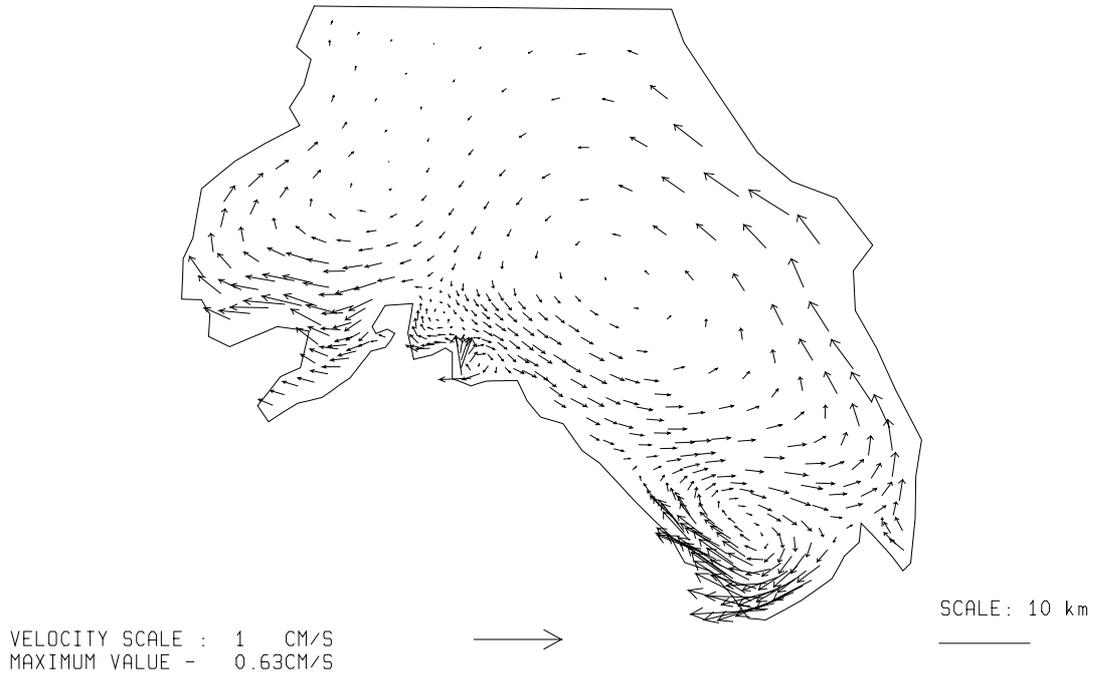
Fig. 3.5.2./40 Calculated depth-averaged flow. Local time 04 h 05.04.97.

FLOW FIELD AT A DEPTH OF   0.50 M

SCALE: 10 km

VELOCITY SCALE :   5   CM/S
MAXIMUM VALUE -   1.01CM/S
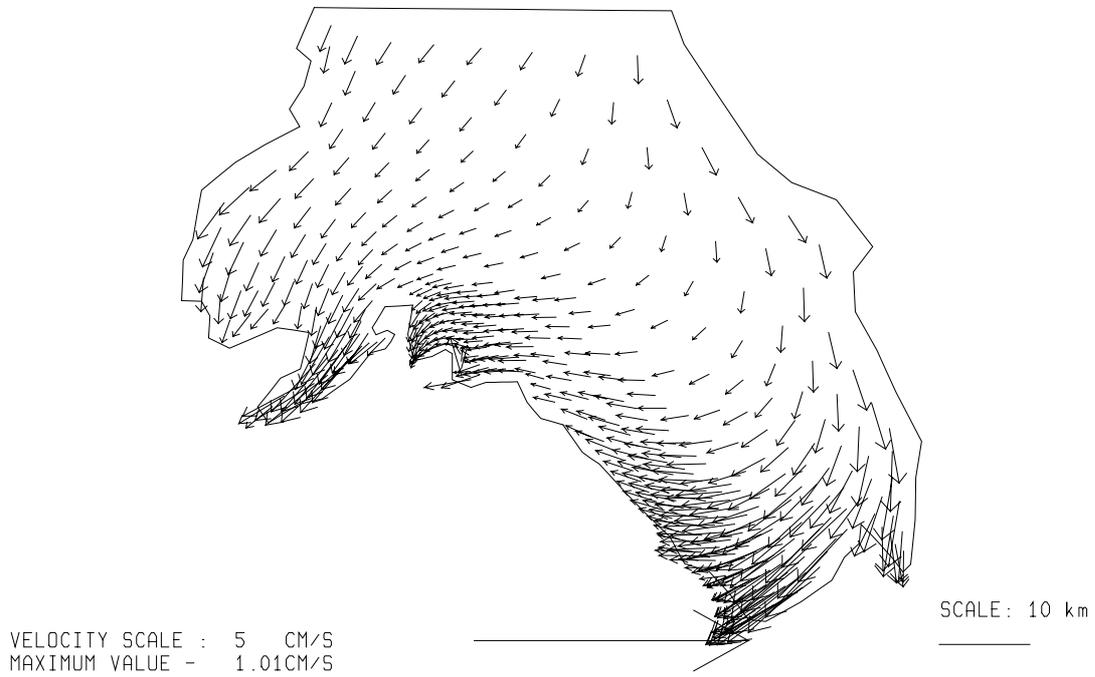
Fig. 3.5.2./41 Calculated flow at a depth of 0.5 m. Local time 12 h 05.04.97.

FLOW FIELD AT A DEPTH OF 50.00 M

SCALE: 10 km

VELOCITY SCALE : 1 CM/S
MAXIMUM VALUE - 0.54CM/S
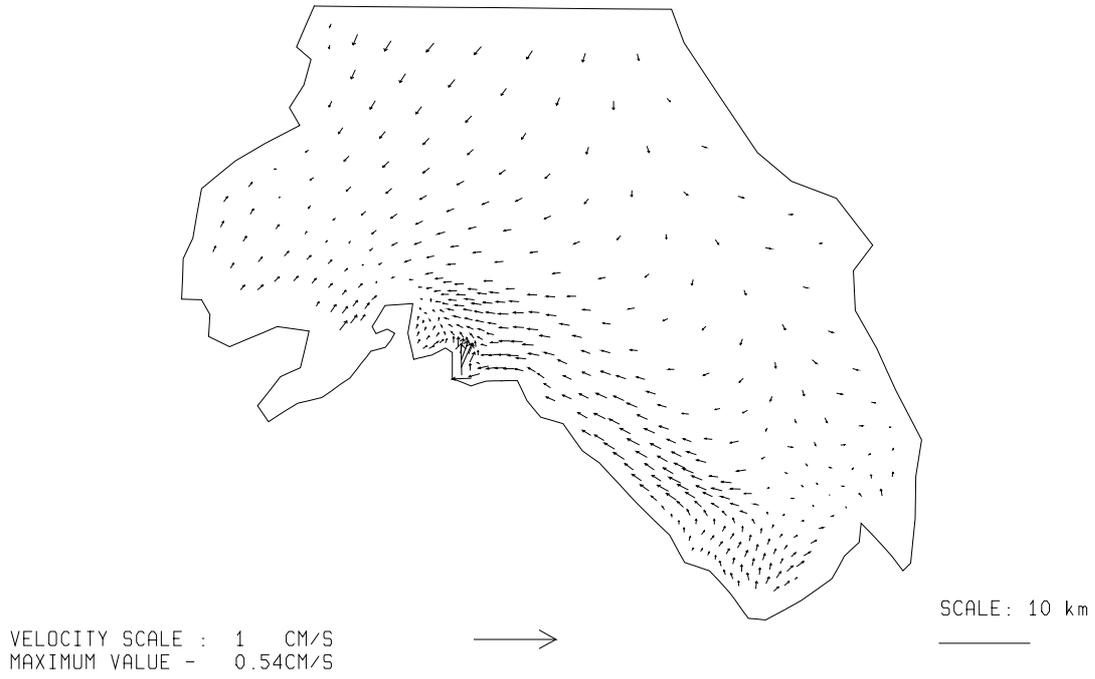
Fig. 3.5.2./42 Calculated flow at a depth of 50 m. Local time 12 h 05.04.97.

FLOW FIELD AT A DEPTH OF 100.00 M

SCALE: 10 km

VELOCITY SCALE : 1 CM/S
MAXIMUM VALUE - 0.27CM/S
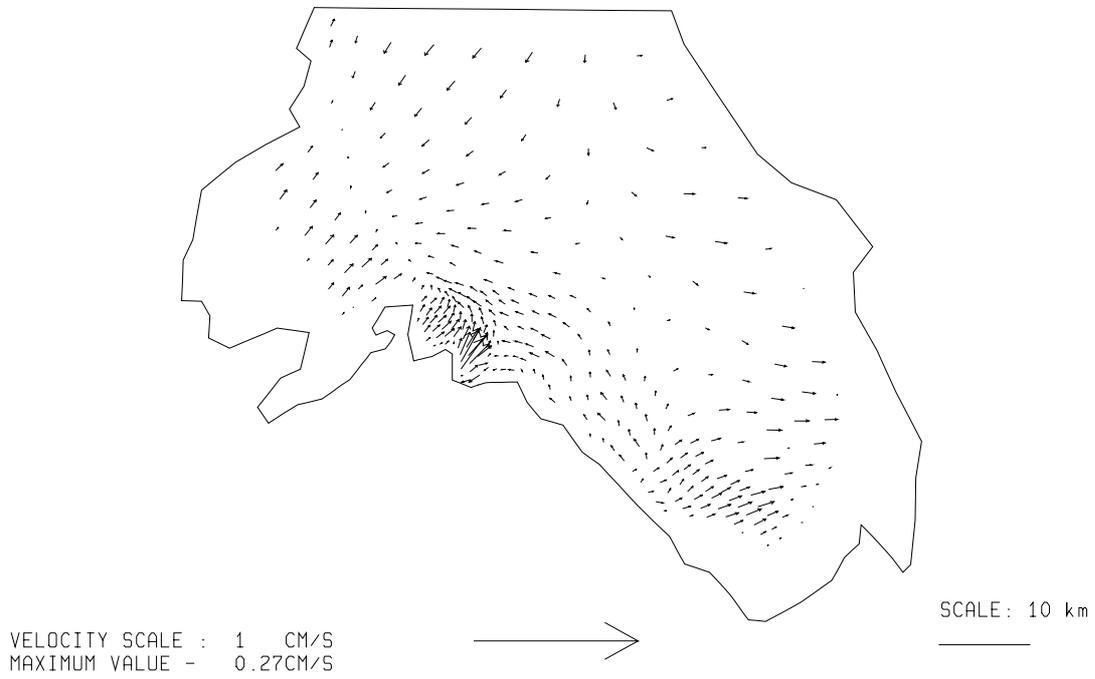
Fig. 3.5.2./43 Calculated flow at a depth of 100 m. Local time 12 h 05.04.97.

NEAR-SURFACE WIND FIELD

SCALE: 10 km

VELOCITY SCALE : 100   CM/S   →
MAXIMUM VALUE - 160.93CM/S
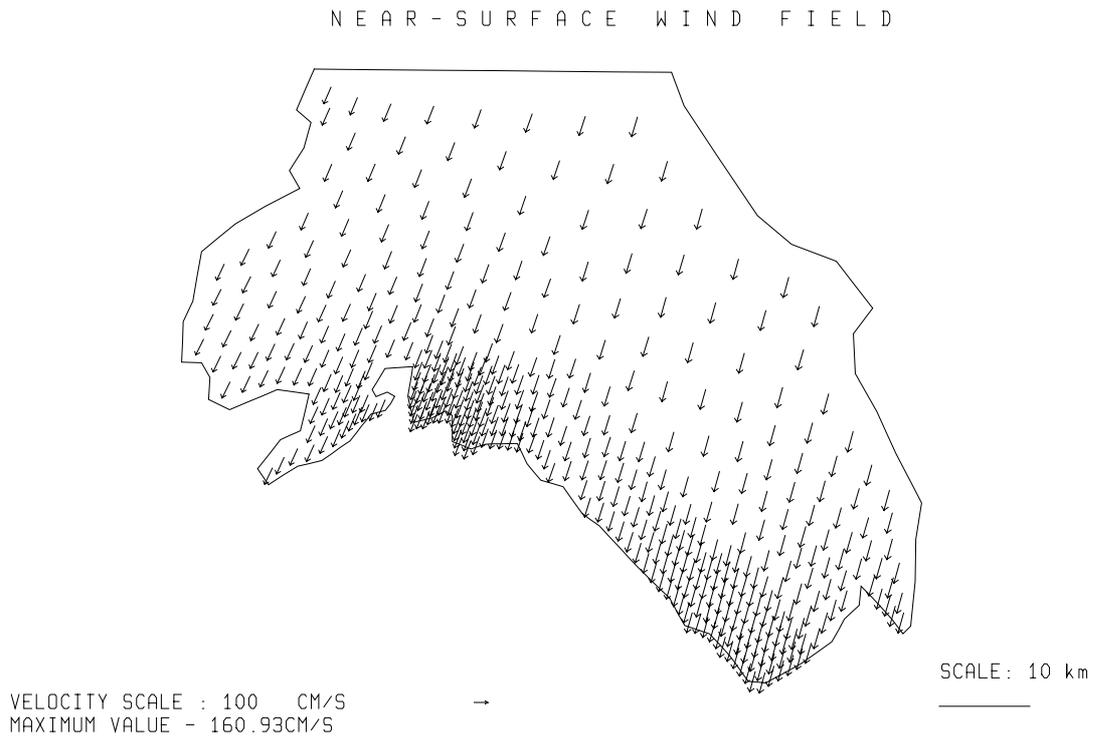
Fig. 3.5.2./44 Simulated near-surface wind. Local time 12 h 05.04.97.

DEPTH-AVERAGED FLOW FIELD

SCALE: 10 km

VELOCITY SCALE :   1   CM/S
MAXIMUM VALUE -   0.44CM/S

Fig. 3.5.2./45 Calculated depth-averaged flow. Local time 12 h 05.04.97.

FLOW FIELD AT A DEPTH OF 0.50 M

VELOCITY SCALE : 5 CM/S
MAXIMUM VALUE - 1.02CM/S

SCALE: 10 km

Fig. 3.5.2./46 Calculated flow at a depth of 0.5 m. Local time 20 h 05.04.97.

FLOW FIELD AT A DEPTH OF 50.00 M

VELOCITY SCALE : 1 CM/S
MAXIMUM VALUE - 0.63CM/S

SCALE: 10 km
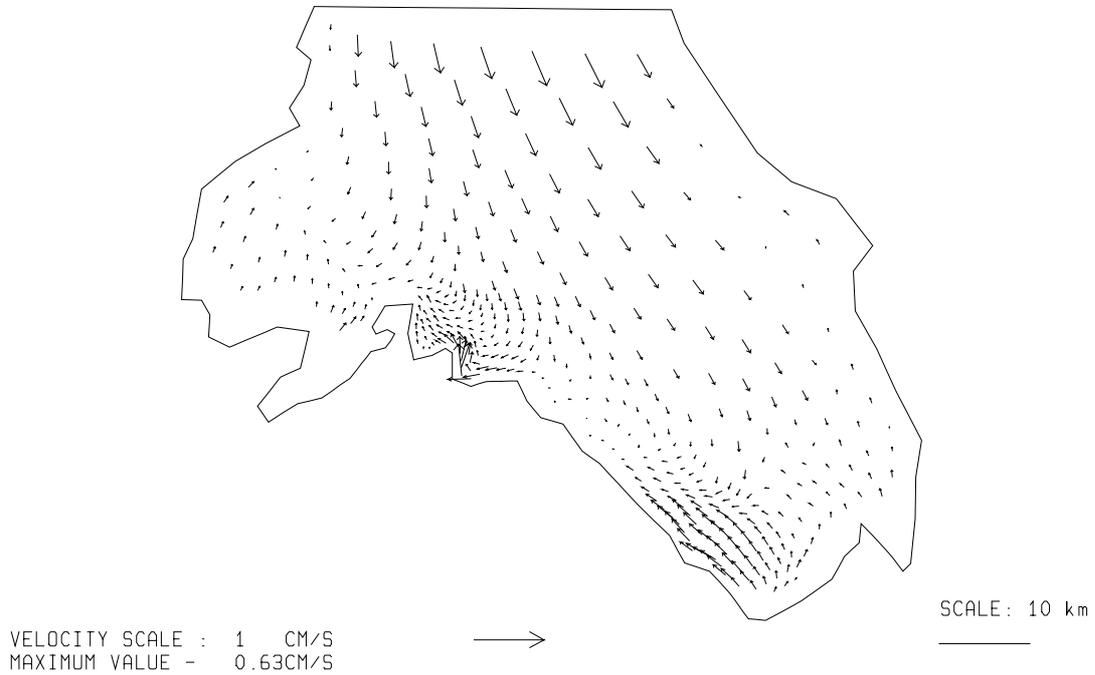
Fig. 3.5.2./47 Calculated flow at a depth of 50 m. Local time 20 h 05.04.97.

FLOW FIELD AT A DEPTH OF 100.00 M

SCALE: 10 km

VELOCITY SCALE : 1 CM/S
MAXIMUM VALUE - 0.40CM/S
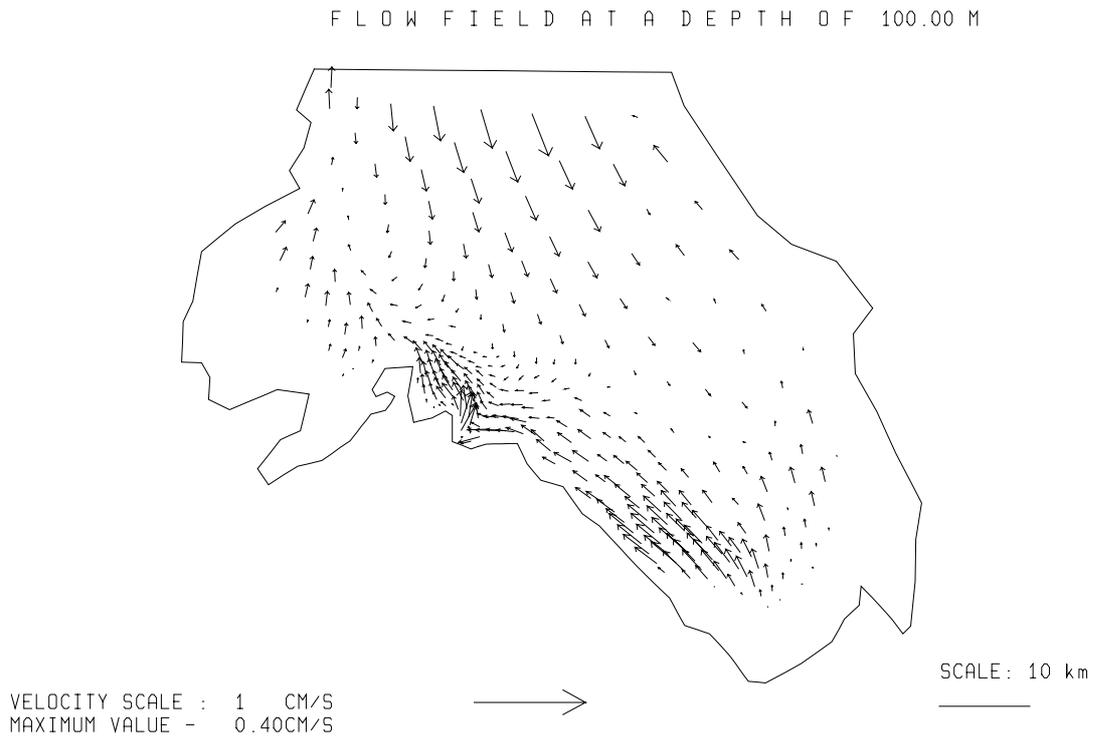
Fig. 3.5.2./48 Calculated flow at a depth of 100 m. Local time 20 h .

NEAR-SURFACE WIND FIELD

SCALE: 10 km

VELOCITY SCALE : 10 CM/S
MAXIMUM VALUE - 32.01CM/S
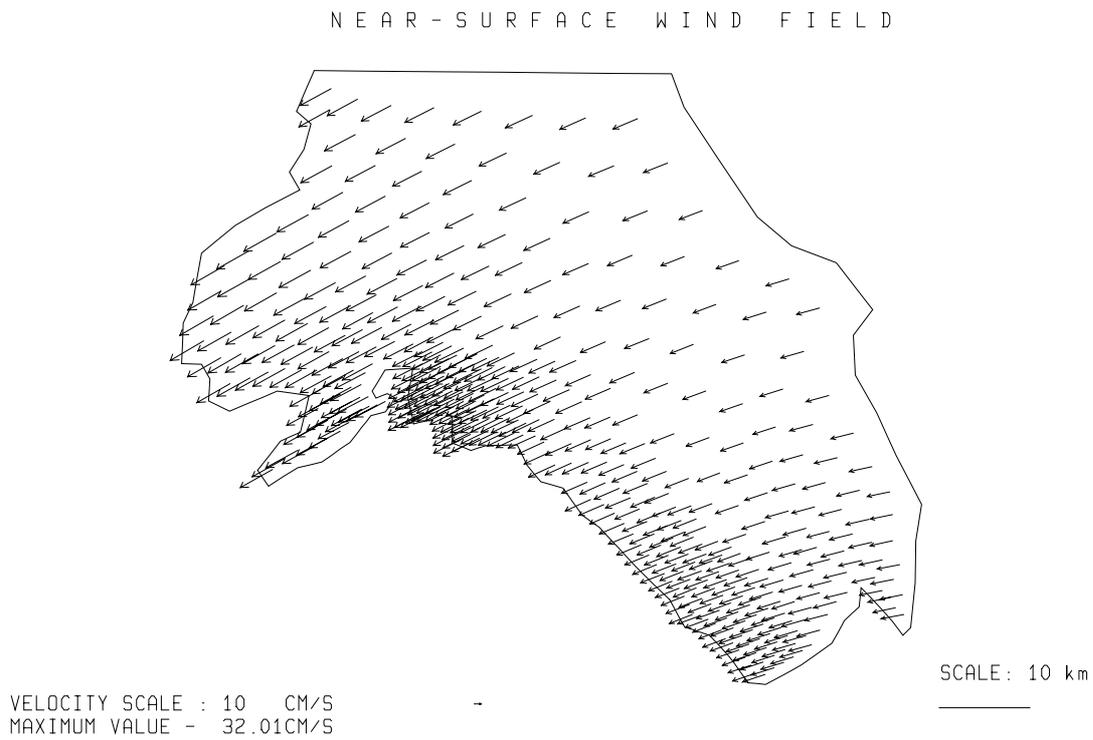
Fig. 3.5.2./49 Simulated near-surface wind. Local time 20 h 05.04.97.

DEPTH-AVERAGED FLOW FIELD

VELOCITY SCALE : 1   CM/S
MAXIMUM VALUE -   0.46CM/S

SCALE: 10 km
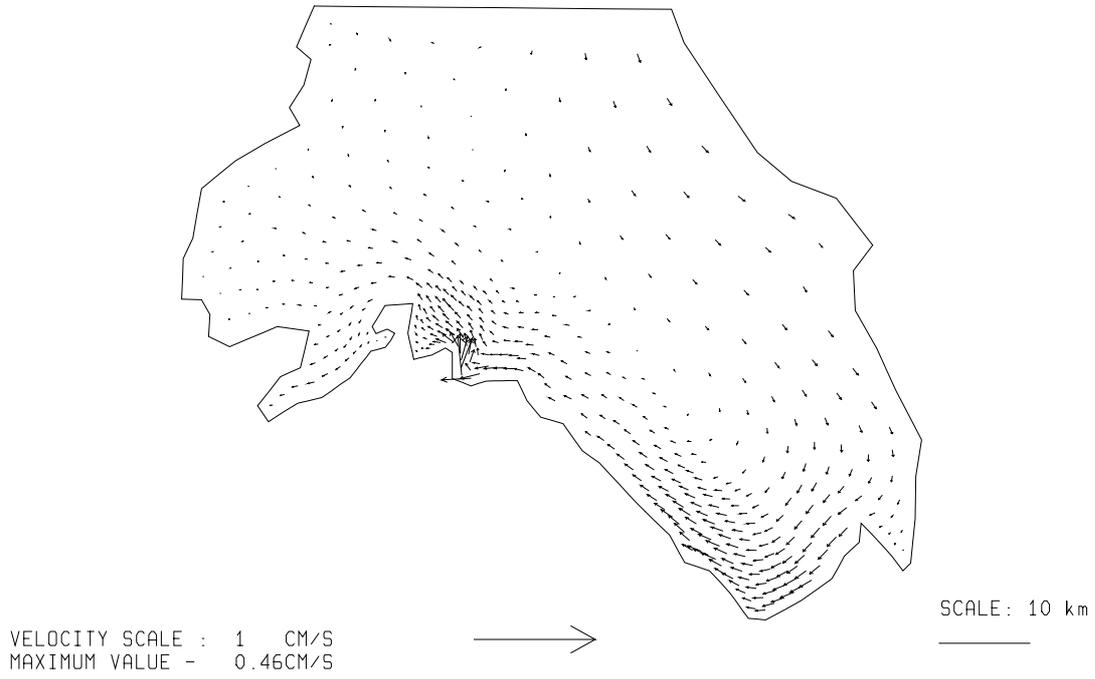
Fig. 3.5.2./50 Calculated depth-averaged flow. Local time 20 h 05.04.97.

FLOW FIELD AT A DEPTH OF 0.50 M

VELOCITY SCALE : 10   CM/S
MAXIMUM VALUE - 12.68CM/S

SCALE: 10 km
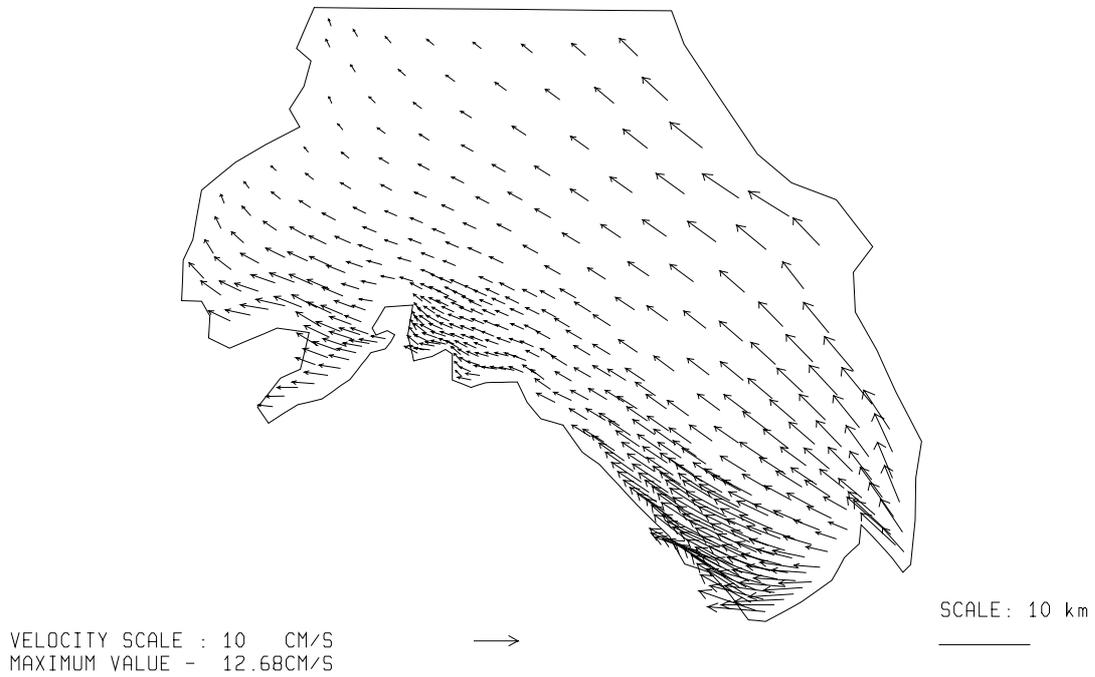
Fig. 3.5.2./51 Calculated flow at a depth of 0.5 m. Local time 04 h 24.08.97.

FLOW FIELD AT A DEPTH OF 50.00 M

VELOCITY SCALE :   5   CM/S
MAXIMUM VALUE -   3.14CM/S
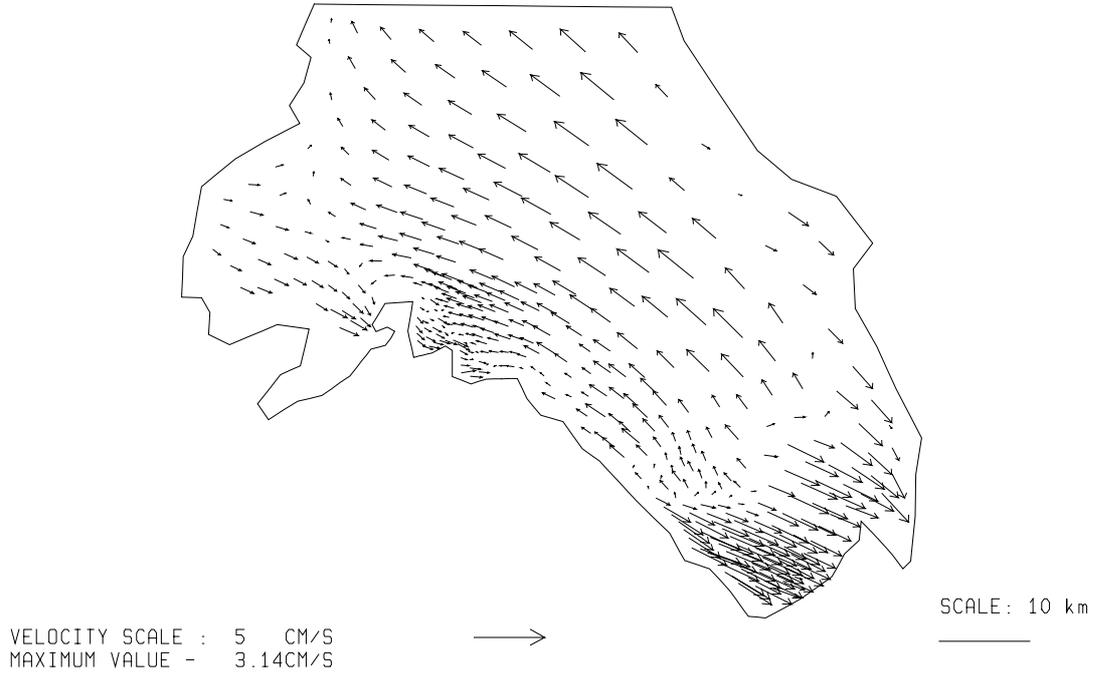
SCALE: 10 km

Fig. 3.5.2./52 Calculated flow at a depth of 50 m. Local time 04 h 24.08.97.

FLOW FIELD AT A DEPTH OF 100.00 M

VELOCITY SCALE :   5   CM/S
MAXIMUM VALUE -   3.19CM/S
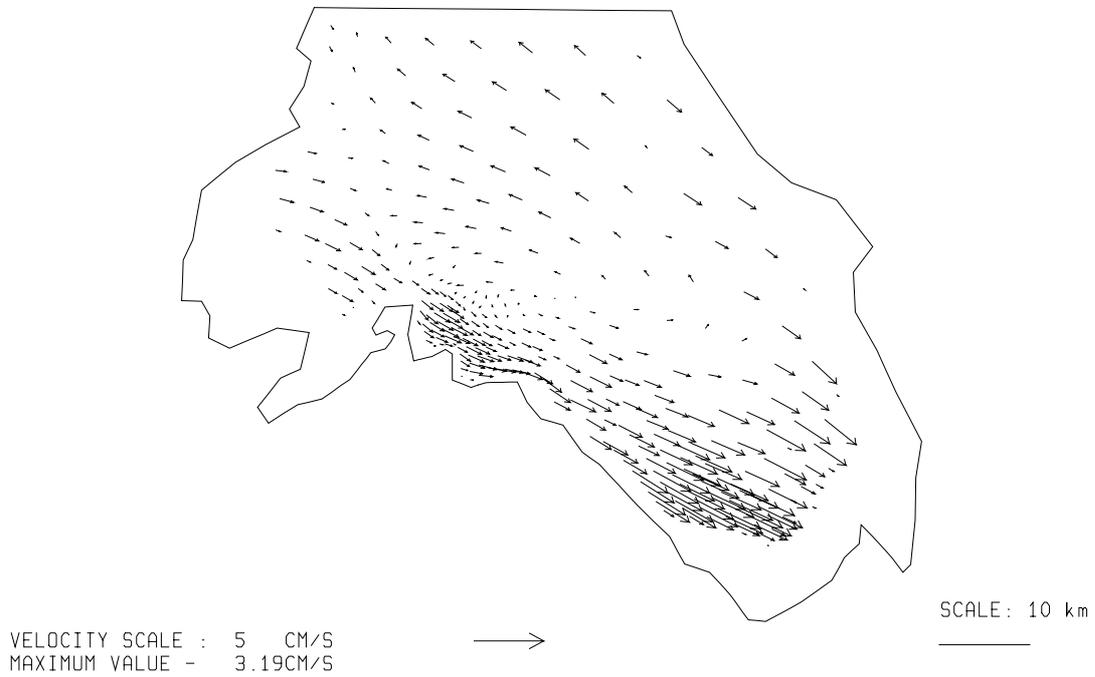
SCALE: 10 km

Fig. 3.5.2./53 Calculated flow at a depth of 100 m. Local time 04 h 24.08.97.

N E A R - S U R F A C E   W I N D   F I E L D
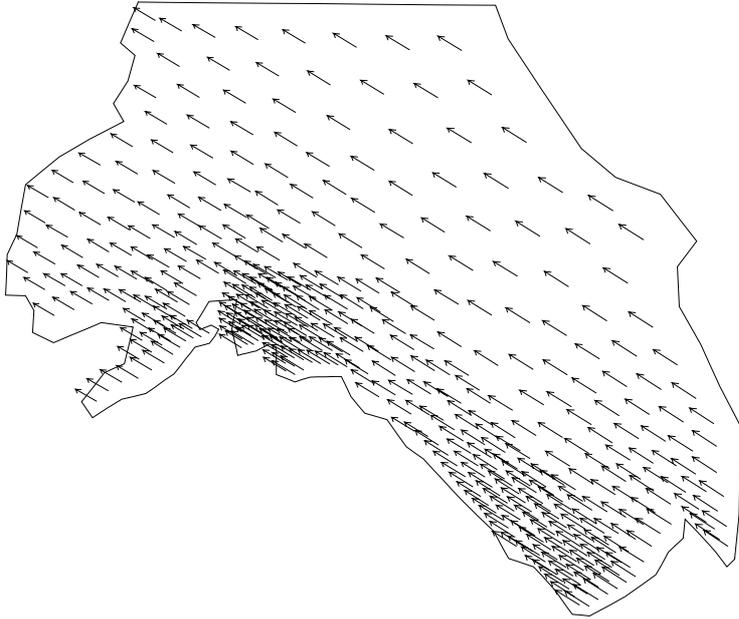
VELOCITY SCALE : 100   CM/S
MAXIMUM VALUE - 557.09CM/S

SCALE: 10 km

Fig. 3.5.2./54 Simulated near-surface wind. Local time 04 h 24.08.97.

D E P T H - A V E R A G E D   F L O W   F I E L D
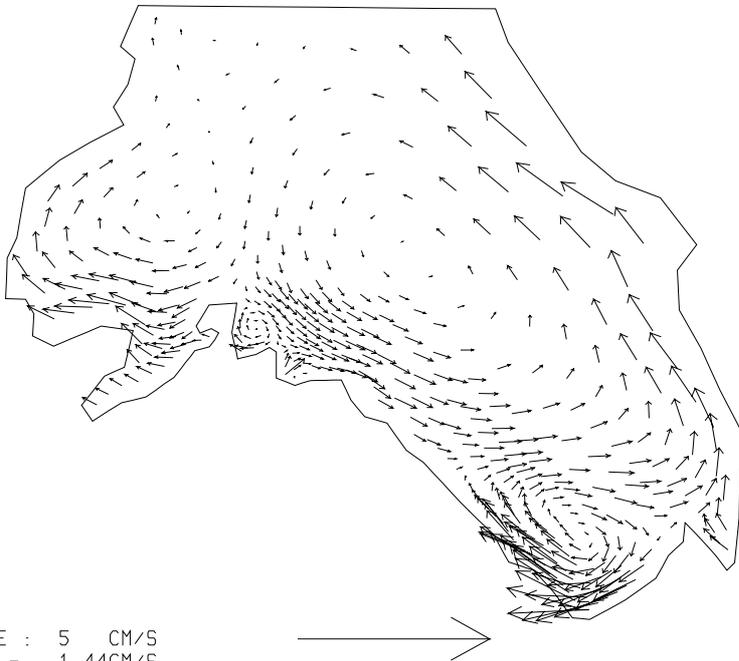
VELOCITY SCALE : 5   CM/S
MAXIMUM VALUE -   1.44CM/S

SCALE: 10 km

Fig. 3.5.2./55 Calculated depth-averaged flow. Local time 04 h 24.08.97.

FLOW FIELD AT A DEPTH OF 0.50 M

VELOCITY SCALE : 5   CM/S
MAXIMUM VALUE -   3.90CM/S

SCALE: 10 km
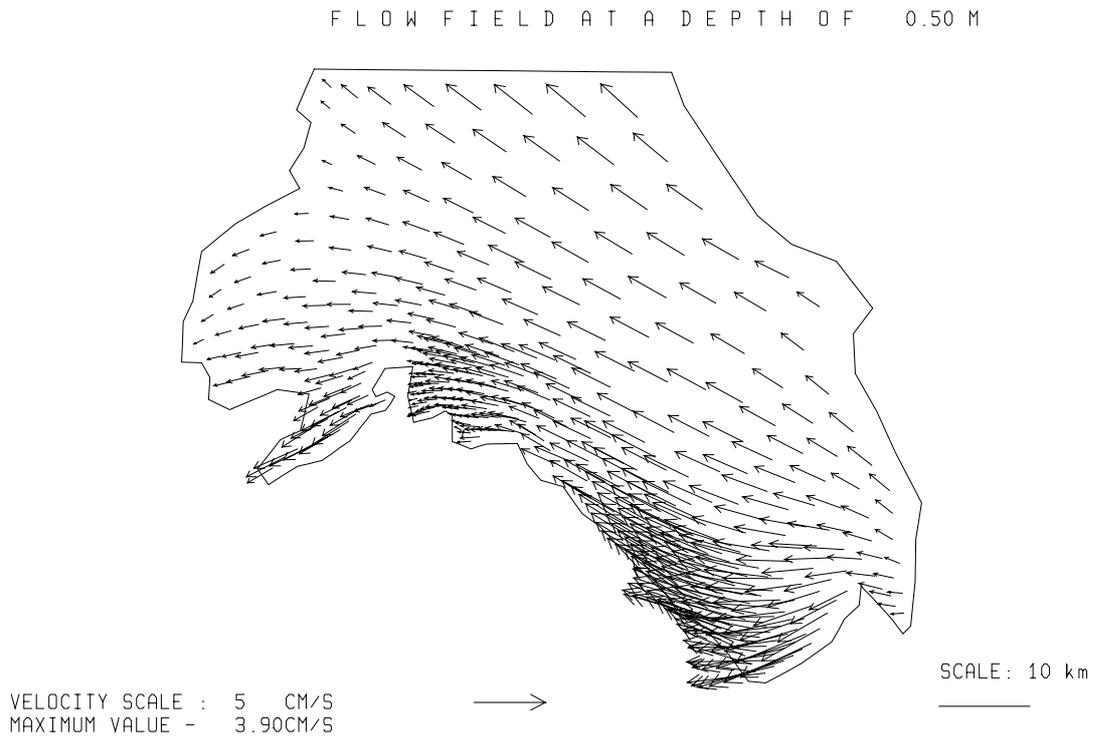
Fig. 3.5.2./56 Calculated flow at a depth of 0.5 m. Local time 12 h 24.08.97.

FLOW FIELD AT A DEPTH OF 50.00 M

VELOCITY SCALE : 5   CM/S
MAXIMUM VALUE -   1.70CM/S

SCALE: 10 km
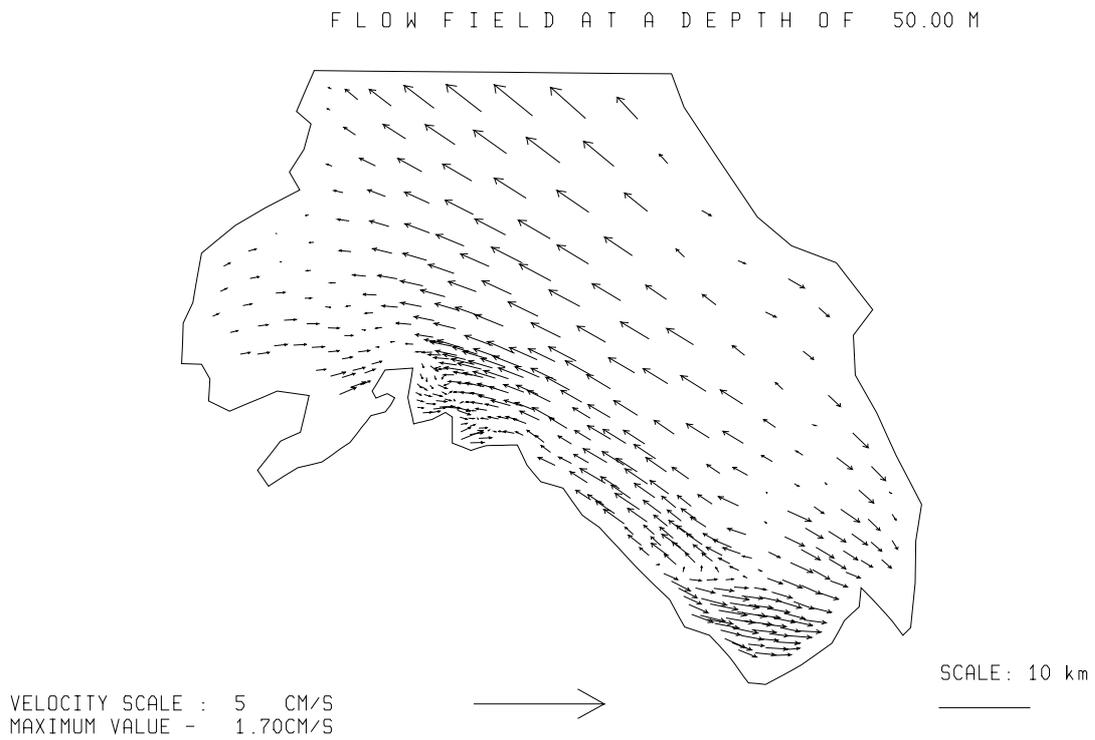
Fig. 3.5.2./57 Calculated flow at a depth of 50 m. Local time 12 h 24.08.97.

FLOW FIELD AT A DEPTH OF 100.00 M

VELOCITY SCALE : 5 CM/S
MAXIMUM VALUE - 1.09CM/S

SCALE: 10 km
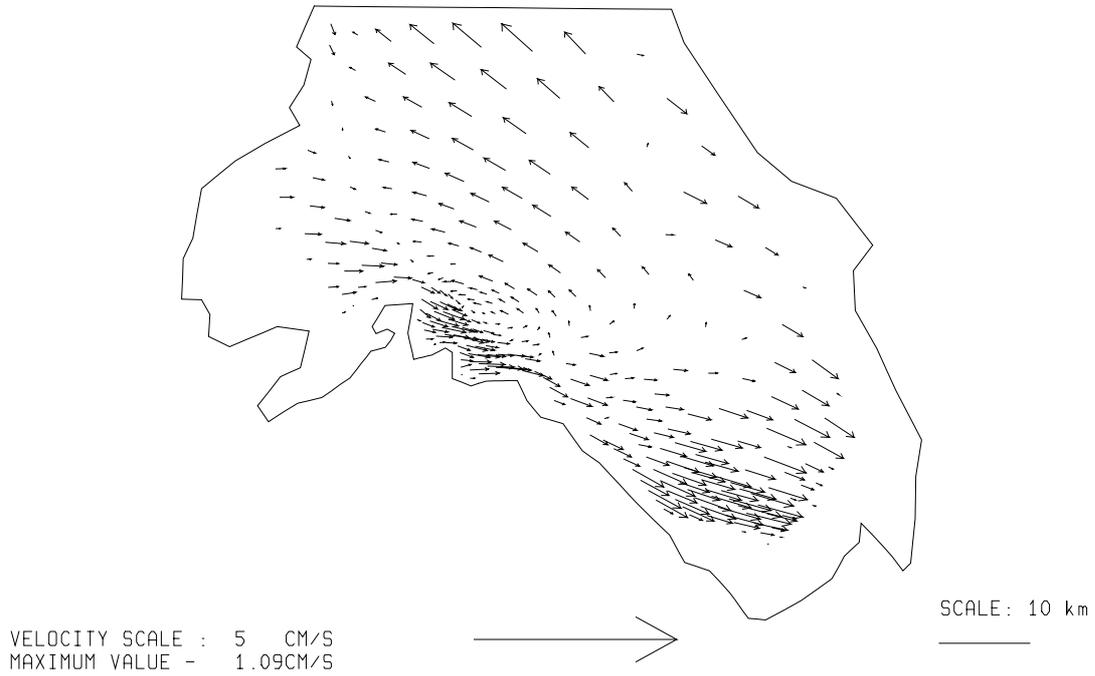
Fig. 3.5.2./58 Calculated flow at a depth of 100 m. Local time 12 h 24.08.97.

NEAR-SURFACE WIND FIELD

VELOCITY SCALE : 100 CM/S
MAXIMUM VALUE - 177.29CM/S

SCALE: 10 km
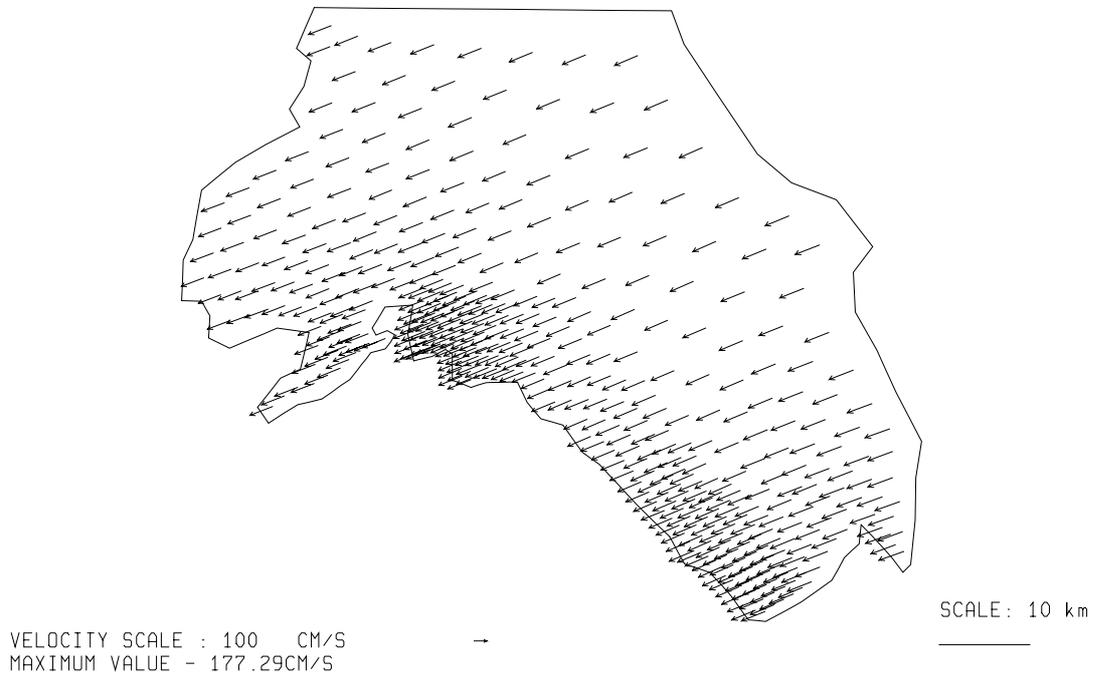
Fig. 3.5.2./59 Simulated near-surface wind. Local time 12 h 24.08.97.

DEPTH-AVERAGED FLOW FIELD

SCALE: 10 km

VELOCITY SCALE : 1 CM/S
MAXIMUM VALUE - 0.67CM/S
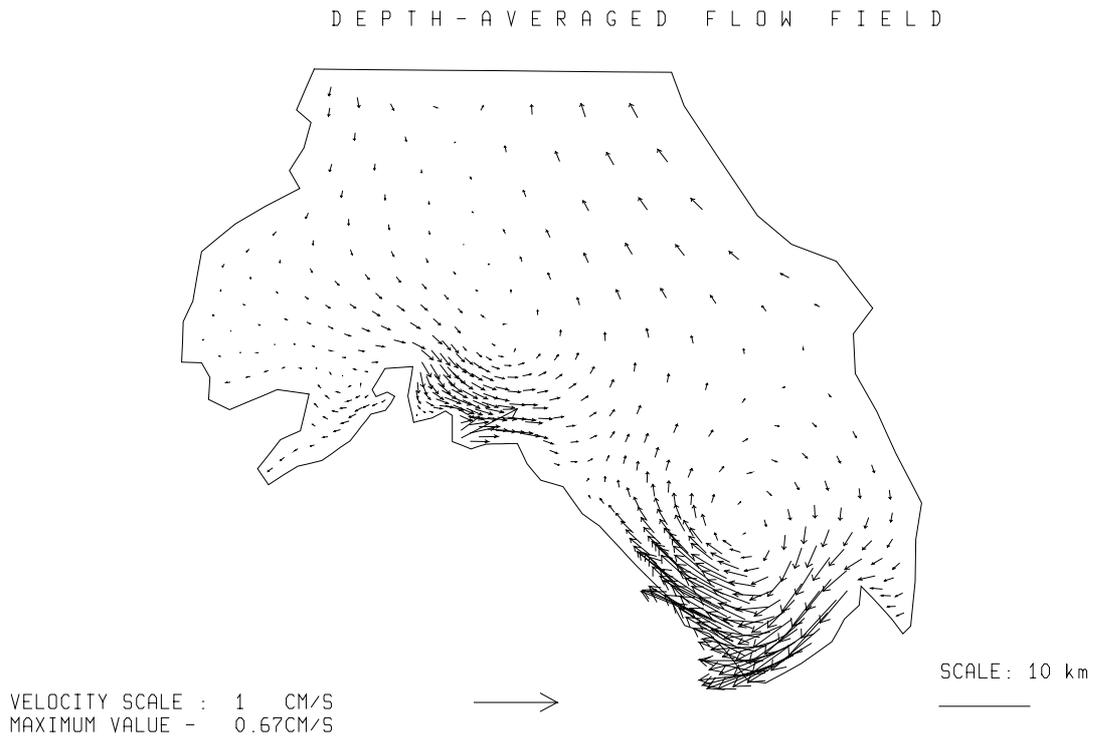
Fig. 3.5.2./60 Calculated depth-averaged flow. Local time 12 h 24.08.97.

FLOW FIELD AT A DEPTH OF 0.50 M

SCALE: 10 km

VELOCITY SCALE : 5 CM/S
MAXIMUM VALUE - 3.58CM/S
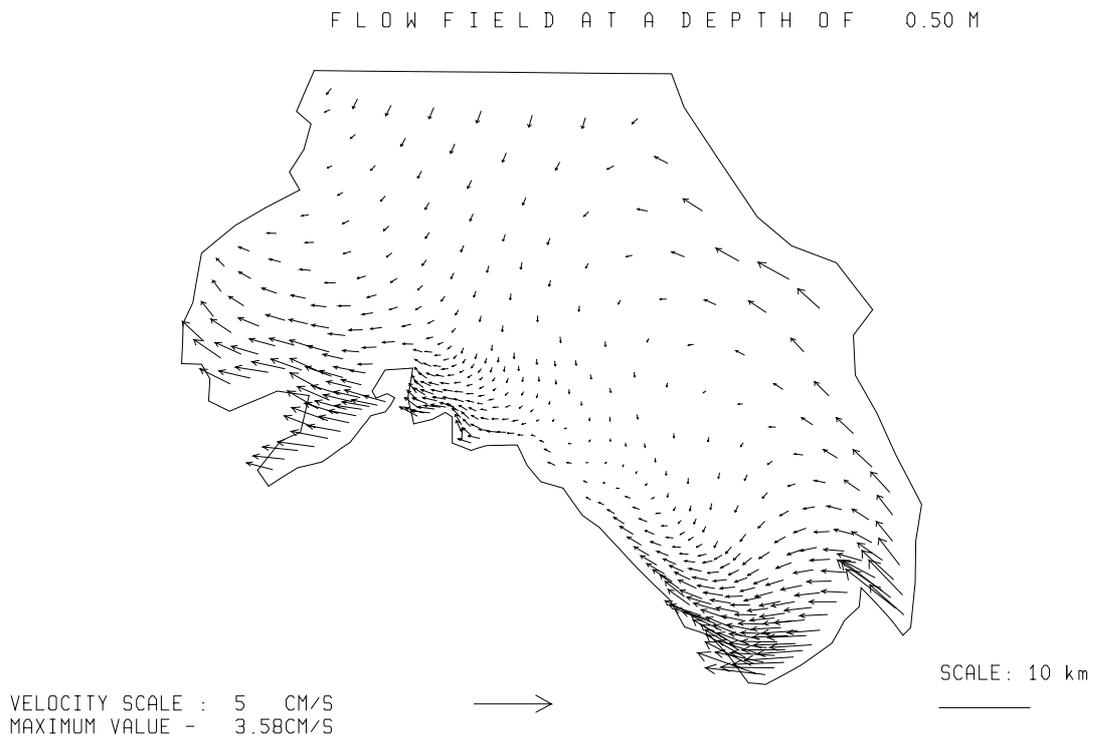
Fig. 3.5.2./61 Calculated flow at a depth of 0.5 m. Local time 20 h 24.08.97.

FLOW FIELD AT A DEPTH OF 50.00 M

SCALE: 10 km

VELOCITY SCALE : 1 CM/S
MAXIMUM VALUE - 0.62CM/S
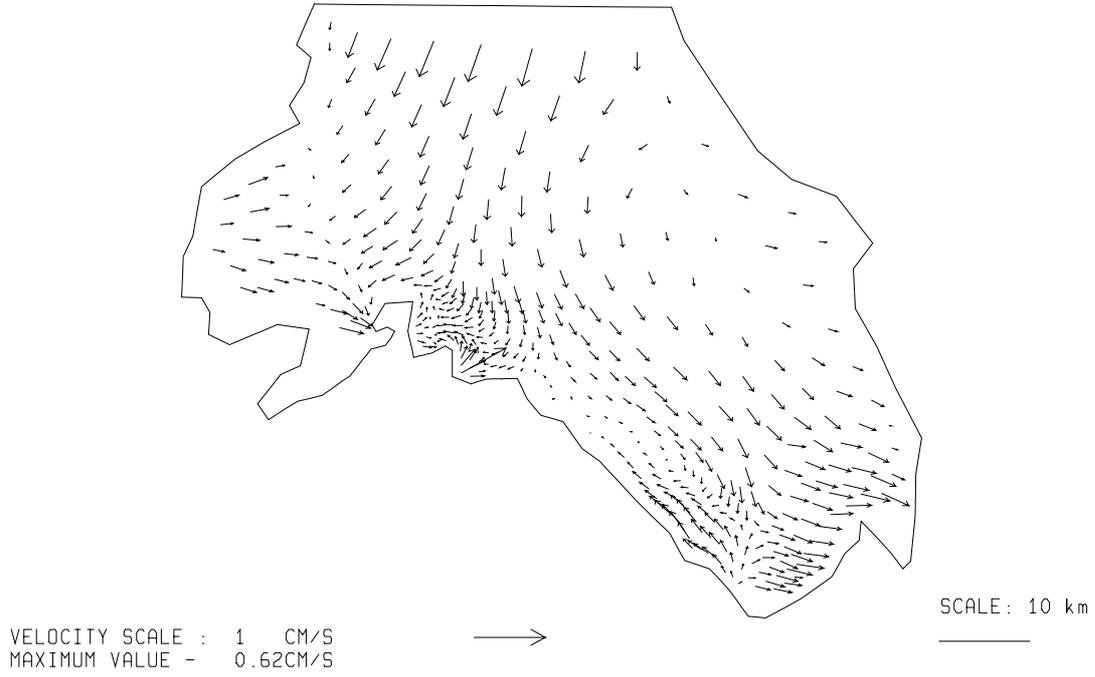
Fig. 3.5.2./62 Calculated flow at a depth of 50 m. Local time 20 h 24.08.97.

FLOW FIELD AT A DEPTH OF 100.00 M

SCALE: 10 km

VELOCITY SCALE : 1 CM/S
MAXIMUM VALUE - 0.39CM/S
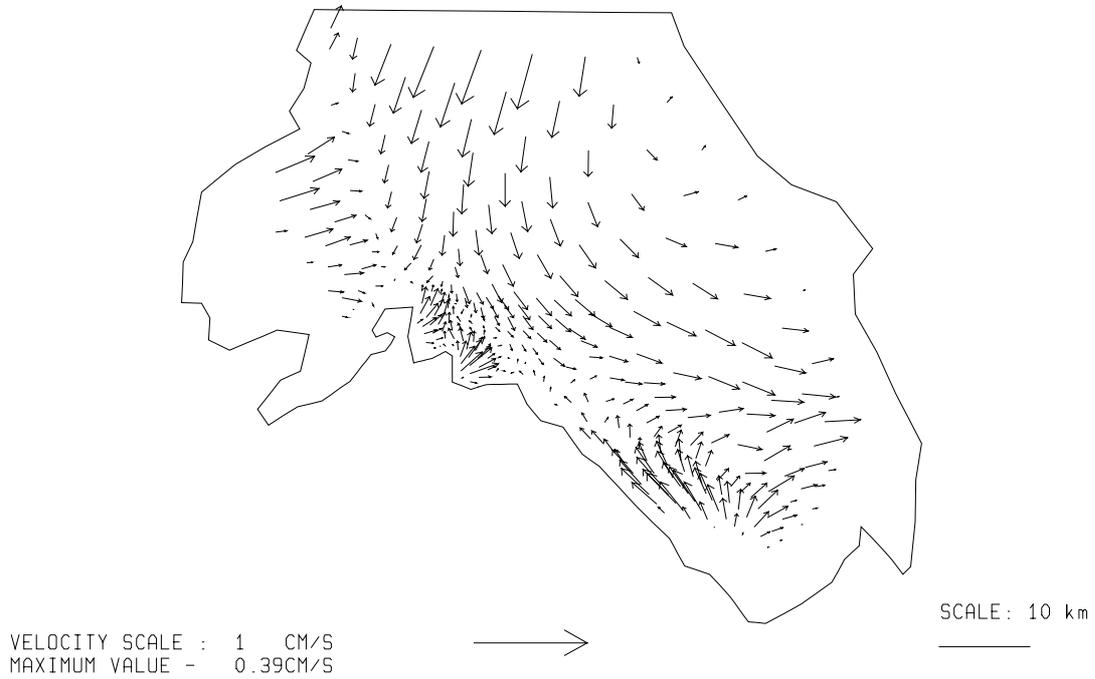
Fig. 3.5.2./63 Calculated flow at a depth of 100 m. Local time 20 h 24.08.97.

N E A R – S U R F A C E   W I N D   F I E L D
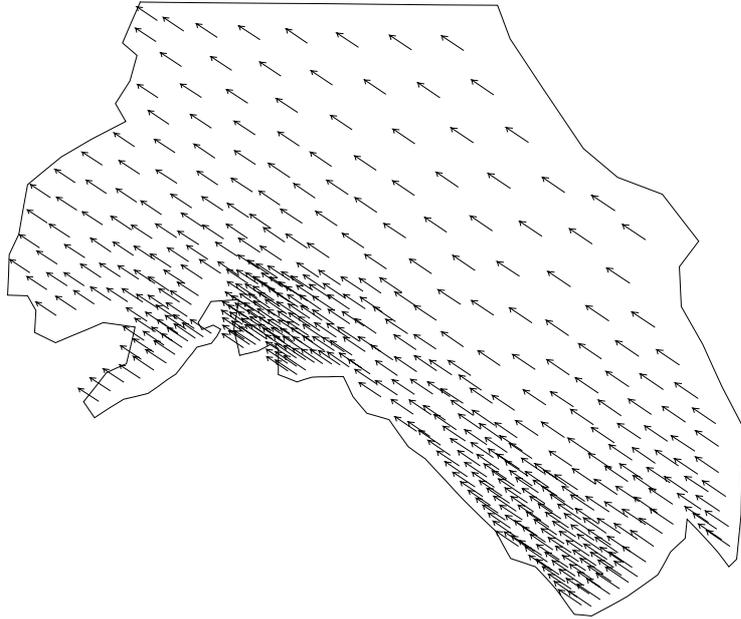
VELOCITY SCALE : 100   CM/S
MAXIMUM VALUE – 349.84CM/S

SCALE: 10 km

Fig. 3.5.2./64 Simulated near-surface wind. Local time 20 h 24.08.97.

D E P T H – A V E R A G E D   F L O W   F I E L D
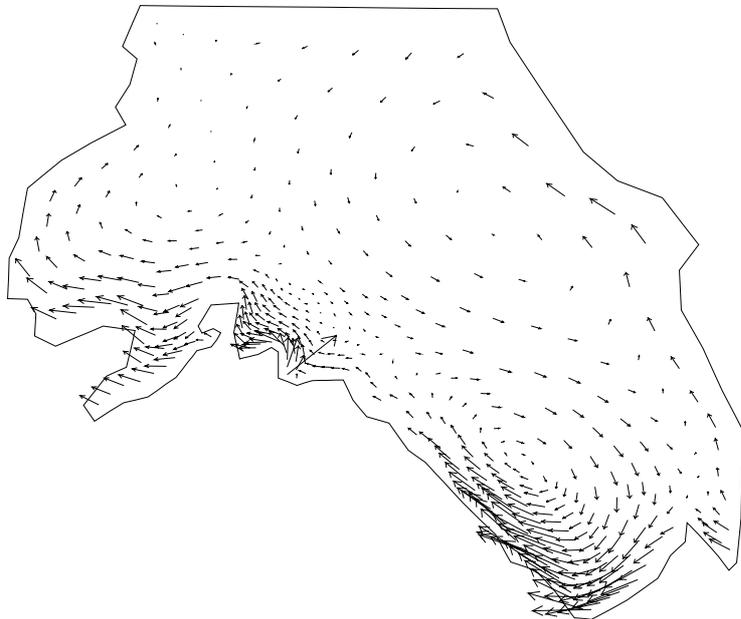
VELOCITY SCALE : 1   CM/S
MAXIMUM VALUE –   0.52CM/S

SCALE: 10 km

Fig. 3.5.2./65 Calculated depth-averaged flow. Local time 20 h 24.08.97.

3.5.3 Sediment transport modelling

According to the experimental findings (Chapter 2.4.3) the sediments in studied areas of Lake Tanganyika can be classified as silt (Raudkivi 1990), varying from fine silt fraction in the region of river Malagarasi to the coarse type near river Lufubu. In the sediment transport models the Suspended Particulate Matter (SPM) was approximated as a single fraction with a grain size equal to the median grain size d_{50} of collected samples. For the Malagarasi region the model parameters were: $d_{50}=15*10^{-6}$ m and $d_{90}=70*10^{-6}$m. In the Lufubu model these values were as follows: $d_{50}=45*10^{-6}$m and $d_{90}=130*10^{-6}$m. Material "constant" $M=10^{-5}$ kg^{-2}s^{-1}, critical shear stress $\tau_{er}=10^{-3}$ N m^{-2}, coefficients of horizontal diffusion Kx = Ky =5 m^2 s^{-1} and timestep $\Delta t = 300$ s were taken equal for both regions. Using the Stokes formula (Raudkivi, 1990) and after preliminary tests the value of the settling velocity was set to be $w_s=5.78*10^{-5}$ m s^{-1} (5 m day^{-1}).

The inflow concentration of SPM was estimated with a simple analogue interpolation method (Chapter 2.4.3). For the wet season it was equal to 3500 mg l^{-1} in river Malagarasi and 1000 mg l^{-1} in the river Lufubu. During the dry season the value of 100 mg l^{-1} was used as the SPM inflow concentration for the river Malagarasi and 50 mg l^{-1} for river Lufubu. There were no direct measurements of SPM concentration in lake waters near the rivers Malagarasi and Lufubu. Turbidity measurements conducted during the expeditions indicate that the SPM concentration is very low in the open lake. This is confirmed by studies performed by Vandelannoote (Vandelannoote et al., 1998) in the northern part of the lake near the mouth of the river Rusizi. It was found that even at 300 m offshore the concentration of suspended solids is 3 - 5 mg l^{-1}. Taking this into consideration and also in order to avoid the appearance of negative values during calculations the initial SPM concentration in all simulations was set equal to 10 mg l^{-1}.

The sediment transport models were used to calculate the transport of suspended solids for the same periods of time as currents were calculated. In figures 3.5.3./1 - 4 calculated changes of SPM concentration in the surface layer with time are shown for wet (2 - 08.04.97) and dry (21 - 28.08.97) season. Three time slices are depicted, namely 22, 82 and 166 hours after beginning of the calculations. The SPM concentrations along a vertical sections extending from river mouths to the lake are illustrated in Figures 3.5.3./5-8.

No erosion or resuspension was found under the simulated meteorological conditions. This can be explained by small values of near bottom current and wave induced shear stresses due to big depths in the lake. These simulation results lead us to important conclusion that in real conditions resuspension of bottom sediments in Lake Tanganyika is bounded in space to the narrow shallow near shore zone. In time re-entrainment of settled particles may take place only during high storms. It should be pointed out that these events are limited both in time and in space. Advective transport by wind-induced currents, turbulent diffusion and gravitational settling are the main factors controlling the spreading of suspended solids incoming with river waters.

Alongshore currents directed toward N - NW are stronger in the shallow area near river Malagarasi mouth. As a result the SS river plume is attenuated in the longitudinal direction and is extended towards N - NW (Figures 3.5.3./1C - 3.5.3./2C). The echo intensity results (Fig. 2.4.4./13) also show that in April the river waters were advected mostly towards N - NW. The observed higher current speeds and their variation during dry season conforms with calculated distribution of SPM. In the vicinity of river Lufubu the simulated currents are weaker and the effect of turbulent diffusion on the distribution of SS is more pronounced. As a result the shape of the plume is closer to semi-

circle. It might be that a closed gyre sometimes found to the NE from river Lufubu mouth blocks the spreading of the river plume in this direction.

The transects along the line AB (Fig. 3.5.2./3) and the line CD (Fig. 3.5.2./4) for the same instants of time in Figures 3.5.3./5 - 3.5.3./8 show mainly homogenous distribution of suspended solids in the vertical direction. Integration period of one week is small to trace the influence of the gravitational settling on the vertical profiles of SPM.
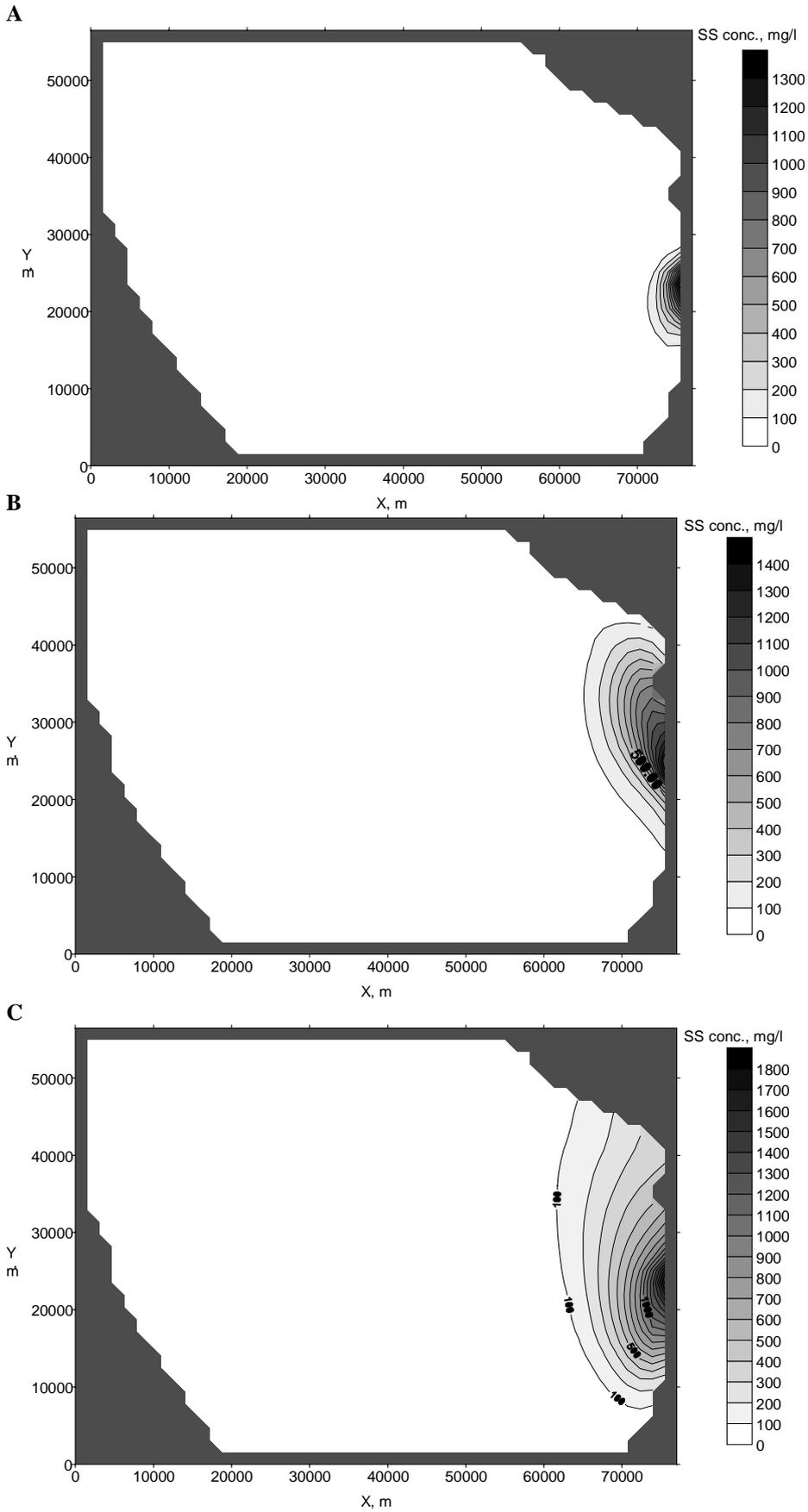
Fig. 3.5.3./1 Calculated SS concentration in the surface layer at 0:00 3.04.97 (A), 12:00 5.04.97 (B) and 0:00 9.04.97 (C) after 22, 82 and 166 hours after the simulation start respectively.
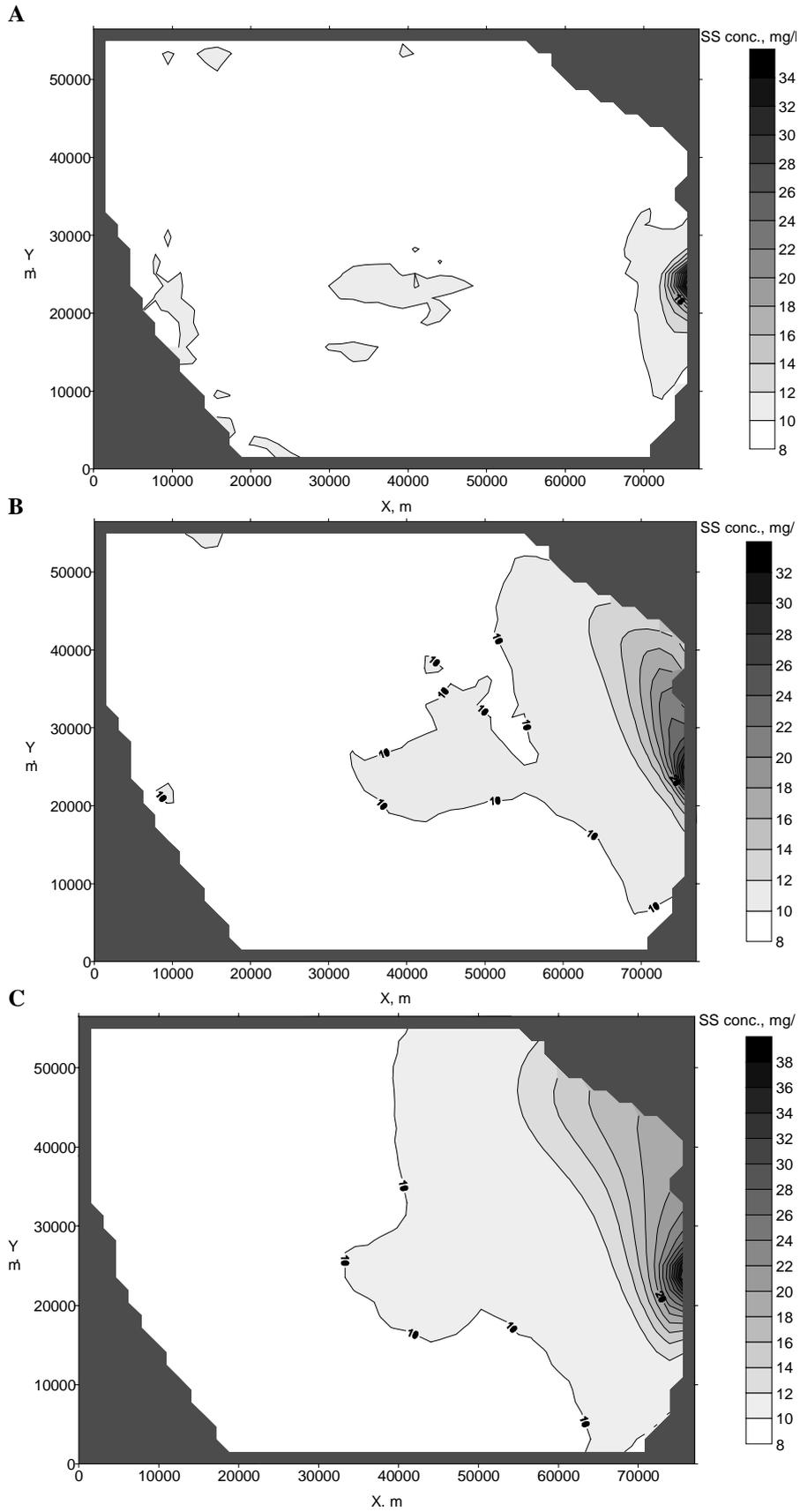
Fig. 3.5.3./2 Calculated SS concentration in the surface layer at 0:00 22.08.97 (A), 12:00 24.08.97 (B) and 0:00 28.08.97 (C) after 22, 82 and 166 hours after the simulation start respectively
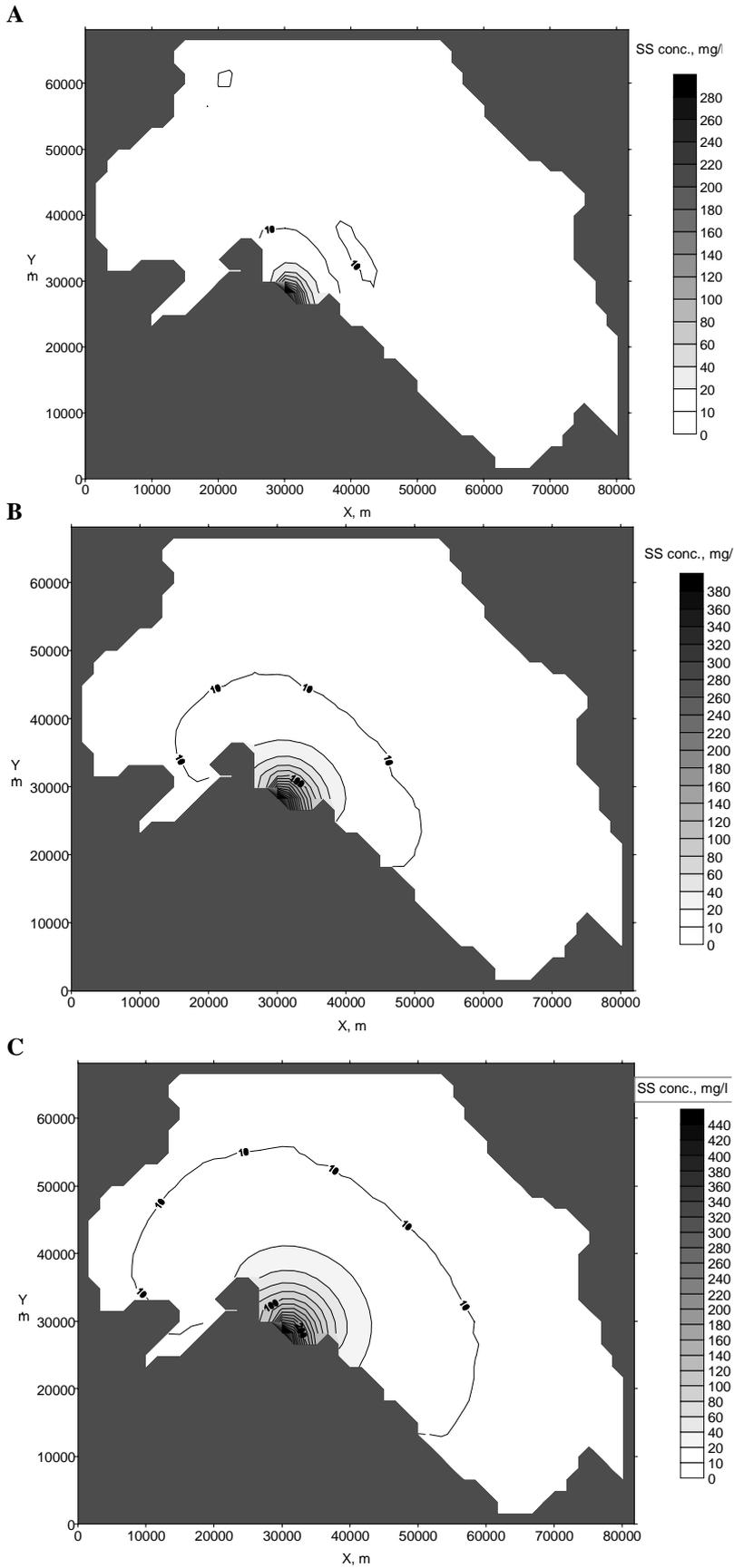
Fig. 3.5.3./3 Calculated SS concentration in the surface layer at 0:00 3.04.97 (A), 12:00 5.04.97 (B) and 0:00 9.04.97 (C) after 22, 82 and 166 hours after the simulation start respectively.

158
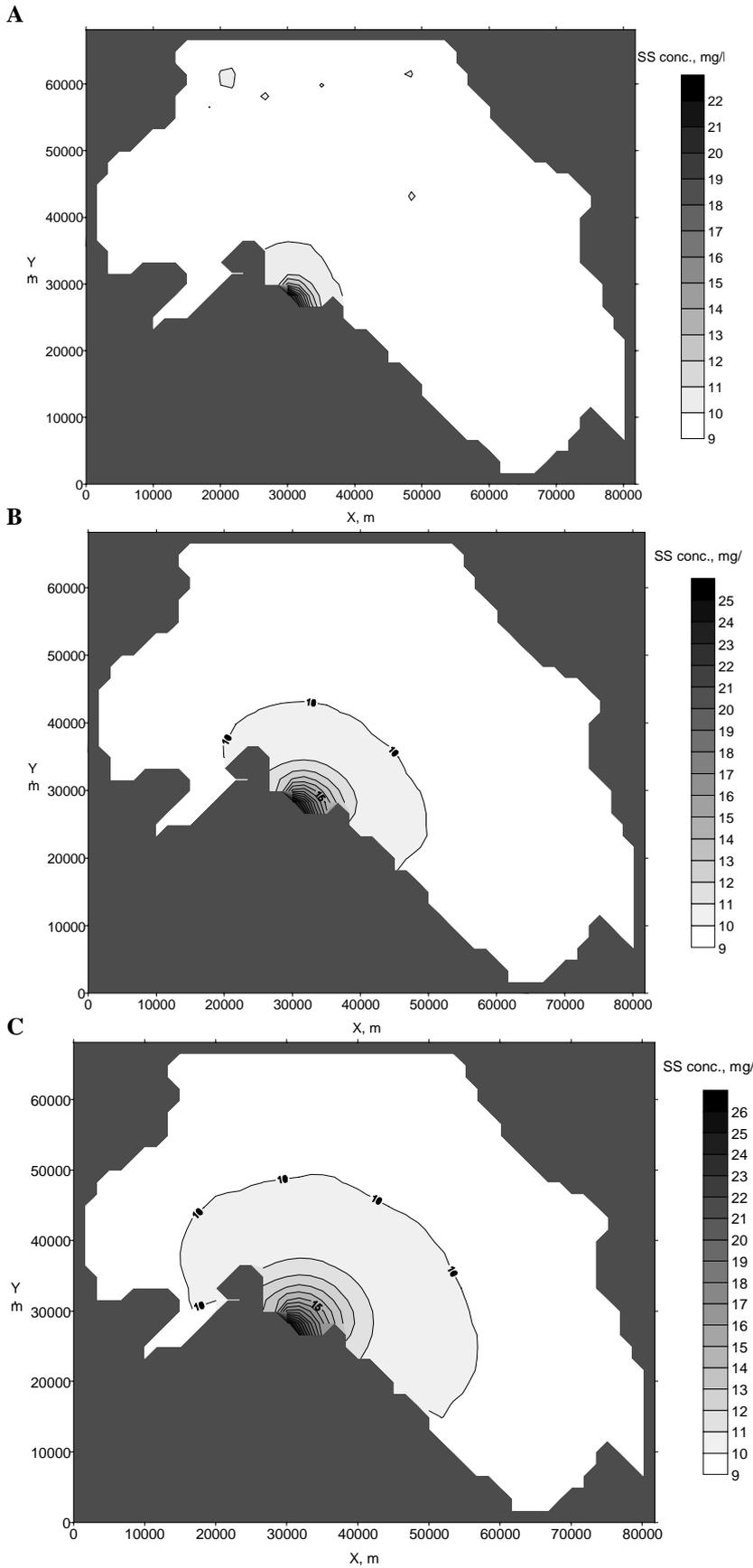
Fig. 3.5.3./4 Calculated SS concentration in the surface layer at 0:00 22.08.97 (A), 12:00 24.08.97 (B) and 0:00 28.08.97 (C) after 22, 82 and 166 hours after the simulation start respectively.
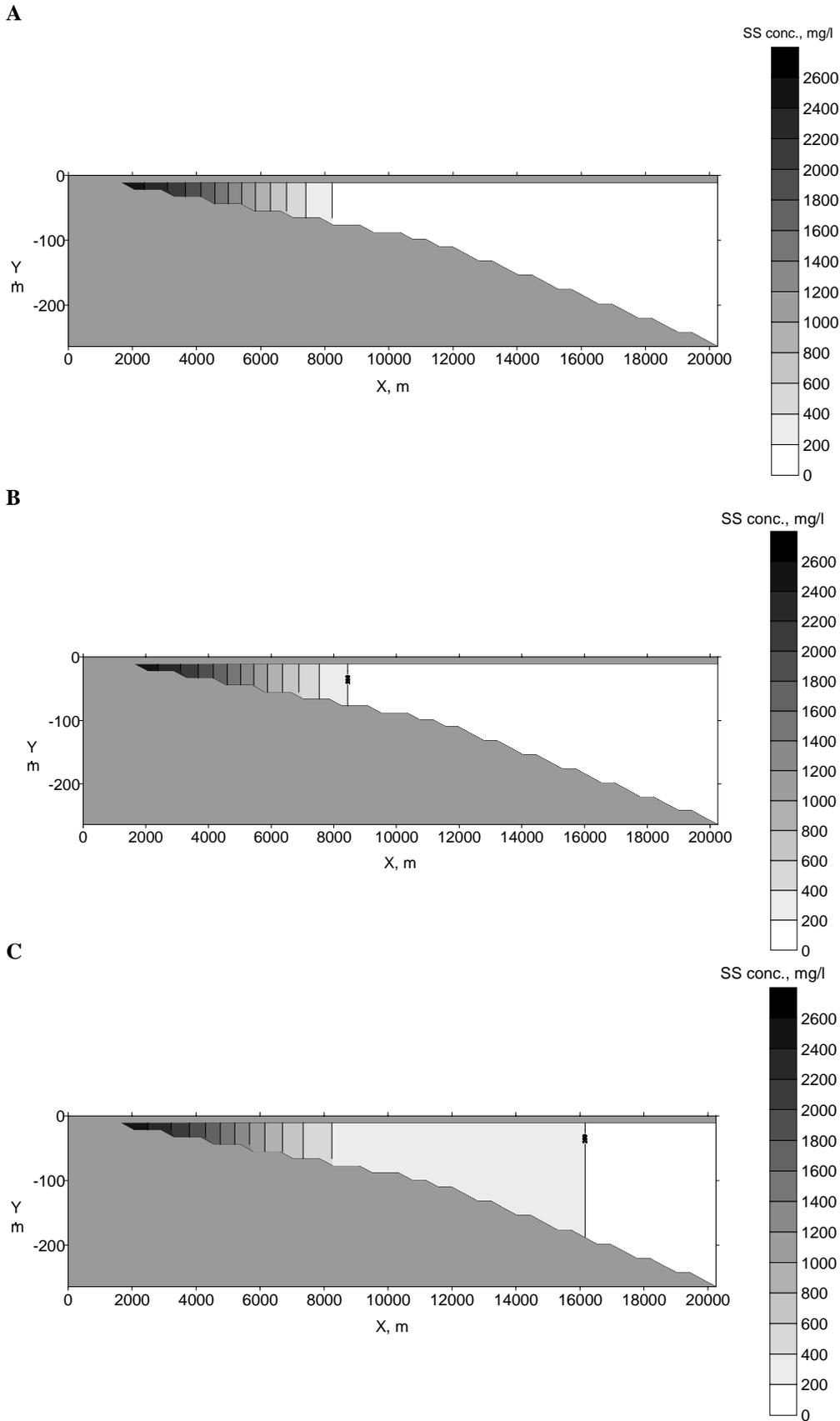
Fig. 3.5.3./5 Calculated SS concentration along a vertical section near river Malagarasi mouth at 0:00 3.04.97 (A), 12:00 5.04.97 (B) and 0:00 9.04.97 (C) after 22, 82 and 166 hours after the simulation start respectively.

A

B

C
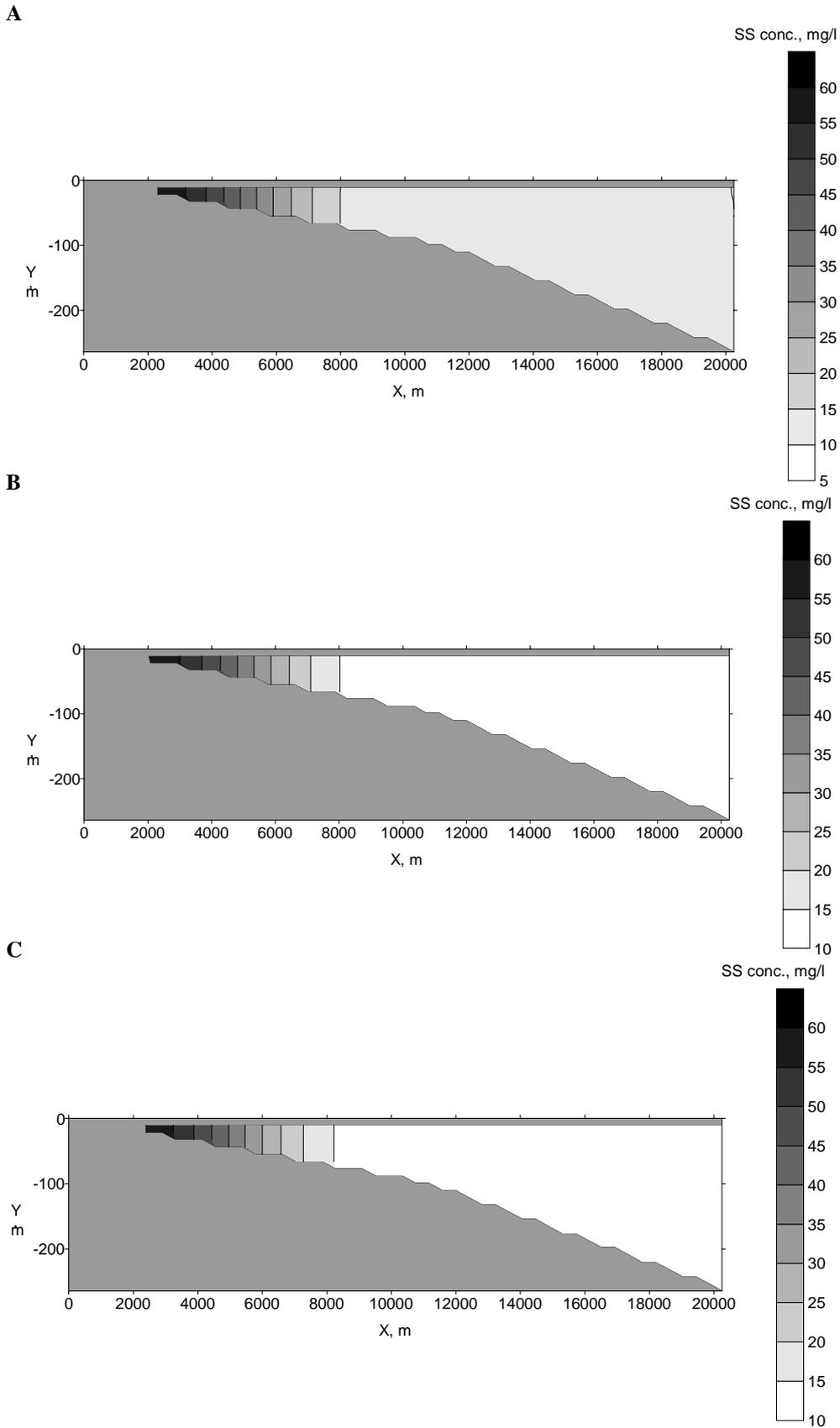
Fig. 3.5.3./6 Calculated SS concentration along a vertical section near river Malagarasi mouth at 0:00 22.08.97 (A), 12:00 24.08.97 (B) and 0:00 28.08.97 (C) after 22, 82 and 166 hours after the simulation start respectively.

161
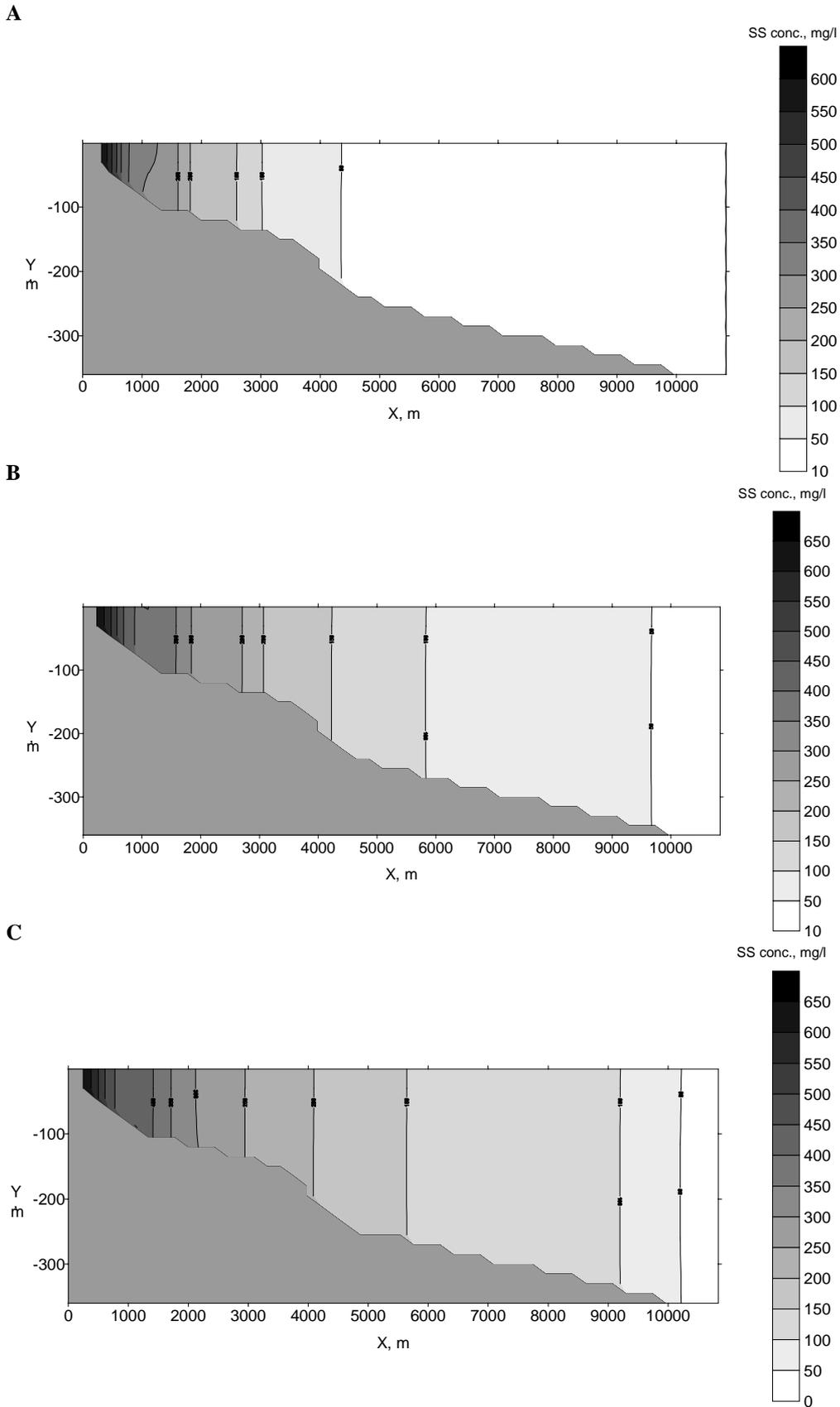
Fig. 3.5.3./7 Calculated SS concentration along a vertical section near river Lufubu mouth at 0:00 3.04.97 (A), 12:00 5.04.97 (B) and 0:00 9.04.97 (C) after 22, 82 and 166 hours after the simulation start respectively.

A

B

C
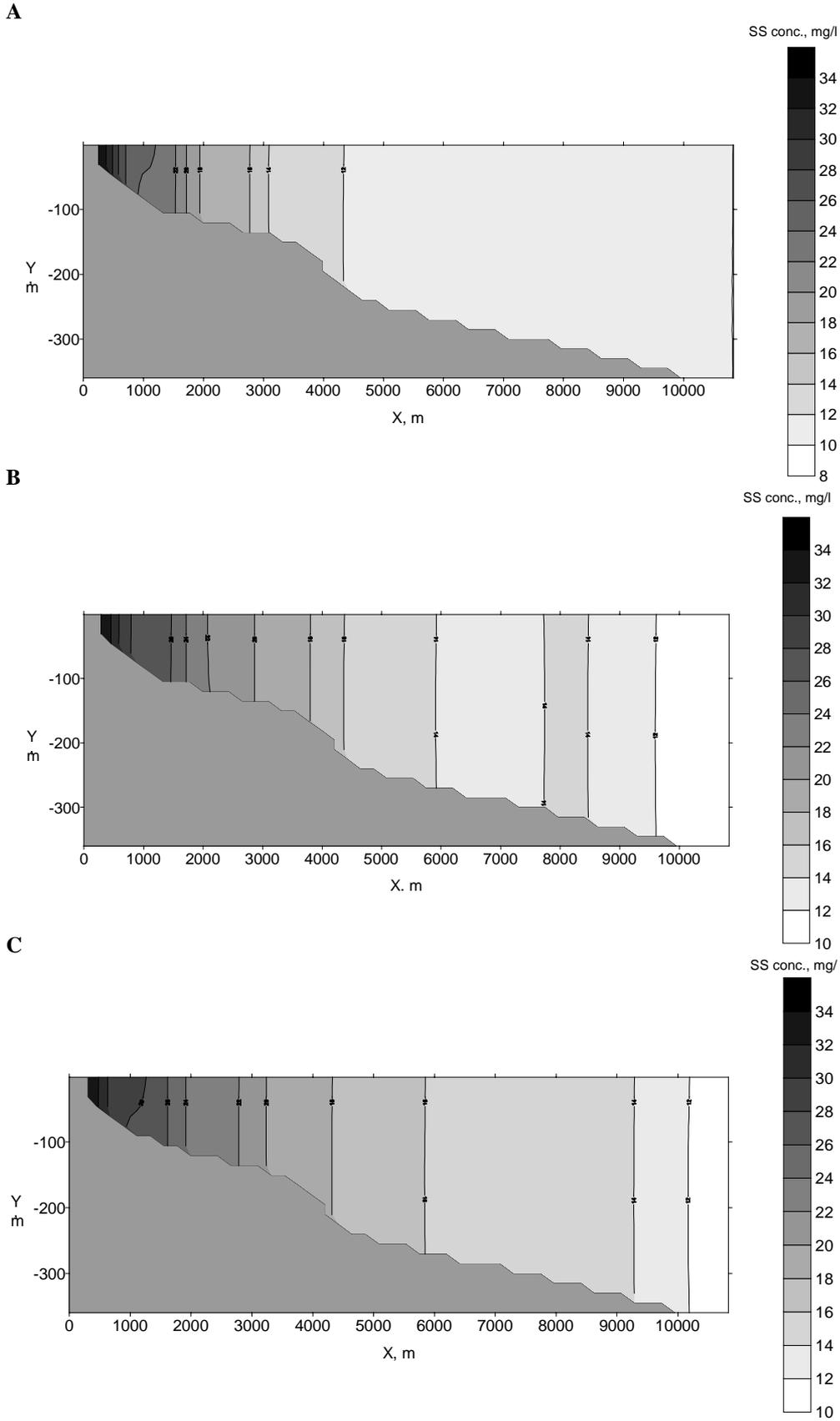
Fig. 3.5.3./8 Calculated SS concentration along a vertical section near river Lufubu mouth at 0:00 22.08.97 (A), 12:00 24.08.97 (B) and 0:00 28.08.97 (C) after 22, 82 and 166 hours after the simulation start respectively.

3.6 Discussion

A set of numerical advanced models have been developed and applied to study the wind and flow regime as well as dynamics of suspended solids in Lake Tanganyika. A state of the art weather forecasting system HIRLAM was used to describe the near surface winds over the Lake Tanganyika region. High spatial and temporal resolution of the model enabled to correctly resolve the main physical mechanisms, combined effects of orography, thermal peculiarities and large scale trade winds, responsible for complicated but quasi regular wind patterns over Lake Tanganyika. The full verification of the model is still in progress, but comparison analysis with vast observations conducted so far show a very reasonable agreement between the observations and simulation results.

Numerical experiments with three-dimensional flow and sediment transport models were focused on two regions adjacent the biggest tributaries of the lake: river Malagarasi in the middle part of the lake and river Lufubu in the south. Lake-wide circulation model was also used to calculate the velocities on liquid boundaries of the regional models. Two time periods were considered, one week during the rainy season in April 1997 and the second week during the dry season in August 1997.

Flow simulation results revealed a very dynamic flow structure, proved by intensive ADCP measurements all over the lake. Calculated currents correlate satisfactory with the observed ones in direction according to comparison with the point measurements conducted with buoy ADCP. The model underestimates the magnitude of the flow due to the high numerical diffusion properties of the selected implicit integration scheme. Simulations showed that the winds over the region and lake bathymetry are the main factors determining the flow structure. Influence of the river inflows is limited to a very small area in the vicinity of the river mouths because of the hydraulic friction. Alongshore N-NW currents prevail in the river Malagarasi region. With the ceasing of the wind and it's turning from a lake breeze to a land breeze, the currents also turn from N-NW to S, but the duration is shorter and the speed of the opposite flow is smaller.

Extremely great depths of the lake considerably reduce the possibility of resuspension of the settled solid particles and limit it in space to the small, shallow coastal areas of the lake. Thus one may conclude that the main source of suspended solids in the lake are the inflowing rivers. Areas with relatively high SPM concentrations in the lake are the river mouths. Under the action of wind-induced currents, the turbulent diffusion and gravitational settling SPM spread in the lake mainly along the narrow coastal zone. The main part of suspended solids settles in the vicinity of the river mouths. Similar types of scenarios were produced with sediment transport models.

4. Summary and conclusions

This work complements the special studies in the UNOPS Project, **"Pollution Control and Other Measures to Protect Biodiversity of Lake Tanganyika"** (RAF/92/G32), or Lake Tanganyika Biodiversity (LTBP), by providing a detailed analysis of water circulation for pollutant and sediment transport in the lake. To attain this goal regional circulation and sediment transport models were developed. The implementation of the work was done through an **Inter-Agency agreement** between the UNOPS and FAO. FAO has been executing a regional project, **"Research for the Management of the Fisheries on Lake Tanganyika"**, Lake Tanganyika Research (LTR) since 1992.

The implementation of the work was divided in **three parts**: **1) improvement of data collection network, 2) development of flow and sediment transport models and 3) application of High Resolution Meteorological Forecast Model (HIRLAM)** to provide accurate wind predictions over the lake for lake models. The last part was **funded by Finnish Academy of Science.**

Data collection network was complemented by current measuring instruments. For this purpose three Acoustic Doppler Profilers (ADCP) were purchased. One was used for ship based measurements and two others for buoy-based measurements. Also a meteorological station for the research vessel was also established.

The LTBP among other subjects focus on the identification of risky areas of pollution through the determination of sediment transport and fate of possible pollutant effluents. The developed regional circulation and sediment transport models **of the River Malagarasi and Lufubu regions serve this purpose**. The model of the south end of the lake also covers the inlet region of the River Kalambo. The results of these studies can be applied to other river mouths too.

Lake Tanganyika is surrounded by high and steep mountains. Gravity winds together with thermal and trade winds create a complicate wind pattern over the lake, where wind direction and magnitude have high temporal and spatial variations. A three-dimensional mesoscale meteorological model **(HIRLAM)** was used to calculate winds over two periods: 2 - 8.04.97 (wet season) and 21 - 28.08.97 (dry season).

The sediment yield from the watershed was estimated from the published literature. There were comparatively good discharge data for the River Malagarasi and scarce and inadequate data for the River Lufubu. The estimations of suspended particulate matter concentration in incoming rivers had been made by an analogue method. For this purpose available sediment discharge rating curves of few small rivers in the basin of River Malagarasi were used. Due to the lack of similar measurements in the southern part of the watershed these estimates were extrapolated to the River Lufubu. In the lake sedimentation fluxes were measured during the dry season of 1997 with sedimentation traps. By this a lower estimate of the sedimentation rate in the lake was obtained. The grain size distribution was determined from the surface sediments samples collected near the three rivers: Ruzisi, Malagarasi and Lufubu.

The hydrodynamic data on water currents, temperature and meteorological variables were collected during the three major expeditions. Two of them were conducted during the wet season. The first one in November 1996 was timed so that the major heating of lake waters had already occurred and the thermal stratification re-established after the dry season. The second

expedition in late April 1997 made it possible to conduct measurements at the end of the wet season before the start of dry season. The third and the most extensive one was conducted at the end of August 1997. At this time the dry season was almost over and the major upwelling and advection of waters from the south already was ceasing. The observational sites during expeditions were selected on the basis of LTR circulation model results and near the river inlets.

The upwelling in the south was observed both in 1996 and 1997, although it was not as extensive as in the year 1993. In Kigoma the thermal stratification was not destroyed at all.

The water temperature data revealed **tilting of thermocline along the main axis of the lake**, which corresponded with the findings of Coulter (1963 and 1968) done more than 30 years ago. Higher temperatures and deeper depth of certain isolines indicated increased heating of waters over the years. The cause of this increase was not studied in the present work, but **the role of climatic change should be studied in future**. The transversal tilting was clear in the Kalemie strait both in the wet season and the dry season as high current speeds were observed. This tilting was obviously connected to the uninodal internal seiching in the lake. The strait is in the vicinity of the seiche node as it was noted by Coulter (1963).

The current measurements revealed high speeds and the variation of the surface currents (down to 20 - 40 m) due to local winds. In several locations (e.q. in Kalemie strait, Kibwesa and near the Lufubu) water flow below this layer had more steady speed and direction and varied on a larger seasonal scale. Due to technical and logistic problems it was possible to deploy ADCP mooring stations only for a short period of time. The longest duration of recorded currents time series was 53 hours. The most powerful ship based ADCP was capable to measure currents at its maximum to the depth of 100 m in the areas with a depth of 600 m. In some test cases it was possible to track the bottom even at a depth of 800 m. The ADCP function is limited by the amount of reflectors and the decay of the bottom tracking beam. The tracking of the ship movement by differential GPs system failed. Still it was possible to collect data from the regions under the special interest in this study, i.e. the shallow areas near the river mouths.

The estimates of baroclinic term in momentum equations during measurement the period were small in comparison with the barotropic one. This fact enabled to neglect the thermal stratification of the water column in flow calculations. **The barotropic flow models** were used to calculate the circulation patterns and their evolution with time. The models are driven by winds calculated with HIRLAM for each hour of the calibration and validation period. High spatial resolution of the regional models (from 0.4 km to 5 km) made it possible to describe in detail the dynamics of the flow regime and its effect on transport of suspended matter. To provide a necessary information the lake wide circulation model developed earlier for the LTR project was used to calculate velocities at liquid boundaries of regional models.

The models were validated mainly with the data collected during the last two expeditions. The comparison of the model results with ADCP current measurements shows that the direction of the calculated flows agrees well with the observed ones in the regions of the River Malagarasi in the central part of the lake and near the River Kalambo in the south. The models underestimate the magnitude of the flow. This can be partially explained by high diffusion properties of the implicit integration scheme. The discrepancy can be also due to the smoothed wind fields produced by the HIRLAM model.

In the dry season the discharge of the river waters and suspended particulate matter concentration in river waters is low. The simulations with **regional sediment transport models** showed that in this time the dilution and the advection of river waters happens in the vicinity of the river mouths. Because of the high hydraulic friction the effect of river plumes on currents is negligibly small. Gravitational settling, advective transport by wind-induced currents and turbulent diffusion are the main governing factors generating the zones of higher SPM concentration mainly in shallow areas near river and creek outlets. The great depth of the lake reduces considerably the probability of erosion and resuspension of already settled solid particles to these narrow areas along the lake shore.

Currents directed N - NW near the River Malagarasi mouth determine the prevailing spreading of suspended matter in the same direction. The river plume is attenuated in longitudinal direction. During the wet season the spatial gradients are higher than during the dry season. This is result of a higher incoming SPM concentration and inflow velocities. But due to the similar wind-induced flow patterns in this region the calculated plume has similar elongated shape during both seasons. The SPM plume from the River Lufubu is spreading to a more limited area than from the River Malagarasi. This is due to the deeper bathymetry and expected lower SPM concentration of river waters.

The PC version of **the particle tracking model** (**TANGPATH)** has been developed in addition to the mainframe models. The model incorporates pre-calculated surface and depth-averaged flow fields of the lake wide and regional model. It gives a user the possibility to study the transport of buoyant and settling particles under the different meteorological conditions of the wet and dry seasons. The model requires a standard PC running Windows operating system and has a user-friendly graphical interface. On-line help is provided to navigate easily through different menu options. **The order form including all details is attached at the end of this report.**

There are lots of complex and challenging scientific problems in Lake Tanganyika deserving more consideration. To tackle some of them developed software tools can be extended further. **The oxygen dynamics** is one of the topics yet to be studied. This is possible by adding an additional block to already developed models. The oxygen model should incorporate the processes of aeration at the upper boundary, biological oxygen demand, sediment oxygen consumption and the oxygen input from river waters. Applications of these type of models has a long tradition in Finland and other countries (Bilatedin et al. 1993, Frisk 1989 and Malve et al. 1991).

LTBP studies also the pollution transport in the lake. Problems of lake pollution have been discussed by Baker (1992) and Coulter (1992) in the case of Lake Tanganyika. Baker even made some hypothetical estimates of oil slicks spreading. T**he oil drift modules** can be incorporated in the present modelling system. The various mechanisms determining the spreading of an oil slick are rather intricate. The processes of oil drift by the wind directly and by currents as well as evaporation, agglomeration and sinking of the oil have to be taken in to account in the model calculations (Koponen et al. 1992).

The development of bottom morphology due to wind waves and water current transportation as well as the fate of cohesive sediments deserves further studies. The connection of these phenomena to the transport of nutrients and pollutants attached to the particles is obvious. They are closely linked to the hydrobiology and even fish biology of the lake. The scale of these studies should cover the full range from synoptic to seasonal and finally even to the geological scale.

ACKNOWLEDGEMENTS

References

Anon. 1993. UNDP Regional Project RAF/88/044 Drought monitoring for Eastern and Southern Africa, Drought monitoring Centres Nairobi/Harare 1993, Drought Monitoring Bulletin: nos. 93/7-94/1.

Anon. 1995. The Technical Manual of Acoustic Doppler Current Profiler. RD Instruments. San Diego. USA.

Asnani, G.C. 1993. Tropical Meteorology. 1202 p.

Badenhuizen, G.R. 1964. Lufubu River Research Notes. Fisheries Research Bulletin 1963-64.

Baker, J.M. 1992. Oil and African Great Lake. Mitt. Internat. Verain. Limnol. Vol 23: 71-77.

Beauchamp, R.S.A. 1939. Hydrology of Lake Tanganyika. Internationale Revue der Gesamten Hydrobiologie und Hydrographie, 39 (34):316-353.

Bilaletdin, Ä., Frisk, T. & Huttula T. 1993. Roineen vedenottoalueen veden laadun riippuvuus lähivalumaalueen kuormituksesta ja Längelmäveden vedenlaadusta. (The water quality of Lake Roine and its depedency on the load from water shed and from Lake Längelmävesi). Vesi- ja ympäristöhallituksen monistesarja nro 512. 56 p.

Blumberg, A.F. & Mellor, G.L. 1987. A description of a three-dimensional coastal ocean circulation model. In. Three-dimensional coastal ocean models Ed. N.S.Heaps Series Coastal and Estuarine Sciences 4. AGU Washington D.C.

Bringfelt, B., Gustafsson, N., Vilmusenaho, P. & Järvenoja, S. 1995. Updating of the HIRLAM physiography and climate data base. HIRLAM Technical Report No. 19, Norrköping, June 1995, 42 pp.

Bultot, F. 1965. Evaporation from a tropical lake: comparison of theory with direct measurements - comment. J. Hydrol. 143 (1993) 513-519.

Camus, C. 1965. Fluctuations du niveau du Lac Tanganyika 1965. Bulletin des Séances 1965:4, Academie Royale des Sciences d'Outre-Mer.

Capart, A. 1949. Sondages et carte bathymétrique du Lac Tanganyika. Résultats scientifiques de l'exploration hydrobiologique du Lac Tanganyika (1946-47), Ins. Roy. Sci. Nat. Belg. 2(2): 1-16.

Capart, A. 1952 Le milieu géographique et géophysique. Results Sci. Exploration Hydrobiol. Lac Tanganyika, (1946-47), Ins. Roy. Sci. Nat. Belg. 1: 3-27.

Cheng, K.J. 1984. Bottom-boundary condition for non-equilibrium transport of sediment. Journal of Geophysical Research, Vol.89, No C5:8209-8214.

Coulter, G.W. 1963. Hydrological changes in relation to biological production in southern Lake Tanganyika. Limnol. Oceanogr. 8:463-477

Coulter, G.W. 1967. Hydrological processes in Lake Tanganyika. Fish. Res. Bull. Zam. 4:53-56.

Coulter, G.W. 1968. Hydrological processes and primary production in Lake Tanganyika. Proc. of 11th Conf. Internat. Assoc. Great Lakes Res. 1968:609-626.

Coulter, G.W. 1981. Biomass, production and potential yield of Lake Tanganyika pelagic fish community. Trans. Am. Fisf.Soc., 110:325-335.

Coulter, G.W. (Ed.), 1991. Lake Tanganyika and its Life. Oxford University Press, London, New York, 354p.

Coulter, G.W. & Spiegel, R.H. 1991. Hydrodynamics of Lake Tanganyika. In: Coulter, G.W. (Ed.): Lake Tanganyika and its Life. British Museum (Natural History) and Oxford University Press. New York, 354p.

Coulter, G.W. 1992. Vulnearability of alke Tanganyika to pollution with comments on socaila aspects. Mitt. Internat. Verain. Limnol. Vol. 23: 67-70

Cunge, J.A., Holly, F.M. & Verwey, A. 1980. Practical aspects of computational river hydraulics. Pitman Advanced Publishing Program, London.

Cunnington, W. A. 1920. The fauna of the African Lakes. A study in comparative limnology with special reference to Lake Tanganyika. Proc. Zool. Soc. Lon. 3:507-622.

Degens, E.T., Von Herzen, R.P. & Wong, H.-K. 1971. Lake Tanganyika: water chemistry, sediments, geological structure. Naturwissenchaften, 58: 229-241.

Dubois, J., Th. 1958. Evolution de la temperature de l'oxygene dissous et de la transparence dans la baie Nord du lac Tanganyika. Hydrobiologia. Vol. X, 1958, 215-240.

Dyer, K.R. 1989. Sediment processes in estuaries: a review. Journal of Geophysical Research. Vol. 94, No C10:14,327 - 14,340.

Frisk, T. 1989. Development of mass balance models for lakes. Publications of Water and Env. Research Institute. No 5. Helsinki. Finland. ISBN 951-47-3089-4

Fukuda, M.K. & Lick, W. 1980. The entrainment of cohesive sediments in fresh water. Journal of Geophysical Research, Vol.85:2813-2824.

Hecky, R.E & Bugenyi, F.W.B. 1992. Hydrology and chemistry of the African Great Lakes and water qulaity issues: Problems and solutions. Mitt. Internat. Verain. Limnol. Vol 23: 45-54.

Hecky, R.E. & Kling, H.J. 1981. The phytoplankton and zooplankton of the euphotic zone of Lake Tanganyika: species composition, biomass, chlorophyll content and spatio-temporal distribution. Limnol. Oceanogr., 26: 548-564.

Henderson-Sellers, B. 1984. Engineering Limnology. Pitman Advancing Publishing Program. London.

Hondzo, M., Ellis, C.R. & Stefan, H.G. 1991. Vertical diffusion in a small stratified lake: data and error analysis. J. Hydr. Eng, ASCE, 117(10): 1352-1369.

Horne, A.J. & Goldman, C.R. 1994 (2nd ed.). Limnology, McGraw-Hill, Inc. New York. 576p.

Hutchinson, G.E, 1957. A treatise on limnology. Vol 1, geography, physics and chemistry. Wiley, New York.

Huttula, T., & Krogerus, K. 1986. Water currents and erosion of celluloose fibers in a short term regulated water course. Aqua Fennica 16,2. Helsinki.

Huttula, T., Peltonen, A. & Nieminen, J. 1993. Hydrodynamic measurements on Lake Tanganyika, FAO/FINNIDA Research for the Management of the Fisheries on Lake Tanganyika. GCP/RAF/271/FIN-FM/02 (En): 48p. Bujumbura, Burundi.

Huttula, T. & Podsetchine, V. 1994. Hydrological Modelling on Lake Tanganyika. FAO/FINNIDA Resarch for the Management of the Fisheries on Lake Tanganyika. GCP/RAF/271/FIN-TD/20 (En):19 p. Bujumbura, Burundi

Huttula, T., Podsetchine, V., Peltonen, A., Kotilainen P. & Mölsä H. 1994. Hydrology of Lake Tanganyika. Nordic Hydrological Conference, Torshavn, Faroe Islands. 2-4 August 1994. NHP-report no 34. pp 43-52.

Järvenoja, S., Eerola, K., Lönnberg, P. & Rontu, L. 1997. Limited area modelling at the Finnish Meteorological Institute in 1996. EWGLAM Newsletter No. 26, 58-61.

Koponen, J., Alasaarela,E., Lehtinen, K., Sarkkula, J., Simbierowicz, Vepsä, H. and Virtanen M.. (1992). Modelling the dynamics of large sea area. Publications of Water and Env. Research Institute. No 7. Helsinki. Finland. ISBN 951-47-4284-2

Kotilainen, P. 1993. Field notes for Hydrodynamics. FAO/FINNIDA Research for the Management of the Fisheries on Lake Tanganyika. GCP/RAF/271/FIN-FM/10 (En): 58p, 5 maps, 8 ann. Bujumbura, Burundi.

Kotilainen, P., Huttula, T. & Peltonen, A. 1995. Lake Tanganyika Hydrodynamics (Results of March 1993-December 1994). FAO/FINNIDA Research for the Management of the Fisheries on Lake Tanganyika. GCP/RAF/271/FIN-TD/42 (En). Bujumbura, Burundi.

Kotilainen, P., Huttula, T., Peltonen, A. & Verburg P. 1995. A Recent View to the Meteorology and Hydrodynamics around Lake Tanganyika. Symposium on Lake Tanganyika Research, Kuopio September 11-15, 1995. Abstracts. Kuopio University publications C. Natural and Environmental Sciences 34. 1995.

Källen, E. 1995. Hirlam Documentation Manual - System 2.5, June 1995.

Lavelle, J.W., Mofjeld, H.O. & Baker, E.T. 1984. An in situ erosion rate for a fine-grained marine sediment. Journal of Geophysical Research, Vol.89, No C4:653-6552.

Lick, W. 1982. Entrainment, deposition and transport of fine-grained sediments in lakes. Hydrobiologia, Vol.91:31-40.

Luettich, R., Harleman, A. Jr., D.R.F. & Somlyody, L. 1990. Dynamic behaviour of suspended sediment concentrations in a shallow lake perturbed by a episodic wind events. Limnol. Oceanogr. 35:1050-1067.

Malve, O., Huttula T. & Lehtinen K. 1991. Modelling of Eutrophication and Oxygen Depletation in the Lake Lappajärvi. In: "First Int. Conference on Water Pollution", Southampton Sept. 1991. ISBN 1-85166-697-4 pp. 111-124

Mehta, J. & Parthenaides, E. 1975. An investigation of the depositional properties of flocculated fine sediments. Journ. of Hydraulic Research 13, 4:361-362.

NORCONSULT, 1982. Kigoma water master plan. Volume 7. Hydrology. Oslo.

Parthenaides, E. 1965. Erosion and deposition of cohesive soils. Journal of the Hydraulic division, ASCE, Vol.91, No HY1.

Patankar, S. 1980. Numerical heat transfer and fluid flow. Hemisphere Publishing Corporation, New York.

Patterson, G. (Ed.). 1996. Baseline review: Sediment Discharge and Its Consequences. Report for Lake Tanganyika Biodiversity Project. NRI. UK.

Pessi, A. 1997. Tanganjika-järven ilmasto havaintojen ja HIRLAM-tulosten mukaan. (Climate of Lake Tanganyika region on the basis of observations and HIRLAM application.). University of Helsinki. Department of Meteorology. Report (in Finnish). 34 p.

Pickens, M.K. & Lick, W.J. 1991. The transport and fate of drilling muds. In Proc. of the 2-nd Int. Conf. Estuarine and Coastal Modelling. pp.202 -214.

Plisnier, P.-D., Langenberg, V., Mwape, L., Chitamwembwa, Tsibangu K. & Coenen. 1996. Limnological sampling during an annual cycle at three stations on Lake Tanganyika (1993-94). FAO/FINNIDA Research for the Management of the Fisheries on Lake Tanganyika. GCP/RAF/271/FIN-TD/46 (En). Bujumbura, Burundi.

Podsetchine, V. & Huttula, T. 1994. Modelling sedimentation and resuspension in lakes Water Pollution Research Journal of Canada, Vol. 29, N 2/3. P.309-342.

Podsetchine, V. & Huttula, T. 1995. Hydrological modelling: Activity report for the period of 1.10.-30.11.94. FAO/FINNIDA Research for the Management of the Fisheries on Lake Tanganyika. GCP/RAF/271/FIN-TD/29 (En). Bujumbura, Burundi.

Podsetchine, V. & Huttula, T. 1996. Hydrological modelling: Activity report for the period of 1.4.-30.09.95. FAO/FINNIDA Research for the Management of the Fisheries on Lake Tanganyika. GCP/RAF/271/FIN-TD/45 (En). Bujumbura, Burundi.

Podsetchine, V., Huttula, T. & Savijärvi, H. 1995. DEVELOPMENT OF A 3D NUMERICAL UPWELLING MODEL FOR LAKE TANGANYIKA. Symposium on Lake Tanganyika Research, Kuopio September 11-15, 1995. Abstracts. Kuopio University publications C. Natural and Environmental Sciences 34. 1995.

Podsetchine, V., Huttula, T. & Savijärvi, H. 1996. Modelling of hydrodynamical regime of Lake Tanganyika. In: Proc. of the second Int. Conf. of Hydrodynamics. Hong Kong 16-19 December 1996. ISBN90 5410 860 6. pp. 661-666.

Raudkivi, A.J. 1990. Loose boundary hydraulics. Third edition. Pergamon Press, Oxford.

Savijärvi, H. 1995. Sea-breeze effects on large-scale atmospheric flow. Contrib. Atmos. Physics, V.68. P.281-292.

Savijärvi, H. 1997. Diurnal winds around Lake Tanganyika. Q. J. R. Meteorol. Soc. Vol.123, P.901-918.

Servais, F. 1957. Etude théorique des oscillations libres (séiches) du Lac Tanganyika. Résultats scientifiques de l'exploration hydrobiologique du Lac Tanganyika (1946-47), Ins. Roy. Sci. Nat. Belg. 2(3): 1-311.

Sheng, Y.P. & Lick, W. 1979. The transport and resuspension of sediments in shallow lake. Journal of Geophysical Research, Vol.84, No C4:1809-1826.

Sheng, Y.P., Eliason, D.E. & Chen X.-J. 1991. Modelling three-dimensional circulation and sediment transport in lakes and estuaries. In Proc. of the 2-nd Int. Conf. Estuarine and Coastal Modelling. pp.105 -115.

Stappers, L. 1914. Recherches bathymétriques sur les Lacs Moero et Tankanyika. An. Biol. Lac, Bruxelles, 7:83-114.

Tabata , M. 1977. A finite element approximation corresponding to the upwind finite differencing. Mem. Numer. Math., 4, 46 - 63.

Tanguy, J.M., Frenette, R. & Dhatt G. 1991. Comparison of numerical methods in sediment transport. In Proc. of Int. Symp. on The transport of suspended sediments and its mathematical modelling, Florence, Italy, September 2-5, 1991:571-585.

Tietze, Kl. 1982. Results of the Lake Tanganyika investigations in December, 1981. Bundesanstalt fur Geowissenschaften und Rohstoffe, Hannover. Memo no: 93356.

Vandelannoote, A., Deelstra, H. & Ollevier, F. 1995. The inflow of the river Rusizi to Lake Tanganyika. In: Mölsä, H. (ed.) Symposium on Lake Tanganyika Research September 11 - 15, 1995 Kuopio, Finland. Abstracts. Department of Applied Zoology and Veterinary Science. University of Kuopio, Finland.

Vandelannote, A., Deelstra, A., & Ollevier. 1997. The inflow of the Rusizi River to Lake Tanganyika. Subimitted to be published: In Mölsä et al. (eds.): Lake Tanganyika: Its water and pelagic fish. Special Volume of Hydrobiologia by Kluwer Publishers (In preparation).

Van Meel, L.I. . 1987. Contribution a la Limnomlogie de quatre Grands Lac du Zaïre oriental: Tanganyika, Kivu, Mobutu Sese Seko (ex Albert) Idi Amin Dada (ex Edouard) d'après des notes et des ébauches inédites de J.Kufferath. Documents de travail no. 41, Fascicule A: Le Lac Tanganyika 1, Institut Royale Sciences Naturelles de Belgique. 118p.

Van Rijn, L.C. 1984. Sediment transport, part II: Suspended load transport. Journal of Hydraulic Engineering, Vol.110, No 11.

Van Rijn, L.C. 1990. Handbook sediment transport by current and waves. Second edition. Delft Hydraulics.

Van Well, P. & Chapman, D.W. 1976. Summary of limnological observations in Lake Tanganyika near Kigoma 1974-75. FI:DP/URT/71/012/39, F.A.O., Rome, 17 pp.

Verburg, P., Huttula T., Kakogozo, B., Kihakwi, A., Kotilainen, P., Makasa, L. and Peltonen A. 1997: Hydrodynamics of Lake Tanganyika and meteorological results. FAO/FINNIDA Research for the Management of the Fisheries on Lake Tanganyika. GCP/RAF/271/FIN-TD/59 (En). Bujumbura, Burundi.

Verburg, P., Huttula T., Kakogozo, B., Kihakwi, A., Kotilainen, P., Makasa, L. and Peltonen A. 1997b: Diurnal variation of meteorological variables on Lake Tanganyika. FAO/FINNIDA Research for the Management of the Fisheries on Lake Tanganyika. (Manuscript). Bujumbura, Burundi.

Verkfrtðistofan, Vatnaskil hf. 1993. Mývatn. Lake circulation and sediment transport. Mininstry of Environment, Iceland.

Appendix 1. A list of acronyms and contributors with their affiliations

Acronyms

FAO	= Food and Agriculture Organization of United Nations
UNDP	= United Nations Development Program
NRI	= Natural Resources Institute
	and in association
	MRAG = Marine Resources Assessment Group
	IFE = Institute of Freshwater Ecology
HIRLAM	= High Resolution Limited Area Model
IAA	= Inter Agency Agreement
REAH	= Regional Environmental Agency of Häme
LTR	= Lake Tanganyika Research
LTBP	= Lake Tanganyka Biodiversity Project
UNOPS	= United Nations Operational Project Service
UN	= United Nations
ADCP	= Acoustic Doppler Current Profiler
MSL	= Mean Sea Level
SPM	= Suspendid particulate matter
FINNIDA	= Finnish International Development Agency
CTD	= Conductivity Temperature and Disolved Oxygen Profiler
IDL-graphics	= Interactive Data Language
GPS	= Global Positioning System
DGPS	= Differential Global Positioning System

Contributors with their affiliations

Hannu Mölsä and
Voitto Tuomainen
University of Kuopio, Department of Applied Zoology and Veterinary Science, POB 1627, Kuopio, Finland

Timo Huttula,
Anu Peltonen and
Victor Podsetchine
Regional Environmental Agency of Häme, POB 297, 33101 Tampere, Finland

Pekka Kotilainen,
Bombi Kagokozo and
Jean-Marie Tumba
FAO Research for the Management of the Fisheries on Lake Tanganyika, POB 1250, Bujumbura, Burundi

Piet Verburg and
Aderico Kihakwi
FAO Research for the Management of the Fisheries on Lake Tanganyika, POB 90, Kigoma, Tanzania

Lawrence Makasa
FAO Research for the Management of the Fisheries on Lake Tanganyika, POB 55, Mpulungu, Zambia

Hannu Savijärvi
University of Helsinki, Department of Meteorology, POB 4 (Yliopistonkatu 3), 00014 University of Helsinki, Finland

Simo Järvenoja
Finnish Meteorological Insitute, POB 503, 00101 Helsinki, Finland

Appendix 2. Used recourses (m/m) in developing the IAA GEF-LT circulation model and related activities during the years 1996-97. AF = Academy of Finland, UKU = University of Kuopio, Other = funding from Ministry of Labour, Finland and from REAH

	IAA	AF	UKU	Other
Co-ordinator			1	
Scientific co-ordinator	6			1
Field co-ordinator	2			
Data collection on field				
- expert in hydrodynamics	16			
- national hydrologists	45			
Expeditions				
- senior researcher	1			
- electric engineer	3			
Data analysis in REAH				
- senior researcher	3	6	2	
- researcher				8
Circulation model development				
- senior researcher	10	3	2	
Total	86	9	4	9

Appendix 4. Collected data in hydrodynamics in March 1993 - May 1997 at LTR stations.

1 9 9 3

STATION	January	February	March	April	May	June	July	August	September	October	November	December
	1 2 3 4	1 2 3 4	1 2 3 4	1 2 3 4	1 2 3 4	1 2 3 4	1 2 3 4	1 2 3 4	1 2 3 4	1 2 3 4	1 2 3 4	1 2 3 4

1. Bujumbura

Weather station

Water level

Flow measurements

2. Kigoma

Lake meteto station

Wind station

Water level

Flow measurements

3. Mpulungu

Lake meteo station

Wind station

Water level

Flow measurements

1 9 9 4

STATION	January	February	March	April	May	June	July	August	September	October	November	December
	1 2 3 4	1 2 3 4	1 2 3 4	1 2 3 4	1 2 3 4	1 2 3 4	1 2 3 4	1 2 3 4	1 2 3 4	1 2 3 4	1 2 3 4	1 2 3 4

1. Bujumbura

Weather station

Water level

Flow measurements

2. Kigoma

Lake meteo station

Wind station

Water level

Flow measurements

3. Mpulungu

Lake meteo station

Wind station

Water level

Flow measurements

Appendix 4. Collected data in hydrodynamics in March 1993 - May 1997 at LTR stations.

1 9 9 5

STATION	January				February				March				April				May				June				July				August				September				October				November				December			
	1	2	3	4	1	2	3	4	1	2	3	4	1	2	3	4	1	2	3	4	1	2	3	4	1	2	3	4	1	2	3	4	1	2	3	4	1	2	3	4	1	2	3	4	1	2	3	4

1. Bujumbura

Weather station

Water level

Flow measurements

2. Kigoma

Lake meteo station

Wind station

Water level

Flow measurements

3. Mpulungu

Lake meteo station

Wind station

Water level

Flow measurements

1 9 9 6

STATION	January				February				March				April				May				June				July				August				September				October				November				December			
	1	2	3	4	1	2	3	4	1	2	3	4	1	2	3	4	1	2	3	4	1	2	3	4	1	2	3	4	1	2	3	4	1	2	3	4	1	2	3	4	1	2	3	4	1	2	3	4

1. Bujumbura

Weather station

Water level

Flow measurements

2. Kigoma

Lake meteo station

Wind station

Water level

Flow measurements

3. Mpulungu

Lake meteo station

Wind station

Water level

Flow measurements

Appendix 4. Collected data in hydrodynamics in March 1993 - May 1997 at LTR stations.

STATION	1 9 9 7 January				February				March				April				May				June				July				August				September				October				November				December			
	1	2	3	4	1	2	3	4	1	2	3	4	1	2	3	4	1	2	3	4	1	2	3	4	1	2	3	4	1	2	3	4	1	2	3	4	1	2	3	4	1	2	3	4	1	2	3	4
1. Bujumbura																																																
Weather station																																																
Water level																																																
Flow measurements																																																
2. Kigoma																																																
Lake meteo station																																																
Wind station																																																
Water level																																																
Flow measurements																																																
3. Mpulungu																																																
Lake meteo station																																																
Wind station																																																
Water level																																																
Flow measurements																																																

Appendix 5. Buoy based ADCP (workhorse) deployments.

SITE	LAT S	LONG E	START DATE	STOP DATE	DEPTH
Utinta	07°06.37	30°28.53	17.11.96 14:20	17.11.96 17:00	70
Lufubu	08°33.71	30°45.21	18.11.96 20:40	19.11.96 08:55	50
Lufubu	08°28.93	30°42.79	18.11.96 21:57	19.11.96 07:50	117
Kibwesa	06°30.41	30°03.03	22.11.96 14:28	22.11.96 18:02	128
Kibwesa	06°28.79	30°07.82	22.11.96 12:54	22.11.96 16:09	112
Malagarasi	05°10.79	29°44.55	25.11.96 14:15	27.11.96 06:14	47
Malagarasi	05°10.50	29°41.61	25.11.96 14:58	27.11.96 06:45	125
Malagarasi	05°10.78	29°44.66	08.04.97 18:00	10.04.97 10:00	38
Malagarasi	05°10.53	29°41.54	08.04.97 18:10	10.04.97 11:00	127
Kalambo	08°35.79	31°10.12	14.04.97 06:00	14.04.97 17:15	39
Kalambo	08°36.10	31°09.60	14.04.97 06:37	14.04.97 16:47	95
Rusizi	03°22.13	29°15.97	21.08.97 14:43	22.08.97 12:26	46
Rusizi	03°24.38	29°15.66	21.08.97 15:16	22.08.97 12:55	108
Malagarasi	05°10.73	29°44.86	25.08.97 14:24	27.08.97 09:52	35
Malagarasi	05°10.65	29°42.50	25.08.97 13:52	27.08.97 09:26	124
Lufubu	08°32.92	30°44.41	30.08.97 17:32	01.09.97 18:00	39
Lufubu	08°32.80	30°44.49	30.08.97 17:53	01.09.97 18:10	95

Appendix 6. CTD stations during expedition 10.

NO	DATE	TIME	LAT S	LON E
1	16.11.96	12:39	06°21.76	29°37.05
3	17.11.96	6:25	07°07.80	30°27.32
4	17.11.96	16:10	07°06.58	30°28.52
5	17.11.96	23:22	08°28.16	30°48.63
6	18.11.96	3:14	08°27.92	30°48.63
7	18.11.96	23:32	08°28.16	30°48.63
8	19.11.96	4:22	08°27.92	30°48.63
9	20.11.96	22:11	08°34.58	31°03.15
11	21.11.96	17:29	07°55.02	30°41.16
12	22.11.96	10:10	06°31.19	30°07.39
13	22.11.96	18:16	06°30.56	30°03.23
14	23.11.96	12:46	05°22.09	29°40.74
16	26.11.96	8:47	05°01.86	29°39.18
17	26.11.96	9:44	05°03.00	29°43.20
18	26.11.96	11:14	05°11.42	29°43.89
19	26.11.96	12:11	05°11.03	29°39.15
20	26.11.96	13:44	05°18.86	29°38.85

Appendix 7. ADCP transects during expedition 10.

LINE	START DATE	START TIME	START LAT, S	START LONG, E	STOP DATE	STOP TIME	STOP LAT, S	STOP LONG, E	RAW DATA FILE	CFG FILE
1	16.11.96	14:50			16.11.96	14:56	06º24.80	29º42.50	ex1004r.80	ex1002.cfg
2	16.11.96	19:30			16.11.96	19:46	06º34.92	30º05.22	ex1008r.000	ex1002d.cfg
3	16.11.96	21:01			16.11.96	21:04	06º35.68	30º12.29	ex10011r.000	ex1002e.cfg
4	16.11.96	21:04	06º35.68	30º12.29	16.11.96	21:23	06º34.76	30º14.50	ex10012r.000	ex100wh.cfg
5	16.11.96	23:35	06º35.64	30º13.85	16.11.96	23:50	06º36.75	30º14.17	ex10014r.000	ex1003.cfg
6	17.11.96	2:55			17.11.96	4:13	06º58.87	30º27.06	ex10015r.000	ex1003b.cfg
7	17.11.96	4:19			17.11.96	5:34	07º06.88	30º27.93	ex10016r.000	ex1003c.cfg
8	17.11.96	9:40	07º08.26	30º25.50	17.11.96	9:44	07º07.96	30º25.81	ex10017r.000	ex1003d.cfg
9	18.11.96	21:09			18.11.96	21:28	08º29.01	30º43.01	ex10024r.000	ex1004b.cfg
10	18.11.96	21:32	08º30.16	30º43.94	18.11.96	21:32	08º29.01	30º43.01	ex10025r.000	ex1004c.cfg
11	18.11.96	22:05	08º28.71	30º42.92	18.11.96	22:55	08º25.60	30º46.46	ex10026r.000	ex1004d.cfg
12	18.11.96	23:00	08º25.85	30º46.67	18.11.96	23:28	08º28.06	30º48.49	ex10027r.000	ex1004e.cfg
13	18.11.96	23:57	08º28.40	30º48.87	19.11.96	0:25	08º30.55	30º50.77	ex10028r.000	ex1004e.cfg
14	19.11.96	0:37	08º31.14	30º49.72	19.11.96	1:29	08º33.35	30º45.12	ex10029r.000	ex1004f.cfg
15	19.11.96	1:38	08º33.10	30º44.72	19.11.96	2:25	08º28.81	30º43.20	ex10030r.000	ex1004g.cfg
16	19.11.96	2:50	08º28.58	30º43.55	19.11.96	3:32	08º25.75	30º46.58	ex10032r.000	ex1004h.cfg
17	19.11.96	3:37	08º28.88	30º46.85	19.11.96	4:05	08º27.92	30º48.63	ex10033r.000	ex1004i.cfg
18	19.11.96	4:45	08º28.29	30º48.91	19.11.96	5:12	08º30.32	30º50.70	ex10034r.000	ex1004i.cfg
19	19.11.96	5:25	08º30.81	30º50.02	19.11.96	6:15	08º33.16	30º45.33	ex10036r.000	ex1004j.cfg
20	19.11.96	6:20	08º33.48	30º45.31	19.11.96	6:21	08º33.68	30º45.25	ex10037r.000	ex1004k.cfg
21	19.11.96	6:33	08º32.81	30º45.01	19.11.96	7:01	08º31.30	30º43.75	ex10038r.000	ex1004l.cfg
22	19.11.96	7:08	08º29.45	30º43.34	19.11.96	7:16	08º28.83	30º42.89	ex10039r.000	ex1004m.cfg
23	19.11.96	7:58	08º29.61	30º43.13	19.11.96	8:44	08º33.45	30º44.10	ex10040r.000	ex1004l.cfg
24	19.11.96	9:15	08º33.46	30º45.54	19.11.96	10:38	08º30.69	30º53.67	ex10041r.000	ex1004m.cfg
25	20.11.96	21:04	08º40.07	31º06.14	20.11.96	22:02	08º34.76	31º03.24	ex10045r.000	ex1005a.cfg
26	20.11.96	23:36	08º33.68	31º02.44	21.11.96	0:08	08º31.94	30º59.92	ex10048r.000	ex1005c.cfg
27	21.11.96	0:17	08º31.35	31º00.06	21.11.96	2:01	08º21.37	31º02.46	ex10049r.000	ex1005d.cfg
28	21.11.96	2:14	08º21.29	31º01.98	21.11.96	5:21	08º35.69	30º48.97	ex10050r.003	ex1005e.cfg
29	21.11.96	5:48	08º34.79	30º49.84	21.11.96	6:50	08º30.17	30º53.88	ex10051r.000	ex1005f.cfg
30	21.11.96	10:22	08º28.56	30º53.95	21.11.96	15:34	07º57.90	30º49.63	ex10053r.005	ex1005h.cfg
31	21.11.96	16:02	07º56.44	30º48.56	21.11.96	16:41	07º55.88	30º44.96	ex10054r.000	ex1005i.cfg
32	21.11.96	16:47	07º55.76	30º44.67	21.11.96	16:55	07º55.62	30º43.98	ex10055r.000	ex1005j.cfg
33	21.11.96	16:57	07º55.59	30º43.78	21.11.96	17:13	07º55.22	30º42.28	ex10056r.000	ex1005k.cfg
34	21.11.96	18:13	07º55.25	30º41.09	21.11.96	18:27	07º54.92	30º39.75	ex10057r.000	ex1005l.cfg
35	21.11.96	18:45	07º53.86	30º39.44	21.11.96	18:50	07º53.49	30º39.36	ex10058r.000	ex1005m.cfg
36	21.11.96	18:52	07º53.39	30º39.35	21.11.96	19:00	07º52.73	30º39.19	ex10059r.000	ex1005n.cfg
37	22.11.96	0:46	07º14.09	30º25.19	22.11.96	5:15	06º49.66	30º22.03	ex10060r.000	ex1005o.cfg
38	22.11.96	6:08	06º47.51	30º22.15	22.11.96	10:05	06º31.66	30º07.92	ex10061r.004	ex1005p.cfg
39	22.11.96	14:41	06º30.96	30º03.25	22.11.96	14:58	06º32.72	30º03.84	ex10070r.000	ex1006a.cfg
40	22.11.96	15:04	06º32.71	30º04.37	22.11.96	15:37	06º31.67	30º07.67	ex10070r.000	ex1006b.cfg
41	22.11.96	15:42	06º31.27	30º07.86	22.11.96	16:00	06º29.56	30º07.53	ex10071r.000	ex1006c.cfg
42	22.11.96	16:05	06º29.18	30º07.66	22.11.96	16:09	06º28.80	30º07.90	ex10072r.000	ex1006d.cfg
43	22.11.96	17:04	06º28.79	30º07.43	22.11.96	17:53	06º30.41	30º03.14	ex10073r.000	ex1006d.cfg
44	22.11.96	18:28	06º30.81	30º02.65	22.11.96	19:46	06º33.67	29º56.17	ex10074r.001	ex1007a.cfg
45	22.11.96	19:54	06º33.60	29º55.20	22.11.96	21:21	06º28.35	29º52.15	ex10075r.000	ex1007b.cfg
46	22.11.96	21:26	06º28.10	29º51.93	22.11.96	22:15	06º26.48	29º50.33	ex10076r.000	ex1007c.cfg
47	22.11.96				22.11.96	23:15	06º22.09	29º47.61	ex10077r.000	ex1007d.cfg
48	23.11.96	1:46	06º08.69	29º40.76	23.11.96	4:11	05º54.97	29º36.28	ex10078r.000	ex1007e.cfg
49	23.11.96	4:23	05º54.49	29º36.80	23.11.96	6:46	05º55.77	29º51.31	ex10079r.000	ex1007f.cfg
50	23.11.96	6:55	05º55.17	29º51.55	23.11.96	11:44	05º25.61	29º43.47	ex10080r.004	ex1007g.cfg

Appendix 7. ADCP transects during expedition 10.

51	23.11.96	11:59	05º24.88	29º42.90	23.11.96	12:28	05º22.39	29º40.77	ex10081r.000	ex1008a.cfg
52	23.11.96	14:59	05º21.68	29º41.21	23.11.96	16:33	05º11.95	29º41.81	ex10082r.001	ex1008b.cfg
53	23.11.96	18:15	05º10.36	29º43.17	23.11.96				ex10086r.000	ex1008f.cfg
54	23.11.96	18:23	05º09.82	29º42.51	23.11.96	18:42	05º08.39	29º40.91	ex10087r.000	ex1008g.cfg
55	23.11.96	18:46	05º08.16	29º40.65	23.11.96	20:11	05º02.29	29º33.56	ex10088r.001	ex1008h.cfg
56	23.11.96	20:57	04º59.36	29º33.63	23.11.96	21:10	04º58.06	29º33.68	ex10089r.000	ex1008i.cfg
57	23.11.96	21:15	04º57.60	29º33.66	23.11.96				ex10090r.000	ex1008j.cfg
58	25.11.96	11:42	05º01.07	29º38.80	25.11.96	12:24	05º05.02	29º40.82	ex10091r.000	ex1009a.cfg
59	25.11.96	12:30	05º05.50	29º41.06	25.11.96	13:16	05º09.94	29º43.28	ex10092r.000	ex1009b.cfg
60	25.11.96	14:20	05º10.86	29º44.27	25.11.96	14:51	05º10.54	29º41.79	ex10093r.000	ex1009c.cfg
61	25.11.96	15:08	05º10.46	29º41.14	25.11.96	15:12	05º10.40	29º40.70	ex10094r.000	ex1009c.cfg
62	25.11.96	15:13	05º10.41	29º40.64	25.11.96	15:15	05º10.38	29º40.33	ex10095r.000	ex1009d.,cfg
63	25.11.96	15:21	05º10.19	29º40.10	25.11.96	16:15	05º04.34	29º40.47	ex10096r.000	ex1009d.cfg
64	25.11.96	16.:17	05º04.13	29º40.47	25.11.96	16:31	05º02.58	29º40.63	ex10097r.000	ex1009f.cfg
65	25.11.96	16:36	05º02.50	29º40.97	25.11.96	17:06	05º02.80	29º44.21	ex10098r.000	ex1009g.cfg
66	25.11.96	17:10	05º02.95	29º44.30	25.11.96	18:20	05º10.52	29º43.80	ex10099r.000	ex1009h.cfg
67	25.11.96	18:25	05º10.60	29º43.41	25.11.96	18:55	05º10.44	29º40.37	ex10100r.000	ex1009i.cfg
68	25.11.96	19:09	05º11.12	29º40.26	25.11.96	20:19	05º18.49	29º39.59	ex10101r.000	ex1009j.cfg
69	25.11.96	20:27	05º18.78	29º40.15	25.11.96	20:38	05º18.77	29º41.40	ex10102r.cfg	ex1009k.cfg
70	25.11.96	20:43	05º18.76	29º41.76	25.11.96	20:55	05º18.75	29º42.99	ex10103r.000	ex1009k.cfg
71	25.11.96	20:57	05º18.75	29º43.19	25.11.96	21:06	05º08.67	29º44.20	ex10104r.000	ex1009l.cfg
72	25.11-96	21:13	05º18.22	29º44.37	25.11.96	21:49	05º14.61	29º44.50	ex10105r.000	ex1009m.cfg
73	25.11.96	21:52	05º14.34	29º44.54	25.11.96	21:59	05º13.49	29º44.58	ex10106r.000	ex1009n.cfg
74	25.11.96	22:20	05º12.19	29º44.36	25.11.96	22:32	05º10.81	29º44.41	ex10107r.000	ex1009o.cfg
75	25.11.96	22:38	05º10.64	29º44.07	25.11.96	23:24	05º10.28	29º39.21	ex10109r.000	ex1010a.cfg
76	25.11.96	23:30	05º09.82	29º39.05	26.11.96	0:42	05º01.98	29º39.15	ex10109r.001	ex1010b.cfg
77	26.11.96	0:51	05º02.03	29º39.82	26.11.96	1:24	05º02.31	29º43.34	ex10110r.000	ex1011o.cfg
78	26.11.96	1:30	05º03.29	29º43.34	26.11.96	1:35	05º03.72	29º43.28	ex10111r.000	ex1010d.cfg
79	26.11.96	1:43	05º04.03	29º43.20	26.11.96	2:48	05º11.84	29º42.62	ex10112r.001	ex1010e.cfg
80	26.11.96	2:53	05º10.96	29º42.19	26.11.96	3:22	05º10.69	29º39.10	ex10113r.000	ex1010f.cfg
81	26.11.96	3:40	05º12.17	29º38.78	26.11.96	4:49	05º18.59	29º40.18	ex10114r.001	ex1010g.cfg
82	26.11.96	4:55	05º18.70	29º40.71	26.11.96	5:18	05º18.80	29º43.05	ex10115r.000	ex1010h.cfg
83	26.11.96	5:24	05º18.27	29º43.20	26.11.96	6:37	05º10.84	29º43.28	ex10116r.002	ex1010i.cfg
84	26.11.96	6:44	05º10.63	29º42.67	26.11.96	7:17	05º10.27	29º39.29	ex10117r.000	ex1010j.cfg
85	26.11.96	7:25	05º09.58	29º39.17	26.11.96	8:36	05º02.02	29º39.10	ex10118r.000	ex1010k.cfg
86	26.11.96	9:04	05º01.85	29º39.52	26.11.96	9:40	05º02.62	29º43.14	ex10119r.000	ex1010l.cfg
87	26.11.96	10:00	05º03.70	29º43.20	26.11.96	10:42	05º08.37	29º43.68	ex10120r.000	ex1010m.cfg
88	26.11.96	10:45	05º08.63	29º43.71	26.11.96	11:00	05º11.20	29º43.88	ex10121r.000	ex1010n.cfg
89	26.11.96	11:24	05º11.38	29º43.45	26.11.96	12:03	05º11.06	29º39.34	ex10122r.000	ex1010o.cfg
90	26.11.96	12:23	05º11.19	29º39.17	26.11.96	13:39	05º18.81	29º38.80	ex10123r.000	ex1010p.cfg
91	26.11.96	14:15	05º18.88	29º39.41	26.11.96	14:52	05º19.02	29º43.30	ex10124r.000	ex1010q.cfg
92	26.11.96	15:07	05º18.88	29º43.74	26.11.96	15:56	05º14.71	29º44.09	ex10125r.000	ex1010r.cfg
93	26.11.96	15:58	05º14.45	29º44.11	26.11.96	16:14	05º12.99	29º44.22	ex10126r.000	ex1010s.cfg
94	26.11.96	16:15			26.11.96	16:32			ex10127r.000	ex1010t.cfg
95	26.11.96	17:26	05º10.77	29º43.80	26.11.96	17:59	05º10.56	29º40.48	ex10129r.000	ex1010u.cfg
96	26.11.96	18:01	05º10.54	29º40.31	26.11.96	18:12	05º10.46	29º39.17	ex10130r.000	ex1010v.cfg
97	26.11.96	18:20	05º10.10	29º38.70	26.11.96	18:33	05º08.71	29º38.77	ex132r.000	ex1010w.cfg
98	26.11.96	19:12	05º07.04	29º38.69	26.11.96	19:23	05º06.15	29º38.73	ex10133r.000	ex1011a.cfg
99	26.11.96	19:27	05º05.91	29º38.72	26.11.96	19:36	05º05.06	29º38.71	ex134r.000	ex1011a.cfg
100	26.11.96	19:40	05º04.94	29º38.71	26.11.96	20:20	05º02.23	29º38.90	ex10135r.000	ex1011b.cfg
101	26.11.96	20:25	05º01.98	29º39.22	26.11.96	21:18	05º02.37	29º43.24	ex10136r.001	ex1011c.cfg
102	26.11.96	21:33	05º03.22	29º43.29	26.11.96	23:09	05º10.55	29º42.95	ex10137r.002	ex1011d.cfg

Appendix 7. ADCP transects during expedition 10.

103	26.11.96	23:15	05°10.61	29°42.58	26.11.96	23:56	05°10.43	29°39.65	ex10138r.000	ex1011e.cfg
104	27.11.96	0:01	05°10.67	29°39.56	27.11.96	1:57	05°18.67	29°39.28	ex10139r.000	ex1011f.cfg
105	27.11.96	2:02	05°18.73	29°39.55	27.11.96	2:39	05°18.69	29°43.17	ex10140.000	ex1011g.cfg
106	27.11.96	2:45	05°18.31	29°43.18	27.11.96	3:26	05°14.23	29°43.13	ex10141.001	ex1010h.cfg
107	27.11.96	3:29	05°13.95	29°43.17	27.11.96	4:01	05°10.91	29°43.19	ex10142r.000	ex1011i.cfg
108	27.11.96	7:04	05°10.29	29°41.75	27.11.96	7:29	05°10.76	29°44.12	ex10143r.000	ex1011j.cfg

Appendix 8. CTD stations during expedition 14.

NO	DATE	TIME	LAT S	LON E
1	8.4.97	6:20	04º49.33	29º24.29
2	8.4.97	19:46	05º02.71	29º41.54
3	8.4.97	21:20	05º02.44	29º46.24
4	9.4.97	2:45	05º17.84	29º35.78
5	9.4.97	4:37	05º16.79	29º41.05
6	9.4.97	9:06	05º02.94	29º42.23
7	9.4.97	10:29	05º02.80	29º37.07
8	9.4.97	19:45	05º16.82	29º41.00
9	9.4.97	21:19	05º17.85	29º35.92
10	10.4.97	3:32	05º02.67	29º42.00
11	10.4.97	4:42	05º02.65	29º37.18
12	10.4.97	23:28	05º25.65	29º32.54
13	11.4.97	1:21	05º25.06	29º37.58
14	11.4.97	2:40	05º24.73	29º72.70
15	11.4.97	6:00	05º40.76	29º44.90
16	11.4.97	9:40	06º00.77	29º42.91
17	11.4.97	12:04	05º57.50	29º38.33
18	11.4.97	13:29	05º55.34	29º34.86
19	11.4.97	14:53	05º54.03	29º32.00
20	11.4.97	16:25	06º01.65	29º27.49
21	11.4.97	18:13	06º04.03	29º32.07
22	11.4.97	19:45	06º06.14	29º36.18
23	11.4.97	21:23	06º08.90	29º41.74
24	11.4.97	22:51	06º13.07	29º41.47
25	12.4.97	0:05	06º14.43	29º36.58
26	12.4.97	10:41	06º31.35	29º56.06
27	12.4.97	12:10	06º36.52	29º55.06
28	12.4.97	13:57	06º42.73	29º54.44
29	12.4.97	15:40	06º48.72	29º55.03
30	12.4.97	17:44	06º47.92	30º03.85
31	12.4.97	20:26	06º46.94	30º13.38
32	12.4.97	22:51	06º47.42	30º22.51
33	12.4.97	0:39	06º54.01	30º24.03
34	13.4.97	2:25	06º59.96	30º26.17
35	13.4.97	4:05	07º05.82	30º28.88
36	13.4.97	5:12	07º08.46	30º26.19
37	13.4.97	7:23	07º21.95	30º23.98
38	13.4.97	10:34	07º40.55	30º36.74
39	13.4.97	12:11	07º38.79	30º39.20
40	13.4.97	13:55	07º51.17	30º42.25
41	13.4.97	15:30	07º49.82	30º45.54
42	13.4.97	18:26	08º12.97	30º46.91
43	13.4.97	20:16	08º10.70	30º51.60
44	13.4.97	21:30	08º09.00	30º55.44
45	13.4.97	23:27	08º19.46	31º00.75
46	14.4.97	2:02	08º26.67	31º07.15
47	14.4.97	3:58	08º33.92	31º04.30
48	14.4.97	20:15	08º34.01	31º04.54

Appendix 8. CTD stations during expedition 14.

49	14.4.97	21:26	08º38.91	31º01.78
50	14.4.97	22:27	08º42.86	31º00.06
51	15.4.97	0:29	08º33.57	31º01.30
52	15.4.97	2:18	08º26.62	31º01.20
53	15.4.97	4:15	08º19.34	31º00.95
54	15.4.97	5:32	08º22.91	31º56.40
55	15.4.97	7:27	08º27.76	31º51.15
56	15.4.97	9:17	08º33.06	31º47.48
57	15.4.97	13:05	08º31.15	31º50.95
58	15.4.97	14:26	08º33.76	31º45.35
59	15.4.97	20:38	08º27.05	31º28.20
60	15.4.97	22:14	08º24.38	31º35.45
61	16.4.97	0:55	08º22.63	30º44.94
62	16.4.97	3.03	08º12.81	30º46.88
63	16.4.97	5:00	08º09.04	30º55.56
64	16.4.97	8:45	07º53.24	30º36.05
65	16.4.97	12:32	07º21.84	30º23.97
66	16.4.97	17:37	06º49.50	29º59.93
67	16.4.97	21:50	06º14.47	29º36.65
68	16.4.97	0:17	05º55.15	29º32.75
69	17.4.97	2:47	05º40.68	29º45.02
70	17.4.97	5:24	05º25.89	29º33.07
71	17.4.97	7:14	05º18.05	29º30.37
72	17.4.97	9:47	04º49.16	29º24.14

Appendix 9. ADCP transects during expedition 14.

LINE	START DATE	START TIME	START LAT, S	START LONG, E	STOP DATE	STOP TIME	STOP LAT, S	STOP LONG, E	RAW DATA FILE	CFG FILE
1	8.4.97	18:30	05º03.34	29º41.44	08.4.97	19:43	05º02.71	29º41.54	cra003r.000	cr14as03.cfg
2	8.4.97	20:26	05º03.03	29º72.25	08.4.97	20:32			c14a004r.000	cr14as03.cfg
3	8.4.97	20:35	05º02.22	29º42.19	08.4.97	21:12			c14as05r.000	cr14as05.cfg
4	8.4.97	20:55	05º02.32	29º44.34	08.4.97	21:12	05º02.39	29º46.24	c14a006r.000	cr14as05.cfg
5	8.4.97	22:56	05º03.03	29º42.25	09.4.97	0:15	510.44	29º41.71	c14a010r.000	cr14as07.cfg
6	9.4.97	0:20	05º10.42	29º41.15	09.4.97	1:08	05º10.42	29º36.68	c14a011r000	cr14as08.cfg
7	9.4.97	1:11	05º10.54	29º36.49	09.4.97	1:36	05º13.12	29º36.32	c14a012r.000	cr14as12.cfg
8	9.4.97	1:41	05º13.33	29º36.33	09.4.97	2:00	05º15.00	29º36.30	c14a013r.000	cr14as13.cfg
9	9.4.97	2:05	05º13.53	29º36.26	09.4.97	2:10	05º15.94	29º36.26	c14a015r.000	cr14as14.cfg
10	9.4.97	2:12	05º16.09	29º36.22	09.4.97	2:32	05º17.85	29º36.06	c14a016r.000	cr14as15.cfg
11	9.4.97	3:33	05º17.87	29º36.06	09.4.97	6:40	05º13.15	29º41.31	c14a001r000	cr14cpi.cfg
12	9.4.97	6:40	05º13.15	29º41.31	09.4.97	9:06	05º02.82	29º42.19	c14a002r000	cr14cp2.cfg
13	9.4.97	9:06	05º02.82	29º42.19	09.4.97	11:05	05º10.76	29º43.30	c14a003r000	cr14cp3.cfg
14	9.4.97	11:05	05º10.76	29º43.30	09.4.97	14:30	05º10.76	29º44.30	c14b004r000	cr14p5.cfg
15	9.4.97	14:30	05º10.76	29º44.30	09.4.97	16:20	05º11.95	29º44.37	c14b005r000	cr147.cfg
16	9.4.97	16:20	05º11.95	29º44.37	09.4.97	16:49	05º14.21	29º42.66	c14b006r000	cr14p8.cfg
17	9.4.97	16:49	05º14.21	29º42.66	09.4.97	20:20	05º16.81	29º39.95	c14b007r000	cr14p9.cfg
18	9.4.97	20:20	05º16.81	29º39.95	09.4.97	20:40	05º17.08	29º38.47	c14b008r000	cr14p10.cfg
19	9.4.97	20:43	05º17.14	29º38.24	09.4.97	20:59	05º17.42	29º37.13	c14b009r000	cr14p11.cfg
20	9.4.97	21:00	05º17.48	29º36.98	09.4.97	22:10	05º16.77	29º35.96	c14b010r000	cr14p12.cfg
21	9.4.97	22:12	05º16.63	29º36.00	09.4.97	23:25	05º10.63	29º36.48	c14b011r000	cr14p13.cfg
22	9.4.97	23:32	05º10.45	29º36.89	10.4.97	0:18	05º10.34	29º40.30	c14b012r000	cr14p14.cfg
23	10.4.97	0:21	05º10.34	29º40.47	10.4.97	0:35	05º10.43	29º41.66	c14b013r000	cr14p15.cfg
24	10.4.97	0:40	05º10.31	29º41.89	10.4.97	3:33	05º02.66	29º41.89	c14b014r000	cr14p16.cfg
25	10.4.97	3:38	05º02.54	29º41.67	10.4.97	7:01	05º10.40	29º36.70	c14b015r001	cr14p17.cfg
26	10.4.97	8:45	05º10.42	29º42.83	10.4.97				c14b016r001	cr14p17.cfg
27	11.4.97	1:21	05º25.04	29º37.55	11.4.97	1:33	05º24.97	29º37.87	c14b018r000	cr14p19.cfg
28	11.4.97	1:33	05º24.97	29º37.87	11.4.97	2:25	05º24.72	29º42.24	c14b019r000	cr14p20.cfg
29	11.4.97	2:25	05º24.72	29º42.24	11.4.97	4:05	05º27.33	29º43.70	c14b020r000	cr14p22.cfg
30	11.4.97	8:59	06º01.15	29º43.01	11.4.97	10:50	06º00.91	29º42.93	c14b021r000	cr14p23.cfg
31	11.4.97	10:50	06º00.91	29º42.93	11.4.97	11:53	05º57.76	29º38.98	c14b022r000	cr14p23.cfg
32	11.4.97	11:55	05º57.65	29º38.73	11.4.97	12:05	05º57.51	29º38.34	c14b023r000	cr14p24.cfg
33	11.4.97	12:06	05º57.52	29º38.35	11.4.97	12:25	05º57.55	29º38.46	c14b024r000	cr14p25.cfg
34	11.4.97	12:26	05º57.49	29º38.49	11.4.97	13:16	05º59.61	29º35.43	c14b025r.000	cr14p26.cfg
35	11.4.97	13:18	05º55.50	29º35.26	11.4.97	13:58	05º54.80	29º33.86	c14b026r.000	cr14p27.cfg
36	11.4.97	14:06	05º54.57	29º33.34	11.4.97	14:19	05º54.19	29º32.36	c14b027r.000	cr14p28.cfg
37	11.4.97	14:24	05º54.19	29º32.36	11.4.97	14:28	05º53.98	29º32.02	c14b028r.000	cr14p29.cfg
38	11.4.97	14:28	05º53.98	29º32.02	11.4.97	14:28	05º53.98	29º32.02	c14b029r.000	cr14p30.cfg
39	11.4.97	17:18	06º01.77	29º28.20	11.4.97	17:28	06º01.77	29º28.20	c14b030r.000	cr14p31.cfg
40	11.4.97	17:32	06º02.26	29º29.04	11.4.97	17:37	06º02.45	29º29.36	c14b031r.000	cr14p32.cfg
41	11.4.97	17:45	06º02.81	29º29.98	11.4.97	17:54	06º03.22	29º30.63	c14b032r.000	cr14p33.cfg
42	11.4.97	17:57	06º03.33	29º30.80	11.4.97	18:44	06º04.03	29º32.07	c14b033r.000	cr14p34.cfg
43	11.4.97	20:46	06º07.57	29º39.21	11.4.97	22:30	06º13.04	29º41.44	c14b034r.000	cr14p36.cfg
44	12.4.97	10:19	06º29.98	29º56.74	12.4.97	11:18	06º32.54	2958.59?	c14b035r.000	cr14p37.cfg
45	12.4.97	11:21	06º32.67	29º55.56	12.4.97	16:13	06º48.47	29º56.53	c14b036r.000	cr14p38.cfg
46	12.4.97	16:14	06º48.47	29º56.53	12.4.97	20:39	06º46.71	30º12.97	c14b037r.000	cr14p39.cfg
47	12.4.97	20:44	06º46.72	30º13.12	12.4.97	23:04	06º47.29	30º22.41	c14b038r.000	cr14p39.cfg
48	12.4.97	23:12	06º47.62	30º22.32	13.4.97	4:05	07º05.82	30º28.88	c14b039r.000	cr14p39.cfg
49	13.4.97	4:18	07º05.74	30º28.98	13.4.97	5:15	07º08.46	30º26.19	c14b040r.000	cr14p40.cfg
50	13.4.97	5:15	07º08.46	30º26.19	13.4.97	5:18	07º08.46	30º26.19	c14b041r.000	cr14p41.cfg

Appendix 9. ADCP transects during expedition 14.

51	13.4.97	11:16	07º39.93	30º36.62	13.4.97	12:13	07º38.75	30º39.20	c14b042r.000	cr14p42.cfg
52	13.4.97	14:35	07º50.58	30º42.33	13.4.97	15:36	07º49.74	30º45.59	c14b043r.000	cr14p43.cfg
53	13.4.97	19:18	08º12.58	30º46.77	13.4.97	21:43	08º09.00	30º55.98	c14b044r.000	cr14p44.cfg
54	14.4.97	0:09	08º19.45	31º00.48	14.4.97	2:12			c14b045r.000	cr14p45.cfg
55	14.4.97	8:02	08º43.11	31º07.74	14.4.97	8:14	08º44.03	31º07.29	c14b046r.000	cr14p46.cfg
56	14.4.97	18:15	08º35.89	31º10.07	14.4.97	20:15	08º34.01	31º04.53	c14b047r.000	cr14p47.cfg
57	14.4.97	20:15	08º34.02	31º04.53	14.4.97	20:36	08º34.93	31º04.01	c14b049r.000	cr14p48.cfg
58	14.4.97	20:36	08º34.93	31º04.01	15.4.97	3:25	08º23.11	31º01.10	c14b049r.000	cr14p48.cfg
59	15.4.97	3:28	08º22.80	31º01.11	15.4.97	11:15	08º30.13	31º54.43	c14b050r.000	cr14p49.cfg
60	15.4.97	11:17	08º30.13	31º54.43	15.4.97	12:20	08º30.18	31º53.51	c14b051r.000	cr14p49.cfg
61	15.4.97	12:26	08º30.35	31º52.96	15.4.97	14:40	08º33.68	30º44.67	c14b052r.000	cr14p50.cfg
62	15.4.97	18:45	08º30.31	31º37.55	15.4.97	21:17	08º26.71	30º29.34	c14b053r.000	cr14p51.cfg
63	15.4.97	21:17	08º26.71	30º29.34	16.4.97	0:01	08º25.36	30º40.74	c14b054r.000	cr14p51.cfg
64	16.4.97	0:11	08º24.89	30º41.62	16.4.97	0:44	08º22.69	30º44.78	c14b055r.000	cr14p52.cfg
65	16.4.97	0:51	08º22.63	30º44.89	16.4.97	3:03	08º12.81	30º46.84	c14b056r.000	cr14p53.cfg
66	16.4.97	3:06	08º12.79	31º46.88	16.4.97	3:23	08º12.51	30º47.06	c14b057r.000	cr14p54.cfg
67	16.4.97	3:24	08º12.51	30º47.06	16.4.97	5:00	08º09.04	30º55.36	c14b058r.000	cr14p55.cfg
68	16.4.97	5:00	08º09.04	30º55.36	16.4.97	5:37	08º09.42	30º53.37	c14b059r.000	cr14p56.cfg
69	16.4.97	5:37	08º09.42	30º53.37	16.4.97	5:53	08º08.92	30º54.11	c14b060r.000	cr14p57.cfg
70	16.4.97	5:53	08º08.92	30º54.11	16.4.97	5:55	08º08.92	30º54.11	c14b061r.000	cr14p58.cfg

Appendix 10. CTD stations during expedition 16.

NO	DATE	TIME	LAT S	LON E
1	21.8.97	14:56	03º22.13	29º15.98
2	21.8.97	15:27	03º24.33	29º15.72
3	21.8.97	16:39	03º24.06	29º17.86
4	21.8.97	17:13	03º22.32	29º17.57
5	21.8.97	18:20	03º22.28	29º14.50
6	21.8.97	20:33	03º24.18	29º17.75
7	21.8.97	21:28	03º22.30	29º17.34
8	21.8.97	22:20	03º22.36	29º14.48
9	21.8.97	22:57	03º24.44	29º14.52
10	22.8.97	12:20	03º25.63	29º15.36
11	22.8.97	14:37	03º25.05	29º19.26
12	22.8.97	15:31	03º28.12	29º19.04
13	22.8.97	16:23	03º28.01	29º16.01
14	22.8.97	17:18	03º30.94	29º16.07
15	22.8.97	18:35	03º30.06	29º19.03
16	22.8.97	20:50	03º44.98	29º19.03
17	22.8.97	22:19	03º45.05	29º14.31
18	22.8.97	23:50	03º44.96	29º09.69
19	23.8.97	2:45	03º59.12	29º22.77
20	23.8.97	4:00	04º01.15	29º19.44
21	23.8.97	5:20	04º01.66	29º15.45
22	23.8.97	8:51	04º19.58	29º18.72
23	23.8.97	11:39	04º19.56	29º26.34
24	23.8.97	13:12	04º19.59	29º33.20
25	24.8.97	12:29	04º49.56	29º34.01
26	24.8.97	15:18	04º48.30	29º24.55
27	25.8.97	13:30	05º10.08	29º41.05
28	25.8.97	15:19	05º10.80	29º41.56
29	25.8.97	17:26	05º02.87	29º43.02
30	25.8.97	19:02	05º02.97	29º37.02
31	25.8.97	21:06	05º10.88	29º36.06
32	25.8.97	22:30	05º10.75	29º41.72
33	25.8.97	23:55	05º16.67	29º40.67
34	26.8.97	1:14	05º16.59	29º35.28
35	26.8.97	2:46	05º10.87	29º36.22
36	26.8.97	4:13	05º10.85	29º41.59
37	26.8.97	5:58	05º03.06	29º42.75
38	26.8.97	7:18	05º02.81	29º36.99
39	26.8.97	9:10	05º10.84	29º36.30
40	26.8.97	10:39	05º10.81	29º41.67
41	26.8.97	11:56	05º16.53	29º40.68
42	26.8.97	13:17	05º16.58	29º35.31
43	26.8.97	15:02	05º10.80	29º36.33
44	26.8.97	16:21	05º10.72	29º41.79
45	26.8.97	18:24	05º03.00	29º42.70
46	26.8.97	19:46	05º02.93	29º30.98
47	26.8.97	21:44	05º10.71	29º36.21
48	26.8.97	23:02	05º10.68	29º41.70

Appendix 10. CTD stations during expedition 16.

49	27.8.97	0:34	05º16.64	29º40.64
50	27.8.97	1:50	05º16.52	29º35.22
51	27.8.97	3:46	05º10.81	29º36.25
52	27.8.97	5:10	05º10.63	29º41.77
53	27.8.97	6:55	05º02.91	29º42.67
54	27.8.97	23:45	05º50.71	29º24.71
55	28.8.97	1:37	05º53.90	29º31.42
56	28.8.97	3:43	05º58.50	29º38.73
57	28.8.97	5:11	06º00.77	29º43.33
58	28.8.97	9:13	06º31.51	29º57.19
59	28.8.97	11:11	06º37.35	29º57.31
60	28.8.97	13:32	06º45.99	29º55.26
61	28.8.97	15:06	06º49.98	29º54.87
62	28.8.97	17:34	06º49.75	30º04.19
63	28.8.97	19:19	06º49.03	30º10.48
64	28.8.97	22:41	06º48.31	30º22.10
65	29.8.97	1:20	06º57.75	30º26.67
66	29.8.97	3:14	07º05.84	30º28.50
67	29.8.97	16:21	07º09.14	30º22.25
68	29.8.97	18:20	07º12.41	30º15.67
69	29.8.97	19:45	07º14.14	30º11.48
70	29.8.97	21:20	07º19.83	30º11.44
71	30.8.97	4:48	08º09.61	30º55.69
72	30.8.97	6:12	08º10.66	30º53.44
73	30.8.97	8:01	08º12.36	30º46.93
74	30.8.97	10:03	08º15.07	30º40.12
75	30.8.97	12:35	08º23.67	30º35.97
76	30.8.97	13:59	08º25.33	30º28.58
77	30.8.97	18:20	08º32.64	30º45.25
78	30.8.97	19:33	08º29.99	30º48.52
79	30.8.97	21:40	08º25.67	30º54.23
80	30.8.97	23:28	08º21.11	30º59.23
81	31.8.97	2:09	08º26.56	31º06.87
82	31.8.97	4:05	08º33.74	33º01.54
83	31.8.97	6:00	08º39.48	30º56.18
84	1.9.97	22:49	07º49.78	30º44.78
85	2.9.97	0:40	07º51.53	30º39.78
86	2.9.97	2:40	07º40.67	30º35.76
87	2.9.97	4:26	07º38.63	30º39.45
88	2.9.97	7:05	07º24.54	30º21.90
89	2.9.97	17:42	06º27.78	29º41.76
90	2.9.97	20:54	06º06.81	29º24.98
91	2.9.97	22:51	06º06.01	29º19.34
92	3.9.97	0:45	05º55.80	29º18.37
93	3.9.97	2:08	05º56.29	29º25.05
94	3.9.97	5:38	05º40.26	29º45.13
95	3.9.97	7:54	05º40.27	29º52.83
96	4.9.97	17:20	04º56.99	29º33.49
97	4.9.97	19:30	04º59.11	29º26.31

Appendix 10. CTD stations during expedition 16.

98	4.9.97	21:22	04º58.94	29º25.67
99	4.9.97	22:19	05º01.01	29º19.09
100	4.9.97	23:10	05º00.77	29º20.82

Appendix 11. ADCP transects during expedition 16.

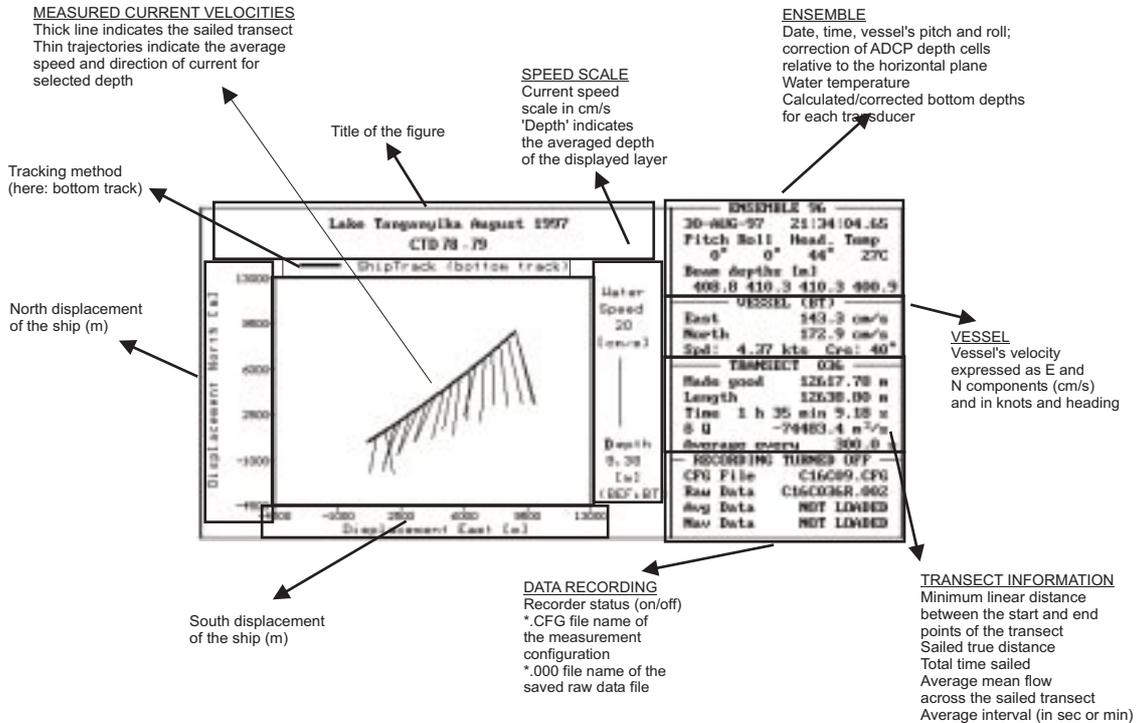| LINE	START DATE	START TIME	START LAT, S	START LONG, E	STOP DATE	STOP TIME	STOP LAT, S	STOP LONG, E	RAW DATA FILE	CFG FILE
1	21.8.97	16:13	03°23.95	29°16.95	21.8.97	16:26	03°24.32	29°17.53	cr16001r.000	cr1601.cfg
2	21.8.97	16:28	03°24.32	29°17.72	21.8.97	17:09	03°22.48	29°17.58	cr16002.000	cr1602.cfg
3	21.8.97	17:22	03°22.09	29°17.64	21.8.97	18:16	03°22.32	29°14.53	cr16003.000	cr1602.cfg
4	21.8.97	18:33	03°22.22	29°14.62	21.8.97	18:42	03°22.46	29°14.49	cr16004.000	cr1602.cfg
5	21.8.97	18:42	03°22.46	29°14.49	21.8.97	19:42	03°24.52	29°14.48	cr16005.000	cr1602.cfg
6	21.8.97	19:40	03°24.68	29°14.75	21.8.97	20.31	03°24.16	29°17.54	cr16006.000	cr1602.cfg
7	21.8.97	20:52	03°24.18	29°17.79	21.8.97	21:21	03°22.45	29°17.45	cr16007.000	cr1602.cfg
8	21.8.97	21:40	03°22.35	29°17.27	21.8.97	22:17	03°22.39	29°14.55	cr16008.000	cr1602.cfg
9	21.8.97	22:29	03°22.50	29°14.34	21.8.97	22:53	03°24.28	29°14.50	cr16009.000	cr1602.cfg
10	21.8.97	23:10	03°24.42	29°14.52	21.8.97	23:54	03°24.51	29°17.64	cr16010.000	cr1602.cfg
11	22.8.97	13:51	03°25.95	29°15.65	22.8.97	14:32	03°25.01	29°19.15	cr16011.000	cr1603.cfg
12	22.8.97	14:53	03°25.70	29°19.30	22.8.97	15:26	03°28.07	29°19.01	cr16012.000	cr1603.cfg
13	22.8.97	15:38	03°28.16	29°19.13	22.8.97	16:20	03°27.96	29°16.03	cr16013.000	cr1604.cfg
14	22.8.97	16:24	03°27.89	29°16.11	22.8.97	16:46	03°28.71	29°16.14	cr16014.000	cr1605.cfg
15	22.8.97	16:48	03°29.02	29°16.16	22.8.97	17:13	03°30.95	29°16.01	cr16015.000	cr1606.cfg
16	22.8.97	17:58	03°30.38	29°16.38	22.8.97	18:32	03°30.95	29°18.96	cr16016.000	cr1606.cfg
17	22.8.97	21:15	03°44.88	29°19.10	22.8.97	21:45			cr16017.000	cr1606.cfg
18	22.8.97	21:47	03°44.77	29°16.55	22.8.97	22:15	03°44.96	29°14.46	cr16018.000	cr1607.cfg
19	22.8.97	22:40	03°44.97	29°14.33	22.8.97	22:48			cr16019.000	cr1607.cfg
20	23.8.97	3:12	03°59.21	29°22.57	23.8.97	3:58	04°01.16	29°19.49	cr16020.000	cr1608.cfg
21	23.8.97	4:24	04°01.24	29°19.03	23.8.97	5:17	04°01.68	29°15.51	cr16021.000	cr1608.cfg
22	23.8.97	5:42	04°02.63	29°15.47	23.8.97	6:21	04°05.07	29°15.81	cr16022.000	cr1609.cfg
23	23.8.97	6:33	04°05.85	29°16.09	23.8.97	6:45	04°06.72	29°16.19	cr16023.000	cr1610.cfg
24	23.8.97	6:48	04°06.94	29°16.17	23.8.97	6:57	04°07.52	29°16.26	cr16024.000	cr1611.cfg
25	23.8.97	7:02	04°07.84	29°16.36	23.8.97	7:39	04°10.57	29°17.02	cr16025.000	cr1612.cfg
26	23.8.97	9:16	04°19.69	29°18.66	23.8.97	9:19	04°19.73	28°18.87	cr16026.000	cr1613.cfg
27	23.8.97	9:20	04°19.74	29°18.95	23.8.97	9:32			cr16027.000	cr1613.cfg
28	23.8.97	9:33	04°19.75	29°19.78	23.8.97	9:42			cr16028.000	cr1613.cfg
29	23.8.97	9:43	04°19.79	29°20.53	23.8.97	9:55			cr16029.000	cr1613.cfg
30	23.8.97	9:55	04°19.82	29°21.47	23.8.97	10:10	04°19.84	29°22.60	cr16030.000	cr1614.cfg
31	23.8.97	10:11	04°19.84	29°22.63	23.8.97	10:20	04°19.82	29°23.20	cr16031.000	cr1614.cfg
32	23.8.97	10:20	04°19.81	29°23.24	23.8.97	10:24	04°19.79	29°23.56	cr16032.000	cr1614.cfg
33	23.8.97		04°19.79	29°23.56	23.8.97	11:01	04°19.58	29°26.20	cr16033.000	cr1614.cfg
34	23.8.97	11:39	04°19.51	29°26.50	23.8.97	13:10	04°19.57	29°33.90	cr16034.000	cr1615.cfg
35	24.8.97	13:09	04°49.37	29°34.10	24.8.97				c16b002.002	c16b01.cfg
36	24.8.97	13:27	04°49.31	29°32.54	24.8.97				c16b003.000	c16b01.cfg
37	24.8.97	13:52	04°49.09	29°30.60	24.8.97				c16b004.000	c16b02.cfg
38	24.8.97	14:10	04°48.90	29°29.19	24.8.97				c16b005.000	c16b02.cfg
39	24.8.97	14:22	04°48.78	28°28.36	24.8.97					
40	24.8.97	14:46	04°48.53	29°26.41	24.8.97					
41	25.8.97	16:13	05°08.48	29°42.19	25.8.97	17:20	05°03.02	29°42.92	c16m002.000	c16m01.cfg
42	25.8.97	17:39	05°02.90	29°43.50	25.8.97	18:59	05°02.95	29°37.03	c16m003.000	c16m01.cfg
43	25.8.97	19:26	05°03.08	29°37.06	25.8.97	19:57	05°05.56	29°36.79	c16m004.000	c16m01.cfg
44	25.8.97	19:57	05°05.60	29°36.78	25.8.97	21:02	05°10.75	29°36.04	c16m005.000	c16m02.cfg
45	25.8.97	21:22	05°10.75	29°36.10	25.8.97	22:24	05°10.74	29°41.50	c16m006.000	c16m02.cfg
46	25.8.97	22:39	05°10.72	29°41.71	25.8.97	22:43	05°11.00	29°41.72	c16m007.000	c16m03.cfg
47	25.8.97	22:50	05°11.55	29°41.64	25.8.97	23:51	05°16.58	29°46.66	c16m010.000	c16m03.cfg
48	26.8.97	0:09	05°16.70	29°40.85	26.8.97	1:08	05°16.56	29°35.46	c16m011.000	c16m02.cfg
49	26.8.97	1:45	05°16.00	29°35.26	26.8.97	2.42	05°10.91	29°36.17	c16m013.001	c16m04.cfg
50	26.8.97	3:06	05°10.85	29°36.19	26.8.97	3:20	05°10.84	29°37.40	c16m014.000	c16m03.cfg

Appendix 11. ADCP transects during expedition 16.

51	26.8.97	3:24	05º10.84	29º37.73	26.8.97	4:10	05º16.95	29º41.57	c16m015.001	c16m05.cfg
52	26.8.97	4.24	05º10.70	29º41.55	26.8.97	5:55	05º03.19	29º42.74	c16m016.001	c16m01.cfg
53	26.8.97	6:08	05º03.26	29º42.70	26.8.97	7:13	05º02.91	29º37.05	c16m017.001	c16m01.cfg
54	26.8.97	7:34	05º02.84	29º36.68	26.8.97	9:07	05º10.70	29º36.18	c16m018.000	c16m02.cfg
55	26.8.97	9:31	05º10.75	29º36.11	26.8.97	9:42	05º10.81	29º36.89	c16m019.000	c16m02.cfg
56	26.8.97	9:44	05º10.81	29º36.89	26.8.97	10:34	05º10.85	29º41.53	c16m021.000	c16m02.cfg
57	26.8.97	10:50	05º10.84	29º41.63	26.8.97	11:55	05º16.45	29º40.65	c16m022.000	c16m03.cfg
58	26.8.97	12:11	05º16.60	29º40.76	26.8.97	13:14	05º16.50	29º35.39	c16m023.001	c16m02.cfg
59	26.8.97	13:43	05º16.50	29º35.83	26.8.97	14:17	05º13.73	29º35.96	c16m024.000	c1604.cfg
60	26.8.97	14:18	05º13.66	29º36.00	26.8.97	14:54	05º10.82	29º36.31	c16m025.001	c16m02.cfg
61	26.8.97	15:19	05º10.92	29º36.14	26.8.97	16:15	05º10.74	29º41.61	c16m026.001	c16m02.cfg
62	26.8.97	16:52	05º10.94	29º42.27	26.8.97	18:22	05º03.12	29º42.81	c16m027.001	c16m01.cfg
63	26.8.97	18:37	05º02.95	29º42.88	26.8.97	19:44	05º02.91	29º37.06	c16m028.001	c16m01.cfg
64	26.8.97	20:02	05º03.00	29º36.87	26.8.97	21:39	05º10.67	29º36.07	c16m029.002	c16m02.cfg
65	26.8.97	22:03	05º10.57	29º36.26	26.8.97	23:01	05º10.67	29º41.50	c16m030.000	c16m05.cfg
66	26.8.97	23:16	05º10.72	29º41.76	27.8.97	00:13	05º16.53	29º40.71	c16m031.000	c16m03.cfg
67	27.8.97	0:47	05º16.54	29º40.56	27.8.97	1:44	05º16.51	29º35.48	c16m032.001	c16m02.cfg
68	27.8.97	2:18	05º16.26	29º35.16	27.8.97	2:55	05º13.07	29º25.86	c16m033.001	c16m04.cfg
69	27.8.97	2:57	05º12.96	29º35.89	27.8.97	3:21	05º10.85	29º36.24	c16m034.000	c16m02.cfg
70	27.8.97	4:01	05º10.81	29º36.26	27.8.97	5:07	05º10.68	29º41.71	c16m035.001	c16m05.cfg
71	27.8.97	5:26	05º09.96	29º41.82	27.8.97	6:53	05º03.01	29º42.67	c16m036.002	c16m01.cfg
72	27.8.97	7:13	05º03.34	29º42.58	27.8.97	8:31	05º09.46	29º42.58	c16m037.000	c16wa.cfg
73	28.8.97	0:16	05º50.68	29º25.34	28.8.97		05º50.68	29º25.34	c16c001.000	c16c01.cfg
74	28.8.97	0:20	05º50.80	29º25.60	28.8.97	1:13	05º52.94	29º29.66	c16c002.000	c16c01.cfg
75	28.8.97	1:15	05º53.10	29º29.95	28.8.97	1:35	05º53.89	29º31.40	c16c003.000	c16c02.cfg
76	28.8.97	2:05	05º53.88	29º31.57	28.8.97	3:40	05º58.48	29º38.60	c16c004.000	c16c02.cfg
77	28.8.97	4:07	05º58.70	29º38.74	28.8.97	5:07	06º00.74	29º43.19	c16c005.000	c16c02.cfg
78	28.8.97	9:51	06º31.57	29º57.37	28.8.97	9:58	06º32.01	29º57.99	c16c006.000	c16c02.cfg
79	28.8.97	10:00	06º32.05	29º58.12	28.8.97	11:07	06º37.14	29º57.27	c16c007.001	c16c02.cfg
80	28.8.97	11:42	06º37.17	29º57.20	28.8.97	13:26	06º45.04	29º55.27	c16c008.000	c16c02.cfg
81	28.8.97	13:58	06º44.87	29º55.19	28.8.97	15:02	06º49.95	29º54.82	c16c009.001	c16c02.cfg
82	28.8.97	15:44	06º49.82	29º55.30	28.8.97	17:32	06º49.77	30º04.13	c16c010.002	c16c02.cfg
83	28.8.97	18:02	06º49.49	30º04.24	28.8.97	19:18	06º49.01	30º10.48	c16c011.002	c16c02.cfg
84	28.8.97	19:19	06º49.02	30º10.51	28.8.97	22:36	06º48.37	30º21.96	c16c012.002	c16c03.cfg
85	28.8.97	22:51	06º48.38	30º22.04	29.8.97	1:16	06º57.82	30º26.64	c16c013.003	c16c03.cfg
86	29.8.97	1:35	06º57.80	03º26.68	29.8.97	3:14	07º05.83	30º28.46	c16c014.002	c16c04.cfg
87	29.8.97	12:56	07º07.29	30º26.90	29.8.97	13:14	07º07.63	30º25.83	c16c017.000	c16c04.cfg
88	29.8.97	13:17	07º07.70	30º25.62	29.8.97	13:30			c16c018.000	c16c05.cfg
89	29.8.97	15:05	07º06.84	30º27.45	29.8.97	16:18	07º09.08	30º22.32	c16c19.000	c16c05.cfg
90	29.8.97	16:50	07º08.93	30º22.27	29.8.97	18:16	07º12.28	30º15.80	c16c23.001	c16c05.cfg
91	29.8.97	18:49	07º12.29	30º15.54	29.8.97	19:39	07º14.15	30º11.50	c16c024.000	c16c06.cfg
92	29.8.97	20:13	07º14.09	30º11.58	29.8.97				c16c025.000	c16c06.cfg
93	30.8.97	5:39	08º09.77	30º55.77	30.8.97	5:39	08º10.59	30º53.40	c16c28.000	c1607.cfg
94	30.8.97	6:39	08º10.84	30º53.44	30.8.97	7:56	08º12.26	30º46.90	c16c29.001	c16c07.cfg
95	30.8.97	8:37	08º12.28	30º46.60	30.8.97	10:00	08º14.97	30º40.22	c16c031.001	c16c07.cfg
96	30.8.97	10:30	08º14.76	30º40.08	30.8.97	12:31	08º23.50	30º35.93	c16c032.002	c11c07.cfg
97	30.8.97	12:51	08º23.54	30º35.64	30.8.97	13:57	08º25.30	30º28.64	c16c033.000	c16c07.cfg
98	30.8.97	14:17	08º25.53	30º28.79	30.8.97	15:54	08º27.47	30º36.58	c16c034.002	c16c08.cfg
99	30.8.97	18:39	08º32.66	30º45.15	30.8.97	19:30	08º30.07	30º48.39	c16c035.000	c16c09.cfg
100	30.8.97	19:58	08º29.91	30º48.52	30.8.97	21:34	08º25.70	30º54.23	c16c036.000	c16c09.cfg
101	30.8.97	22:02	08º25.62	30º54.30	30.8.97	23:25	08º21.14	30º59.17	c16c037.000	c16c09.cfg
102	30.8.97	23:57	08º21.29	30º59.36	31.8.97	0:34	08º20.52	31º01.74	c16c038.000	c16c09.cfg

Appendix 11. ADCP transects during expedition 16.

103	31.8.97	0:35	08°20.63	31°01.83	31.8.97	2:04	08°26.48	31°06.83	c16c039.000	c16c09.cfg
104	31.8.97	2:23	08°26.83	31°06.83	31.8.97	3:19	08°30.64	31°03.70	c16c040.000	c16c09.cfg
105	31.8.97	3:21	08°30.82	31°03.56	31.8.97	4:01	08°33.70	33°01.66	c16c041.000	c16c09.cfg
106	31.8.97	4:23	08°33.67	31°01.55	31.8.97	5:56	08°39.38	30°56.15	c16c042.000	c16c09.cfg
107	1.9.97	23:33	07°49.89	30°44.87	2.9.97	0:36	07°51.40	30°39.84	c16c043.000	c16c10.cfg
108	2.9.97	3:09	07°40.50	30°35.76	2.9.97	3:58	07°38.77	30°39.47	c16c044.000	c16c10.cfg
109	2.9.97	21:40	06°06.35	29°24.96	2.9.97	22:47	06°06.02	29°19.50	c16c045.000	c16c10.cfg
110	2.9.97	23:02	06°05.88	29°19.26	3.9.97	0:42	05°56.90	29°18.28	c16c046.000	c16c10.cfg
111	3.9.97	0:58	05°56.92	29°18.60	3.9.97	2:05	05°56.29	29°24.88	c16c047.000	c16c10.cfg
112	3.9.97	6:26	05°40.00	29°45.65	3.9.97	7:51	05°40.20	29°32.76	c16c048.000	c16c10.cfg
113	4.9.97	18:09	04°56.93	29°33.17	4.9.97	19:25	04°59.16	29°26.46	c16k001.001	c16c06.cfg
114	4.9.97	20:05	04°58.92	29°26.05	4.9.97	20:08	04°58.95	29°25.72	c16k002.000	c16c06.cfg
115	4.9.97	20:09	04°58.94	29°25.64	4.9.97	22:16	05°00.97	24°18.92	c16k003.000	c16c06.cfg
116	4.9.97	22:49	05°00.77	29°18.98	4.9.97	22:57			c16k004.000	c16c06.cfg
117	4.9.97	22:59	05°00.77	29°19.91	4.9.97	23:10	05°00.79	29°20.82	c16k005.000	c16c06.cfg

Appendix 12.

Acoustic Doppler Current Profiler (ADCP)
Quick guide: How to read a shiptrack figure

MEASURED CURRENT VELOCITIES
Thick line indicates the sailed transect
Thin trajectories indicate the average speed and direction of current for selected depth

SPEED SCALE
Current speed scale in cm/s
'Depth' indicates the averaged depth of the displayed layer

ENSEMBLE
Date, time, vessel's pitch and roll; correction of ADCP depth cells relative to the horizontal plane
Water temperature
Calculated/corrected bottom depths for each transducer

Title of the figure

Tracking method
(here: bottom track)

North displacement
of the ship (m)

VESSEL
Vessel's velocity expressed as E and N components (cm/s) and in knots and heading

South displacement
of the ship (m)

DATA RECORDING
Recorder status (on/off)
*.CFG file name of the measurement configuration
*.000 file name of the saved raw data file

TRANSECT INFORMATION
Minimum linear distance between the start and end points of the transect
Sailed true distance
Total time sailed
Average mean flow across the sailed transect
Average interval (in sec or min)

Acoustic Doppler Current Profiler (ADCP)
Quick guide: How to read a profile figure

MEASURED CURRENT VELOCITIES
Dark raster i.e. positive values indicate flow to north and light raster i.e. negative values to south

SPEED SCALE
Current speed scale in cm/s
'Bad' indicates unreliable data or bottom

ENSEMBLE
Date, time, vessel's pitch and roll; correction of ADCP depth cells relative to the horizontal plane
Water temperature
Calculated/corrected bottom depths for each transducer

Title of the figure

Projection angle in
degrees from N

Layer depth
in meters

VESSEL
Vessel's velocity expressed as E and N components (cm/s) and in knots and heading

Displacement in time

DATA RECORDING
Recorder status (on/off)
*.CFG file name of the measurement configuration
*.000 file name of the saved raw data file

TRANSECT INFORMATION
Minimum linear distance between the start and end points of the transect
Sailed true distance
Total time sailed
Average mean flow across the sailed transect
Averaged interval (in sec or min)

TANGPATH - LAKE TANGANYIKA PARTICLE TRACKING MODEL ORDER FORM

TANGPATH is a computer program for calculation and visualisation of particle trajectories in Lake Tanganyika with special emphasis on the Malagarasi and Lufubu river inlet regions.

Requirements: PC 386/486/Pentium running Microsoft Windows 3.1/95/NT, math coprocessor, 4 MB RAM (8 MB recommended).

A sum of US $ 30.00 is charged for shipping and handling for each item ordered.

This is to order ___ copies of the program:

Name:_____

Institution:_____

Street address:_____

Postal address:_____

Herewith we confirm that total US $ _____ has been paid to the bank account of Kuopio University, project 6781, Account nr: 800011- 47092 Postipankki, 00007 Helsinki 7, Finland,

_____

Signature

Please send the order to:

Prof. Hannu Mölsä
University of Kuopio
Department of Applied Zoology and Veterianary Medicine
University of Kuopio
P.O. Box 1627
FIN-70211 KUOPIO
FINLAND
Tel. +358 17 163145
Fax +358 17 163148